Identification of a *cis*-regulatory module for bundle sheath-specific gene expression and transcriptome analysis of the chilling response of the C_4 grass *Zea mays*

Inaugural-Dissertation

zur Erlangung des Doktorgrades
der Mathematisch-Naturwissenschaftlichen Fakultät
der Heinrich-Heine-Universität Düsseldorf

vorgelegt von

Sandra Kirschner
aus Neuss

Düsseldorf, August 2017

aus dem Institut für Entwicklungs- und Molekularbiologie der Pflanzen
der Heinrich-Heine-Universität Düsseldorf

Gedruckt mit der Genehmigung der
Mathematisch-Naturwissenschaftlichen Fakultät der
Heinrich-Heine-Universität Düsseldorf

Referent: Prof. Dr. Peter Westhoff

Korreferentin: Prof. Dr. Maria von Korff Schmising

Tag der mündlichen Prüfung: 09.11.2017

Erklärung

Ich versichere an Eides Statt, dass die Dissertation von mir selbstständig und ohne unzulässige fremde Hilfe unter Beachtung der "Grundsätze zur Sicherung guter wissenschaftlicher Praxis an der Heinrich-Heine-Universität Düsseldorf" erstellt worden ist. Die Dissertation habe ich in der vorgelegten oder in ähnlicher Form noch bei keiner anderen Institution eingereicht. Ich habe bisher keine erfolglose Promotionsversuche unternommen.

Neuss, 04.08.2017

Sandra Kirschner

Contents

Abbreviations

°C	Degree Celsius
3-PGA	3-Phosphoglycerate
3'/5'UTR	3'/5' Untranslated region
5'RACE	Rapid amplification of 5' complementary DNA ends
A	Rate of CO_2 uptake
A. thaliana	*Arabidopsis thaliana*
ABA	Abscisic Acid
ACR8	ACT domain repeat 8
ARF	Auxin response factor
A_{sat}	Light-saturated rate of CO_2 uptake
ATP	Adenosine triphosphate
AuxRE	Auxin response element
bp	Base pairs
BS	Bundle sheath
bZIP	Basic leucine zipper
C_2, C_3, C_4	Two-, three-, four-carbon molecule
CA	Carbonic anhydrase
CAM	Crassulaceaen acid metabolism
CaMV35S	35S promoter of the cauliflower mosaic virus
CBP	Calmodulin-binding protein
cDNA	Complementary DNA
CDS	Coding sequence
cm	Centimetre
cM	Centimorgan
CO_2	Carbon dioxide
Col-0	Columbia-0
Cyt *f*	Cytochrome *f*
DAT	Days after transplanting
dH_2O	Distilled water
DNA	Desoxyribonucleic acid
DNase	Desoxyribonuclease
DR	Distal region of Mem1

DST element	Downstream element
DW	Dry weight
ETIF3SU4	Eukaryotic translation initiation factor 3 subunit 4
F. bidentis/Fb	*Flaveria bidentis*
F. pringlei/Fp	*Flaveria pringlei*
F. trinervia/*Ft*	*Flaveria trinervia*
FDR	False discovery rate
G. gynandra/Gg	*Gynandropsis gynandra*
GDC	Glycine decarboxylase complex
GFP	Green fluorescent protein
GLDPA	Glycine decarboxylase PA gene of *Flaveria trinervia*
GO	Gene ontology
GSH	Glutathione
GST	Glutathione S-transferase
GUS	β-glucuronidase
h	Hour(s)
H2B	Histone 2B
H_2O_2	Hydrogen peroxide
HCO_3^-	Bicarbonate
HSF	Heat shock factor
Hz	Hertz
kb	Kilo base pairs
k_{cat}	Catalytic turnover rate
kDa	Kilodalton
ke-1	*Kühlempfindlich-1*
K_m	Michaelis constant
l	Litre
LSU	Large subunit of Rubisco
LT_{50}	50 % rhizome mortality
M	Mesophyll
M x *g*	*Miscanthus* x *giganteus*
MAP	Mitogen activated protein
Mb	Mega base pairs
MDH	Malate dehydrogenase

ME	Malic enzyme
Mem1/2	Mesophyll expression module 1/2
MeSA	Methyl salicylate
mg	Milligram
min	Minute(s)
MJ	Megajoule
ml	Millilitre
mRNA	Messenger ribonucleic acid
Mt	Megatonne
MU	4-methylumbelliferone
MUG	4-methylumbelliferone β-D-glucuronide
my	Million years
mya	Million years ago
N. benthamiana	*Nicotiana benthamiana*
NAD	Nicotinamide adenine dinucleotide
NAD-ME	Nicotinamide adenine dinucleotide-malic enzyme
NADP	Nicotinamide adenine dinucleotide phosphate
NADP-MDH	Nicotinamide adenine dinucleotide phosphate-malate dehydrogenase
NADP-ME	Nicotinamide adenine dinucleotide phosphate-malic enzyme
NADPH	Nicotinamide adenine dinucleotide phosphate, reduced form
NH_3	Ammonia
NIL	Near isogenic line
nm	Nanometre
nM	Nanomolar
NUE	Nitrogen use efficiency
O_2	Molecular oxygen
OAA	Oxalacetate
PCA	Principal component analysis
pCO_2	Carbon dioxide partial pressure
PCR	Polymerase chain reaction
PEP	Phospho*enol*pyruvate
PEP-CK	Phospho*enol*pyruvate carboxykinase
PEPC	Phospho*enol*pyruvate carboxylase
PFD	Photon flux density

PG	Phosphoglycolate
pH	Potential of hydrogen
PIP	Plasma membrane intrinsic protein
PNUE	Photosynthetic nitrogen use efficiency
ppcA	Phospho*enol*pyruvate carboxylase gene A of *Flaveria*
PPDK	Pyruvate, orthophosphate dikinase
ppm	Parts per million
PPFD	Photosynthetic photon flux density
PR	Proximal region of Mem1
PSII	Photosystem II
qRT-PCR	Quantitative real-time polymerase chain reaction
QTL	Quantitative trait locus
R^2	Coefficient of determination
RNA	Ribonucleic acid
RNase	Ribonuclease
ROS	Reactive oxygen species
RPKM	Reads per million mapped reads and kb transcript length
Rubisco	Ribulose-1,5-bisphosphate carboxylase/oxygenase
RuBP	Ribulose-1,5-bisphosphate
RUE	Radiation use efficiency
s	Second(s)
S. pectinata	*Spartina pectinata*
SAUR	*SMALL AUXIN-UP RNA*
SDS-PAGE	Sodium dodecyl sulfate polyacrylamid gel electrophoresis
SULTR2;2	Sulfate transporter gene 2;2
TCA	Tricarboxylic acid
TEL_{50}	50 % electrolyte leakage
THI	Thiamine thiazole synthase
TSS	Transcription start site
V_{max}	Substrate saturated enzyme activity
WUE	Water use efficiency
YFP	Yellow fluorescent protein
Z. mays/Zm	*Zea mays*
θ	Light response curve

µg	Microgram
µl	Microliter
Φ	Maximum quantum efficiency
Φ_{CO2}	Efficiency of CO_2 assimilation

Nucleobases of the DNA

A	Adenine
C	Cytosine
G	Guanine
T	Thymine

Amino acids

A	Alanine	M	Methionine
C	Cysteine	N	Asparagine
D	Aspartic acid	P	Proline
E	Glutamic acid	Q	Glutamine
F	Phenylalanine	R	Arginine
G	Glycine	S	Serine
H	Histidine	T	Threonine
I	Isoleucine	V	Valine
K	Lysine	W	Tryptophan
L	Leucine	Y	Tyrosine

I. Introduction

1. C_4 photosynthesis

1.1. The dark side of Rubisco

Photosynthesis is an elementary process performed by plants, algae and some bacteria. Atmospheric and inorganic CO_2 as well as water are transformed in dependence of light energy into organic carbohydrates and O_2. Three photosynthetic mechanisms are known: C_3, C_4 and crassulacean acid metabolism (CAM) that can be differentiated by the location and time of CO_2 fixation. The majority of plants use the C_3 mechanism (Ehleringer *et al.* 1991) that is initiated by the enzyme ribulose-1,5-bisphosphate carboxylase/oxygenase (Rubisco).

Rubisco is the only enzyme able to fix atmospheric CO_2 (Andrews and Lorimer 1987). In one year, it is estimated that Rubisco fixes 10^{11} tons of atmospheric CO_2 (Andersson 2008, Field *et al.* 1998). The reaction is the first of the Calvin-Benson-Bassham cycle. Ribulose-1,5-bisphosphate (RuBP) becomes carboxylated, resulting in two molecules of 3-phosphoglycerate (3-PGA) (Calvin and Benson 1948, Lorimer 1981). However, the reaction is very slow (Andrews and Lorimer 1987). In light-saturated leaves, the carboxylation reaction by Rubisco is the rate-limiting step of photosynthesis (Carmo-Silva *et al.* 2015). The enzyme is of ancient origin: 2.7 and 2.9 billion years old fossils evidence the presence of the Rubisco I isoform (Nisbet *et al.* 2007). But there are indications that the oxygenic photosynthesis and Rubisco evolved earlier (Buick 2008), two processes that are inherently correlated (Nisbet *et al.* 2007).

Afore, the earth's atmosphere contained more CO_2 and much less O_2 than today (Sage 1999, Sage 2004), in contrast to today where the opposite is true. Now, the atmosphere contains 21.95 % O_2 and only 0.04 % CO_2, which makes an O_2/CO_2 ratio of nearly 550. And this is the key issue: apart from carboxylation, Rubisco is able to catalyse the oxygenation of RuBP (Andrews *et al.* 1973). This reaction was negligible in the anoxic atmosphere of the Archean when the enzyme was recruited for photosynthesis. However, due to the changing composition of the atmosphere 280 million years ago (mya) the oxygenation reaction became (in terms of fitness) for the first time relevant (Sage 2004). Although Rubisco favours CO_2 over O_2 as a substrate (Jordan and Ogren 1984), the atmospheric composition of today as well as the photosynthetic oxygen formation (Andrews and Lorimer 1987) lead to substantial fractions of oxygenation. For example, in crude spinach leaf extract at 25 °C, the

oxygenase/carboxylase rate is 0.25 (Andrews *et al.* 1973). Oxygenation of RuBP results in one molecule 3-PGA and one molecule phosphoglycolate (PG) (Andrews and Lorimer 1987, Andrews *et al.* 1973). Furthermore, detrimental H_2O_2 is formed as a byproduct (Kim and Portis 2004).

PG is metabolically useless and even toxic for cells (Jordan and Ogren 1984). Thus, PG needs to be rapidly eliminated. The process comprising PG formation and its recycling to 3-PGA under release of CO_2 and NH_3 is called photorespiration. Photorespiration involves the three compartments mitochondria, chloroplasts and peroxisomes and is quite expensive for the cell. It may rescue 75 % of the carbon in PG, but it also consumes ATP and reduction equivalents (Ogren 1984, Peterhänsel *et al.* 2010). Assuming an oxygenation rate of 25 % relative to carboxylation, the energy costs of photosynthesis increase by about 50 % (Peterhänsel *et al.* 2010).

However, these figures only apply for temperate conditions. Heat favours the oxygenation reaction over carboxylation (Jordan and Ogren 1984). On the one hand, rising temperatures are correlated with an increased O_2/CO_2 solubility ratio in leaves (Ku and Edwards 1977). On the other hand, the oxygenase specificity constant of Rubisco increases more strongly than the carboxylase specificity constant when temperature is rising (Jordan and Ogren 1984). Heat also promotes stomata closure, thus impeding CO_2 uptake; albeit this effect may be marginal (Farquhar and Sharkey 1982). As a consequence of all these deficiencies and the absolute requirement of this enzyme for plant photosynthesis, Rubisco is the most abundant protein in the world (Ellis 1979). In C_3 plants, Rubisco makes up 30 to 50 % of the soluble leaf protein. Improvement of Rubisco, therefore, may improve biomass production as plants invest a lot of nitrogen for the synthesis of the enzyme (Carmo-Silva *et al.* 2015). However, although there is some variation for the specificity of Rubisco (Galmés *et al.* 2005), engineering of an improved Rubisco had little success so far (Carmo-Silva *et al.* 2015). But why should one improve Rubisco since nature has already circumvented the oxygenation problem by the invention of C_4 photosynthesis?

1.2. C_4 plants have a distinct anatomy and concentrate CO_2 around Rubisco to supress photorespiration

C_4 plants have evolved an efficient CO_2 pump system to concentrate CO_2 around Rubisco (Hatch 1987, Pearcy and Ehleringer 1984, von Caemmerer and Furbank 2003), resulting in a reduced CO_2 compensation point as compared to C_3 species (Kanai and Edwards 1999). In C_4 photosynthesis, CO_2 is initially fixed by the oxygen-insensitive enzyme phospho*enol*pyruvate

carboxylase (PEPC) and the resulting C_4 acid is usually transported into a different cell type where Rubisco is exclusively localised. There, the C_4 acid is decarboxylated, resulting in CO_2 enrichment at the site of Rubisco (Hatch 1987). This process demands for certain anatomic changes. C_4 plants commonly exhibit Kranz anatomy (Dengler and Nelson 1999), a term early coined by the Austrian botanist Gottlieb Haberlandt (Haberlandt 1881). Two cell types typically – but not always – form the "Kranz" (German for wreath): one layer of bundle sheath (BS) cells concentrically surrounds the vasculature and is itself wrapped by a concentric layer of mesophyll (M) cells (Dengler and Nelson 1999). C_3 plants also have a BS, however, the BS cells are smaller and contain only a few chloroplasts (Kinsman and Pyke 1998). C_4 plants display a higher vein density (Dengler and Nelson 1999). Furthermore, many C_4 plants have evolved mechanisms to impede CO_2 diffusion back into the M cells, like a suberin lamella in the BS cell wall or a certain arrangement of chloroplasts and/or mitochondria in the BS cells (Sage 2004, von Caemmerer and Furbank 2003). A comparison of the leaf anatomy of the C_3 plant *Arabidopsis thaliana* and the C_4 plant *Zea mays* is shown in Figure 1.

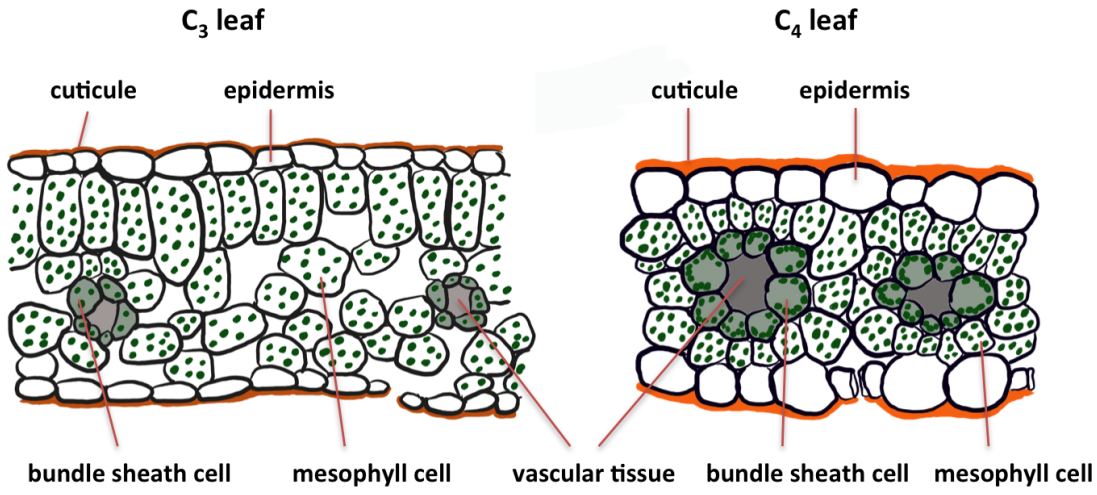

Figure 1: Schematic cross-sections of a typical C_3 plant (*Arabidopsis thaliana*) and C_4 plant (*Zea mays*)
C_4 plants have in general enlarged BS cells that are usually parted by two M cells (Kranz anatomy). BS chloroplasts of C_4 plants are often differently distributed as those from the mesophyll. In case of maize, the BS chloroplasts are orientated adjacent to the cell part next to the M cells. Adapted from self-made cross-sections.

A few exceptions from two-celled C_4 photosynthesis, i.e. single-cell C_4 photosynthesis, are found in the Chenopodiaceae. In single-cell C_4 photosynthesis, the photosynthetic cells are polarised and the two carboxylating enzymes are located in different parts of the cell (Akhani *et al.* 2005, Voznesenskaya *et al.* 2002, Voznesenskaya *et al.* 2001).

Three types of two-cell C_4 photosynthesis types can be distinguished by the abundance of the enzyme responsible for the decarboxylation in the BS: the NADP-malic enzyme (NADP-

ME) type, the NAD-malic enzyme (NAD-ME) type and the phospho*enol*pyruvate carboxykinase (PEP-CK) type (Hatch *et al.* 1975, Kanai and Edwards 1999). All types initially fix CO_2 by PEPC, resulting in oxaloacetate (OAA) (Kanai and Edwards 1999). PEPC uses bicarbonate instead of CO_2 as the substrate and has a high capacity for assimilation of bicarbonate even at low internal bicarbonate concentrations (Hatch 1987). In the NADP-ME type (Figure 2), OAA is imported into the chloroplasts of the M cells where it is reduced to malate by the NADP-malate dehydrogenase (NADP-MDH). Exported from the M cell chloroplasts into the cytosol, malate diffuses along the concentration gradient through the plasmodesmata into the BS cells (Hatch 1987, Stitt and Heldt 1985). Following transport to the BS cell chloroplasts, malate is decarboxylated. This is performed – as the name of the type indicates – by the NADP-ME, resulting in atmospheric CO_2 and pyruvate. The CO_2 is then assimilated by the Rubisco in the Calvin-Benson-Bassham cycle (Hatch 1987). Due to this enrichment, Rubisco can work close to its substrate saturated enzyme activity (V_{max}) (von Caemmerer and Furbank 2003). Pyruvate, however, is transported back into the M chloroplasts, where it is converted to PEP via the pyruvate, orthophosphate dikinase (PPDK). PEP can be carboxylated again, thus closing the cycle. In the NAD-ME type, the C_4 acid aspartate is the major transport form of carbon. Once arrived in the BS mitochondria, aspartate is converted to OAA, which is then reduced to malate. Malate is finally decarboxylated to pyruvate by the NAD-ME in order to feed Rubisco with CO_2. Similar to the NAD-ME type, aspartate is the main transport form of carbon in the PEP-CK type. Contrastingly, aspartate is decarboxylated by the PEP-CK in the BS cytosol. Also, some malate is formed in the PEP-CK type that is decarboxylated by the NAD-ME in the BS mitochondria (Hatch 1987, Kanai and Edwards 1999).

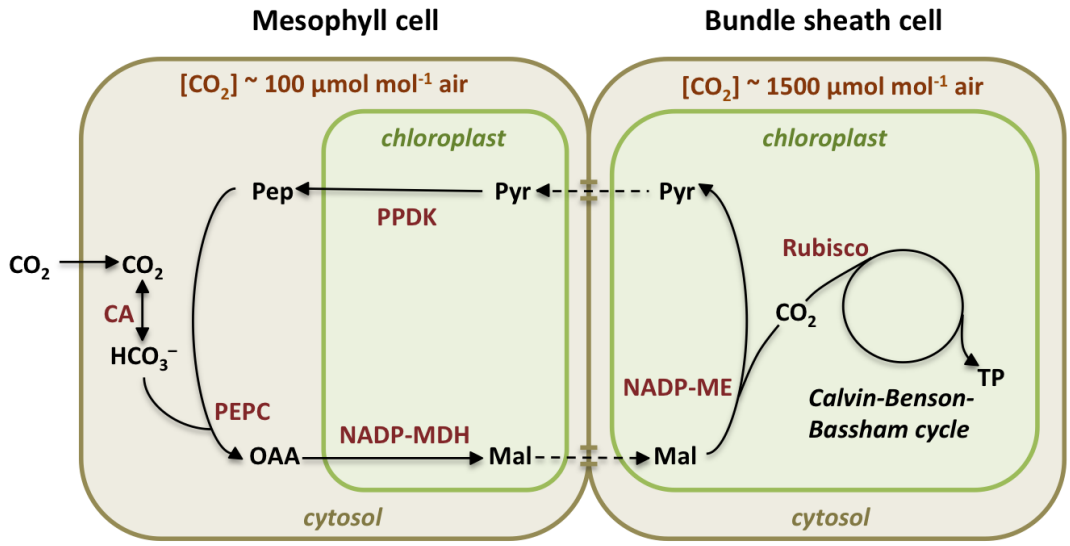

Figure 2: C_4 photosynthetic pathway performed by plants of the NADP-malic enzyme subtype
A simplified schematic model of the C_4 photosynthetic pathway that is performed by plants of the NADP-malic enzyme subtype is shown. The different CO_2 concentrations in both cell types indicate the CO_2 concentration mechanism of C_4 photosynthesis.
CA, carbonic anhydrase; PEPC, phospho*enol*pyruvate carboxylase; NADP-MDH, NADP-malate dehydrogenase; NADP-ME, NADP-malic enzyme; Rubisco, ribulose-1,5-bisphosphate carboxylase/oxygenase; PPDK, pyruvate, orthophosphate dikinase; Pep, phospho*enol*pyruvate; OAA, oxaloacetate; Mal, malate; Pyr, pyruvate
Adapted and simplified from Sage *et al.* (2012) and Furbank (2011).

However, the subdivision into the three types is not strict. For example, PEP-CK accumulates also in the BS of maize and other plants thought to be NADP-ME plants (Walker *et al.* 1997). Indeed, PEP-CK catalyses at least 20 % of the decarboxylation reactions, indicating that the C_4 cycle is rather branched than linear (Pick *et al.* 2011). This mechanism is thought to confer robustness of photosynthesis at changing environmental conditions (Wang *et al.* 2014). In general, C_4 photosynthesis is not considered as a single pathway but as different pathways with PEP as first carbon acceptor (Kellogg 1999).

Nevertheless, independent of the type(s), C_4 plants succeed in elevating the CO_2 concentration at the location of Rubisco. In doing so, the oxygenase activity and thus photorespiration are largely supressed (Hatch 1987, Sage 2004). This results in a higher conversions efficiency of solar energy to biomass at present atmospheric conditions when compared to C_3 plants (Zhu *et al.* 2008).

1.3. The benefits of the CO_2 concentrating mechanism

In comparison to C_3 plants, C_4 plants display a higher radiation use efficiency (RUE), nitrogen use efficiency (NUE) and water use efficiency (WUE) at temperatures and

conditions promoting photorespiration (Ehleringer and Monson 1993, Pearcy and Ehleringer 1984, Sage 2004). These parameters define the efficiency of a plant in producing dry matter (Brown 1999).

The RUE describes how efficiently radiation is transformed in energy and biomass (Mitchell and Sheehy 2007) and is expressed as g shoot dry weight (DW) per MJ (Sheehy *et al.* 2007). After all, production of biomass depends on photosynthetically active radiation (Beadle and Long 1985). The RUE is in turn dependant on the maximum quantum yield (Sage and Zhu 2011). Modelling shows that C_4 plants can convert 6.0 % and C_3 plants 4.6 % of the solar energy into biomass at 30 °C and atmospheric CO_2 concentrations (Zhu *et al.* 2008, Zhu *et al.* 2010). Other models also support the superiority of C_4 plants in conversion efficiency (Beadle and Long 1985, Wang *et al.* 2012). Experiments substantiated the models with facts: C_4 plants appeared to have a greater RUE or quantum yield when compared with C_3 plants (e.g. Ehleringer and Pearcy (1983), Ludlow (1981), Sheehy *et al.* (2007)). In contrast to C_3 plants, the quantum yield of C_4 plants does not decrease at increasing temperatures (Ehleringer and Pearcy 1983, Ku and Edwards 1978).

In general, the high RUE of C_4 plants is a result of the strongly diminished photorespiration (Ehleringer and Monson 1993, Yin and Struik 2009). For example, a model shows that at high light, the concentration of CO_2 in C_4 leaves is about 8 to 10 times higher than in C_3 leaves, thus nearly eliminating photorespiration (Yin and Struik 2009). However, without taking photorespiration and respiration into account, C_3 plants are estimated to have a higher maximum energy conversion efficiency than C_4 plants, due to the extra ATP costs of the CO_2 concentrating mechanism (Zhu *et al.* 2008, Zhu *et al.* 2010). Conversely, elimination of photorespiration in rice would result into a 31 % higher RUE (Mitchell *et al.* 1998). Furthermore, low light promotes CO_2 leakage from the BS back to the M, thus reducing quantum yield (Furbank and Hatch 1987, Yin and Struik 2009). Also C_4 Rubisco and RuBP may be limiting at low light (Sage and Seemann 1993).

Nevertheless, at temperatures above 25 °C, C_4 photosynthesis is superior to C_3 photosynthesis (Ehleringer and Pearcy 1983, Ehleringer and Monson 1993, Sage and Zhu 2011). This could be visualised by a comparison of growth of rice (C_3), maize (C_4) and *Echinochloa glabrescens* (C_4) in the warm tropical climate in the Philippines (Figure 3). In numbers, maize reached a RUE of 4.4 g DW MJ^{-1}, *E. glabrescens* of 4.0 g DW MJ^{-1} and rice of only 2.9 g DW MJ^{-1}. The grain yield of maize was double as of rice (Sage and Zhu 2011, Sheehy *et al.* 2007).

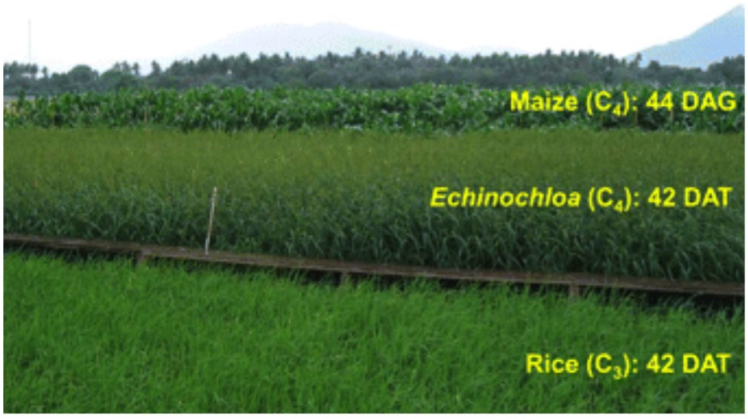

Figure 3: Differences in biomass accumulation of two C_4 species and one C_3 species
The results of a field trial at the warm tropical climate in the Philippines, comparing the C_4 species maize and *Echinochloa glabrescens* and the C_3 species rice, is displayed.
DAG, days after germination; DAT, days after transplanting
Taken with permission from Sage and Zhu (2011).

It was early recognised that tropic C_4 grasses are superior to temperate C_3 grasses at high temperature as well as high light. They exhibited a smaller loss of water but accumulated more biomass (Downes 1969). Many other studies displayed comparable results: a higher ratio of net CO_2 assimilation rate and transpiration rate in C_4 plants (e.g. Gillies *et al.* (1983), Kocacinar *et al.* (2008), Taylor *et al.* (2010)). In short, at equivalent water loss rates, C_4 plants outperform C_3 plants concerning photosynthetic carbon gain (Ehleringer and Monson 1993). High WUEs were found in independent C_4 grass lineages, which indicate a common cause. One possibility is the CA-PEPC system (Taylor *et al.* 2010). PEPC fixes carbon much faster than Rubisco (von Caemmerer 2000), thus allowing for a lower stomatal conductance (Osborne and Sack 2012). Furthermore, the anatomical adaptions enhance the WUE. Enlarged BS cells are able to store more water. The reduction of M cells in relation to water conducting and storing cells also leads to a reduction of the transpiration area (Sage 2001). The elevated WUE offer some advantages for the plants. In dry, saline regions with shallow substrates, plants with an increased WUE are able to survive easier and can propagate (Sage 2001). Additionally, an improved WUE allows C_4 grasses to balance carbon costs of mycorrhiza (Heckathorn *et al.* 1999). Some C_4 plants – especially those of wetter habitats – invest their savings in canopy development (Kocacinar *et al.* 2008, Kocacinar and Sage 2003). A better WUE resulted also in an adaption of the xylem. C_4 plants often display shorter and thinner xylem vessels and thus a decreased hydraulic efficiency. However, the costs of reduction in hydraulic efficiency denote also an improved protection against embolism, a trait beneficial in dry habitats (Kocacinar 2015, Kocacinar *et al.* 2008, Kocacinar and Sage 2003).

In quantitative terms, nitrogen is the most important nutrient, which limits both growth and development of plants (Kraiser *et al.* 2011). The NUE, defined as the ratio of increase in plant biomass to the increase in plant nitrogen (Long 1999), can be twice as high in C_4 plants as in C_3 plants (Brown 1985). This was also shown for the photosynthetic NUE (PNUE), the net rate of CO_2 uptake in full sunlight per unit leaf nitrogen content (Long 1999). However, several studies demonstrate some limitations or contradictions. One study exhibited that the C_4 *Amaranthus retroflexus* showed superior NUE to the C_3 *Chenopodium album* when grown on high nitrogen, however, the opposite was true when plants were kept at low nitrogen (Sage and Pearcy 1987a, Sage *et al.* 1987). Also high CO_2 levels (Schmitt and Edwards 1981) or low temperatures can compromise NUE of C_4 plants (Sage and Pearcy 1987b). The latter was contradicted by a study comparing maize and wheat: the C_4 plant maize always exhibited a higher NUE than the C_3 plant wheat, independent of temperature (Schmitt and Edwards 1981). But on the bottom line, C_4 plants generally have a higher NUE and PNUE than C_3 plants at conditions favouring C_4 photosynthesis (Long 1999, Sage and Pearcy 1987b, Schmitt and Edwards 1981).

It was proposed that C_4 plants could exploit these advantages in two ways. On the one hand, they can produce more leaf area, resulting in an improved photosynthetic capacity. On the other hand, they can invest their nitrogen in roots to ameliorate water and mineral uptake (Long 1999, Sage and Pearcy 1987a). Interestingly, the C_4 subspecies of *Alloteropsis semialata*, exhibiting superior NUE than the C_3 subspecies, allocates biomass to sexual reproduction organs and corms (Ripley *et al.* 2008).

The high NUE of C_4 plants is based on their CO_2 concentrating mechanism (Long 1999, Schmitt and Edwards 1981). C_4 leaves contain only about half of the Rubisco amount of C_3 leaves. Consequently, Rubisco accounts for 10-30 % of total leaf nitrogen in C_3 plants but only for 5-10 % in C_4 plants (Carmo-Silva *et al.* 2015). However, one should not forget that the C_4 cycle requires investment in additional enzymes like PEPC. But due to the 10 times higher catalytic turnover rate (k_{cat}) of PEPC, C_4 plants do not invest into high amounts of PEPC, thus still allowing a positive NUE balance (Long 1999, Sage *et al.* 1987). Furthermore, the K_m of Rubisco for CO_2 is increased in C_4 plants. Thus, Rubisco binds CO_2 less stably, resulting in a faster release and a twice as high k_{cat}. This could further reduce the required amount of Rubisco and improves NUE (Seemann *et al.* 1984). In contrast to C_3 plants missing the CO_2 concentrating mechanism, C_4 plants can afford a higher K_m to raise k_{cat} (Ghannoum *et al.* 2011, Sage 2002). A comparison of grasses of either NADP-ME or NAD-ME type demonstrates the correlation of Rubiscos k_{cat} and NUE/PNUE. NADP-ME grasses exhibited a

higher NUE and PNUE and a higher k_{cat} of Rubisco than NAD-ME grasses (Ghannoum *et al.* 2005).

All in all, the higher photosynthetic capacity and the superior RUE, WUE and NUE of C_4 plants account for the higher yields of these (Sage and Zhu 2011).

1.4. The convergent evolution of C_4 photosynthesis

C_4 species make up about 3 % of all land plant species (Sage and Stata 2015) but account for 25 % of the terrestrial photosynthesis (Edwards *et al.* 2010, Still *et al.* 2003). Regarding global agriculture, merely maize, Sorghum and sugar cane are of significance (Sage 2016, Sage and Zhu 2011). Only angiosperms, but neither gymnosperms, lower vascular plants nor bryophytes perform C_4 photosynthesis (Sage 2016, Sage *et al.* 2012). Concerning the life form, C_4 plants are organised as graminoids, herbaceous and small woody eudicots, shrubs, vines and aquatic herbs (Sage 2016). Only few C_4 plants are trees with a trunk (Sage 2016, Sage and Sultmanis 2016). Those belong to the genus *Euphorbia* and are restricted to Hawaii. They have a well-developed Kranz anatomy and grow up to 9 m (Pearcy 1975).

Despite the complexity of the trait, C_4 photosynthesis has evolved repeatedly, thus being convergent and polyphyletic (Sage *et al.* 2011). The C_4 photosynthesis evolved independently from C_3 ancestors (Kellogg 1999). By now, 61 de novo lineages are assumed, developed in 19 families and comprising 8145 species (Sage 2016). Considering the increase of discoveries over time, one can assume that the number of de novo lineages might be revised upwards in the future. For example, in 1999, 31 independent origins were proposed (Kellogg 1999) and five years later already 45 lineages (Sage 2004).

The majority of C_4 plants are monocots, comprising 5044 grasses and 1322 sedges. Eudicots amount to at least 1750 species (Sage 2016). Some are species of intermediate C_3-C_4 photosynthesis (Sage *et al.* 2011) like the Asteracean genus *Flaveria* with 9 intermediate species (McKown *et al.* 2005) that serve as a model for studying C_4 evolution (McKown *et al.* 2005, Sage *et al.* 2012).

Low atmospheric CO_2 partial pressure (pCO_2) is a precondition for C_4 evolution (Sage *et al.* 2011, Sage and Stata 2015). In middle to late Oligocene, 30 to 25 mya, the pCO_2 declined from roughly 800 to 400 ppm (Zhang *et al.* 2013). In this time frame, the first C_4 plants evolved. The oldest C_4 monocots are possibly those of the Chloridoidae and evolved 28.5 mya (Grass Phylogeny Working Group II 2012, Sage 2016). The *Portulaca* species are the oldest

C_4 eudicots and are estimated to have evolved 28.8 mya. Therefore, C_4 eudicots are not younger than monocots, which has been assumed for a long time (Christin *et al.* 2011).

Besides low pCO_2, ecological and climatic conditions also promoted C_4 evolution (Christin *et al.* 2008, Sage 2016). In total, C_4 photosynthesis evolved in six arid and semi-arid regions, namely in North- and South America, central Asia, northeast Africa and Arabia, the south of Africa and Australia. However, these hotspots are mainly verified for eudicots as grasses are more dispersed and thus their origins are not easy to trace (Sage *et al.* 2011). C_4 grasses now exist in low latitudes and altitudes where they dominate warm grasslands and savannahs (Edwards *et al.* 2010).

In the Miocene, C_4 grasses were rare (Christin *et al.* 2008), but at the transition of Miocene to Pliocene, about 3 to 8 mya, a sudden shift from C_3- to C_4-dominated vegetation occurred (Cerling *et al.* 1998, Edwards *et al.* 2010, Strömberg 2011). Regional factors like aridity, nutrient-deficient soils, herbivory and fire triggered the expansion of C_4 grasses (Bond 2008, Sage and Stata 2015, Strömberg 2011). Interestingly, there might be a possible connection between the expansion of C_4 biomass and the evolution of humans (van der Merwe and Tschauner 1999). Examinations on 1.9 to 1.4 million years (my) old fossils of the East African *Paranthropus boisei* exhibited that those Hominins have largely fed on C_4 grasses and sedges (Cerling *et al.* 2011). During the last 4.3 my, a time characterised by increasing aridity and climate instability, C_4 biomass gradually accumulated in the Turkana basin in Kenya. Especially this site is a true treasure trove for Hominin fossils dated in this period (Wood and Leakey 2011).

Also in these times, C_4 evolution continues (Sage 2016). But whereas expansion of C_4 plants might have triggered human evolution (van der Merwe and Tschauner 1999), human influence might negatively affect C_4 expansion in the future. Sage (2016) assumed and warned that humans and their intervention in the ecosystems might endanger the diversity of C_4 species.

1.5. A model for the step-by-step evolution of C_4 photosynthesis

C_4 photosynthesis independently evolved at least 61 times (Sage 2016), indicating that this process has to be, in genetic terms, quite simple (Gowik and Westhoff 2011). Sage (2004) proposed a model for the gradual evolution of C_4 photosynthesis, which was refined by Sage *et al.* (2012). Each stage is thought to present an adaptive advantage (Gowik and Westhoff 2011). The five phases comprise (1) preconditioning of C_3 plants, (2) evolution of proto-

Kranz anatomy, (3) evolution of a photorespiratory CO_2 pump, (4) establishment of the C_4 cycle and (5) optimisation of the C_4 cycle (Gowik and Westhoff 2011, Sage *et al.* 2012) (Figure 4).

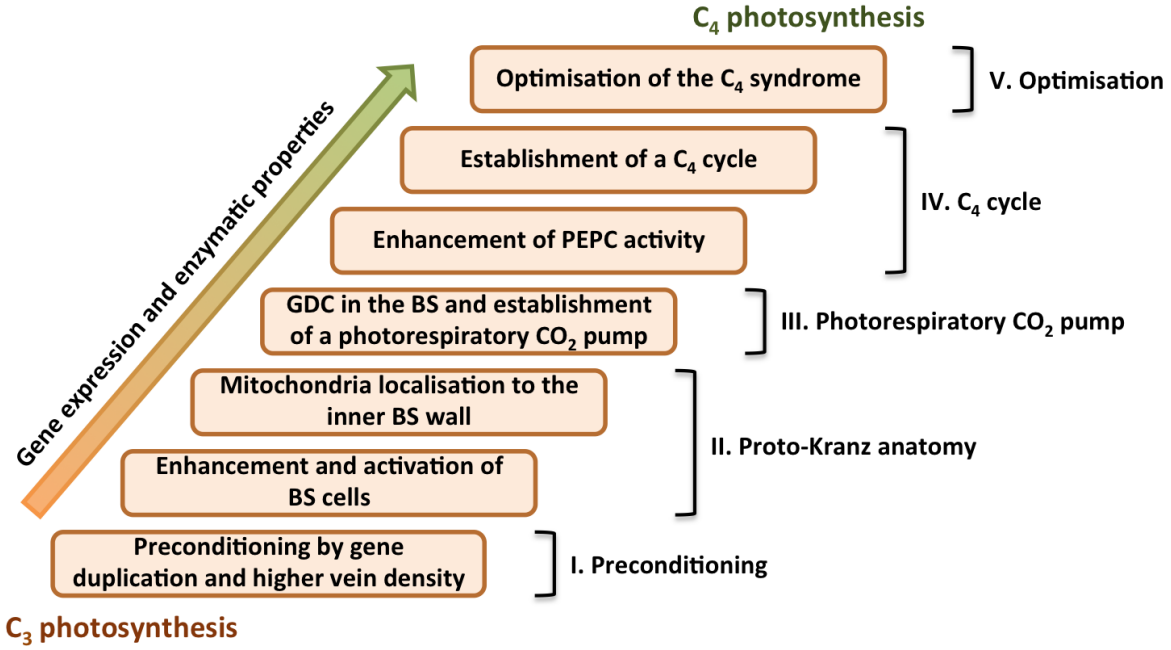

Figure 4: Conceptual model for the evolution of C_4 photosynthesis.
Displayed are the steps and the five major phases for the progressive evolution of C_4 photosynthesis. BS, bundle sheath; GDC, glycine decarboxylase complex; PEPC, phospho*enol*pyruvate carboxylase
Adapted from Gowik and Westhoff (2011) and Sage *et al.* (2012).

The first phase comprises a general preconditioning of plants. The observation that some clades did not produce C_4 photosynthesis and other exhibited a number of independent origins of C_4 photosynthesis led to the assumptions that the latter clades are predisposed for C_4 evolution (Sage 2004, Sage *et al.* 2011, Sage *et al.* 2014). Several traits might raise the possibility of C_4 evolution. One trait is an increase in vein density (Sage *et al.* 2012). The C_3 species *Flaveria robusta* of the basal clade has already achieved a higher vein density. This indicates that the common ancestor of *F. robusta* and the residual C_4 *Flaveria* species had already evolved this trait (McKown and Dengler 2007). Similar observations were made in the clades of *Cleome*, *Euphorbia*, *Heliotropium* and *Mollugo* (Sage *et al.* 2012). The higher vein density is thought to be an adaption to dry climates (Muhaidat *et al.* 2007, Sage *et al.* 2012) as it maintains hydraulic integrity and reduces the evaporative surfaces of photosynthetic cells (Sage 2001). Besides, higher vein density enables an improved exchange of metabolites between M and BS cells. Another trait is the duplication of genes or whole genomes, leading to neo- or subfunctionalisation of genes that can be adapted for evolution in general or evolution of C_4 photosynthesis (Monson 2003, Moore and Purugganan 2005, Sage

2004, Sage *et al.* 2012). In a recent study, it was shown that duplication and neofunctionalisation are key factors for the C_4 evolution of monocots (Emms *et al.* 2016). Another precondition might be the adoption of gene regulatory elements and their modification to achieve C_4 photosynthetic expression patterns (Sage *et al.* 2012).

A decrease of vein density causes a problem as the higher BS to M ratio decreases the photosynthetic capacity of the plant. To compensate, plants enlarge their BS cells and increase the amount of cell organelles in this tissue – the BS gets "activated" (Gowik and Westhoff 2011, Sage 2004, Sage *et al.* 2012). This leads to the second phase, the formation of the proto-Kranz anatomy. This pattern comprises not only the afore mentioned anatomic changes but also a centripetal (inner) distribution of mitochondria in the BS cells (Muhaidat *et al.* 2011), resulting in a one-cell glycine shuttle (Morton *et al.* 2014, Sage *et al.* 2013). In the mitochondria, one important step of the photorespiration takes place: the decarboxylation of glycine catalysed by the P-subunit of the glycine decarboxylase complex (GDC) (Oliver 1994). The inner part of the BS cell is considered to function as a glycine sink (Sage *et al.* 2013). The CO_2 released from glycine is concentrated in this cell part and can be scavenged by Rubisco of the inner-located chloroplasts (Muhaidat *et al.* 2011). Furthermore, the vacuole of the BS cell hinders the diffusion of CO_2, thereby improving the enrichment of CO_2. This mechanism partially compensates for photorespiratory costs and results together with the one-cell glycine shuttle in a slight decrease of the CO_2 compensation point (Sage *et al.* 2012, Sage *et al.* 2013). This photorespiratory CO_2 scavenging system within the BS is found in C_3 species closely related to C_3-C_4 intermediate species (Sage *et al.* 2012) like *Heliotropium karwinskyi, H. procumbens* and *F. pringlei* (Sage *et al.* 2013, Muhaidat *et al.* 2011). The glycine sink in the BS might also attract excess glycine from the M, thereby entailing selective pressure for an increased amount of chloroplasts in this tissue (Sage and Stata 2015). In this stage, a mutation causing deletion of GDC activity in the M would be safe (Muhaidat *et al.* 2011, Sage and Stata 2015).

This leads to the transition to the third phase, the establishment of a photorespiratory CO_2 pump. This key step of C_4 evolution (Gowik and Westhoff 2011, Muhaidat *et al.* 2011, Sage *et al.* 2012, Sage and Stata 2015) involves the loss of GDC activity in the M cells, a process that evolved stepwise in *Flaveria* (Schulze *et al.* 2013). Glycine produced in the M has to move to the BS where it gets decarboxylated (Rawsthorne 1992, Rawsthorne *et al.* 1988, Sage 2004). The plants no longer rely on a one-cell but on a two-cell glycine shuttle. This has two advantages. First of all, central accumulation of CO_2 minimises its chance for escape due to the long diffusion part. Secondly, CO_2 accumulates in the BS (Gowik and Westhoff 2011).

Consequently, photorespiration changes from a negative process to a source of CO_2 in the BS (Sage *et al.* 2012). The CO_2 compensation points drops to a lower level (McKown and Dengler 2007, Voznesenskaya *et al.* 2010). Often the photorespiratory CO_2 pump is termed analogous to the other photosynthetic mechanisms C_2 photosynthesis as a two-carbon photorespiratory metabolite is shuttled and decarboxylated (Sage *et al.* 2012, Sage and Stata 2015, Vogan *et al.* 2007). The photorespiratory CO_2 pump is associated with further changes of anatomy. BS are enlarged, the M to BS ratio further decreases, the number and size of BS organelles rise. Additionally, the centripetal location of BS organelles gets more pronounced (Marshall *et al.* 2007, McKown and Dengler 2007, Muhaidat *et al.* 2011, Voznesenskaya *et al.* 2010). All in all, the leaf anatomy of these intermediate species is well-adapted to the C_2 photosynthesis (Muhaidat *et al.* 2011) and furthermore might promote expression of C_4 photosynthetic enzymes (McKown and Dengler 2007). In some intermediate species, low amounts of several C_4 cycle transcripts or enzymes, respectively, accumulate (Marshall *et al.* 2007, Voznesenskaya *et al.* 2010). In case of *Flaveria*, transcriptome analysis of five intermediate species revealed also upregulation of typical C_4 genes as well as C_4-associated transporter genes. The expression of the genes increased with increased degrees of "C_4-ness" of the species (Mallmann *et al.* 2014).

This heralds the transition to the fourth phase, the establishment of the C_4 metabolic cycle. That step involves enhanced and compartmentalised expression of key enzymes like PEPC, Rubisco and CA (Sage *et al.* 2012). In case of PEPC, the increased activity of the enzyme is linked to recycling of escaped CO_2 from the BS (Monson 1999, Monson and Moore 1989, Sage 2004). PEPC expression steadily increased from *Flaveria* C_3 species over C_3-C_4 intermediates and C_4-likes up to true C_4 species, whereas the C_4-like species exhibited near-similar expression strength and activity as the C_4 species (Engelmann *et al.* 2003, Ku *et al.* 1991, Mallmann *et al.* 2014, Svensson *et al.* 2003). Only few base pair changes are necessary and sufficient to enhance and restrict the expression of the *Flaveria* PEPC gene *PpcA* to the M in C_4-like and C_4 species (Akyildiz *et al.* 2007). This highlights the necessary prerequisite of BS- and M-specific expression of C_4 cycle genes (Gowik and Westhoff 2011, Sage *et al.* 2012). However, the C_4-like species still show an incomplete localisation of Rubisco in the BS (Bauwe 1984, Moore *et al.* 1989, Sage *et al.* 2014), also indicated by low but measurable O_2 inhibition rates (Ku *et al.* 1991). Yet the increase in PEPC activity is thought to select for an increase in other C_4 enzymes in order to regenerate the substrate PEP (Engelmann *et al.* 2003, Monson 1999, Monson and Moore 1989, Sage 2004).

With the restriction of Rubisco to the BS, C_2 photosynthesis became obsolete (Mallmann *et al.* 2014) and the fifth and last phase, the optimisation phase, set in. For a fully operating C_4 cycle, the regulatory and kinetic properties of C_4 enzymes need to be changed and optimised (Gowik and Westhoff 2011, Sage 2004, Sage *et al.* 2012). This has been intensely studied for the *ppcA* genes of *Flaveria*. When compared to the PEPC of the C_3 species *F. pringlei*, the C_4 isoform of *F. trinervia* exhibited a higher K_m for PEP (Svensson *et al.* 1997). Regions 2 and 5 of PEPC are associated with the lower PEP affinity of the C_4 enzyme. Especially an alanine to serine substitution at position 774 (region 5) was found to be important for the evolution of the C_4 isoform (Blasing *et al.* 2000, Engelmann *et al.* 2002). Strikingly, only C_4 *Flaveria* species contain this serine (Svensson *et al.* 2003). Furthermore, C_4 PEPC enzymes are inhibited to a lesser extent by malate (Engelmann *et al.* 2003), which is necessary as the enzyme has to work in a high malate environment (Hatch 1987). The lower affinity to PEP of the C_4 isoforms might be surprising but it was proposed that the higher tolerance for malate or the observed lower K_m for bicarbonate is of greater importance (Svensson *et al.* 2003). A similar trade-off was found for Rubisco. The C_4 enzyme exhibits concerning CO_2 a higher k_{cat} at the expense of a higher K_m (Seemann *et al.* 1984).

2. *Cis*-regulatory modules for BS- and M-specific expression

2.1. Implementation of the C_4 cycle in C_3 plants

The world faces serious problems. During the last 50 years, the world population doubled to 7.3 billion people in 2015. In 2050, a population of 9.7 billion people is estimated (United Nations 2015). Consequently, sufficient nourishment of people will be compromised, not least by increasing demand for meat, climate change and restricted agricultural land (Miflin 2000). The most important grain crop for human nutrition is possibly the C_3 plant rice, with a total yield of 741.5 Mt in the year 2014. Only another cereal beats rice concerning total yield (FAOSTAT 2017), however, the C_4 plant maize is also deployed for the production of fodder and biofuel (FAO 2015, Sheehy *et al.* 2007). It was estimated that the rise of population during the next 50 years likewise demands for an increase of rice yields of 50 % (Hibberd *et al.* 2008). However, rice yields could not be improved in breeder's trials of the international rice research institute (IRRI) during the last 30 years (Sheehy 2001). Thus, a second green revolution is required (Kajala *et al.* 2011, von Caemmerer *et al.* 2012).

Many important crops are C_3 plants (Matsuoka *et al.* 2001). C_4 plants are concerning biomass production and yield under certain conditions superior to C_3 plants. A direct comparison of rice and maize exhibited for the C_4 plant strikingly higher NUE, WUE and RUE figures. Therefore, it is not unreasonable to estimate a yield increase of 50 % by implementing C_4 photosynthesis in rice (Mitchell and Sheehy 2006, Sheehy *et al.* 2007). There were already some attempts to integrate a one-cell C_4 photosynthesis mechanism in C_3 plants, however, the outcomes were not convincing (Häusler *et al.* 2002, Hibberd and Covshoff 2010, Kajala *et al.* 2011). Consequently, a two-cell mechanism as established in most C_4 plants might be the better option. The implementation of C_4 photosynthesis is very ambitious. Yet there is the fact of the polyphyletic origin of C_4 photosynthesis. It was hypothesised that C_4 evolution – in genetic terms – must have been a quite facile process (Gowik and Westhoff 2011), a point supporting the idea of creating C_4 rice.

Beside the necessary changes in anatomy of rice leaves, genes required for the C_4 photosynthesis cycle have to be expressed specifically in the BS or M cells (Hibberd and Covshoff 2010, Peterhänsel 2011, Schuler *et al.* 2016). To achieve this, a diverse "toolbox" of gene regulatory modules specific for those cell types is necessary (Schuler *et al.* 2016).

2.2. Modules conferring BS- and M-specific gene expression on diverse regulatory levels

Transcriptome studies in maize have revealed that between 21 and 25 % of the genes are differentially expressed in M and BS cells (Chang *et al.* 2012, Li *et al.* 2010). Even the C_3 plant *Arabidopsis thaliana* exhibited differential expression: about 15 % of the total transcripts accumulated preferentially in BS cells (Aubry *et al.* 2014). These are quite high percentages and thus it seems surprising that the mechanisms of BS- and M-specific expression are not well understood (Hibberd and Covshoff 2010, Schuler *et al.* 2016).

Yet some regulatory modules have been extensively studied, like the mechanism that confers M-specific expression of the *ppcA1* gene of the C_4 species *Flaveria trinervia* (Figure 5). This gene encodes the PEPC isoform involved in C_4 photosynthesis. Assays with the *GUS* reporter gene exhibited that the region +2185 to +1 (relative to the translational start site) was sufficient to induce GUS accumulation in the M cells of the C_4 plant *Flaveria bidentis*. However, M-specific GUS expression could not be directed by the 5' region of the closely related C_3 counterpart *ppcA1* gene from *Flaveria pringlei* (Stockhaus et al. 1997). A deletion series of the *F. trinervia ppcA1* 5' region revealed two regions necessary for high M-specific expression: a more distal region of 575 bp (DR) responsible for M-specific expression and

repression of expression in the BS and a proximal region of 571 bp (PR) enabling basal activity. Further deletions of DR led to the discovery of a 41 bp element necessary for M-specific expression that was called Mesophyll expression module 1 (Mem1). A comparison with C_3, C_4-like and C_4 *Flaveria* species revealed a G to A transition and an insertion of the tetranucleotide CACT in C_4-like and C_4 species. It was further shown that both sub-modules are mandatory for M-specific expression. Interestingly, integration of both sub-modules in the *F. pringlei* promoter-reporter gene construct induced GUS accumulation specifically in the M. Conversely, deletion of the sub-modules in the *F. trinervia* promoter-reporter gene construct abolished M-specific expression. However, Mem1 was not able to direct M-specific expression in the phylogenetically more distant species Arabidopsis (Akyildiz *et al.* 2007, Gowik *et al.* 2004).

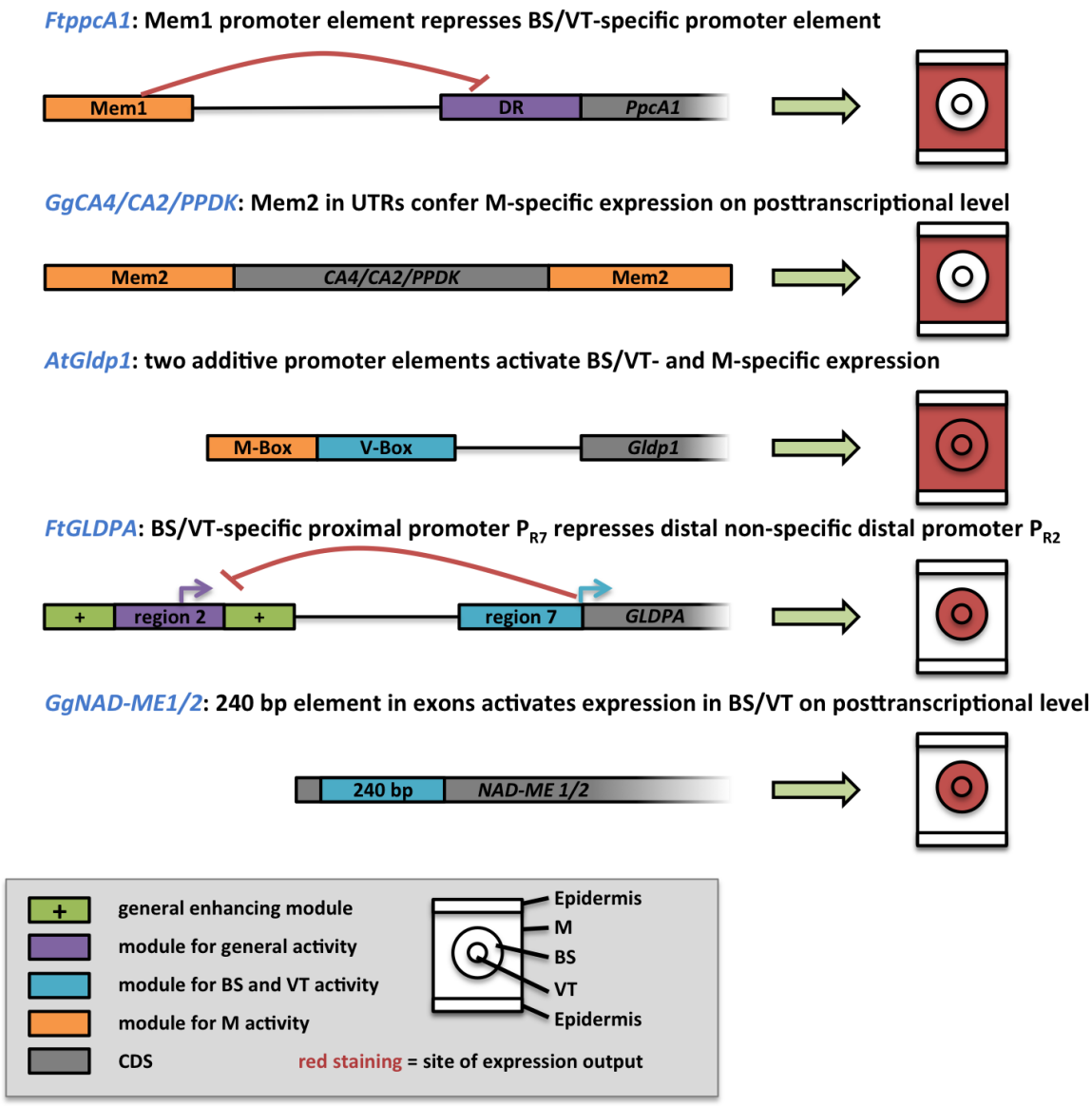

Figure 5: *Cis*-regulatory modules for cell-specific expression function in multiple ways
The simplified mechanisms of several *cis*-regulatory modules that promote cell-specific expression in leaves are shown on the left side. On the right hand side, the sites of the expression output (simplified leaf cross-section) are marked in red.
FtppcA1, *phosphoenolpyruvate carboxylase A1* of *Flaveria trinervia*; *GgCA4/CA2/PPDK*, *carbonic anhydrase 4/ carbonic anhydrase 2/pyruvate, phosphate dikinase* of *Gynandropsis gynandra*; *AtGldp1*, *glycine decarboxylase P-subunit 1* of *Arabidopsis thaliana*; *FtGLDPA*, *glycine decarboxylase P-subunit* of *Flaveria trinervia*; *GgNAD-ME1/2*, *NAD-malic enzyme1/2* of *Gyndandropsis gynandra*; M, mesophyll; BS, bundle sheath; VT, vascular tissue

In recent studies, another M-specific module has been identified (Figure 5). In combination with the 35S promoter of the cauliflower mosaic virus (CaMV35S), the 5' or 3' UTRs of the carbonic anhydrase gene *CA4* of the C_4 plant *Gynandropsis gynandra* or of the closely related *A. thaliana* were sufficient to drive accumulation of GUS in the M cells in *G. gynandra* (Kajala *et al.* 2012). Two sequences of 13 or seven nucleotides, respectively, both individually necessary for M-specific expression, were found via a deletion series of the

5' UTR of *G. gynandra*. By means of sequence analysis of 10 UTRs of *G. gynandra* and Arabidopsis *CA4*, *CA2* and *PPDK* genes, a conserved nine-nucleotide motif partly overlapping with the 13 nucleotides was detected. Three nucleotides of this motif were conserved among all analysed sequences. Site-directed mutagenesis of five nucleotides (containing the conserved ones) of the motif in either *G. gynandropis CA4* and *PPDK* 5' or 3' UTR abolished M-specific GUS accumulation in *G. gynandropsis*. Instead, GUS staining was observed in M and BS cells. Therefore, the motif was henceforward called Mem2. Mem2 functions – in contrast to Mem1 – posttranscriptionally as the endogenous *CA4* mRNAs accumulated to a higher level in the BS cells of *G. gynandra*. However, the exact mechanism of Mem2 remains unclear. It was proposed that Mem2 promotes translation in M cells or represses this process in BS cells. But interestingly, Mem2 is present in C_3 and C_4 species and in the UTRs of different enzyme genes. The latter evidence led to the suggestion that Mem2 regulates more genes (Williams *et al.* 2016).

A mechanism regulating at the transcriptional level was found for a gene encoding the P-subunit of glycine decarboxylase (*Gldp1*) of Arabidopsis (Figure 5). By means of deletion analysis of the 5' region fused to the *GUS* gene, two regions necessary for spatial expression of *Gldp1* were identified. The whole promoter directed expression of *GUS* in all leaf cell types. Deletion of −576 to −379 resulted in solely GUS-stained vascular tissue cells, thus this region was called M-Box. Further removal of −379 to −113 abolished visible *GUS* expression in the leaves. This region was accordingly named V-Box. Additional deletions pinned the M-Box down to 59 bp. This element was sufficient to generate M-specific expression when combined with a CaMV35S minimal promoter. The authors concluded that the M-Box functions as a tissue-specific "enhancer". It was also shown that the vasculature module conferred GUS expression not only in the vascular tissue but also in the BS (Adwy *et al.* 2015). Both modules are interesting as they are derived from a C_3 plant and are able to confer BS- and M-specific expression in this C_3 plant. These modules are most desirable for the establishment of C_4 photosynthesis in C_3 plants (Peterhänsel 2011).

A similar but more sophisticated mechanism was found for the regulation of the *GLDPA* gene from *F. trinervia* (Figure 5) that encodes the P-subunit of the glycine decarboxylase. The 5' region that was sufficient to drive *GUS* expression in the BS and vascular tissue of *F. bidentis* was dissected into seven sub-regions. Originally, it was thought that regions 1 and 2 work as a general enhancing element and 3 as a M-specific repressor of gene expression (Engelmann *et al.* 2008). However, further studies uncovered that two tandem promoters regulate *GLDPA* expression. The weak proximal promoter P_{R7} is active in the BS and vascular

tissue and is enhanced by regions 1 and 3. The strong distal promoter P_{R2} is also enhanced by regions 1 and 3 but promotes non-specific expression in leaves, thus being a general leaf promoter. Both promoters can work independently, however, when combined, P_{R7} probably serves as a roadblock and represses the activity of P_{R2}. Nonsense-mediated RNA-decay degrades most of the mRNAs derived from P_{R2} as they contain an unspliced intron. Intriguingly, the promoter regions had a very similar output when transformed in Arabidopsis (Wiludda *et al.* 2012). A subsequent study exhibited that the tandem promoter structure is conserved in the *GLDPA1/2* genes of *F. pringlei* and the *GLDPA* gene of *F. robusta*. Moreover, they were able to drive BS-specific or at least BS-preferential expression in *A. thaliana* and *F. bidentis*. This confirms that C_3 plants possess elements enabling expression restricted to the BS (Schulze *et al.* 2016).

The previously described mechanisms of cell-specific expression are based on promoter regions or UTRs. However, BS-specific expression can also be regulated posttranscriptionally by transcribed regions apart from UTRs (Figure 5). The exons of *G. gynandra NAD-ME1* and *2* under control of the CaMV35S promoter are sufficient to induce GUS-staining in the BS cells of the *G. gynandra*. A 3' deletion series of *NAD-ME1* led to the discovery of 240 bp located in the 5' region of the gene. This module has to be inserted in the transcribed region to promote cell-specific expression, arguing for a posttranscriptional mechanism. The module is present not only in *NAD-ME1* and *2* of *G. gynandra* but also in *NAD-ME* genes of *A. thaliana*. Interestingly, the Arabidopsis genes are not specifically expressed in the endogenous context but were able to drive GUS-accumulation in the BS when transformed in *G. gynandra*. Furthermore, similar modules from *NAD-ME* genes of maize and rice elicited BS-specific expression of *GUS*, proving the conserved function of these modules.

2.3. More modules for C_4 expression patterns are required

The compilation of examples for modules conferring BS- or M-specific gene expression shows that spatial expression is regulated on transcriptional or posttranscriptional levels or even on a combination of both levels. One example for epigenetic regulation is also known (Danker *et al.* 2008). Most of the identified regulatory mechanisms concerning BS- and M-specific expression have been reviewed by Hibberd and Covshoff (2010). Yet the number of regulatory modules so far found might be insufficient. Concerning implementation of C_4 photosynthesis in C_3 plants, it was proposed that at least 14 genes are necessary. Yet these genes only include core components of the C_4 cycle and key transporters (Covshoff and Hibberd 2012). A cluster analysis of transcriptomes of C_3, C_{3-4} and C_4 *Flaveria* species

exhibited 3582 transcripts showing C_4 expression patterns. However, the number of genes absolutely required for C_4 photosynthesis is unknown (Gowik *et al.* 2011) and might be somewhere between 14 and 3582. These numbers indicate that the toolbox containing regulatory modules for implementation of C_4 photosynthesis in rice or other C_3 plants has to be further filled. By means of a transcriptome study with de-etiolating maize and rice seedlings, numerous possible *cis*-regulatory elements related to C_4 photosynthesis were predicted. Still, the authors concluded that a further analysis of these motifs is required to prove their C_4 expression pattern (Xu *et al.* 2016). Consequently, one aim of this thesis is the identification and analysis of another *cis*-regulatory module that can be put in the toolbox

3. C_4 photosynthesis and temperature

3.1. C_4 crop plants are often susceptible to low temperatures

The C_4 photosynthesis pathway evolved in regions that can be characterised by high temperatures like arid tropics, subtropics and warm temperate zones (Sage 2004). Most C_4 species are generally found in these areas but are quite uncommon in chilly temperate or cold regions (Kubien and Sage 2003, Long 1983, Long and Spence 2013). The temperature optimum and range of photosynthesis reflect the origin of the species (Sage and Kubien 2007). Most C_4 plants fail to maintain their photosynthetic capacity at temperatures below 14 °C (Long and Spence 2013). A number of crops are C_4 plants and have a great economic importance as indicated by the worldwide production in the year 2014. Sugar cane and maize are with a yield of 1884.2 Mt or 1037.8 Mt, respectively, the most important crops. Also Sorghum is with a production of 68.9 Mt among the major crops (FAOSTAT 2017). To a certain degree, all these crops are susceptible to chilling. Sugarcane kept at 15 °C exhibited low chlorophyll a contents and a reduction of Hill reaction in contrast to the control plants grown at 27 °C (Ebrahim *et al.* 1998). The *Saccharum officinale* L. cultivar Badira, adapted to the subtropics, shows poor performance in response to chilling as well. Exposing the plants to 52 h chilling stress at 10 °C reduced the photosynthetic rate to a level of about 20 % (Du *et al.* 1999a). However, sugarcane has some potential for adaption as various hybrids perform well upon temperatures of 10 °C or below (Du *et al.* 1999a, Du *et al.* 1999b, Khan *et al.* 2013). Sorghum is usually drought tolerant since this crop evolved in warm regions where water is the limiting factor (Blum and Sullivan 1986). Conversely, Sorghum seedlings are strongly affected by chilling. Low temperature treatment resulted in development of necrosis during recovery. The duration and temperature of stress treatment were correlated with the growth

rate during recovery: longer periods and lower temperature resulted in reduced growth resumption. Eight days at 2 °C eventually led to permanent damage of Sorghum plants (Ercoli *et al.* 2004). Similar to Sorghum and sugarcane, maize has its origin in the tropics and subtropics (Greaves 1996). The optimum for growth of maize is 30-35 °C (Miedema 1982). Temperatures below 10-15 °C in combination with high light result in development of chlorosis (Greaves 1996, Miedema 1982). The light-saturated rate of CO_2 uptake (A_{sat}) can be decreased to a level of 17.6 % when warm grown seedlings are subjected to 14° C (Nie *et al.* 1992). Furthermore, maize seedlings suffer serious injuries (often beyond repair) at temperatures below 6 °C (Miedema 1982).

3.2. Chilling susceptibility in relation to photosynthetic enzymes

A number of C_4 crop plants are susceptible to chilling stress (Long and Spence 2013). But what are the reasons for the poor performance of C_4 plants at low temperatures? Several photosynthetic enzymes may contribute to the failure of C_4 plants in response to low temperatures (Long 1983, Long and Spence 2013, Yamori *et al.* 2014). Rubisco is not only the limiting factor in C_3 plants subjected to high temperatures but also in some cases in C_4 plants grown during chilling periods. A study using antisense constructs of *Rbc*S in *Flaveria bidentis* indicated that Rubisco nearly completely controls C_4 photosynthesis at low temperatures (Kubien *et al.* 2003). Also in the C_4 grass *Bouteloua gracilis*, Rubisco was found to be the rate-limiting factor for temperatures below 17 °C as the rate of CO_2 uptake (A) was CO_2-satured (Pittermann and Sage 2000). An increase of Rubisco content would overcome the problem, however, the C_4-specific restriction of this enzyme to the BS cells in C_4 plants prevents this solution (Dengler and Nelson 1999, Kubien *et al.* 2003, Pittermann and Sage 2000). Furthermore, a higher amount of Rubisco would diminish the C_4 plants' advantage of a high NUE (Pittermann and Sage 2000). A study about PPDKs, originated from *Flaveria* species of C_3, C_3-C_4 intermediate, C_4-like and C_4 photosynthetic types, revealed differential activities of this enzyme when tested at 0 °C. Curiously, the PPDK of the C_4-like species *F. brownii* was found to be cold tolerant (Burnell 1990) and cold tolerance is attributed to some residues in the C-terminus of the enzyme (Ohta *et al.* 1996). In a different study, the maize line A188 was transformed with the *F. brownii* PPDK cDNA and an antisense construct of the endogenous PPDK. The resulting PPDK heterotetramers exhibited a breakpoint temperature about 3 °C lower than the endogenous enzyme (Ohta *et al.* 2004). In maize, the PPDK protein and mRNA decreased to low levels when plants were shifted from 25 to 14 °C. Likewise,

V_{max} decreased more than 50 % and the authors suggested that the PPDK is crucial for continuation of C_4 photosynthesis in the cold (Wang *et al.* 2008b). Similar findings were made by Naidu *et al.* (2003), however, chilling treatment changed only the maize PPDK protein and not the mRNA level. In *Zoysia japonica*, a C_4 grass of the PEP-PCK subtype, PEP-PCK was the rate-limiting enzyme at cold temperatures and the probable cause for chilling sensitivity of this plant (Matsuba *et al.* 1997). However, it should be noted that the C_4 cycle is by now not considered to be per se the reason for susceptibility of C_4 plants to low temperatures. The true reason may be the warm origin of C_4 plants, resulting in neglected adaption to chilling conditions (Long and Spence 2013, Pearcy and Ehleringer 1984, Sage *et al.* 2015).

3.3. Low temperature tolerance of C_4 grasses

Interestingly, there are exceptions proving the rule (and by the way evidencing that the C_4 cycle is not the problem): a number of C_4 plants are found in cold climates. Some species avoid low temperature in these regions by growing in warm microsites. For instance, the C_4 grass *Muhlenbergia richardsonis* can grow in altitudes up to 3960 m in the White Mountains of California. Between 3500-3800 m, the grass preferentially grows on east-, south- and west-facing slopes and at higher altitudes on those facing the southeast. There, the plants are able to warm their leaves to 10 to 20 °C above air temperature, and those conditions favour C_4 photosynthesis (Sage and Sage 2002). Other species – like C_4 prairie grasses – evade the cold by restricting their growth to summer months.

However, there are also species actually facing the cold but that are able to maintain photosynthetic capacity. The probably most prominent member of these plants is the perennial grass hybrid *Miscanthus* x *giganteus* (*M* x *g*). Due to its high cellulose content and dry matter yield, *M* x *g* is an excellent crop for energy production (Lee and Kuan 2015, McKendry 2002), also in temperate climates (Beale and Long 1995). In a field study in Essex, *M* x *g* was exposed to chilling stress for one week. Yet, the maximum quantum efficiency (Φ) and the convexity of the light response curve (θ) were not reduced and not significantly different from the rates measured in the warmer June and July. A decrease of Φ and θ were only noticed in October but was possibly a result of natural leaf senescence at the end of the growing season (Beale *et al.* 1996). Several other studies demonstrated the superior chilling tolerance of *M* x *g* over maize. Both plants have the same temperature optimum but only *M* x *g* exhibited similar CO_2 uptake rates at 25/20 °C (day/night) and 14/11 °C (day/night). Conversely, maize plants exhibited an 80 % reduction of CO_2 uptake when grown at 14/11 °C (day/night) (Naidu *et al.*

2003). In a later study performed at the same conditions, maize displayed in all cases, when compared to *M* x *g*, stronger reductions in photosynthetic parameters, such as A_{sat}, the efficiency of CO_2 assimilation (Φ_{CO2}) and θ. The maintenance of CO_2 uptake and electron transport of *M* x *g* in adverse conditions provides an explanation of the high biomass production in the field (Naidu and Long 2004). A closer look at two whole growing seasons in the US corn belt revealed that *M* x *g* produced leaves earlier and maintained them longer than maize. *M* x *g* benefited from an average 59 % longer growth period and thus had a 61 % higher biomass yield (Dohleman and Long 2009).

The mechanisms of this extraordinary chilling tolerance are partly elucidated. On the one hand, at 10 °C, *M* x *g* strongly accumulated zeaxanthin and increased non-photochemical and photochemical quenching for the protection of photosystem II (Farage *et al.* 2006). On the other hand, *M* x *g* maintained or even upregulated the levels of photosynthetic enzymes in response to low temperatures. In contrast to maize, PEPC and LSU/Rubisco levels were quite stable and PPDK contents even increased in cold grown or cold treated plants, respectively (Naidu *et al.* 2003, Wang *et al.* 2008b). Interestingly, the Rubisco of *M* x *g* and maize displayed similar properties concerning sequence, activation energy and k_{cat} (Wang *et al.* 2008a), indicating an active and constant regulation of protein expression in *M* x *g*. PPDK also exhibited similar properties in maize and *M* x *g* and the authors concluded due to its upregulation that this enzyme is crucial for efficient C_4 photosynthesis under chilling conditions (Wang *et al.* 2008b). In a most recent study performed by Spence *et al.* (2014), young leaf samples of *M* x *g* grown for 14 days at 14 °C were compared to those grown at 25 °C by microarray. MapMan analysis revealed that the amounts for 30 transcripts related to the light reactions were significantly increased in the chilling treated plants and none of this category was decreased. Two genes encoding Rubisco activases exhibited enhanced expression as well. Therefore, *M* x *g* sustained A_{sat} and Φ_{CO2} at chilling by enhancing or maintaining levels of key photosynthetic proteins. An improved D1 repair was suggested to contribute to high Φ_{CO2} as a D1 protease gene, too, and *psbA* were upregulated in concert with zeaxanthin accumulation (Fryer *et al.* 1995, Spence *et al.* 2014).

M x *g* has a restricted frost tolerance (Friesen *et al.* 2015, Glowacka *et al.* 2015). But there are frost-adapted C_4 plants. The perennial grass *Spartina pectinata*, growing in high latitudes of North America, exhibits an improved frost tolerance in contrast to *M* x *g*. Two accessions of *S. pectinata* displayed temperatures corresponding to 50 % rhizome mortality (LT_{50}) of −23 to in all cases −14 °C (*M* x *g*: LT_{50} of −4 °C). Also the temperature related to 50 % electrolyte leakage (TEL_{50}) in leaves was with −9 to −10 °C improved in *S. pectinata* (*M* x *g*:

TEL_{50} of −5 °C). After a frosty night in spring, Φ_{CO2max} was about 50 % higher in *S. pectinata* as in *M* x *g* (Friesen *et al.* 2015*)*. The mechanism of this remarkable frost tolerance is not well characterised but a transcriptome study indicates a rapid signal reception and transduction in response to frost (Nah *et al.* 2016). The winter tolerance and high yields of biomass suggest an enormous potential of *S. pectinata* for cultivation in high latitudes (Potter *et al.* 1995, Sage *et al.* 2015).

These facts, together with the many other C_4 species reported to be cold tolerant (Sage *et al.* 2015), indicate that low temperature does not necessarily compromise performance of C_4 plants.

3.4. The need for chilling tolerant crops

Considering the rapidly increasing world population and their needs for nourishment and energy, cold tolerant C_4 species are required. In times of global warming, this approach seems strange. However, the climate change also affects the temperate and boreal regions, resulting in elongated growth seasons (Sage and Kubien 2007, Walther *et al.* 2002). These would favour cold-adapted species (Sage and Kubien 2007). Also in present times, C_4 crops with an improved performance upon chilling are required. In early spring, temperatures below 5 °C can occur in northern Europe, Canada and USA (Greaves 1996). These temperatures are below the minimum temperature of 6 to 8 °C required for germination and growth of leaves, shoots and roots of maize (Miedema 1982). Exposure of maize seedlings under this threshold results in chilling injuries or even in death (Greaves 1996, Miedema 1982). Therefore, early vigour is a major trait for maize breeders. In general, implementation of low temperature tolerance in maize was suggested to be as important as the realization of the C_4 cycle in rice (Long and Spence 2013). The direct comparison of maize and *M* x g, exhibiting superior biomass yield of the chilling tolerant *M* x *g* (Dohleman and Long 2009), supports this notion. To improve chilling tolerance of maize, a general understanding of responses to chilling is necessary. Hence, the second aim of this thesis is the analysis of chilling response of maize by means of transcriptome. Furthermore, the base of chilling tolerance of a maize near isogenic line (NIL) should be examined.

II. Scientific Aims

The thesis consists of two different sub-projects analysing BS-specific gene expression in Arabidopsis and chilling response of maize.

(1) *BS-specific expression mechanism of the Arabidopsis* SULTR2;2 *promoter*. The model organism *Arabidopsis thaliana*, a C_3 plant, possesses a BS. This indicates that the BS is an ancient invention in terms of evolution and occurs in C_3 and C_4 plants. However, the role of the BS in C_3 plants – in contrast to C_4 plants – is poorly explored. It was suggested that the C_3 BS is involved in regulation of metabolic flux. The promoter of the low-affinity sulphate transporter *AtSULTR2;2* from *A. thaliana* promotes BS-specific gene expression in the same plant. To gain insight into the mechanisms of BS-specific gene expression, the 5' region of *AtSULTR2;2* was analysed in detail. In order to accomplish this goal, two approaches were chosen. Firstly, promoter-reporter gene constructs were designed, transformed in Arabidopsis and analysed. Secondly, bioinformatics were applied. Studying the conservation of BS-specific gene expression amongst distantly related species was achieved by transformation of *Flaveria bidentis* with the full-length *AtSULTR2;2* promoter from Arabidopsis fused with a reporter gene and subsequent analysis of the resulting transgenic plants (Manuscript 1).

(2) *Low temperature-regulated gene expression and chilling tolerance of maize.* A QTL for fresh matter yield, QTL4, has been identified previously and explains 33.7 % of the phenotypic variance. Initially, the QTL comprised more than half of chromosome 4 but was reduced to a short segment containing only the *SAUR31* gene. Maize plants containing the positive allele of the QTL4 show an improved early vigour and are chilling tolerant. For future breeding, it is important to understand the molecular answers of maize seedlings in response to chilling and the nature of chilling tolerance. To achieve these aims, RNA-seq was employed with aerial parts and root tissue of maize lines exhibiting contrasting chilling susceptibility. The obtained sequencing data provided a deep insight in the processes affected by low temperature and the nature of QTL4 (Manuscript 2).

III.A Summary

The thesis comprises two thematically different sub-projects.

C_4 plants locate the necessary enzymes for the photosynthetic cycle in two different compartments, the bundle sheath and the mesophyll. Analyses of the associated genes revealed control for spatial gene expression at the transcriptional, posttranscriptional and even posttranslational level. Implementing the C_4 cycle in C_3 plants requires understanding of mechanisms conferring BS- and M-specific expression as well as a "toolbox" of respective modules.

In the first sub-project, the promoter of the *Arabidopsis thaliana SULTR2;2* gene was analysed to reveal *cis*-regulatory elements generating BS-specific expression by means of deletion analyses of promoter-reporter gene constructs. 5' deletions led to the discovery of a 741 bp region for specific expression. Further 3' deletions shortened the region to a 350 bp core module that is absolutely necessary for moderate BS-specific expression. A quantitative module located 5' of the core module was also identified. This module enhances the activity of the core module in the natural context of the promoter and is able to raise the activity of a heterologous minimal promoter. In total, BS-specific expression of *AtSULTR2;2* is regulated transcriptionally and driven by a 350 bp core region surrounded by a negligible region conferring robustness to expression. Furthermore, conservation of *trans*-regulatory factors for BS-specific expression over the border of asterids and rosids was implied as the *AtSULTR2;2* promoter was able to direct BS-specific gene expression in *Flaveria bidentis*.

Maize has its origin in tropical and subtropical regions but is by now cultivated in more temperate regions. There, yields might be limited by low temperature in the early growth season. Obtaining a greater knowledge of chilling response and basis of chilling tolerance of maize might help breeders to generate chilling tolerant maize lines.

In the second sub-project, the chilling answer of maize with respect to a quantitative trait locus for fresh matter yield and chilling tolerance was analysed. This was achieved by a transcriptome experiment analysing aerial organs and roots before and during chilling. Chilling stress quickly induced differential gene expression in the double haploid and chilling sensitive line SL. These transcripts largely included those related to phytohormone regulation, expression regulation, reactive oxygen species scavenging and signal transduction. The quality indicates that SL actively pauses growth during unfavourable conditions. The output can be seen in field and growth chamber experiments. Perturbations of photosynthesis and the

circadian clock were implied. A comparison of the tolerant and the sensitive near isogenic lines N4-8X-tol and N4-8X-sen hinted preconditioning of N4-8X-tol for chilling tolerance at favourable temperatures. Additionally, it seemed that the tolerant NIL prepared for rapid growth resumption during chilling. Furthermore, differential expression was verified for the candidate gene *ke-1*.

III.B Zusammenfassung

Die Arbeit ist in zwei thematisch unterschiedliche Teilprojekte unterteilt.

C_4 Pflanzen haben die für den Photosynthesezyklus benötigten Enyzme in zwei verschiedene Kompartimente, der Bündelscheide und dem Mesophyll, aufgeteilt. Analysen der zugehörigen Gene zeigten, dass die räumliche Expression auf transkriptioneller, posttranskriptioneller und sogar posttranslationaler Ebene reguliert werden kann. Der Einbau des C_4 Zyklus in C_3 Pflanzen bedarf der Kenntnis von Mechanismen, die bündelscheiden- und mesophyllspezifische Expression bedingen sowie ein Repertoire der entsprechenden Module.

Im ersten Teilprojekt wurde der Promoter des *SULTR2;2* Gens aus *Arabidopsis thaliana* mittels Deletionsanalyse von Promoter-Reportergen Konstrukten auf *cis*-regulatorische Elemente für bündelscheidenspezifische Expression untersucht. Durch 5' Deletionen konnte eine 741 bp lange Region für spezifische Expression abgegrenzt werden. Weitere 3' Deletionen verkürzten diese Region zu einem 350 bp langen Kernmodul, das zwingend für moderate bündelscheidenspezifische Expression erforderlich ist. Ein quantitatives Modul, das 5' vor dem Kernmodul liegt, konnte identifiziert werden. Dieses Modul steigert im natürlichen Kontext des Promoters die Aktivität des Kernmoduls und kann die Aktivität eines heterologen Minimialpromotors potenzieren. Zusammenfassend kann gesagt werden, dass die bündelscheidenspezifische Expression von *AtSULTR2;*2 auf der Transkriptionsebene reguliert wird. Die Regulation erfolgt durch eine 350 bp lange Kernregion, umgeben von einer nicht zwingend notwendigen, aber Robustheit verleihenden Region. Zudem wurde gezeigt, dass der *AtSULTR2;2* Promoter auch in *Flaveria bidentis* bündelscheidenspezifische Expression initiieren kann. Daraus wurde gefolgert, dass die nötigen *trans*-regulatorischen Faktoren über die Grenze der Asteriden und Rosiden hinaus konserviert sind.

Mais hat seinen Ursprung in tropischen und subtropischen Regionen, wird aber mittlerweile auch in gemäßigteren Regionen kultiviert. Dort kann die Ernte aufgrund von geringen Temperaturen geschmälert werden. Ein größeres Verständnis über die Reaktion von Mais auf Kühle sowie über die Basis von Kühletoleranz kann dem Züchter helfen, kühletolerante Pflanzen zu generieren.

Im zweiten Teilprojekt wurde die Reaktion von Mais auf Kühle mit Bezug auf einen Quantitative Trait Locus für Frischmasseertrag analysiert. Dies wurde mittels eines Transkriptomexperiments, bei dem oberirdische Organe sowie Wurzeln untersucht wurden, erreicht. Kühlestress induzierte schnell differenzielle Genexpression in der doppelhaploiden

und kühlesensitiven Linie SL. Diese Transkripte umfassten oft solche, die mit Phytohormonen, Regulation von Expression, Bereinigung von reaktiven Sauerstoffspezies und Signaltransduktion assoziiert sind. Die Qualität dieser deutete darauf hin, dass SL während der ungünstigen Zeit aktiv das Wachstum einstellte. Dies kann tatsächlich in Feld- oder in Klimakammer-Experimenten beobachtet werden. Störungen der Photosynthese und der circadianen Uhr wurden angedeutet. Bei dem Vergleich der toleranten nahe isogenen Linie N4-8X-tol und der sensitiven nahe isogenen Linie N4-8X-sen wurde angedeutet, dass die tolerante NIL schon bei günstigen Temperaturen die entsprechende Voraussetzung für Kühletoleranz aufweist. Außerdem schien N4-8X-tol sich während der Kälte auf eine schnelle Wiederaufnahme des Wachstums vorzubereiten. Ferner wurde für das Kühletoleranz-Kandidatengen *ke-1* differenzielle Expression nachgewiesen.

IV. Literature

Adwy, W., Laxa, M. and Peterhansel, C. (2015) A simple mechanism for the establishment of C(2)-specific gene expression in Brassicaceae. *Plant J*, **84**, 1231-1238.

Akhani, H., Barroca, J., Koteeva, N., Voznesenskaya, E.V., Franceschi, V.R., Edwards, G.E., Ghaffari, S.M., Ziegler, H. and Lammers, T.G. (2005) Bienertia sinuspersici (Chenopodiaceae): A New Species from Southwest Asia and Discovery of a Third Terrestrial C4 Plant Without Kranz Anatomy. *Syst Bot*, **30**, 290-301.

Akyildiz, M., Gowik, U., Engelmann, S., Koczor, M., Streubel, M. and Westhoff, P. (2007) Evolution and Function of a cis-Regulatory Module for Mesophyll-Specific Gene Expression in the C4 Dicot Flaveria trinervia. *Plant Cell*, **19**, 3391-3402.

Andersson, I. (2008) Catalysis and regulation in Rubisco. *J Exp Bot*, **59**, 1555-1568.

Andrews, T.J. and Lorimer, G.H. (1987) Rubisco: structure, mechanisms, and prospects for improvement. *Hatch MD, Boardman NK (eds) The biochemistry of plants, Vol. 10. Academic Press, New York, NY, USA*, 131-218.

Andrews, T.J., Lorimer, G.H. and Tolbert, N.E. (1973) Ribulose diphosphate oxygenase. I. Synthesis of phosphoglycolate by fraction-1 protein of leaves. *Biochemistry*, **12**, 11-18.

Aubry, S., Kelly, S., Kumpers, B.M., Smith-Unna, R.D. and Hibberd, J.M. (2014) Deep evolutionary comparison of gene expression identifies parallel recruitment of trans-factors in two independent origins of C4 photosynthesis. *PLoS Genet*, **10**, e1004365.

Bauwe, H. (1984) Photosynthetic enzyme activities and immunofluorescence studies on the localization of ribulose-1,5-bisphosphate carboxylase/oxygenase in leaves of C3, C4, and C3−C4 intermediate species of Flaveria (Asteraceae). *Biochem Physiol Pflanz*, **179**, 253-268.

Beadle, C.L. and Long, S.P. (1985) Photosynthesis — is it limiting to biomass production? *Biomass*, **8**, 119-168.

Beale, C.V., Bint, D.A. and Long, S.P. (1996) Leaf photosynthesis in the C4-grass Miscanthus x giganteus, growing in the cool temperate climate of southern England. *J Exp Bot*, **47**, 267-273.

Beale, C.V. and Long, S.P. (1995) Can perennial C4 grasses attain high efficiencies of radiant energy conversion in cool climates? *Plant Cell Environ*, **18**, 641-650.

Blasing, O.E., Westhoff, P. and Svensson, P. (2000) Evolution of C4 phosphoenolpyruvate carboxylase in Flaveria, a conserved serine residue in the carboxyl-terminal part of the enzyme is a major determinant for C4-specific characteristics. *J Biol Chem*, **275**, 27917-27923.

Blum, A. and Sullivan, C.Y. (1986) The Comparative Drought Resistance of Landraces of Sorghum and Millet From Dry and Humid Regions*. *Ann Bot*, **57**, 835-846.

Bond, W.J. (2008) What Limits Trees in C4 Grasslands and Savannas? *Annu Rev Ecol Evol Sys*, **39**, 641-659.

Brown, R.H. (1985) Growth of C3 and C4 Grasses Under Low N Levels. *Crop Sci*, **25**, 954-957.

Brown, R.H. (1999) Agronomic Implications of C4 Photosynthesis. *In C4 Plant Biology, ed. R. F. Sage, R. K. Monson, San Diego: Academic*, 473-507.

Buick, R. (2008) When did oxygenic photosynthesis evolve? *Philosophical transactions of the Royal Society of London. Series B, Biological sciences*, **363**, 2731-2743.

Burnell, J.N. (1990) A Comparative Study of the Cold-Sensitivity of Pyruvate,Pi Dikinase in Flaveria Species. *Plant Cell Physiol*, **31**, 295-297.

Calvin, M. and Benson, A.A. (1948) The Path of Carbon in Photosynthesis. *Science*, **107**, 476-480.

Carmo-Silva, E., Scales, J.C., Madgwick, P.J. and Parry, M.A. (2015) Optimizing Rubisco and its regulation for greater resource use efficiency. *Plant Cell Environ*, **38**, 1817-1832.

Cerling, T.E., Ehleringer, J.R. and Harrism J. M (1998) Carbon dioxide starvation, the development of C4 ecosystems, and mammalian evolution. *Phil Trans R Soc Lond B*, **353**, 159-171.

Cerling, T.E., Mbua, E., Kirera, F.M., Manthi, F.K., Grine, F.E., Leakey, M.G., Sponheimer, M. and Uno, K.T. (2011) Diet of Paranthropus boisei in the early Pleistocene of East Africa. *Proc Natl Acad Sci U S A*, **108**, 9337-9341.

Chang, Y.M., Liu, W.Y., Shih, A.C., Shen, M.N., Lu, C.H., Lu, M.Y., Yang, H.W., Wang, T.Y., Chen, S.C., Chen, S.M., Li, W.H. and Ku, M.S. (2012) Characterizing regulatory and functional differentiation between maize mesophyll and bundle sheath cells by transcriptomic analysis. *Plant Physiol*, **160**, 165-177.

Christin, P.A., Besnard, G., Samaritani, E., Duvall, M.R., Hodkinson, T.R., Savolainen, V. and Salamin, N. (2008) Oligocene CO2 decline promoted C4 photosynthesis in grasses. *Curr Biol*, **18**, 37-43.

Christin, P.A., Osborne, C.P., Sage, R.F., Arakaki, M. and Edwards, E.J. (2011) C4 eudicots are not younger than C4 monocots. *J Exp Bot*, **62**, 3171-3181.

Covshoff, S. and Hibberd, J.M. (2012) Integrating C4 photosynthesis into C3 crops to increase yield potential. *Curr Opin Biotech*, **23**, 209-214.

Danker, T., Dreesen, B., Offermann, S., Horst, I. and Peterhänsel, C. (2008) Developmental information but not promoter activity controls the methylation state of histone H3 lysine 4 on two photosynthetic genes in maize. *Plant J*, **53**, 465-474.

Dengler, N.G. and Nelson, T. (1999) Leaf Structure and Development in C 4 Plants. *C4 Plant Biology*, 133-172.

Dohleman, F.G. and Long, S.P. (2009) More productive than maize in the Midwest: How does Miscanthus do it? *Plant Physiol*, **150**, 2104-2115.

Downes, R.W. (1969) Differences in transpiration rates between tropical and temperate grasses under controlled conditions. *Planta*, **88**, 261-273.

Du, Y.C., Nose, A. and Wasano, K. (1999a) Effects of chilling temperature on photosynthetic rates, photosynthetic enzyme activities and metabolite levels in leaves of three sugarcane species. *Plant Cell Environ*, **22**, 317-324.

Du, Y.C., Nose, A. and Wasano, K. (1999b) Thermal Characteristics of C4 Photosynthetic Enzymes from Leaves of Three Sugarcane Species Differing in Cold Sensitivity. *Plant Cell Physiol*, **40**, 298-304.

Ebrahim, M.K.H., Vogg, G., Osman, M.N.E.H. and Komor, E. (1998) Photosynthetic performance and adaptation of sugarcane at suboptimal temperatures. *J Plant Physiol*, **153**, 587-592.

Edwards, E.J., Osborne, C.P., Stromberg, C.A., Smith, S.A., Bond, W.J., Christin, P.A., Cousins, A.B., Duvall, M.R., Fox, D.L., Freckleton, R.P., Ghannoum, O., Hartwell, J., Huang, Y., Janis, C.M., Keeley, J.E., Kellogg, E.A., Knapp, A.K., Leakey, A.D., Nelson, D.M., Saarela, J.M., Sage, R.F., Sala, O.E., Salamin, N., Still, C.J. and Tipple, B. (2010) The origins of C4 grasslands: integrating evolutionary and ecosystem science. *Science*, **328**, 587-591.

Ehleringer, J. and Pearcy, R.W. (1983) Variation in Quantum Yield for CO2 Uptake among C3 and C4 Plants. *Plant Physiol*, **73**, 555-559.

Ehleringer, J.R. and Monson, R.K. (1993) Evolutionary and Ecological Aspects of Photosynthetic Pathway Variation. *Annu Rev Ecol Syst*, **24**, 411-439.

Ehleringer, J.R., Sage, R.F., Flanagan, L.B. and Pearcy, R.W. (1991) Climate change and the evolution of C4 photosynthesis. *Trends Ecol Evol*, **6**, 95-99.

Ellis, R.J. (1979) The most abundant protein in the world. *Trends Biochem Sci*, **4**, 241-244.

Emms, D.M., Covshoff, S., Hibberd, J.M. and Kelly, S. (2016) Independent and Parallel Evolution of New Genes by Gene Duplication in Two Origins of C4 Photosynthesis Provides New Insight into the Mechanism of Phloem Loading in C4 Species. *Mol Biol Evol*, **33**, 1796-1806.

Engelmann, S., Bläsing, O.E., Gowik, U., Svensson, P. and Westhoff, P. (2003) Molecular evolution of C4 phosphoenolpyruvate carboxylase in the genus Flaveria--a gradual increase from C3 to C4 characteristics. *Planta*, **217**, 717-725.

Engelmann, S., Bläsing, O.E., Westhoff, P. and Svensson, P. (2002) Serine 774 and amino acids 296 to 437 comprise the major C4 determinants of the C4 phosphoenolpyruvate carboxylase of Flaveria trinervia. *FEBS Lett*, **524**, 11-14.

Engelmann, S., Wiludda, C., Burscheidt, J., Gowik, U., Schlue, U., Koczor, M., Streubel, M., Cossu, R., Bauwe, H. and Westhoff, P. (2008) The gene for the P-subunit of glycine decarboxylase from the C4 species Flaveria trinervia: analysis of transcriptional control in transgenic Flaveria bidentis (C4) and Arabidopsis (C3). *Plant Physiol*, **146**, 1773-1785.

Ercoli, L., Mariotti, M., Masoni, A. and Arduini, I. (2004) Growth responses of Sorghum plants to chilling temperature and duration of exposure. *Eur J Agron*, **21**, 93-103.

FAO (2015) FAO Statistical Pocketbook World food and agriculture 2015. *Food and Agriculture Organization of the United Nations, Rome, 2015, ISBN 978-92-5-108802-9*.

FAOSTAT (2017) *FAOSTAT. Rome: Food and Agriculture Organization of the United Nations* http://www.fao.org/faostat/ *(accessed 13 February 2017)*.

Farage, P.K., Blowers, D., Long, S.P. and Baker, N.R. (2006) Low growth temperatures modify the efficiency of light use by photosystem II for CO2 assimilation in leaves of two chilling-tolerant C4 species, Cyperus longus L. and Miscanthus x giganteus. *Plant Cell Environ*, **29**, 720-728.

Farquhar, G.D. and Sharkey, T.D. (1982) Stomatal Conductance and Photosynthesis. *Ann Rev Plant Physiol*, **33**, 317-345.

Field, C.B., Behrenfeld, M.J., Randerson, J.T. and Falkowski, P. (1998) Primary production of the biosphere: integrating terrestrial and oceanic components. *Science*, **281**, 237-240.

Friesen, P.C., Peixoto Mde, M., Lee, D.K. and Sage, R.F. (2015) Sub-zero cold tolerance of Spartina pectinata (prairie cordgrass) and Miscanthus x giganteus: candidate bioenergy crops for cool temperate climates. *J Exp Bot*, **66**, 4403-4413.

Fryer, M.J., Oxborough, K., Martin, B., Ort, D.R. and Baker, N.R. (1995) Factors Associated with Depression of Photosynthetic Quantum Efficiency in Maize at Low Growth Temperature. *Plant Physiol*, **108**, 761-767.

Furbank, R.T. (2011) Evolution of the C4 photosynthetic mechanism: are there really three C4 acid decarboxylation types? *J Exp Bot*, **62**, 9.

Furbank, R.T. and Hatch, M.D. (1987) Mechanism of C4 photosynthesis: the size and composition of the inorganic carbon pool in bundle sheath cells. *Plant Physiol*, **85**, 958-964.

Galmés, J., Flexas, J., Keys, A.J., Cifre, J., Mitchell, R.A.C., Madgwick, P.J., Haslam, R.P., Medrano, H. and Parry, M.A.J. (2005) Rubisco specificity factor tends to be larger in plant species from drier habitats and in species with persistent leaves. *Plant Cell Environ*, **28**, 571-579.

Ghannoum, O., Evans, J.R., Chow, W.S., Andrews, T.J., Conroy, J.P. and von Caemmerer, S. (2005) Faster Rubisco is the key to superior nitrogen-use efficiency in NADP-malic enzyme relative to NAD-malic enzyme C4 grasses. *Plant Physiol*, **137**, 638-650.

Ghannoum, O., Evans, J.R. and von Caemmerer, S. (2011) Nitrogen and Water Use Efficiency of C4 Plants. *In C4 Photosynthesis and Related CO2 Concentration Mechanisms, ed. A. S. Raghavendra, R. F. Sage, Springer Netherlands*, **32**, 129-146.

Gillies, S.D., Morrison, S.L., Oi, V.T. and Tonegawa, S. (1983) A Tissue-specific Transcription Enhancer Element Is Located in the Major lntron of a Rearranged lmmunoglobulin Heavy Chain Gene. *Cell*, **33**, 717-728.

Glowacka, K., Jorgensen, U., Kjeldsen, J.B., Korup, K., Spitz, I., Sacks, E.J. and Long, S.P. (2015) Can the exceptional chilling tolerance of C4 photosynthesis found in Miscanthus x giganteus be exceeded? Screening of a novel Miscanthus Japanese germplasm collection. *Ann Bot*, **115**, 981-990.

Gowik, U., Bräutigam, A., Weber, K.L., Weber, A.P.M. and Westhoff, P. (2011) Evolution of C4 Photosynthesis in the Genus Flaveria: How Many and Which Genes Does It Take to Make C4? *Plant Cell*, **23**, 2087-2105.

Gowik, U., Burscheidt, J., Akyildiz, M., Schlue, U., Koczor, M., Streubel, M. and Westhoff, P. (2004) cis-Regulatory elements for mesophyll-specific gene expression in the C4 plant Flaveria trinervia, the promoter of the C4 phosphoenolpyruvate carboxylase gene. *Plant Cell*, **16**, 1077-1090.

Gowik, U. and Westhoff, P. (2011) The Path from C3 to C4 Photosynthesis. *Plant Physiol*, **155**, 56-63.

Grass Phylogeny Working Group II. (2012) New grass phylogeny resolves deep evolutionary relationships and discovers C4 origins. *New Phytol*, **193**, 304-312.

Greaves, J.A. (1996) Improving suboptimal temperature tolerance in maize— the search for variation. *J Exp Bot*, **47**, 307-323.

Haberlandt, G. (1881) Vergleichende Anatomie des assimilatorischen Gewebesystems bei Pflanzen. . *Jahrbuch der Wissenschaftlichen Botanik* **13**, 74-188.

Hatch, M.D. (1987) C4 photosynthesis: a unique blend of modified biochemistry, anatomy and ultrastructure. *Biochim Biophys Acta, ER. Reviews on bioenergetics*, **895**, 81-106.

Hatch, M.D., Kagawa, T. and Craig, S. (1975) Subdivision of C4-pathway species based on differing C4 decarboxylating systems and ultrastructural features. *Aust J Plant Physiol*, **2**, 111-128.

Häusler, R.E., Hirsch, H.J., Kreuzaler, F. and Peterhansel, C. (2002) Overexpression of C4-cycle enzymes in transgenic C3 plants: a biotechnological approach to improve C3-photosynthesis. *J Exp Bot*, **53**, 591-607.

Heckathorn, S.A., McNaughton, S.J. and Coleman, J.S. (1999) C4 Plants and Herbivory. *In C4 Plant Biology, ed. R. F. Sage, R. K. Monson, San Diego: Academic*, 285-312.

Hibberd, J.M. and Covshoff, S. (2010) The regulation of gene expression required for C4 photosynthesis. *Annu Rev Plant Biol*, **61**, 181-207.

Hibberd, J.M., Sheehy, J.E. and Langdale, J.A. (2008) Using C4 photosynthesis to increase the yield of rice-rationale and feasibility. *Curr Opin Plant Biol*, **11**, 228-231.

Jordan, D.B. and Ogren, W.L. (1984) The CO2/O 2 specificity of ribulose 1,5-bisphosphate carboxylase/oxygenase : Dependence on ribulosebisphosphate concentration, pH and temperature. *Planta*, **161**, 308-313.

Kajala, K., Brown, N.J., Williams, B.P., Borrill, P., Taylor, L.E. and Hibberd, J.M. (2012) Multiple Arabidopsis genes primed for recruitment into C4 photosynthesis. *Plant J*, **69**, 47-56.

Kajala, K., Covshoff, S., Karki, S., Woodfield, H., Tolley, B.J., Dionora, M.J.A., Mogul, R.T., Mabilangan, A.E., Danila, F.R., Hibberd, J.M. and Quick, W.P. (2011) Strategies for engineering a two-celled C4 photosynthetic pathway into rice. *J Exp Bot*, **62**, 3001-3010.

Kanai, R. and Edwards, G.E. (1999) The Biochemistry of C4 Photosynthesis. *In C4 Plant Biology, ed. R. F. Sage, R. K. Monson, San Diego: Academic*, 49-87.

Kellogg, E.A. (1999) Phylogenetic Aspects of the Evolution of C4 Photosynthesis. *In C4 Plant Biology, ed. R. F. Sage, R. K. Monson, San Diego: Academic*, 411-444.

Khan, N.A., Bedre, R., Parco, A., Bernaola, L., Hale, A., Kimbeng, C., Pontif, M. and Baisakh, N. (2013) Identification of cold-responsive genes in energycane for their use in genetic diversity analysis and future functional marker development. *Plant Sci*, **211**, 122-131.

Kim, K. and Portis, A.R., Jr. (2004) Oxygen-dependent H2O2 production by Rubisco. *FEBS Lett*, **571**, 124-128.

Kinsman, E.A. and Pyke, K.A. (1998) Bundle sheath cells and cell-specific plastid development in Arabidopsis leaves. *Development*, **125**, 1815-1822.

Kocacinar, F. (2015) Photosynthetic, hydraulic and biomass properties in closely related C3 and C4 species. *Physiol Plant*, **153**, 454-466.

Kocacinar, F., McKown, A.D., Sage, T.L. and Sage, R.F. (2008) Photosynthetic pathway influences xylem structure and function in Flaveria (Asteraceae). *Plant Cell Environ*, **31**, 1363-1376.

Kocacinar, F. and Sage, R.F. (2003) Photosynthetic pathway alters xylem structure and hydraulic function in herbaceous plants. *Plant Cell Environ*, **26**, 2015-2026.

Kraiser, T., Gras, D.E., Gutierrez, A.G., Gonzalez, B. and Gutierrez, R.A. (2011) A holistic view of nitrogen acquisition in plants. *J Exp Bot*, **62**, 1455-1466.

Ku, M.S., Wu, J., Dai, Z., Scott, R.A., Chu, C. and Edwards, G.E. (1991) Photosynthetic and photorespiratory characteristics of Flaveria species. *Plant Physiol*, **96**, 518-528.

Ku, S.B. and Edwards, G.E. (1977) Oxygen Inhibition of Photosynthesis: I. Temperature Dependence and Relation to O2/CO2 Solubility Ratio. *Plant Physiol*, **59**, 986-990.

Ku, S.B. and Edwards, G.E. (1978) Oxygen inhibition of photosynthesis : III. Temperature dependence of quantum yield and its relation to O2/CO 2 solubility ratio. *Planta*, **140**, 1-6.

Kubien, D.S. and Sage, R.F. (2003) C4 grasses in boreal fens: their occurrence in relation to microsite characteristics. *Oecologia*, **137**, 330-337.

Kubien, D.S., von Caemmerer, S., Furbank, R.T. and Sage, R.F. (2003) C4 photosynthesis at low temperature. A study using transgenic plants with reduced amounts of Rubisco. *Plant Physiol*, **132**, 1577-1585.

Lee, W.C. and Kuan, W.C. (2015) Miscanthus as cellulosic biomass for bioethanol production. *Biotechnol J*, **10**, 840-854.

Li, P., Ponnala, L., Gandotra, N., Wang, L., Si, Y., Tausta, S.L., Kebrom, T.H., Provart, N., Patel, R., Myers, C.R., Reidel, E.J., Turgeon, R., Liu, P., Sun, Q., Nelson, T. and Brutnell, T.P. (2010) The developmental dynamics of the maize leaf transcriptome. *Nat Genet*, **42**, 1060-1067.

Long, S.P. (1983) C4 photosynthesis at low temperatures. *Plant Cell Environ*, **6**, 345-363.

Long, S.P. (1999) Environmental responses. *In C4 Plant Biology, ed. R. F. Sage, R. K. Monson, San Diego: Academic*, 215-249.

Long, S.P. and Spence, A.K. (2013) Toward cool C4 crops. *Annu Rev Plant Biol*, **64**, 701-722.

Lorimer, G.H. (1981) The carboxylation and oxygenation of ribulose 1,5-bisphosphate: the primary events in photosynthesis and photorespiration. *Ann Rev Plant Physiol*, **32**, 349-383.

Ludlow, M.M. (1981) Effect of temperature on light utilization efficiency of leaves in C3 legumes and C 4 grasses. *Photosynth Res*, **1**, 243-249.

Mallmann, J., Heckmann, D., Brautigam, A., Lercher, M.J., Weber, A.P., Westhoff, P. and Gowik, U. (2014) The role of photorespiration during the evolution of C4 photosynthesis in the genus Flaveria. *eLife*, **3**, e02478.

Marshall, D.M., Muhaidat, R., Brown, N.J., Liu, Z., Stanley, S., Griffiths, H., Sage, R.F. and Hibberd, J.M. (2007) Cleome, a genus closely related to Arabidopsis, contains species spanning a developmental progression from C3 to C4 photosynthesis. *Plant J*, **51**, 886-896.

Matsuba, K., Imaizumi, N., Kaneko, S., Samejima, M. and Ohsugi, R. (1997) Photosynthetic responses to temperature of phosphoenolpyruvate carboxykinase type C4 species differing in cold sensitivity. *Plant Cell Environ*, **20**, 268-274.

Matsuoka, M., Furbank, R.T., Fukayama, H. and Miyao, M. (2001) MOLECULAR ENGINEERING OF C4 PHOTOSYNTHESIS. *Annu Rev Plant Physiol Plant Mol Biol*, **52**, 297-314.

McKendry, P. (2002) Energy production from biomass (Part 1): Overview of biomass. *Bioresour Technol*, **83**, 37-46.

McKown, A.D. and Dengler, N.G. (2007) Key innovations in the evolution of Kranz anatomy and C4 vein pattern in Flaveria (Asteraceae). *Am J Bot*, **94**, 382-399.

McKown, A.D., Moncalvo, J.M. and Dengler, N.G. (2005) Phylogeny of Flaveria (Asteraceae) and inference of C4 photosynthesis evolution. *Am J Bot*, **92**, 1911-1928.

Miedema, P. (1982) The effects of low temperature on Zea mays. *Adv Agron*, **35**, 93-128.

Miflin, B. (2000) Crop improvement in the 21st century. *J Exp Bot*, **51**, 1-8.

Mitchell, P.L. and Sheehy, J.E. (2006) Supercharging rice photosynthesis to increase yield. *New Phytol*, **171**, 688-693.

Mitchell, P.L. and Sheehy, J.E. (2007) The case for C4 rice. *In: Sheey, J. E., Mitchell, P. L., Hardy, B., editors. Charting new pathways to C4 rice. Los Baños (Phillipines): International Rice Research Institute*, 27-36.

Mitchell, P.L., Sheehy, J.E. and Woodward, F.I. (1998) Potential yields and the efficiency of radiation use in rice. *Discussion Paper No. 32. Manila (Philippines): International Rice Research Institute*.

Monson, R.K. (1999) The Origins of C4 Genes and Evolutionary Pattern in the C4 Metabolic Phenotype. *In C4 Plant Biology, ed. R. F. Sage, R. K. Monson, San Diego: Academic*, 377-410.

Monson, R.K. (2003) Gene Duplication, Neofunctionalization, and the Evolution of C4 Photosynthesis. *Int J Plant Sci*, **164**, S43-S54.

Monson, R.K. and Moore, B.d. (1989) On the significance of C3—C4 intermediate photosynthesis to the evolution of C4 photosynthesis. *Plant Cell Environ*, **12**, 689-699.

Moore, B.D., Ku, M.S.B. and Edwards, G.E. (1989) Expression of C4-like photosynthesis in several species of Flaveria. *Plant Cell Environ*, **12**, 541-549.

Moore, R.C. and Purugganan, M.D. (2005) The evolutionary dynamics of plant duplicate genes. *Curr Opin Plant Biol*, **8**, 122-128.

Morton, T., Petricka, J., Corcoran, D.L., Li, S., Winter, C.M., Carda, A., Benfey, P.N., Ohler, U. and Megraw, M. (2014) Paired-end analysis of transcription start sites in Arabidopsis reveals plant-specific promoter signatures. *Plant Cell*, **26**, 2746-2760.

Muhaidat, R., Sage, R.F. and Dengler, N.G. (2007) Diversity of Kranz anatomy and biochemistry in C4 eudicots. *Am J Bot*, **94**, 362-381.

Muhaidat, R., Sage, T.L., Frohlich, M.W., Dengler, N.G. and Sage, R.F. (2011) Characterization of C3–C4 intermediate species in the genus Heliotropium L. (Boraginaceae): anatomy, ultrastructure and enzyme activity. *Plant Cell Environ*, **34**, 1723-1736.

Nah, G., Lee, M., Kim, D.S., Rayburn, A.L., Voigt, T. and Lee, D.K. (2016) Transcriptome Analysis of Spartina pectinata in Response to Freezing Stress. *PLoS One*, **11**, e0152294.

Naidu, S.L. and Long, S.P. (2004) Potential mechanisms of low-temperature tolerance of C4 photosynthesis in Miscanthus x giganteus: an in vivo analysis. *Planta*, **220**, 145-155.

Naidu, S.L., Moose, S.P., AK, A.L.-S., Raines, C.A. and Long, S.P. (2003) Cold tolerance of C4 photosynthesis in Miscanthus x giganteus: adaptation in amounts and sequence of C4 photosynthetic enzymes. *Plant Physiol*, **132**, 1688-1897.

Nie, G.Y., Long, S.P. and Baker, N.R. (1992) The effects of development at sub - optimal growth temperatures on photosynthetic capacity and susceptibility to chilling - dependent photoinhibition in Zea mays. *Physiol Plant*, **85**, 554-560.

Nisbet, E.G., Grassineau, N.V., Howe, C.J., Abell, P.I., Regelous, M. and Nisbet, R.E.R. (2007) The age of Rubisco: the evolution of oxygenic photosynthesis. *Geobiology*, **5**, 311-335.

Ogren, W.L. (1984) Photorespiration: Pathways, Regulation, and Modification. *Annu Rev Phys*, **35**, 415-442.

Ohta, S., Ishida, Y. and Usami, S. (2004) Expression of cold-tolerant pyruvate, orthophosphate dikinase cDNA, and heterotetramer formation in transgenic maize plants. *Transgenic Res*, **13**, 475-485.

Ohta, S., Usami, S., Ueki, J., Kumashiro, T., Komari, T. and Burnell, J.N. (1996) Identification of the amino acid residues responsible for cold tolerance in Flaveria brownii pyruvate,orthophosphate dikinase. *FEBS Lett*, **396**, 152-156.

Oliver, J.O. (1994) The glycine dercarboxylase complex from plant mitochondria. *Annu Rev Plant Physiol*, **45**, 323-337.

Osborne, C.P. and Sack, L. (2012) Evolution of C4 plants: a new hypothesis for an interaction of CO2 and water relations mediated by plant hydraulics. *Philos Trans R Soc Lond B Biol Sci*, **367**, 583-600.

Pearcy, R.W. (1975) C4 photosynthesis in tree form euphorbia species from hawaiian rainforest sites. *Plant Physiol*, **55**, 1054-1056.

Pearcy, R.W. and Ehleringer, J. (1984) Comparative ecophysiology of C3 and C4 plants. *Plant Cell Environ*, **7**, 1-13.

Peterhänsel, C. (2011) Best practice procedures for the establishment of a C4 cycle in transgenic C3 plants. *J Exp Bot*, **62**, 3011-3019.

Peterhänsel, C., Horst, I., Niessen, M., Blume, C., Kebeish, R., Kurkcuoglu, S. and Kreuzaler, F. (2010) Photorespiration. *The Arabidopsis book*, **8**, e0130.

Pick, T.R., Brautigam, A., Schluter, U., Denton, A.K., Colmsee, C., Scholz, U., Fahnenstich, H., Pieruschka, R., Rascher, U., Sonnewald, U. and Weber, A.P. (2011) Systems analysis of a maize leaf developmental gradient redefines the current C4 model and provides candidates for regulation. *Plant Cell*, **23**, 4208-4220.

Pittermann, J. and Sage, R.F. (2000) Photosynthetic performance at low temperature of Bouteloua gracilis Lag., a high-altitude C4 grass from the Rocky Mountains, USA. *Plant Cell Environ*, **23**, 811-823.

Potter, L., Bingham, M.J., Baker, M.G. and Long, S.P. (1995) The Potential of Two Perennial C4 Grasses and a Perennial C4 Sedge as Ligno-cellulosic Fuel Crops in N.W. Europe. Crop Establishment and Yields in E. England. *Ann Bot*, **76**, 513-520.

Rawsthorne, S. (1992) C3–C4 intermediate photosynthesis: linking physiology to gene expression. *Plant J*, **2**, 267-274.

Rawsthorne, S., Hylton, C.M., Smith, A.M. and Woolhouse, H.W. (1988) Photorespiratory metabolism and immunogold localization of photorespiratory enzymes in leaves of C3 and C 3-C 4 intermediate species of Moricandia. *Planta*, **173**, 298-308.

Ripley, B.S., Abraham, T.I. and Osborne, C.P. (2008) Consequences of C4 photosynthesis for the partitioning of growth: a test using C3 and C4 subspecies of Alloteropsis semialata under nitrogen-limitation. *J Exp Bot*, **59**, 1705-1714.

Sage, R.F. (1999) Why C4 photosynthesis? *In: Sage RF, Monson RK, eds. C4 plant biology. San Diego, CA, USA: Academic Press*, 3-16.

Sage, R.F. (2001) Environmental and Evolutionary Preconditions for the Origin and Diversification of the C4 Photosynthetic Syndrome. *Plant biology (Stuttgart, Germany)*, **3**, 202-213.

Sage, R.F. (2002) Variation in the kcat of Rubisco in C3 and C4 plants and some implications for photosynthetic performance at high and low temperature. *J Exp Bot*, **53**, 609-620.
Sage, R.F. (2004) The evolution of C4 photosynthesis. *New Phytol*, **161**, 341-370.
Sage, R.F. (2016) A portrait of the C4 photosynthetic family on the 50th anniversary of its discovery: species number, evolutionary lineages, and Hall of Fame. *J Exp Bot*, **67**, 4039-4056.
Sage, R.F., Christin, P.A. and Edwards, E.J. (2011) The C4 plant lineages of planet Earth. *J Exp Bot*, **62**, 3155-3169.
Sage, R.F., de Melo Peixoto, M., Friesen, P. and Deen, B. (2015) C4 bioenergy crops for cool climates, with special emphasis on perennial C4 grasses. *J Exp Bot*, **66**, 4195-4212.
Sage, R.F., Khoshravesh, R. and Sage, T.L. (2014) From proto-Kranz to C4 Kranz: building the bridge to C4 photosynthesis. *J Exp Bot*, **65**, 3341-3356.
Sage, R.F. and Kubien, D.S. (2007) The temperature response of C3 and C4 photosynthesis. *Plant Cell Environ*, **30**, 1086-1106.
Sage, R.F. and Pearcy, R.W. (1987a) The Nitrogen Use Efficiency of C3 and C4 Plants: I. Leaf Nitrogen, Growth, and Biomass Partitioning in Chenopodium album (L.) and Amaranthus retroflexus (L.). *Plant Physiol*, **84**, 954-958.
Sage, R.F. and Pearcy, R.W. (1987b) The Nitrogen Use Efficiency of C3 and C4 Plants: II. Leaf Nitrogen Effects on the Gas Exchange Characteristics of Chenopodium album (L.) and Amaranthus retroflexus (L.). *Plant Physiol*, **84**, 959-963.
Sage, R.F., Pearcy, R.W. and Seemann, J.R. (1987) The Nitrogen Use Efficiency of C3 and C4 Plants : III. Leaf Nitrogen Effects on the Activity of Carboxylating Enzymes in Chenopodium album (L.) and Amaranthus retroflexus (L.). *Plant Physiol*, **85**, 355-359.
Sage, R.F. and Sage, T.L. (2002) Microsite characteristics of Muhlenbergia richardsonis (Trin.) Rydb., an alpine C4 grass from the White Mountains, California. *Oecologia*, **132**, 501-508.
Sage, R.F., Sage, T.L. and Kocacinar, F. (2012) Photorespiration and the Evolution of C4 Photosynthesis. *Annu Rev Plant Biol*, **63**, 19-47.
Sage, R.F. and Seemann, J.R. (1993) Regulation of Ribulose-1,5-Bisphosphate Carboxylase/Oxygenase Activity in Response to Reduced Light Intensity in C4 Plants. *Plant Physiol*, **102**, 21-28.
Sage, R.F. and Stata, M. (2015) Photosynthetic diversity meets biodiversity: the C4 plant example. *J Plant Physiol*, **172**, 104-119.
Sage, R.F. and Sultmanis, S. (2016) Why are there no C4 forests? *J Plant Physiol*, **203**, 55-68.
Sage, R.F. and Zhu, X.G. (2011) Exploiting the engine of C4 photosynthesis. *J Exp Bot*, **62**, 2989-3000.
Sage, T.L., Busch, F.A., Johnson, D.C., Friesen, P.C., Stinson, C.R., Stata, M., Sultmanis, S., Rahman, B.A., Rawsthorne, S. and Sage, R.F. (2013) Initial events during the evolution of C4 photosynthesis in C3 species of Flaveria. *Plant Physiol*, **163**, 1266-1276.
Schmitt, M.R. and Edwards, G.E. (1981) Photosynthetic Capacity and Nitrogen Use Efficiency of Maize, Wheat, and Rice: A Comparison Between C3 and C4 Photosynthesis. *J Exp Bot*, **32**, 459-466.
Schuler, M.L., Mantegazza, O. and Weber, A.P. (2016) Engineering C4 photosynthesis into C3 chassis in the synthetic biology age. *Plant J*, **87**, 51-65.
Schulze, S., Mallmann, J., Burscheidt, J., Koczor, M., Streubel, M., Bauwe, H., Gowik, U. and Westhoff, P. (2013) Evolution of C4 Photosynthesis in the Genus Flaveria: Establishment of a Photorespiratory CO2 Pump. *Plant Cell*, **25**, 2522-2535.
Schulze, S., Westhoff, P. and Gowik, U. (2016) Glycine decarboxylase in C3, C4 and C3-C4 intermediate species. *Curr Opin Plant Biol*, **31**, 29-35.
Seemann, J.R., Badger, M.R. and Berry, J.A. (1984) Variations in the Specific Activity of Ribulose-1,5-bisphosphate Carboxylase between Species Utilizing Differing Photosynthetic Pathways. *Plant Physiol*, **74**, 791-794.
Sheehy, J.E. (2001) Will yield barriers limit future rice production? *In Nösberger, J., Geiger, H. H., Struik, P. C., editors. Crop science: progress and prospects. Wallingford (UK): CABI Publishing*, 281-305.
Sheehy, J.E., Ferrer, A.B., Mitchell, P.L., Elmido-Mabilangan, A., Pablico, P. and Dionora, M.J.A. (2007) How the rice crop works and why it needs a new engine. *In: Sheey, J. E.,*

Mitchell, P. L., Hardy, B., editors. Charting new pathways to C4 rice. Los Baños (Phillipines): International Rice Research Institute, 3-26.

Spence, A.K., Boddu, J., Wang, D., James, B., Swaminathan, K., Moose, S.P. and Long, S.P. (2014) Transcriptional responses indicate maintenance of photosynthetic proteins as key to the exceptional chilling tolerance of C4 photosynthesis in Miscanthus × giganteus. *J Exp Bot*, **65**, 3737-3747.

Still, C.J., Berry, J.A., Collatz, G.J. and DeFries, R.S. (2003) Global distribution of C3 and C4 vegetation: Carbon cycle implications. *Global Biochem Cy*, **17**, 6-1-6-14.

Stitt, M. and Heldt, H.W. (1985) Generation and maintenance of concentration gradients between the mesophyll and bundle sheath in maize leaves. *BBA-Bioenergetics*, **808**, 400-414.

Stockhaus, J., Schlue, U., Koczor, M., Chitty, J.A., Taylor, W.C. and Westhoff, P. (1997) The Promoter of the Gene Encoding the C4 Form of Phosphoenolpyruvate Carboxylase Directs Mesophyll-Specific Expression in Transgenic C4 Flaveria spp. *Plant Cell*, **9**, 479-489.

Strömberg, C.A.E. (2011) Evolution of Grasses and Grassland Ecosystems. *Annu Rev Earth Planet Sci*, **39**, 517-544.

Svensson, P., Blasing, O.E. and Westhoff, P. (1997) Evolution of the enzymatic characteristics of C4 phosphoenolpyruvate carboxylase--a comparison of the orthologous PPCA phosphoenolpyruvate carboxylases of Flaveria trinervia (C4) and Flaveria pringlei (C3). *Eur J Biochem*, **246**, 452-460.

Svensson, P., Blasing, O.E. and Westhoff, P. (2003) Evolution of C4 phosphoenolpyruvate carboxylase. *Arch Biochem Biophys*, **414**, 180-188.

Taylor, S.H., Hulme, S.P., Rees, M., Ripley, B.S., Woodward, F.I. and Osborne, C.P. (2010) Ecophysiological traits in C3 and C4 grasses: a phylogenetically controlled screening experiment. *New Phytol*, **185**, 780-791.

United Nations, D.o.E.a.S.A., Population Division (2015) World Population Prospects: The 2015 Revision, Key Findings and Advance Tables. *Working Paper No. ESA/P/WP.241*.

van der Merwe, N.J. and Tschauner, H. (1999) C4 Plants and the Development of Human Societies. *In C4 Plant Biology, ed. R. F. Sage, R. K. Monson, San Diego: Academic*, 509-549.

Vogan, P.J., Frohlich, M.W. and Sage, R.F. (2007) The functional significance of C3–C4 intermediate traits in Heliotropium L. (Boraginaceae): gas exchange perspectives. *Plant Cell Environ*, **30**, 1337-1345.

von Caemmerer, S. (2000) Biochemical models of leaf photosynthesis. *Victoria, Australia: CSIRO Publishing*.

von Caemmerer, S. and Furbank, R.T. (2003) The C4 pathway: an efficient CO2 pump. *Photosynth Res*, **77**, 191-207.

von Caemmerer, S., Quick, W.P. and Furbank, R.T. (2012) The development of C4rice: current progress and future challenges. *Science*, **336**, 1671-1672.

Voznesenskaya, E.V., Franceschi, V.R., Kiirats, O., Artyusheva, E.G., Freitag, H. and Edwards, G.E. (2002) Proof of C4 photosynthesis without Kranz anatomy in Bienertia cycloptera (Chenopodiaceae). *Plant J*, **31**, 649-662.

Voznesenskaya, E.V., Franceschi, V.R., Kiirats, O., Freitag, H. and Edwards, G.E. (2001) Kranz anatomy is not essential for terrestrial C4 plant photosynthesis. *Nature*, **414**, 543-546.

Voznesenskaya, E.V., Koteyeva, N.K., Edwards, G.E. and Ocampo, G. (2010) Revealing diversity in structural and biochemical forms of C4 photosynthesis and a C3-C4 intermediate in genus Portulaca L. (Portulacaceae). *J Exp Bot*, **61**, 3647-3662.

Walker, R.P., Acheson, R.M., Técsi, L.I. and Leegood, R.C. (1997) Phosphoenolpyruvate Carboxykinase in C4 Plants: Its Role and Regulation. *Func Plant Biol*, **24**, 459-468.

Walther, G.R., Post, E., Convey, P., Menzel, A., Parmesan, C., Beebee, T.J., Fromentin, J.M., Hoegh-Guldberg, O. and Bairlein, F. (2002) Ecological responses to recent climate change. *Nature*, **416**, 389-395.

Wang, C., Guo, L., Li, Y. and Wang, Z. (2012) Systematic comparison of C3 and C4 plants based on metabolic network analysis. *BMC Syst Biol*, **6 Suppl 2**, S9.

Wang, D., Naidu, S.L., Portis, A.R., Jr., Moose, S.P. and Long, S.P. (2008a) Can the cold tolerance of C4 photosynthesis in Miscanthus x giganteus relative to Zea mays be explained by differences in activities and thermal properties of Rubisco? *J Exp Bot*, **59**, 1779-1987.

Wang, D., Portis, A.R., Jr., Moose, S.P. and Long, S.P. (2008b) Cool C4 photosynthesis: pyruvate Pi dikinase expression and activity corresponds to the exceptional cold tolerance of carbon assimilation in Miscanthus x giganteus. *Plant Physiol*, **148**, 557-567.

Wang, Y., Brautigam, A., Weber, A.P. and Zhu, X.G. (2014) Three distinct biochemical subtypes of C4 photosynthesis? A modelling analysis. *J Exp Bot*, **65**, 3567-3578.

Williams, B.P., Burgess, S.J., Reyna-Llorens, I., Knerova, J., Aubry, S., Stanley, S. and Hibberd, J.M. (2016) An Untranslated cis-Element Regulates the Accumulation of Multiple C4 Enzymes in Gynandropsis gynandra Mesophyll Cells. *Plant Cell*, **28**, 454-465.

Wiludda, C., Schulze, S., Gowik, U., Engelmann, S., Koczor, M., Streubel, M., Bauwe, H. and Westhoff, P. (2012) Regulation of the Photorespiratory GLDPA Gene in C4 Flaveria: An Intricate Interplay of Transcriptional and Posttranscriptional Processes. *Plant Cell*, **24**, 137-151.

Wood, B. and Leakey, M. (2011) The Omo-Turkana Basin Fossil Hominins and Their Contribution to Our Understanding of Human Evolution in Africa. *Evol Anthropol*, **20**, 264-292.

Xu, J., Brautigam, A., Weber, A.P. and Zhu, X.G. (2016) Systems analysis of cis-regulatory motifs in C4 photosynthesis genes using maize and rice leaf transcriptomic data during a process of de-etiolation. *J Exp Bot*, **67**, 5105-5117.

Yamori, W., Hikosaka, K. and Way, D.A. (2014) Temperature response of photosynthesis in C3, C4, and CAM plants: temperature acclimation and temperature adaptation. *Photosynth Res*, **119**, 101-117.

Yin, X. and Struik, P.C. (2009) C3 and C4 photosynthesis models: An overview from the perspective of crop modelling. *NJAS - Wageningen Journal of Life Sciences*, **57**, 27-38.

Zhang, Y.G., Pagani, M., Liu, Z., Bohaty, S.M. and DeConto, R. (2013) A 40-million-year history of atmospheric CO2. *Phil Trans R Soc*, **371**.

Zhu, X.G., Long, S.P. and Ort, D.R. (2008) What is the maximum efficiency with which photosynthesis can convert solar energy into biomass? *Curr Opin Biotechnol*, **19**, 153-119.

Zhu, X.G., Long, S.P. and Ort, D.R. (2010) Improving Photosynthetic Efficiency for Greater Yield. *Annu Rev Plant Biol*, **61**, 235-261.

V. Manuscripts

1. Sandra Kirschner, Helen Woodfield, Katharina Prusko, Maria Koczor, Udo Gowik, Julian M. Hibberd, Peter Westhoff (2017). **The *SULTR2;2* promoter from *Arabidopsis thaliana* contains a positive regulator for gene expression in the bundle sheath.** In Progress.

2. **Transcriptome analysis of maize subjected to chilling stress.** Unpublished work.

Manuscript 1

The *SULTR2;2* promoter from *Arabidopsis thaliana* contains a positive regulator for gene expression in the bundle sheath

Running title: The *SULTR2;2* promoter from *Arabidopsis thaliana* contains a positive regulator for gene expression in the bundle sheath

Sandra Kirschner[1], Helen Woodfield [2], Katharina Prusko[1], Maria Koczor[1], Udo Gowik[1], Julian M. Hibberd[2], Peter Westhoff[1]

[1] Institute for Plant Molecular and Developmental Biology, Heinrich-Heine-Universität Düsseldorf, Universitätsstraße 1, D-40225 Düsseldorf, Germany

[2] Department of Plant Sciences, University of Cambridge, Downing Street, Cambridge CB2 3EA, United Kingdom

Author's contributions:

SK and **HW** wrote this manuscript. **SK** performed all experiments with the exceptions of those listed below.

HW designed, created and analysed seven constructs listed in the Supplemental.

KP designed and created eight constructs and analysed five of them.

MK transformed the *F. bidentis* plants.

UG, **JMH** and **PW** participated in drafting the manuscript and revised it.

Status of the manuscript:

In progress

Introduction

The evolution of multicellularity is associated with individual cell types that are able to undertake specialised roles within a tissue. In leaves, the bundle sheath (BS) cells form a wreath-like structure around the vasculature that appears analogous to the endodermis of roots (Esau 1965). The role of BS cells is best characterized in C_4 species that partition photosynthesis between the BS and mesophyll (M) cells. In most C_4 plants, CO_2 is initially fixed into a C_4 acid in the M cells by the enzyme phospho*enol*pyruvate carboxylase (PEPC). Subsequently, the C_4 acid diffuses into the BS where CO_2 is released and refixed by the enzyme ribulose-1,5-bisphosphate carboxylase/oxygenase (Rubisco). The decarboxylation of the C_4 acids in the BS generates a high concentration of CO_2 around Rubisco that suppresses the oxygenase activity of the enzyme and hence reduces photorespiration (Hatch 1987). Thus, in C_4 species, the BS is specialized to allow an efficient fixation of CO_2 in the Calvin-Benson-Bassham cycle. In some C_4 plants, the BS is also modified in terms of light capture. For example, in maize and Sorghum, components of the cyclic electron transport are more abundant in the BS compared with the mesophyll cells (Takabayashi *et al.* 2005), whereas photosystem II does not assemble in the BS (Kubicki *et al.* 1994). In addition to these changes associated with photosynthesis, the C_4 BS is also modified to preferentially undertake starch synthesis and degradation, as well as the initial steps of sulphur assimilation (Friso *et al.* 2004).

The mechanisms underpinning preferential gene expression in the BS have been investigated in various species that have evolved C_4 photosynthesis independently (Hibberd and Covshoff 2010). For example, in the C_4 dicotyledon *Flaveria trinervia*, the glycine decarboxylase P-subunit (*GLDPA*) gene contains two promoters, one proximal to the coding region, and the other more distal. The activity of the distal promoter is high but not cell-specific. However, in the presence of the proximal promoter, transcripts derived from the distal promoter are degraded in the M cells by nonsense-mediated RNA decay of incompletely spliced transcripts (Engelmann *et al.* 2008, Wiludda *et al.* 2012). The *GLDPA* promoter from *F. trinervia* is able to generate BS-specific activity in the C_3 species *Arabidopsis thaliana* despite the phylogenetic distance between the Brassicaceae and the Asteraceae (Engelmann *et al.* 2008, Wiludda *et al.* 2012). In *Amaranthus hybridus*, 5' and 3' untranslated regions of the *RbcS1* gene act to restrict accumulation of the glucuronidase (GUS) reporter to the BS of C_4 *F. bidentis* and appear to function as enhancers of translation (Patel *et al.* 2004). Lastly, in the C_4 *Gynandropsis gynandra*, preferential expression of *NAD-ME1&2* genes is associated with coding sequence rather than UTRs or promoter elements

(Brown *et al.* 2011). When this regulatory sequence from *NAD-ME* is placed adjacent to the constitutive CaMV35S promoter, accumulation of GUS is restricted to the BS, indicating that it acts to repress expression in mesophyll cells (Brown *et al.* 2011). Thus, the BS of C_4 species is highly specialized and gene expression in this cell type is controlled by a variety of mechanisms.

In C_3 plants, the role of the BS is less clearly defined. It is supposed to maintain hydraulic integrity of the xylem (Sade *et al.* 2014), regulate flux of metabolites in and out of the leaf (Leegood 2008) and act as a starch store (Miyake and Maeda 1976). Although the C_3 BS is less important for photosynthesis than the BS of C_4 species, the BS cells account to 15 % of the chloroplast containing cells in *A. thaliana* leaves (Kinsman and Pyke 1998). Reducing photosynthesis in chloroplasts of the vasculature and the BS compromises growth and seed-set (Janacek *et al.* 2009). Overall, this physiological analysis indicates that the C_3 BS is specialized, a notion that is supported by analysis of gene expression in this cell type. For example, a quantification of transcripts available for translation indicated that the *A. thaliana* BS is likely important in sulphur metabolism, glucosinolate biosynthesis, trehalose metabolism and detoxification of active oxygen species (Aubry *et al.* 2014). However, the mechanisms underpinning gene expression in the C_3 BS are poorly understood. A small number of promoters including *SHORT-ROOT* (Dhondt *et al.* 2010), *SCARECROW* (Wysocka-Diller *et al.* 2000) and *SULTR2;2* (Takahashi *et al.* 2000) have been reported to drive BS-specific expression in *A. thaliana*, but the molecular nature of the *cis*-regulatory elements controlling their expression is unclear. Further analyses of these processes could give more insight into the cell-specific gene expression in multicellular leaves. Moreover, it would help to answer the question whether or not C_4 gene expression is built on pre-existing mechanisms found in C_3 species. To better understand mechanisms associated with expression in the BS cells of *A. thaliana*, we targeted the Arabidopsis *SULTR2;2* gene that encodes a low-affinity sulphate transporter (Takahashi *et al.* 2000). An in-depth analysis of *AtSULTR2;2* revealed both qualitative and quantitative regulatory modules within the promoter sequence. The preferential expression of *AtSULTR2;*2 in the BS is mediated by a repetitive region that is highly conserved within orthologous genes from Brassicaceaen species. Furthermore, the *SULTR2;2* promoter from *A. thaliana* generates BS specificity in the Asteraceaen C_4 species *F. bidentis*. The most parsimonious explanation for this result is that a common transcription factor or multiple factors are shared by these phylogenetically dispersed species, and that it functions in both C_3 and C_4 BS.

Results

The nucleotides –2815 to +123 relative to the translational start site predicted by TAIR have previously been reported to generate expression in the BS of *A. thaliana* (Takahashi *et al.* 2000). To verify if the sequence downstream of the predicted start codon is required for expression in the BS, a second construct that terminated at nucleotide –1 relative to the predicted translational start site annotated in the TAIR database was generated (Figure 1A).

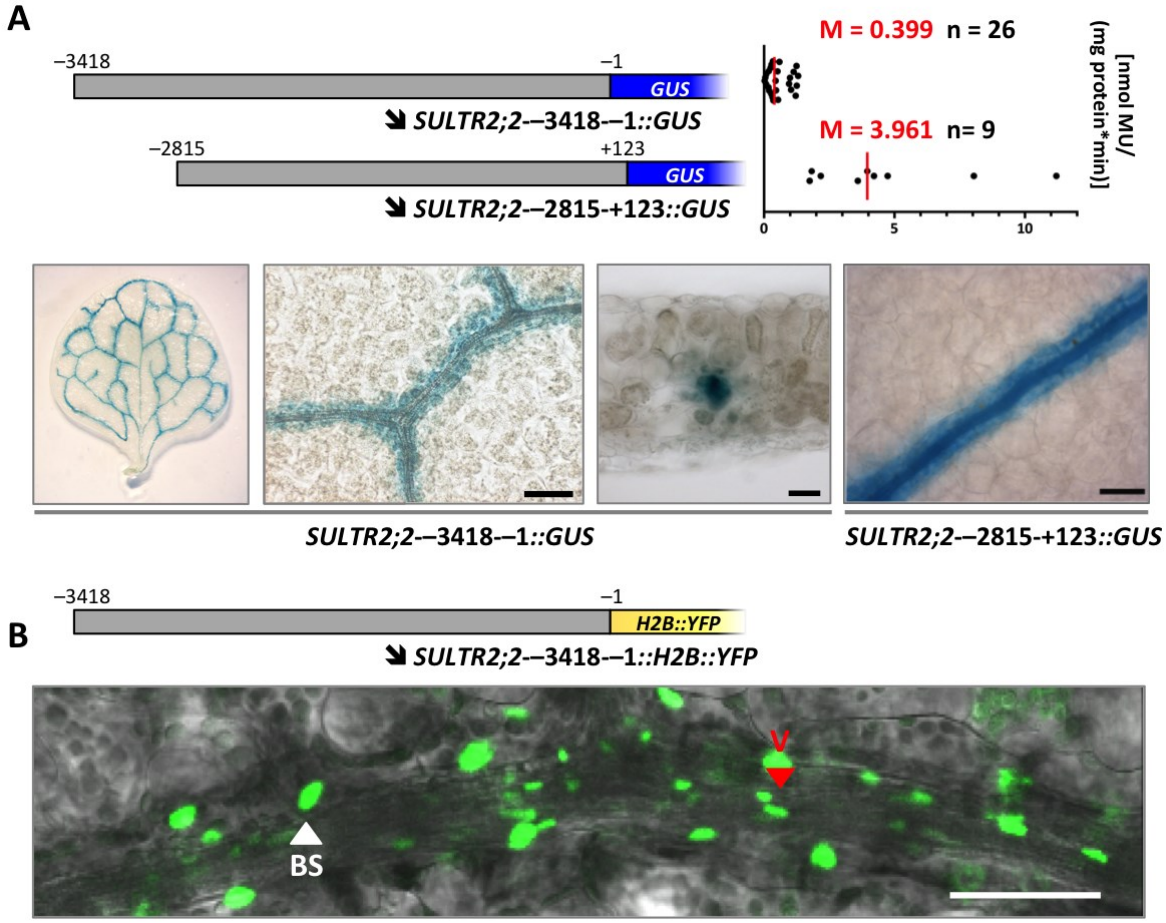

Figure 1: Analysis of the expression of the full-length promoter reveals BS-specific expression
(A) Schematic presentation of promoter regions of the sulphate transporter *SULTR2;2* from *Arabidopsis thaliana* cloned in front of the *GUS* gene, corresponding quantitative data and histochemical localisation of *GUS* expression. The GUS-activity of transgenic T_0 Arabidopsis leaves is measured in nmol 4-methylumbelliferone (MU) per min and mg protein. At the top of the associated data the median (M) and the number of independent analysed transgenic plants (n) are indicated. The positions of the medians are marked as red lines. Both promoter-*GUS* fusions show qualitative expression in the BS of transgenic T_0 Arabidopsis plants. Histological staining of cross-sections indicates expression in the vasculature in addition to the BS. Incubation times were 3 h (whole rosette leaf of *SULTR2;2*-–3418-–1::*GUS*), 16 h (detail of whole rosette leaf of *SULTR2;2*-–3418-–1::*GUS*), 5 h (cross-section of *SULTR2;2*-–3418-–1::*GUS*) and 6 h (*SULTR2;2*-–2815-+123::*GUS*).
(B) Display of the Arabidopsis *SULTR2;2* full-length promoter fused to *H2B::YFP*. The promoter-*H2B::YFP* fusion exhibits expression in the BS (white arrowheads) as well as in the vasculature (red arrowhead).
Scale bars = 50 µm.

Both constructs were transformed into *A. thaliana* and multiple T_0 lines were analysed in terms of the spatial localization and the activity of GUS within the leaf. The promoter activity

was quantified using the MUG fluorimetric assay (Figure 1A). Interestingly, the activity driven by the construct that contained 123 base pairs of coding sequence, but 603 fewer base pairs at the 5' end was about tenfold higher. This difference could either be due to a negative regulator located between −3418 and −2185 nucleotides, or a positive regulator in the 123 base pairs downstream of the predicted translational start site. However, histological staining of mature rosette leaves showed a strong accumulation of GUS in the BS for both constructs (Figure 1A). There was no evidence that GUS accumulated in M or epidermal cells from either construct although staining was evident in the vascular tissue as well as the BS (Figure 1A). GUS accumulated both in young and mature leaves of the *A. thaliana* rosette (Supplemental Figure 1). To confirm that the activity of *GUS* in the vascular tissue was due to gene expression and not diffusion of the dye from the BS to the vascular tissue, a translational fusion between YFP and the nuclear localized Histone 2B protein was placed under control of the *AtSULTR2;2* promoter (Figure 1B). The rosette leaves containing this construct exhibited YFP in the nuclei of BS cells and vascular tissue (Figure 1B). In agreement with a previous report (Chytilova *et al.* 1998), it was noticeable that the vascular nuclei were elongated and rod-like compared with the more spherical ones from the BS (Figure 1B).

Overall, these findings imply that the presence of GUS in each cell-type can be explained by a *AtSULTR2;2* promoter-driven expression in both vascular tissue and BS cells and not by diffusion of the *GUS* product between cell-types.

A small region that is necessary and sufficient to activate gene expression in the BS

Since the nucleotides −2815 to −1 of the *AtSULTR2;2* promoter contain *cis*-regulatory elements necessary to generate expression in BS cells of *A. thaliana*, a 5' deletion series was generated to identify the responsible elements. The deleted sequences are hereafter referred to as regions 1 to 5 (Figure 2).

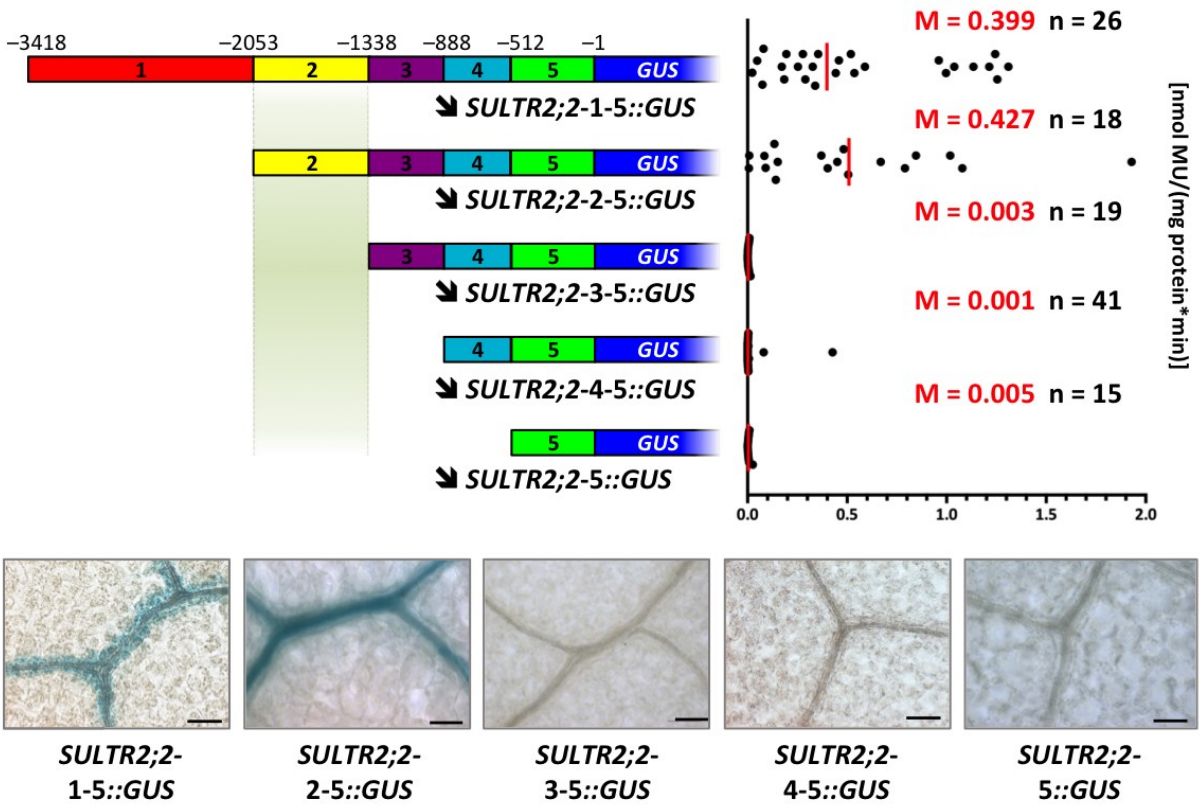

Figure 2: Analysis of 5‘ promoter deletions indicates importance of region 2
Overview of the deletion constructs based on *SULTR2;2*-–3418-–1*::GUS* (henceforward designated as *SULTR2;2-1*-5*::GUS*), corresponding GUS-activity and representative images of spatial *GUS*-expression. The promoter fused to the GUS gene was dissected into five regions (namely region 1 to region 5) and deleted subsequently from the 5’ end. Deletion of region 2 resulted into a loss of activity. Quantitative GUS-activity of transgenic T_0 Arabidopsis leaves was measured in nmol 4-methylumbelliferone (MU) per min and mg protein. At the top of the corresponding data, the medians (M) and the numbers of independent analysed transgenic plants (n) are indicated. The positions of the median are marked as red lines. The spatial expression of the *GUS* gene in transgenic T_0 Arabidopsis plants supports the outcome of quantitative data. Deletion of region 2 (highlighted in light green) revealed the probable region necessary for BS-specific expression. Leaves were incubated for 23 h (*SULTR2;2-1*-5*::GUS*), 4 h *(SULTR2;2*-2-5*::GUS*) and 6 d *(SULTR2;2*-3-5*::GUS*, *SULTR2;2*-4-5*::GUS* and *SULTR2;2*-5*::GUS*). Scale bars = 50 µm.

The removal of region 1 had no significant effect on either activity (p = 0.5948) or spatial accumulation of GUS (Figure 2), which indicates that no essential *cis*-regulatory elements are located within this section. Deletion of region 2 resulted in total loss of MUG activity when assessed by either the quantitative fluorimetric MUG assay or GUS staining to identify spatial patterns of gene expression (Figure 2). Deletion of regions 3 and 4 had no further effect on activity or localization (Figure 2). Hence, these data indicate that the nucleotides in region 1 (–3418 to –2053 relative to the predicted translational start site) do not impact the promoter activity, but that region 2 is necessary for BS expression in mature leaves. There are two possibilities that could explain the lack of GUS accumulation in the BS and the loss of promoter activity once region 2 is absent. Firstly, region 2 could harbour *cis*-regulatory elements that generate expression in BS cells. Secondly, region 2 could contain the *cis*-

regulatory elements for overall promoter activity whereas regions 3 to 5 contain elements that restrict this activity to the BS.

To assess whether region 2 alone is sufficient to drive BS-specific expression, it was fused to the *AtSULTR2;2* core promoter. To define the core promoter, the position of the *AtSULTR2;2* transcription start site was identified with 5' rapid amplification of cDNA ends. No single transcription start site was detected, with 5' ends of transcripts being found between −125 and +71 relative to the predicted translational start site (Supplemental Figure 3). To ensure that all necessary components of the core promoter were present, a region spanning −349 to −1 nucleotides relative to the predicted translational start site (sub-region 5.2) was fused to region 2 and the *GUS* gene (Figure 3).

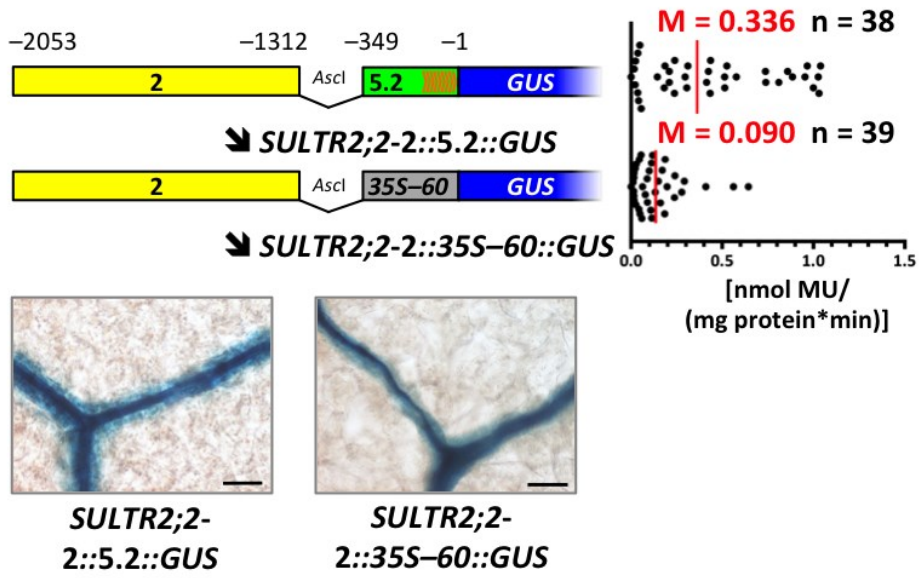

Figure 3: Analysis of region 2 shows that this part of the promoter is sufficient for specificity and activity
Display of region 2 fusion construct, quantification of GUS-activity and representative images of spatial expression. The region 2 was combined with −349 bp of region 5 (sub-region 5.2) or a minimal promoter (−60 - +1 bp of the CaMV35S promoter of the cauliflower mosaic virus), respectively, and cloned in front of the *GUS* gene. Both constructs maintain activity. The orange arrowheads mark the range of 5' cDNA ends obtained by 5'-RACE PCR. The quantitative GUS-activity of transgenic T_0 Arabidopsis leaves was measured in nmol 5-methylumbellyferone (MU) per min and mg protein. At the top of the corresponding data, the medians (M) and the numbers of independent analysed transgenic plants (n) are indicated. The positions of the median are marked as red lines. Visualisation of *GUS* expression of transgenic T_0 Arabidopsis plants shows that both fusion constructs are able to sustain BS-specific expression. Incubation was stopped after 5 h (*SULTR2;2-2::5.2::GUS*) and 22 h (*SULTR2;2-2::35S-60::GUS*). Scale bars = 50 µm.

The fluorimetric MUG assay indicated that the activity from this fusion was comparable to that of the full-length promoter ($p = 0.2212$) and GUS was detectable in both BS and vascular tissue (Figure 3).

To exclude the possibility that the core promoter (nucleotides −349 to −1) includes *cis*-regulatory elements necessary for BS-specific expression, region 2 was also fused to the

minimal CaMV35S promoter (Figure 3). The minimal promoter alone cannot drive significant expression of the *GUS* gene (Supplemental Figure 4). Although the activity of this construct was tenfold lower than that of the full-length promoter ($p<0.0001$), GUS accumulation was still restricted to the BS and vascular tissue (Figure 3). This analysis indicates that the sub-region 5.2 likely represents the core promoter of *SULTR2;2* and contains elements enabling high activity, however, it is not capable of driving BS expression. In contrast, the nucleotides −2053 to −1312 contain all necessary *cis*-regulatory elements required to restrict expression to the BS and vascular tissue of *A. thaliana*.

AtSULTR2;2 contains multiple redundant sequences mediating BS expression

Having established that the nucleotides −2053 to −1338 relative to the predicted translational start site are both necessary and sufficient for BS expression, an unbiased approach to further dissect this region was adopted. Ten consecutive deletions were made to this region (Figure 4). Each construct was fused to the core promoter.

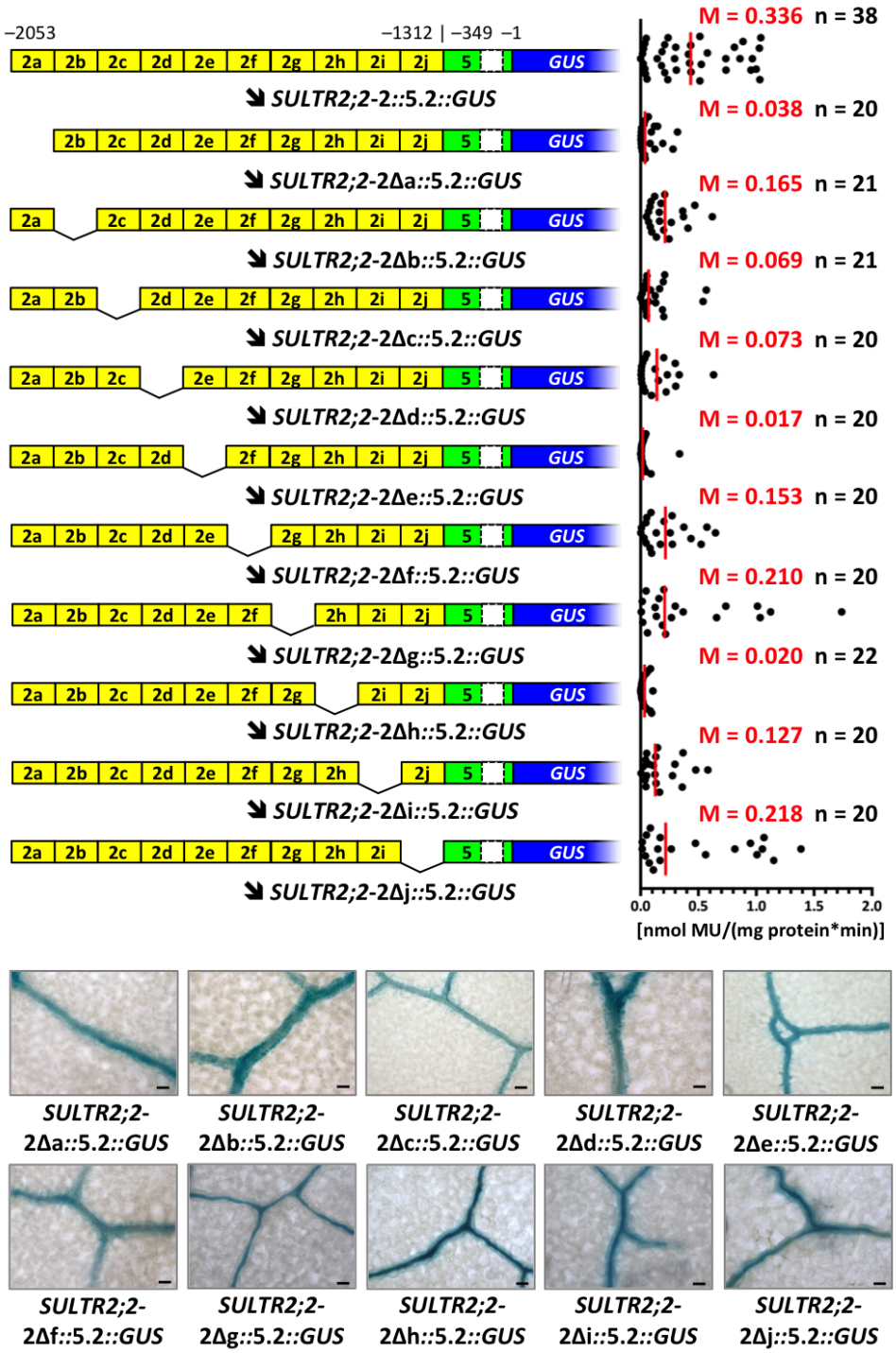

Figure 4: Analysis of internal deletions of region 2 exhibits redundancy of BS elements
Illustration of the internal deletion constructs of region 2, quantification of GUS-activity and representative images of spatial *GUS* expression. Ten constructs with subsequent internal deletions (each 75 bp or 66 bp for the last construct, respectively) of region 2 in combination with –349 of region 5 (sub-region 5.2) fused to the *GUS* gene were generated. All constructs maintain GUS-activity. Quantitative GUS-activity of transgenic T_0 Arabidopsis leaves was measured in nmol 4-methylumbelliferone (MU) per min and mg protein. At the top of the corresponding data, the medians (M) and the numbers of independent analysed transgenic plants (n) are indicated. The positions of the median are marked as red lines. Histochemical images of the spatial expression of transgenic T_0 Arabidopsis plants exhibited BS-specific expression of all promoter-reporter gene fusion constructs. Staining times were 23 h (SULTR2;2-2Δa::5.2::GUS, 16 h (*SULTR2;2*-2Δb*::5.2::GUS*), 48 h (*SULTR2;2*-2Δc*::GUS*), 23 h (*SULTR2;2*-2Δd*::GUS*), 48 h (*SULTR2;2*-2Δe*::GUS*), 8 h (*SULTR2;2*-2Δf*::GUS*), 3 h (*SULTR2;2*-2Δg*::GUS*), 7 h (*SULTR2;2*-2Δh*::GUS*), 3 h (*SULTR2;2*-2Δi*::GUS*) and 19 h (*SULTR2;2*-2Δj*::GUS*). Scale bars = 50 µm.

Interestingly, none of the deletions resulted in a total loss of GUS activity, nor was GUS staining lost from the BS (Figure 4). This indicates a significant redundancy in *cis*-regulatory elements mediating BS-specific expression within region 2. However, it was notable that the GUS activity declined to varying degrees compared with the intact region. This finding strongly suggests that either these redundant *cis*-elements act additively, or that this region contains quantitative elements.

To better understand the redundant *cis*-regulatory elements contained in this section of the promoter, larger deletions were made from either the 5' (Figure 5A) or 3' end (Figure 5B) of this fragment. This generated five sub-regions, hereafter referred to as sub-regions 2.1 to 2.5.

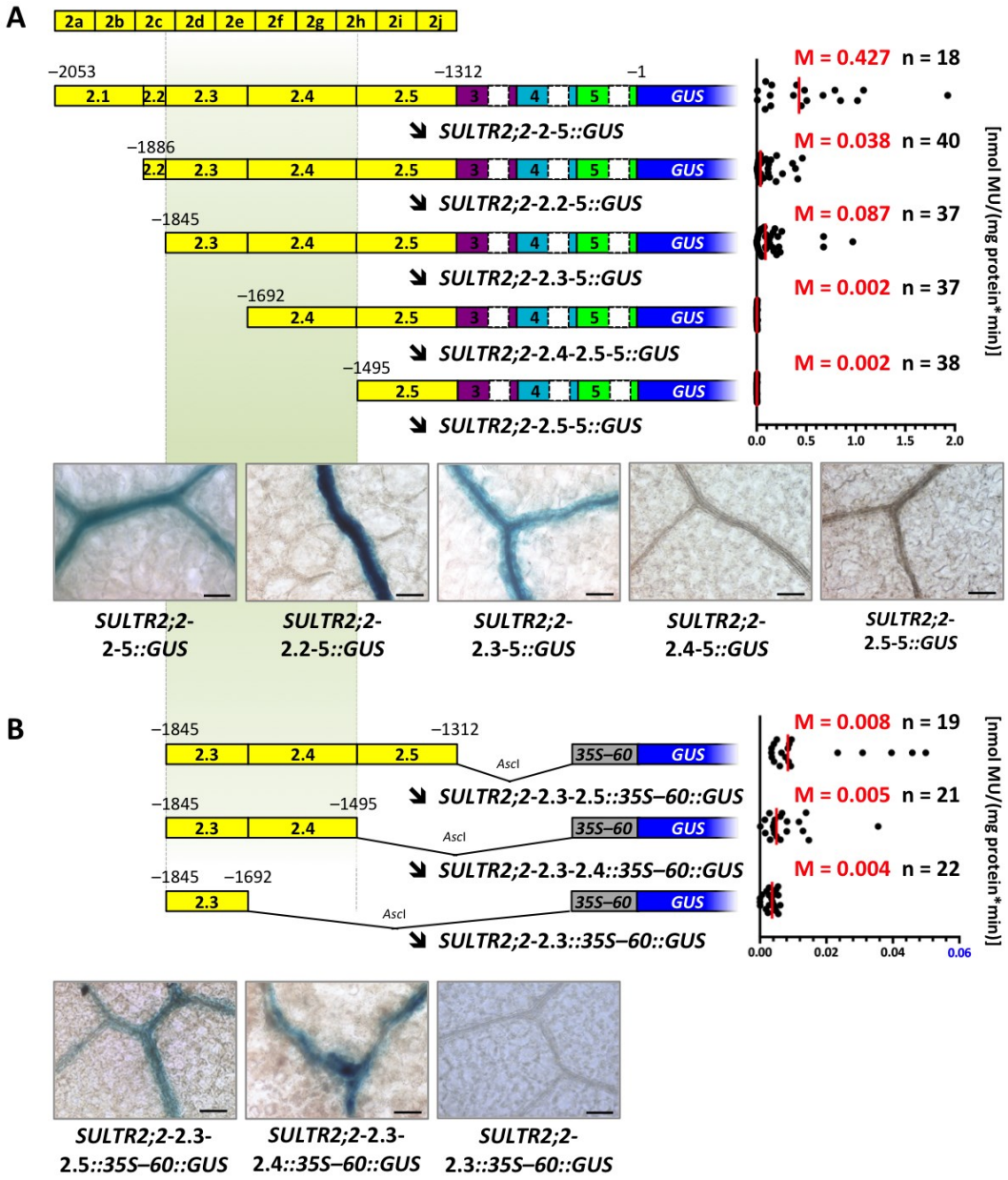

Figure 5: In-depth analysis reveals sections necessary for BS expression maintenance and high activity
(A) Schematic overview of the 5' deletion constructs, their GUS-activity and representative histochemical images of *GUS* expression. Region 2 was further dissected into five sub-regions (2.1 to 2.5). In context of regions 3-5, region 2 was shortened from the 5' end. A significant decline of activity ($p < 0.0001$) was achieved by eliminating sub-region 2.1 and a total loss of activity was recorded by deleting sub-regions 2.1. to 2.3. In compliance to the activity data, BS-specific expression (and expression at all) of transgenic T_0 Arabidopsis plants was lost by deletion of 2.1 to 2.3. Incubation times were 4 h (*SULTR2;2*-2-5*::GUS*), 47 h (*SULTR2;2*-2.2-5*::GUS*), 4 h (*SULTR2;2*-2.3-5*::GUS*) and 6 d (*SULTR2;2*-2.4-5*::GUS* and *SULTR2;2*-2.5-5*::GUS*).
(B) Illustration of the 3' deletion constructs, their GUS-activity and representative images of *GUS* expression. Region 2 was deleted from the 3' end and combined with the minimal promoter of CaMV35S. The expression strength was nearly at the wild type level and dropped with the decrease of length. Note the different scale of the horizontal axis. The spatial expression of *GUS* of transgenic T_0 Arabidopsis plants reveals that the sub-regions 2.3 and 2.4 (highlighted in light green) are necessary for BS expression and activity. Staining times were 5 d (*SULTR2;2*-2.3-2.5*::35S–60::GUS*), 2 d (*SULTR2;2*-2.3-2.4*::35S–60::GUS*) and 29 h (*SULTR2;2*-2.3*::35S–60::GUS*).
The quantitative GUS-activity of transgenic T_0 Arabidopsis leaves was measured in nmol 4-methylumbelliferone (MU) per min and mg protein. At the top of the corresponding data, the medians (M) and the numbers of independent analysed transgenic plants (n) are indicated. The positions of the median are marked as red lines. Scale bars = 50 µm.

The deletion of sub-region 2.1 resulted in a strong reduction of MUG activity but BS-specific accumulation of GUS was maintained (Figure 5A). This finding implies that sub-region 2.1 contains a quantitative enhancer element. Deleting sub-region 2.2 had no clear impact on either BS specificity or activity (Figure 5A). However, the subsequent deletion of sub-regions 2.3 and 2.4 caused a loss of MUG activity and also a loss of GUS staining in the BS and vascular tissue (Figure 5A). This indicates that the *cis*-regulatory elements mediating BS expression may be situated in sub-region 2.3, or that quantitative elements in this region mask qualitative elements in distal sub-regions. To address these options, 3' deletions of region 2 were created. Since the sub-regions 2.1 and 2.2 had little impact on BS-specific expression, the last three sub-regions were fused to the minimal CaMV35S promoter (Figure 5B). The expression from each of these three constructs was low, however, BS expression could be observed for the constructs harbouring sub-regions 2.3, 2.4 and 2.5 (Figure 5B). The removal of sub-region 2.5 resulted in a loss of GUS in rosette leaves although cotyledons still showed patchy staining restricted to the BS and vascular tissue (Figure 5B). Once sub-region 2.4 was removed, MUG activity was further reduced and GUS staining was no longer detectable even in seedlings (Figure 5B). Hence, we conclude that sub-regions 2.3 and 2.4, which comprise a total of 350 base pairs, contain the necessary *cis*-regulatory elements for BS expression of *AtSULTR2;2* and acts as a BS-specific module. It was not possible to identify smaller sections in this 350 base pair region of the promoter.

As previously stated, the deletion of sub-region 2.1 (−2053 to −1886) resulted in a strong reduction of activity but staining of GUS in the BS was maintained. This result was also observed in a separate truncation that consisted of nucleotides −2333 to −1813, which led to a significant decrease in GUS-activity ($p = 0.0009$, Supplemental Figure 1) and confirmed the presence of an additional *cis*-regulatory element in this region. To test if this region acts to enhance activity, it was combined with the heterologous sequence from the *GLDPA* promoter of *F. trinervia* that is known to generate low but detectable GUS activity in the BS and vasculature of *A. thaliana* (Wiludda *et al.* 2012) (Supplemental Figure 2). Interestingly, when combined with this section of the *GLDPA* promoter, the nucleotides −2333 to −1813 from *AtSULTR2;2* increased the MUG activity about thirtyfold. Furthermore, GUS was detectable in both the vasculature and BS (Supplemental Figure 2). These data support the notion that the nucleotides −2333 to −1813 operate as a quantitative enhancing module for expression in the *A. thaliana* BS.

The regulator of BS expression in *AtSULTR2;2* is highly conserved in the Brassicaceae

The *cis*-regulatory elements necessary for BS-specific expression of *AtSULTR2;2* appear to be located within a 350 nucleotide region of the promoter. Since the various deletions failed to identify the responsible *cis*-elements for this phenotype, a phylogenetic approach was performed. Orthologs of *AtSULTR2;2* were identified from *Arabidopsis lyrata*, *Arabidopsis halleri*, *Capsella rubella*, *Capsella grandiflora*, *Boechera stricta*, *Brassica rapa* and *Eutrema salsiguneum*, which represent seven species from the Brassicaceae. Alignments of the sequences 5 kb upstream of each ortholog indicated that region 2 is highly conserved in the Brassicaceae, except *A. lyrata*, which contained an insertion of 446 nucleotides (Figure 6).

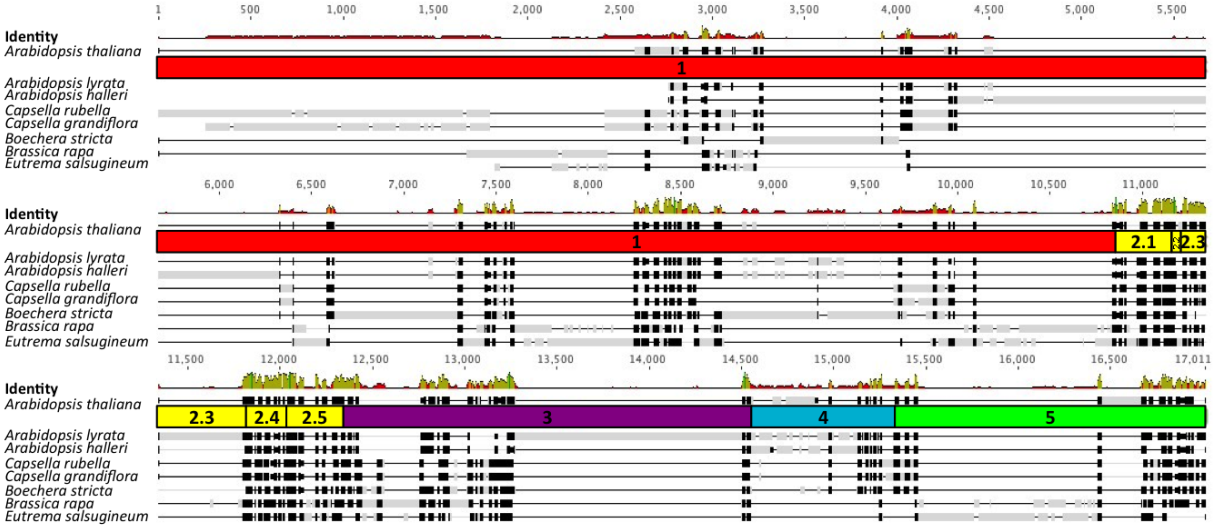

Figure 6: Alignment of *SULTR2;2* promoters of Brassicaceae species shows strong conservation of region 2
The full-length promoter (3418 bp) of *AtSULTR2;2* and each about 5 kb of promoters from orthologs of different Brassicaceae species were aligned globally. Especially region 2 (with exception of a 446 bp insertion of *Arabidopsis lyrata*) and parts of region 3 and 5 are conserved within the Brassicaceae. Region 2 exhibits a pairwise identity of 53.8 %, in contrast to 21.5 % of the whole alignment. The black boxes indicate a strong similarity of the sequences, grey boxes conversely sequences not matching the consensus sequence and black lines gaps. The level of similarity is also specified on the top of the alignment. High peaks in green mark strong similarity, low red peaks highlight poor similarity.

No short sequences or motifs within region 2 that may restrict the expression to the BS could be identified. Hence, the results of this alignment do not identify a specific *cis*-element that could be bound by a transcription factor responsible for generating BS expression, but they do support the functional analysis and implicate region 2 as a critical component of the *SULTR2;2* promoter for BS-specific expression.

The *AtSULTR2;2* promoter is capable of driving BS-specific expression in C_4 *Flaveria bidentis*

Since the *GLDPA* promoter from the C_4 species *F. trinervia* is able to confer BS-specific expression in C_3 *A. thaliana* (Engelmann *et al.* 2008), we next tested whether or not the *A. thaliana SULTR2;2* promoter leads to BS-specific expression in *F. bidentis*. The GUS activity in the transgenic *F. bidentis* plants was about fourfold higher than in *A. thaliana* (Figure 7).

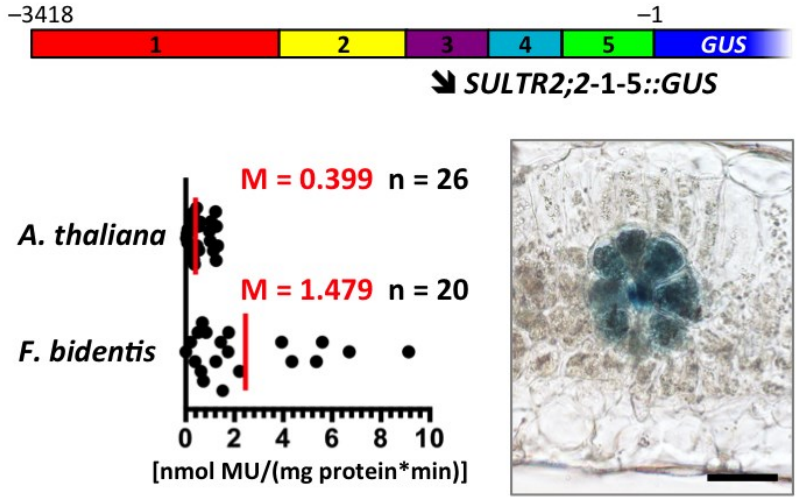

Figure 7: Analysis of the Arabidopsis *SULTR2;2* promoter in *Flaveria bidentis* reveals strong conservation of BS-specific expression
Schematic overview of the *AtSULTR2;2* full-length promoter transformed in *Flaveria bidentis*, its GUS-activity and a representative histochemical image of *GUS* expression. To facilitate a comparison, the *GUS* expression data from *A. thaliana* are added. An about threefold higher activity was observed. The quantitative GUS-activity of transgenic T_0 *Flaveria bidentis* or Arabidopsis leaves, respectively, was measured in nmol 4-methylumbelliferone (MU) per min and mg protein. At the top of the corresponding data, the medians (M) and the numbers of independent analysed transgenic plants (n) are indicated. The positions of the medians are marked as red lines. The image of the cross section of a transgenic T_0 Flaveria plant shows staining in both vasculature and BS. Staining time was 4 d. Scale bar = 50 µm.

However, the histochemical analysis of mature leaves revealed a similar expression pattern to that in *A. thaliana* with strong GUS accumulation in the BS and vascular tissue but not in mesophyll cells (Figure 7). These data indicate that transcription factors from *F. bidentis*, which belongs to the Asteraceae, recognise BS *cis*-regulatory elements from the Brassicaceae. The most parsimonious explanation for this finding is that these sequences represent a part of an ancient and conserved mechanism that restricts gene expression to BS cells of dicotyledenous leaves.

Discussion

In this study, the promoter of *AtSULTR2;2* was analysed to identify Arabidopsis *cis*-regulatory elements of transcription capable driving C_4-like expression pattern in a C_3 environment. The characterisation of the expression from the full-length promoter revealed that the gene activity persisted throughout the life of the leaf (Supplemental Figure 1). This is consistent with the proposed role of *AtSULTR2;2* as a low affinity sulphate transporter for moving sulphate from the vascular bundle to the palisade cells in the leaf (Takahashi *et al.* 2000). In addition to the BS, expression was also seen in the vasculature, which conflicts with previous evidences that *AtSULTR2;2* expression is specific to the BS as stated in Takahashi *et al.* (2000). However, *AtSULTR2;2* transcripts could be detected in the vasculature of Arabidopsis by the sequencing of tissue-specific translatomes (Mustroph *et al.* 2009) that confirmed our findings regarding the *AtSULTR2;2* promoter activity. This expression pattern, which was also detected for the *F. trinervia GLDPA* promoter in Arabidopsis and *F. bidentis* (Engelmann *et al.* 2008), may arise from a possible common origin of the BS and the vasculature. Although there are still ambiguities about the derivation of BS, several studies suggest that the BS develops at least in several C_4 grasses in a lineage specific manner from procambial strands (which give rise to the vasculature) and not in a position-dependent manner (Dengler and Nelson 1999, Jankovsky *et al.* 2001, Soros and Dengler 2001). This possible relationship of the BS and vasculature argues for the parallel activity of the *AtSULTR2;2* promoter in those tissues.

Two separate transcriptional regulatory regions were identified. The first one is qualitative, hence responsible for driving expression in the BS, whereas the second one is of quantitative nature, thus enhancing the activity of the qualitative module. A region of 350 bp was found to be sufficient to drive moderate BS-specific expression when fused to a minimal promoter.

Redundant elements in a 350 bp promoter region drive moderate BS-specific expression in *Arabidopsis thaliana*

The only comprehensive analysis of the mechanism responsible for driving BS specificity in a C_3 plant is the dissection of the *F. trinervia GLDPA,* which is BS-specific in Arabidopsis. Initially, the mechanism proposed for the regulation of *GLDPA* was rather simple and involved two regions: one responsible for BS-specificity via a negative regulator in the M, and the second for enhanced expression (Engelmann *et al.* 2008). However, further investigations revealed that BS-specificity is achieved by a complex interplay between

transcriptional and post-transcriptional processes mediated by both distal and proximal sequences relative to the translational start site (Wiludda *et al.* 2012).

In case of the *AtSULTR2;2* promoter, the regulation appears to be more straightforward. The most parsimonious explanation for our observations is that *AtSULTR2;2* is under regulation of positive factors for BS-specific expression rather than negative regulators for M-specific expression, for which deletion of regulatory domains would have resulted in ubiquitous activity. In contrast to *F. trinervia GLDPA* (Wiludda *et al.* 2012) or *NADME1* and *2* of *Gynandropsis gynandra,* where a 240 bp fragment within the transcribed region supresses expression in the M (Brown *et al.* 2011), there were no evidences for negative regulators for the M in in the *AtSULTR2;2* promoter. Either there was BS-specific expression or no expression at all. This is a further indication that the BS-specific elements concurrently confer activity or that they are tightly linked to quantitative elements.

The subsequent deletions of ten short regions of 75 bp or 66 bp within region 2 were not sufficient to extinguish BS-specific expression. This result implies the existence of several BS-specific elements located in this region that act in a redundant way and together act as a BS-specific module. Only the activity inclined to different level, which suggests that these elements have a kind of additive effect or that additional quantitative elements exist. This redundancy of elements driving specific expression has been shown before. The promoter of the *PAL2* gene coding for the phenylalanine ammonia-lyase of *Phaseolus vulgaris* L. exhibits a similar redundancy for xylem-specific expression when transformed in tobacco. The deletion of the nucleotides −289 to −74 of the promoter prevented xylem-specific expression of the *GUS* reportergene. However, when only the proximal or the distal parts were eliminated, expression in the xylem was maintained (Leyva *et al.* 1992). In a later study, this region was further examined by means of more internal deletions, confirming a redundancy of several xylem-specific elements (Hatton *et al.* 1995).

Phylogenetic shadowing within several Brassicaceae species was used to identify conserved elements in the promoter of the *DORNRÖSCHEN-LIKE* (*DRNL*) gene of Arabidopsis. Three conserved enhancers were found, whereof two showed functional redundancy (Comelli *et al.* 2016). These findings may fit to some extent to the idea of "shadow enhancers", firstly described for Drosophila. Shadow enhancers are secondary enhancers, which show a similar or the same activity in comparison to the primary enhancers, both for one gene (Hong *et al.* 2008). These "distributed" enhancers, as they are also called, may confer robustness for expression e.g. in times of environmental perturbations or to mutations. The also may increase patterning precision (Barolo 2011, Payne and Wagner

2015). The deletion of each 75 base pairs of region 2 of the *AtSULTR2;2* promoter was always "shadowed" by other elements. When only the sub-region 2.3 and 2.4 were left, the GUS-staining in the BS was rather patchy (Figure 5). This finding indicates that the deleted elements usually increase similar to shadow enhancers the accuracy of the activity pattern. Certainly, the BS specificity elements of *AtSULTR2;2* are rather tightly packed within a short region than distributed. This idea is confirmed by the alignment of the *SULTR2;2* promoters from several Brassicaceae species since the outcome did not reveal single conserved elements but a conservation of the whole region 2 within the Brassicaceae. This indicates that the whole region 2 is quite important for the species belonging to this plant family. It is also tempting to state that the whole region 2 functions as a BS-specific module or a "BS enhancer". This BS enhancer comprises a 350 bp core region (sub-regions 2.3 and 2.4) conferring the moderate BS-specific expression and a surrounding negligible region that enhances the robustness of expression. A similar result was found for the regulation of the *even-skipped* (*eve*) gene of *Drosophila melanogaster*. The so-called "eukaryotic minimal enhancer" with 480 bp length was sufficient for normal gene expression of *eve* in the second stripe, but the surrounding binding sites, extending the enhancer region to 800 base pairs, were needed for a robust gene expression during genetic and environmental perturbations (Ludwig *et al.* 2011).

The high expression level of *AtSULTR2;2* is mediated by an upstream located quantitative element

Enhancer elements are important because they often have a leading role in the initiation of gene expression or increasing expression to significant levels (Bulger and Groudine 2011, Spitz and Furlong 2012). Enhancers have been first described by Banerji *et al.* (1981), working on the SV40 virus, and the first eukaryotic enhancer was identified by Gillies *et al.* (1983). The original definition of an enhancer comprises several elements. It should strongly stimulate transcription, the activation being independent of the position and orientation of the enhancer relative to the gene. Additionally, an enhancer should be capable to induce the transcription of heterologous genes (Khoury and Gruss 1983, Serfling *et al.* 1985).

A promoter region driving high expression was identified by the deletion of sub-region 2.1 (Figure 5) as well as by deletion of region II in the second set of truncation constructs (Supplemental Figure 1), both overlapping by 167 base pairs. To test if region II is an enhancer according to the above-mentioned definition, it was in first instance combined with region 7 of the promoter of *GLDPA* from *F. trinervia* and the *GUS* gene. Actually, region II

was capable to enhance *GUS* expression to about thirtyfold in comparison to *GLDPA*-Ft-7 alone (Supplemental Figure 2). Hence, the region fulfils the prerequisite of inducing transcription in a heterologous system. Secondly, the orientation of region II was inverted in context of the full-length promoter to prove that this module acts orientation-independent. The BS specificity was maintained, however, the inversion resulted into a significant reduction in activity ($p = 0.0030$) compared to the full-length promoter. The expression level was even as low as the construct containing the subsequent regions III to VI ($p = 0.2757$) (Supplemental Figure 1 and 2). This outcome reveals that the region in inverse orientation is inoperable and thus does not fulfil the second prerequisite of the original definition of a quantitative enhancer. However, in the last decades much more became known about their nature and enhancer characteristics were subsequently extended (Li *et al.* 2016, Smith and Shilatifard 2014). It might be that region II, which contains the proximal part of region 2, should rather be considered as a quantitative part of the BS-enhancer. In this case, it would lead to high activity of BS-specific expression but would also be able to increase activity of heterologous elements. Hence, one can conclude that region 2 is a rather sophisticated platform for the recruitment of different, partially redundant transcription factors that initiate qualitative and quantitative expression. Therefore, it would be illuminating to know if the whole region 2 would operate inverted in the same way as in the natural direction.

The BS-specific expression of *AtSULTR2;2* in a heterologous context implies the conservation of BS-specific *trans*-regulatory elements

C_4 photosynthesis has evolved at least 61 times independently (Sage 2016). This implies that the development of this type of photosynthesis might be easy in genetic terms (Gowik and Westhoff 2011). For most C_4 plants, an important prerequisite is differential gene expression in the BS and the M cells. Additionally, even in C_3 plants, genes are expressed BS-specific such as *SCARECROW* (*SCR*), *SCR-LIKE23* (*SCL23*) or *AtSULTR2;2* in Arabidopsis (Cui *et al.* 2014, Takahashi *et al.* 2000). The regulation of spatial expression that is necessary for the genes encoding components of the C_4 pathway may have been adopted from those BS-specific genes during C_4 evolution (Covshoff and Hibberd 2012). Together with the independent parallel evolution of C_4 photosynthesis, this implies a possible conservation of *cis*- and *trans*-regulatory elements for BS- and M-specific expression in higher plants.

To test if the BS-specific expression of *AtSULTR2;2* is conserved among Brassicaceae and Asteraceae, the full-length promoter-reporter gene construct was transformed into the C_4

species *Flaveria bidentis*. Indeed, the promoter construct exhibited a similar activity pattern as in transformants of Arabidopsis (Figure 7).

In promoters of orthologous genes, which are divided since the last ten to hundred million years, similar cluster of transcription factor binding sites were found (Wray *et al.* 2003). Presumably, the BS enhancer is not conserved in *A. thaliana* and *F. bidentis*, as region 2 appears to be conserved within Brassicaceae but cannot be found in the closely related Brassicales-Malvales. This indicates a parallel evolution or recruitment of pre-existing *cis*-regulatory elements from other genes for the *AtSULTR2;2* promoter as well as the conservation of the necessary *trans*-regulatory elements. Since *trans*-regulatory elements are more robust to mutations (Payne and Wagner 2015), it is possible that elements that are necessary for BS-specific expression were already present in a common ancestor of rosids (containing the Brassicaceae) and asterids (containing the Asteraceae). Considering that the clades rosids and asterids diverged in the Early Cretaceous – the crown ages are estimated to 108-117 million years ago (mya) for rosids and 107-117 mya for asterids (Sanderson *et al.* 2004, Wikström *et al.* 2001, Wikström *et al.* 2003) – it is quite astonishing that *trans*-regulatory elements still confer a similar expression pattern. On the other hand, it is known that the plant vasculature started to evolve 450 to 430 mya (Furuta *et al.* 2014, Sperry 2003, Ye 2002). It is unclear to the authors of the study when exactly the BS evolved but it should be considered that the BS and vasculature might share the same origin (Dengler and Nelson 1999, Jankovsky *et al.* 2001, Soros and Dengler 2001). This implies an early evolution of a *cis*- and *trans*-regulatory network for these tissues, which may have been conserved over the time. The *GLDPA* promoter of *F. trinervia* is a further example for the possible conservation of these elements since it also exhibits the same expression pattern in Arabidopsis and *F. bidentis* (Engelmann *et al.* 2008, Wiludda *et al.* 2012). Additionally, the promoter of one of the *GLDP* genes of Arabidopsis, *Gldp1*, gives rise to specific expression in the BS and vasculature if a segment conferring expression in the M (M box) is deleted. In short, there are two separate modules, one for M- and one for BS-specific expression (Adwy *et al.* 2015). Interestingly, *AtSULTR2;2* is not a gene involved in photorespiration (like *GLDPA*) or photosynthesis (like *NAD-ME*). These are further hints that the BS-specific expression has been established not only in C_4 plants and this type of expression pattern must be ancient.

Taken together, the BS-specific expression pattern of *AtSULTR2;2* in a C_3 plant and in a C_4 plant of different phylogenetic positions is not *that* surprising.

Materials and methods

Cloning of promoter-reporter gene constructs

DNA manipulations were performed according to Sambrook and Russell (2001). All DNA fragments created by PCR were confirmed by DNA sequencing. The generation of the full-length promoter construct via PCR was executed with *Arabidopsis thaliana* Columbia-0 (Col-0) genomic DNA, which was extracted according to (Fulton et al. 1995). All following constructs were generated by using this promoter construct as a template for PCR. Restriction sites were added to the respective fragments by PCR. Afterwards, the fragments were inserted in the pBI121 (Chen *et al.* 2003, Jefferson *et al.* 1987) or a partially modified pBI121. The region 2 with internal deletions was synthesised by GenScript (Hong Kong, China) and then swapped with the full-length region 2 of *SULTR2;2*-2::5.2::*GUS* to generate the internal deletion constructs. As template for region 7 of *GLDPA* from *Flaveria trinervia* to produce *SULTR2;2-II::GLDPA*-Ft-7*::GUS* served *GLDPA*-Ft (Cossu 1997, Engelmann *et al.* 2008). All used oligonucleotides; restriction sites/enzymes and vectors are listed in the Supplemental Tables 1-3.

Transformation of *Arabidopsis thaliana* and *Flaveria bidentis*

A. thaliana ecotype Col-0 was stably transformed according to the floral dip protocol (Clough and Bent 1998) modified by Logemann *et al.* (2006). The *Agrobacterium tumefaciens* strain AGL1 (Lazo *et al.* 1991) was used, containing the respective construct that was transformed via electroporation. *F. bidentis* was transformed with the appropriate construct as stated in Chitty *et al.* (1994), using AGL1 (Lazo *et al.* 1991). The successful transformations of *A. thaliana* and *F. bidentis* T_0 plants were tested by PCR.

Growth of plant material

Before transplanting to soil, positive T_0 transformants of *A. thaliana* were selected for kanamycin resistance by means of tissue culture. Seeds were sterilized by washing two times for 5 min with 20 % DanKlorix (Colgate-Palmolive, New York City, USA) and 0.02 % Triton-X 100 (Fluka Analyticals, Buchs, Switzerland), and four times with sterile water. The stratification of the seeds was performed for 4 °C for 48 h. Afterwards, seeds were spread on ½ MS selective growth medium containing 10 g l^{-1} (w/v) sucrose (Sigma-Aldrich, St. Louis, USA), 0.5 g l^{-1} MES (Biomol, Hamburg, Germany), 2.13 g l^{-1} (w/v) Murashige-Skoog basal salts (Duchefa Biochemie, Haarlem, Netherlands), 0.75 % agar (SERVA Electrophoresis,

Heidelberg, Germany), 50 µg ml^{-1} kanamycin (Sigma-Aldrich, St. Louis, USA) and 100 mg l^{-1} Cefotaxim (Fresenius Kabi Deutschland, Bad Homburg, Germany) with a final pH of 5.7. Then the petri dishes were transferred to a long day (14 h light/10 h dark) growth cabinet with temperatures of 23 °C at day and 20 °C at night, ambient humidity and CO_2 concentration and a light intensity of 90 µmol m^{-2} s^{-1} PFD.

Visual and quantitative analysis of GUS accumulation in situ

The histochemical analyses were performed as described in Engelmann *et al.* (2008). For *A. thaliana*, three- to four-week old rosette leaves (whole blades or transverse sections) and 10- to 14-day old seedlings were used, for *F. bidentis* the sixth leaves of 40-50 cm tall plants (transverse sections). The transverse sections were prepared manually using a razor blade. By means of light microscopy, stained leaves and transverse sections were visualised. The quantification of GUS-activity was performed via fluorimetric assay according to Jefferson *et al.* (1987) and Kosugi *et al.* (1990), using two to four leaves of 3- to 4-week old T_0 *A. thaliana* plants or the fifth leave of 40-50 cm tall T_0 *F. bidentis* plants, respectively. At least 15 independent T_0 plants were analysed for each construct. With the Mann-Whitney U test (Prism 6, GraphPad Software, La Jolla, USA), statistical differences between data sets were determined.

YFP visualisation

The imaging of H2B::YFP was performed on a Zeiss LSM 780 confocal laser-scanning microscope (Zeiss Microscopy, Jena, Germany) equipped with a 40x water immersion objective, NA 1.2. The YFP fluorescence was excited at 514 nm using an argon laser at an output power of 5 %. The fluorescence signal was detected between 517 and 569 nm using a spectral detector.

5' RACE PCR

The total RNA from leaves of wild type *A. thaliana* Col-0 plants was extracted according to Westhoff *et al.* (1991). The RNA was treated with DNase I (Thermo Fisher Scientific, Waltham, USA) and further purified with the RNeasy® Plant Mini Kit (Qiagen, Hilden, Germany). An amount of 1 µg RNA was used for generating cDNA by means of the SMARTer™ RACE cDNA Amplification Kit (Clontech Laboratories, Mountain View, USA). The 5' RACE-PCR was performed with the same kit, using the Advantage® 2 DNA

Polymerase Mix (Clontech Laboratories, Mountain View, USA) or the Phusion® HF DNA Polymerase (Thermo Fisher Scientific, Waltham, USA). Two nested 3' oligonucleotides, At Sultr2;2-11 and At Sultr2;2-13, both binding in the cDNA of *AtSULTR2;2*, were used. The PCR products were cloned with the CloneJET PCR Cloning Kit (Thermo Fisher Scientific, Waltham, USA) and clones were checked via colony PCR using the pJET1.2 Forward Sequencing Primer and the pJET1.2 Reverse Sequencing Primer oligonucleotides of the Kit. Correct clones were subjected for plasmid preparation and sequencing.

Phylogenetic analysis of the *SULTR2;2* promoters

The promoter sequences of *Arabidopsis lyrata*, *Arabidopsis halleri*, *Capsella rubella*, *Capsella grandiflora*, *Boechera stricta*, *Brassica rapa* and *Eutrema salsiguneum* were retrieved from the Phytomine tool implemented in the Phytozome database (Goodstein *et al.* 2011). The alignment of these sequences as well as the *AtSULTR2;2* full-length promoter was performed with the Genious multiple alignment algorithm (Kearse *et al.* 2012).

Acknowledgments

We thank the Center for Advanced imaging (HHU Düsseldorf) for provision and technical assistance of the Zeiss LSM 780 laser-scanning microscope.

Literature

Adwy, W., Laxa, M. and Peterhansel, C. (2015) A simple mechanism for the establishment of C(2)-specific gene expression in Brassicaceae. *Plant J*, **84**, 1231-1238.

Aubry, S., Smith-Unna, R.D., Boursnell, C.M., Kopriva, S. and Hibberd, J.M. (2014) Transcript residency on ribosomes reveals a key role for the Arabidopsis thaliana bundle sheath in sulfur and glucosinolate metabolism. *Plant J*, **78**, 659-673.

Banerji, J., Rusconi, S. and Schaffner, W. (1981) Expression of a β-Globin Gene Is Enhanced by Remote SV40 DNA Sequences. *Cell*, **27**, 299-308.

Barolo, S. (2011) Shadow enhancers: Frequently asked questions about distributed cis- regulatory information and enhancer redundancy. *Bioessays*, **24**, 135-141.

Brown, N.J., Newell, C.A., Stanley, S., Chen, J.E., Perrin, A.J., Kajala, K. and Hibberd, J.M. (2011) Independent and Parallel Recruitment of Preexisting Mechanisms Underlying C4 Photosynthesis. *Science*, **331**, 1436-1439.

Bulger, M. and Groudine, M. (2011) Functional and Mechanistic Diversity of Distal Transcription Enhancers. *Cell*, **144**, 327-339.

Chen, P.Y., Wang, C.K., Soong, S.C. and To, K.Y. (2003) Complete sequence of the binary vector pBI121 and its application in cloning T-DNA insertion from transgenic plants. *Mol Breeding*, **11**, 287-293.

Chitty, J.A., Furbank, R.T., Marshall, J.S., Chen, Z. and Taylor, W.C. (1994) Genetic transformation of the C4 plant, Flaveria bidentis. *Plant J*, **6**, 949-956.

Chytilova, E., Macas, J. and Galbraith, D.W. (1998) Green Fluorescent Protein Targeted to the Nucleus, a Transgenic Phenotype Useful for Studies in Plant Biology. *Ann Bot*, **83**, 645-654.

Clough, S.J. and Bent, A.F. (1998) Floral dip: a simplified method for Agrobacterium-mediated transformation of Arabidopsis thaliana. *Plant J*, **16**, 735-743.

Comelli, P., Glowa, D., Chandler, J.W. and Werr, W. (2016) Founder-cell-specific transcription of the DORNROSCHEN-LIKE promoter and integration of the auxin response. *J Exp Bot*, **67**, 143-155.

Cossu, R. (1997) Charakterisierung der Glycindecarboxylase-Gene von Flaveria trinervia (C4) und ihre Expression in transgenen Nicotiana tabacum, Flaveria pubescens und Solanum tuberosum. *PhD thesis. Universität Hannover, Hannover, Germany*.

Covshoff, S. and Hibberd, J.M. (2012) Integrating C4 photosynthesis into C3 crops to increase yield potential. *Curr Opin Biotech*, **23**, 209-214.

Cui, H., Kong, D., Liu, X. and Hao, Y. (2014) SCARECROW, SCR-LIKE 23 and SHORT-ROOT control bundle sheath cell fate and function in Arabidopsis thaliana. *Plant J*, **78**, 319-327.

Dengler, N.G. and Nelson, T. (1999) Leaf Structure and Development in C 4 Plants. *C4 Plant Biology*, 133-172.

Dhondt, S., Coppens, F., De Winter, F., Swarup, K., Merks, R.M., Inze, D., Bennett, M.J. and Beemster, G.T. (2010) SHORT-ROOT and SCARECROW regulate leaf growth in Arabidopsis by stimulating S-phase progression of the cell cycle. *Plant Physiol*, **154**, 1183-1195.

Engelmann, S., Wiludda, C., Burscheidt, J., Gowik, U., Schlue, U., Koczor, M., Streubel, M., Cossu, R., Bauwe, H. and Westhoff, P. (2008) The gene for the P-subunit of glycine decarboxylase from the C4 species Flaveria trinervia: analysis of transcriptional control in transgenic Flaveria bidentis (C4) and Arabidopsis (C3). *Plant Physiol*, **146**, 1773-1785.

Esau, K. (1965) Plant Anatomy. *New York: John Wiley and Sons*, 767pp.

Friso, G., Giacomelli, L., Ytterberg, A.J., Peltier, J.B., Rudella, A., Sun, Q. and Wijk, K.J. (2004) In-depth analysis of the thylakoid membrane proteome of Arabidopsis thaliana chloroplasts: new proteins, new functions, and a plastid proteome database. *Plant Cell*, **16**, 478-499.

Fulton, T.M., Chunwongse, J. and Tanksley, S.D. (1995) Microprep Protocol for Extraction of DNA from Tomato and other Herbaceous Plants. *Plant Mol Biol Report*, **13**, 207-209.

Furuta, K.M., Hellmann, E. and Helariutta, Y. (2014) Molecular control of cell specification and cell differentiation during procambial development. *Annu Rev Plant Biol*, **65**, 607-638.

Gibson, D.G., Young, L., Chuang, R.Y., Venter, C., Hutchison, C.A. and Smith, H.O. (2009) Enzymatic assembly of DNA molecules up to several hundred kilobases. *Nat Methods*, **6**, 343-345.

Gillies, S.D., Morrison, S.L., Oi, V.T. and Tonegawa, S. (1983) A Tissue-specific Transcription Enhancer Element Is Located in the Major lntron of a Rearranged lmmunoglobulin Heavy Chain Gene. *Cell*, **33**, 717-728.

Goodstein, D.M., Shu, S., Howson, R., Neupane, R., Hayes, R.D., Fazo, J., Mitros, T., Dirks, W., Hellsten, U., Putnam, N. and Rokhsar, D.S. (2011) Phytozome: a comparative platform for green plant genomics. *Nucleic Acids Res*, **40**, D1178-D1186.

Gowik, U. and Westhoff, P. (2011) The Path from C3 to C4 Photosynthesis. *Plant Physiol*, **155**, 56-63.

Hatch, M.D. (1987) C4 photosynthesis: a unique blend of modified biochemistry, anatomy and ultrastructure. *Biochim Biophys Acta, ER. Reviews on bioenergetics*, **895**, 81-106.

Hatton, D., Sablowski, R., Yung, M.H., Smith, C., Schuch, W. and Bevan, M. (1995) Two classes of cis sequences contribute to tissue-specific expression of a PAL2 promoter in transgenic tabacoo. *Plant J*, **7**, 859-876.

Hibberd, J.M. and Covshoff, S. (2010) The regulation of gene expression required for C4 photosynthesis. *Annu Rev Plant Biol*, **61**, 181-207.

Higo, K., Ugawa, Y., Iwamoto, M. and Korenaga, T. (1999) Plant cis-acting regulatory DNA elements (PLACE) database: 1999. *Nucleic Acids Res*, **27**, 297-300.

Hong, J.W., Hendrix, D.A. and Levine, M.S. (2008) Shadow Enhancers as a Source of Evolutionary Novelty. *Science*, **321**, 1314.

Janacek, S.H., Trenkamp, S., Palmer, B., Brown, N.J., Parsley, K., Stanley, S., Astley, H.M., Rolfe, S.A., Quick, W.P., Fernie, A.R. and Hibberd, J.M. (2009) Photosynthesis in cells around veins of the C3 plant Arabidopsis thaliana is important for both the shikimate pathway and leaf senescence as well as contributing to plant fitness. *Plant J*, **59**, 329-343.

Jankovsky, J.P., Smith, L.G. and Nelson, T. (2001) Specification of bundle sheath cell fates during maize leaf development: roles of lineage and positional information evaluated through analysis of the tangled1 mutant. *Development*, **128**, 2747-2753.

Jefferson, R.A., Kavanagh, T.A. and Bevan, M.W. (1987) GUS fusions: beta-glucuronidase as a sensitive and versatile gene fusion marker in higher plants. *EMBO*, **6**, 3901-3907.

Kearse, M., Moir, R., Wilson, A., Stones-Havas, S., Cheung, M., Sturrock, S., Buxton, S., Cooper, A., Markowitz, S., Duran, C., Thierer, T., Ashton, B., Meintjes, P. and Drummond, A. (2012) Geneious Basic: An integrated and extendable desktop software platform for the organization and analysis of sequence data. *Bioinformatics*, **28**, 1647-1649.

Khoury, G. and Gruss, P. (1983) Enhancer Elements. *Cell*, **33**, 313-314.

Kinsman, E.A. and Pyke, K.A. (1998) Bundle sheath cells and cell-specific plastid development in Arabidopsis leaves. *Development*, **125**, 1815-1822.

Koncz, C. and Schell, J. (1986) The promoter of TL-DNA gene 5 controls the tissue-specific expression of chimaeric genes carried by a novel type of Agrobacterium binary vector. *Mol Gen Genet*, **204**, 383-396.

Kosugi, S., Ohashi, Y., Nakajima, K. and Arai, Y. (1990) An improved assay for β-glucuronidase in transformed cells: Methanol almost completely suppresses a putative endogenous β-glucuronidase activity. *Plant Sci*, **70**, 133-140.

Kubicki, A., Steinmuller, K. and Westhoff, P. (1994) Differential transcription of plastome-encoded genes in the mesophyll and bundle-sheath chloroplasts of the monocotyledonous NADP-malic enzyme-type C4 plants maize and Sorghum. *Plant Mol Biol*, **25**, 669-679.

Lazo, G.R., Stein, P.A. and Ludwig, R.A. (1991) A DNA transformation-competent Arabidopsis genomic library in Agrobacterium. *Nat Biotechnol*, **9**, 963-967.

Leegood, R.C. (2008) Roles of the bundle sheath cells in leaves of C3 plants. *J Exp Bot*, **59**, 1663-1673.

Leyva, A., Liang, X., Pintor-Toro, J.A., Dixon, R.A. and Lamb, C.J. (1992) cís-Element Combinations Determine Phenylalanine Ammonia-Lyase Gene Tissue-Specific Expression Patterns. *Plant Cell*, **4**, 263-271.

Li, W., Notani, D. and Rosenfeld, M.G. (2016) Enhancers as non-coding RNA transcription units: recent insights and future perspectives. *Nat Rev Genet*, **17**, 207-223.

Logemann, E., Birkenbihl, R.P., Ulker, B. and Somssich, I.E. (2006) An improved method for preparing Agrobacterium cells that simplifies the Arabidopsis transformation protocol. *Plant Methods*, **2**, 16.

Ludwig, M.Z., Manu, Kittler, R., White, K.P. and Kreitman, M. (2011) Consequences of eukaryotic enhancer architecture for gene expression dynamics, development, and fitness. *PLoS Genet*, **7**, e1002364.

Miyake, H. and Maeda, E. (1976) Development of bundle sheath chloroplasts in rice seedlings. *Can J Bot*, **54**, 556-565.

Mustroph, A., Zanetti, M.E., Jang, C.J., Holtan, H.E., Repetti, P.P., Galbraith, D.W., Girke, T. and Bailey-Serres, J. (2009) Profiling translatomes of discrete cell populations resolves altered cellular priorities during hypoxia in Arabidopsis. *Proc Natl Acad Sci U S A*, **106**, 18843-18848.

Nakagawa, T., Kurose, T., Hino, T., Tanaka, K., Kawamukai, M., Niwa, Y., Toyooka, K., Matsuoka, K., Jinbo, T. and Kimura, T. (2007) Development of series of gateway binary vectors, pGWBs, for realizing efficient construction of fusion genes for plant transformation. *J Biosci Bioeng*, **104**, 34-41.

Patel, M., Corey, A.C., Yin, L.P., Ali, S., Taylor, W.C. and Berry, J.O. (2004) Untranslated regions from C4 amaranth AhRbcS1 mRNAs confer translational enhancement and preferential bundle sheath cell expression in transgenic C4 Flaveria bidentis. *Plant Physiol*, **136**, 3550-3561.

Payne, J.L. and Wagner, A. (2015) Mechanisms of mutational robustness in transcriptional regulation. *Front Genet*, **6**.

Prusko, K. (2010) Identifizierung cis-regulatorischer Elemente der Transkriptionskontrolle in photosynthetisch aktiven Blattzellen von Arabidopsis thaliana. *PhD thesis, HHU Düsseldorf, Düsseldorf, Germany*.

Sade, N., Shatil-Cohen, A., Attia, Z., Maurel, C., Boursiac, Y., Kelly, G., Granot, D., Yaaran, A., Lerner, S. and Moshelion, M. (2014) The role of plasma membrane aquaporins in regulating the bundle sheath-mesophyll continuum and leaf hydraulics. *Plant Physiol*, **166**, 1609-1620.

Sage, R.F. (2016) A portrait of the C4 photosynthetic family on the 50th anniversary of its discovery: species number, evolutionary lineages, and Hall of Fame. *J Exp Bot*, **67**, 4039-4056.

Sambrook, J. and Russell, D.W. (2001) Molecular cloning: a laboratory manual 3rd edition. *Coldspring-Harbour Laboratory Press, UK*.

Sanderson, M.J., Thorne, J.L., Wikstrom, N. and Bremer, K. (2004) Molecular evidence on plant divergence times. *Am J Bot*, **91**, 1656-1665.

Serfling, E., Jasin, M. and Schaffner, W. (1985) Enhancers and eukaryotic gene transcripton. *Trends Genet*, **1**, 224-230.

Smith, E. and Shilatifard, A. (2014) Enhancer biology and enhanceropathies. *Nat Struct Mol Biol*, **21**, 210-219.

Soros, C.L. and Dengler, N.G. (2001) Ontogenetic Derivation and Cell Differentiation in Photosynthetic Tissues of C3 and C4 Cyperaceae. *Am J Bot*, **88**, 992-1005.

Sperry, J.S. (2003) Evolution of water transport and xylem structure. *Int J Plant Sci*, **164**, S115-S127.

Spitz, F. and Furlong, E.E. (2012) Transcription factors: from enhancer binding to developmental control. *Nat Rev Genet*, **13**, 613-626.

Takabayashi, A., Kishine, M., Asada, K., Endo, T. and Sato, F. (2005) Differential use of two cyclic electron flows around photosystem I for driving CO2-concentration mechanism in C4 photosynthesis. *Proc Natl Acad Sci U S A*, **102**, 16898-16903.

Takahashi, H., Watanabe-Takahashi, A., Smith, F.W., Blake-Kalff, M., Hawkesford, M.J. and Saito, K. (2000) The roles of three functional sulphate transporters involved in uptake and translocation of sulphate in Arabidopsis thaliana. *Plant J*, **23**, 171-182.

Westhoff, P., Offermann-Steinhard, K., Höfer, M., Eskins, K., Oswald, A. and Streubel, M. (1991) Differential accumulation of plastid transcripts encoding photosystem II components in the mesophyll and bundle-sheath cells of monocotyledonous NADP-malic enzyme-type C4 plants. *Planta*, **184**, 377-388.

Wikström, N., Savolainen, V. and Chase, M.W. (2001) Evolution of the angiosperms: calibrating the family tree. *Proceedings. Biological sciences / The Royal Society*, **268**, 2211-2220.

Wikström, N., Savolainen, V. and Chase, M.W. (2003) Angiosperm divergence times: congruence and incongruence between fossils and sequence divergence estimates. *In P. C. J. Donoghue and M. P. Smith [eds.], Telling the evolutionary time: molecular clocks and the fossil record, 142–165. Taylor & Francis, London, UK.*

Wiludda, C., Schulze, S., Gowik, U., Engelmann, S., Koczor, M., Streubel, M., Bauwe, H. and Westhoff, P. (2012) Regulation of the Photorespiratory GLDPA Gene in C4 Flaveria: An Intricate Interplay of Transcriptional and Posttranscriptional Processes. *Plant Cell*, **24**, 137-151.

Wray, G.A., Hahn, M.W., Abouheif, E., Balhoff, J.P., Pizer, M., Rockman, M.V. and Romano, L.A. (2003) The evolution of transcriptional regulation in eukaryotes. *Mol Biol Evol*, **20**, 1377-1419.

Wysocka-Diller, J.W., Helariutta, Y., Fukaki, H., Malamy, J.E. and Benfey, P.N. (2000) Molecular analysis of SCARECROW function reveals a radial patterning mechanism common to root and shoot. *Development*, **127**, 595-603.

Ye, Z.H. (2002) Vascular tissue differentiation and pattern formation in plants. *Annu Rev Plant Biol*, **53**, 183-202.

Supplemental Figures

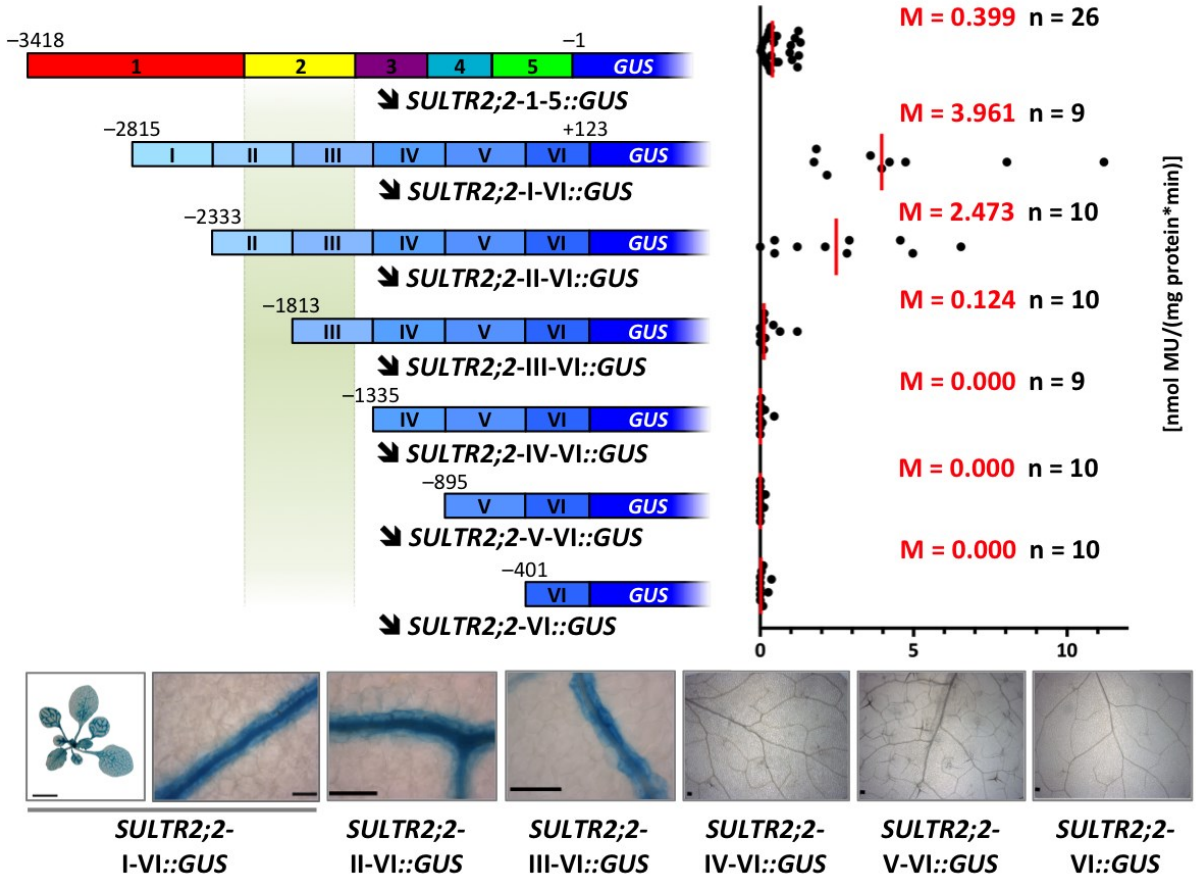

Supplemental Figure 1: Analysis of the expression of the full-length promoter reveals BS-specific expression in the second set of constructs generated at the University of Cambridge

Schematic display of the deletion constructs generated at University of Cambridge (UoC) (in comparison of the full-length promoter from the Heinrich-Heine-University of Düsseldorf (HHU); the region necessary for BS-specific expression is indicated in light green), their GUS-activity and representative images of spatial *GUS* expression. The promoter fused to the *GUS* gene was cut-down from the 5' end to create six constructs, deleting approximately 400 bp each time. The positions of each cut were designed to avoid *cis*-regulatory elements predicted by the software PLACE (Higo *et al.* 1999). Each deleted section is referred to as regions I to VI. The deletion of regions I and II resulted into a decline of activity and deletion of regions I to III led to a total loss of expression. The quantitative GUS-activity of transgenic T_0 Arabidopsis leaves was measured in nmol 4-methylumbelliferone (MU) per min and mg protein. At the top of the corresponding data, the medians (M) and the numbers of independent analysed transgenic plants (n) are indicated. The positions of the median are marked as red lines. The visualisation of *GUS* expression in transgenic T_0 Arabidopsis plants exhibits a loss of staining at deletion of region I to III, demonstrating that region III is necessary for BS-specific expression. Whole plant and leaves were incubated for 6 h. Scale bars = 50 µm with the exception of the image showing the whole rosette of *SULTR2;2*-I-VI*::GUS* = 2 mm.

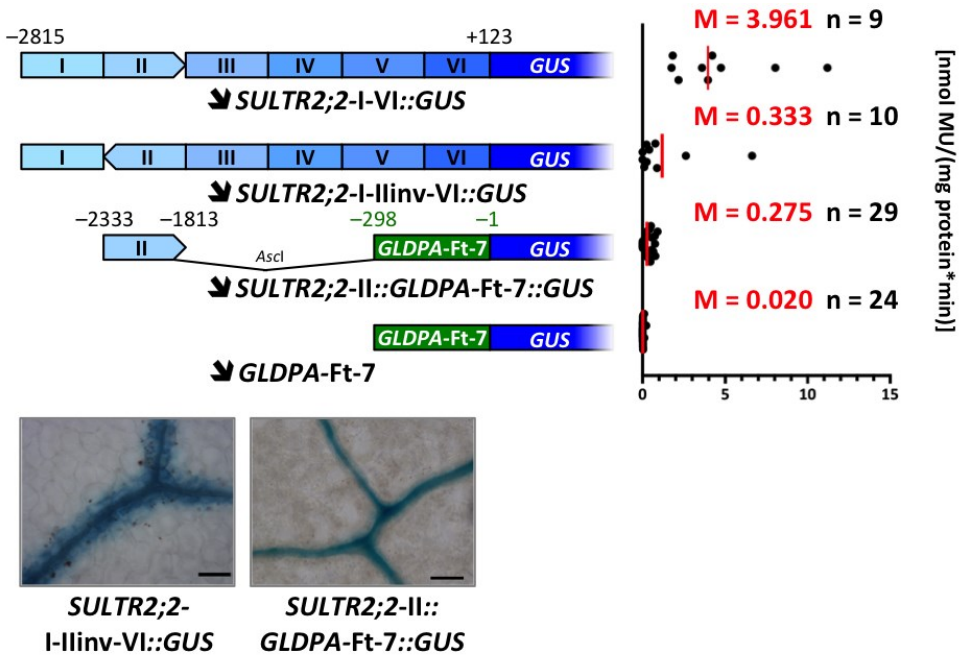

SULTR2;2-I-IIinv-VI::GUS

SULTR2;2-II::GLDPA-Ft-7::GUS

Supplemental Figure 2: Region II is able to enhance activity in a chimeric construct
Illustration of the enhancer-promoter constructs, their GUS-activity and spatial expression in comparison to the UoC full-length promoter. Region II was inverted in context of the full-length promoter (construct created at UoC), resulting into an incline of activity. Additionally, region II was combined with region 7 of the *Flaveria trinervia GLDPA* promoter (created at HHU), leading to an enhanced expression in comparison to *GLDPA*-Ft-7 alone. The quantitative GUS-activity of transgenic T_0 Arabidopsis leaves was measured in nmol 4-methylumbelliferone (MU) per min and mg protein. At the top of the corresponding data, the medians (M) and the numbers of independent analysed transgenic plants (n) are indicated. The positions of the median are marked as red lines. The inversion of region II had no effect on the BS-specific expression of transgenic T_0 Arabidopsis plants (*SULTR2;2*-I-IIinv-VI*::GUS*) compared to the full-length promoter with a non-inverted region II. The chimeric construct *SULTR2;2*-II*::GLDPA*-Ft-7*::GUS* exhibited a strong staining in the vasculature and in the BS cells. Incubation times were each 6 h. Scale bars = 50 µm.

Supplemental Figure 3: 5‘ RACE PCR reveals no distinct transcription start site

Alignment of 5’ ends of cDNAs obtained via 5’ RACE PCR. The first line shows the template for alignment, the 3’ end is the same as in *SULTR2;2*-I-VI*::GUS*. No distinct transcription start site was found. Different Translational start sites are marked in blue (TAIR annotated and used at HHU, TAIR Accession 1009028759) and red (used by UoC and Takahashi *et al.* (2000)). A TATA box motif found by the PLACE database (Higo *et al.* 1999) is underlined. The black arrowhead marks the TAIR annotated transcription start site (TAIR Accession 1009028759).

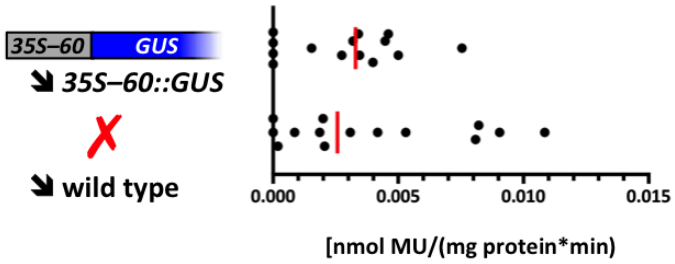

Supplemental Figure 4: Analysis of the minimal promoter –60 - +1 of CaMV35S reveals no difference in activity compared to the wild type
Schematic display of the analysed samples and their GUS-activity. The activity of the empty vector pBIMCS2II transformed in Arabidopsis was compared to that of Arabidopsis Col-0 wild type by means of GUS-fluorimetric assay. It was exhibited that the medians are not significantly different (p = 0.5312). Thus, this minimal promoter cannot drive expression on its own. The quantitative GUS-activity of transgenic T_0 or wild type Arabidopsis leaves, respectively, was measured in nmol 4-methylumbelliferone (MU) per min and mg protein. At the top of the corresponding data the medians (M) and the numbers of independent analysed transgenic or wild type plants (n) are indicated. The positions of the median are marked as red lines.

Generation of HHU constructs

Supplemental Table 1: Oligonucleotides used for generating the *AtSULTR2;2* constructs and the according restriction enzymes used

Oligonucleotid name	Sequence (5' to 3'), restriction sites underlined	Restriction enzyme
Sulfvorw HindIII	AAAAAGCTTGCTAATTCTTAGTCATCTTCGTTTGAC	*Hin*dIII
Sulfruck XmaI2	ATACCCGGGTCAGCTCTCTCTCTAGATATATATTAAC	*Xma*I
SULTRVORWAsiSI	AAAGCGATCGCGCTAATTCTTAGTCATCTTCGTTTGAC	*Asi*SI
SULTRRUECKAscI	ATAGGCGCGCCTCAGCTCTCTCTCTAGATATATATTAAC	*Asc*I
Sulf HindIII a	TTAAAGCTTATGCATCCAAAACATGGCGCCTTCC	*Hin*dIII
Sulf HindIII b	TTAAAGCTTCTGATCATCTAACATTGTTGGTATGC	*Hin*dIII
Sulf AscI c	TTAGGCGCGCCTCTACTATACCAGGTAAGTATACGCT	*Asc*I
Sulf HindIII d	TTAAAGCTTATCTCAAGCATGAGTGATAATTTCAAC	*Hin*dIII
Sultr22SbAscI rev	ATAGGCGCGCCGCATACCAACAATGTTAGATGATCAG	*Asc*I
Sultr22 AscIF	ATTGGCGCGCCGATTGTAGAAATGATTATAACATTC	*Asc*I
Sulf HindIIIaI	TATAAGCTTGTAAATAAGTGAATAAGAATTGGTTC	*Hin*dIII
At Sultr2;2-6	CTCAAGCTTACCTATATGACTCATGCGTAGT	*Hin*dIII
At Sultr2;2-5	GACCCCGGGTCAGCTCTCTCTCTAGATATATATTAAC	*Xma*I
At Sultr2;2-8	GTTAAGCTTGTGACCACATCACATCCGTTCA	*Hin*dIII
At Sultr2;2-10	GGCAAGCTTGCAACGCTGACATCTCCACTTA	*Hin*dIII
At Sultr2;2-18	TCTGGCGCGCCGCATACCAACAATGTTAGATGATCAG	*Asc*I
At Sultr2;2-16	TCTGGCGCGCCCAAACAAAACAAGAATGGTTTGA	*Asc*I
At Sultr2;2-14	TCTGGCGCGCCTGGGCATGTTCGGTCCACATT	*Asc*I
At Sultr2;2-20	TATAAGCTTACTACAGGAACACCAGTGTGGC	*Hin*dIII
At Sultr2;2-9	AGAGGCGCGCCCTATCTTTCCACTACGCATGAGTC	*Asc*I
Ft GLDPA-7-2	TAAGGCGCGCCCATTTGATCTATAAC	*Asc*I
gdcsPA-XMA-verandert	AAATCCCGGGAGTGTAAGATGGG	*Xma*I

Supplemental Table 2: Oligonucleotides used for various purposes

Oligonucleotid name	Sequence (5' to 3')	Usage
At Sultr2;2-11	TCTTGCCACATGCTTGGTGGTTCCG	5' RACE-PCR
At Sultr2;2-13	AGGACTGGCTTCTTCATGGTGGCTC	5' RACE-PCR
Long UP	CTAATACGACTCACTATAGGGCAAGCAGTGGTATCA ACGCAGAGT	5' RACE-PCR
Short UP	CTAATACGACTCACTATAGGGC	5' RACE-PCR
NUP	AAGCAGTGGTATCAACGCAGAGT	5' RACE-PCR
pJET1.2 Forward Sequencing Primer	CGACTCACTATAGGGAGAGCGGC	Sequencing, colony PCR
pJET1.2 Reverse Sequencing Primer	AAGAACATCGATTTTCCATGGCAG	Sequencing, colony PCR
pBI121 gus3-1	ACTGCCTGGCACAGCAATTGC	Colony PCR, test PCR

Supplemental Table 3: Promoter-reporter constructs, oligonucleotide combinations and vector used
Modified pBI121 vectors and their creation are described in Prusko (2010).

Construct	PCR product	5'-oligonucleotid	3'-oligonucleotid	vector
SULTR2;2-At-1-5::*GUS*	*SULTR2;2*-At-1-5	Sulfvorw HindIII	Sulfruck XmaI2	pBI121
SULTR2;2-At-1-5::*H2B::YFP*	*SULTR2;2*-At-1-5	SULTRVORWAsiSI	SULTRRUECKAscI	pBIMCSH2B YFP
SULTR2;2-At-2-5::*GUS*	*SULTR2;2*-At-2-5	Sulf HindIII a	Sulfruck XmaI2	pBI121
SULTR2;2-At-3-5::*GUS*	*SULTR2;2*-At-3-5	Sulf HindIII b	Sulfruck XmaI2	pBI121
SULTR2;2-At-4-5::*GUS*	*SULTR2;2*-At-4-5	Sulf AscI c	Sulfruck XmaI2	pBIMCS4
SULTR2;2-At-5::*GUS*	*SULTR2;2*-At-5	Sulf HindIII d	Sulfruck XmaI2	pBI121
SULTR2;2-At-2::5.2::*GUS*	*SULTR2;2*-At-2	Sulf HindIII a	Sultr22SbAscI rev	pBI121
	SULTR2;2-At-5.2	Sultr22 AscIF	Sulfruck XmaI2	
SULTR2;2-At-2::35S-60::*GUS*	*SULTR2;2*-At-2	SulfHindIII a	Sultr22SbAscIrev	pBIMCS2II
SULTR2;2-At-2Δa **to** j::*GUS*	-	-	-	pBI121
SULTR2;2-At-2.2-5::*GUS*	*SULTR2;2*-At-2.2-5	Sulf HindIIIaI	Sulfruck XmaI2	pBI121
SULTR2;2-At-2.3-5::*GUS*	*SULTR2;2*-At-2.3-5	At Sultr2;2-6	At Sultr2;2-5	pBIMCS4
SULTR2;2-At-2.4-5::*GUS*	*SULTR2;2*-At-2.4-5	At Sultr2;2-8	At Sultr2;2-5	pBIMCS4
SULTR2;2-At-2.5::*GUS*	*SULTR2;2*-At-2.5	At Sultr2;2-10	At Sultr2;2-5	pBIMCS4
SULTR2;2-At-2.3-2.5::35S-60::*GUS*	*SULTR2;2*-At-2.3-2.5	At Sultr2;2-6	At Sultr2;2-18	pBIMCS2II
SULTR2;2-At-2.3-2.4::35S-60::*GUS*	*SULTR2;2*-At-2.3-2.4	At Sultr2;2-6	At Sultr2;2-16	pBIMCS2II
SULTR2;2-At-2.3::35S-60::*GUS*	*SULTR2;2*-At-2.3	At Sultr2;2-6	At Sultr2;2-14	pBIMCS2II
SULTR2;2-At-1.2-2.1-2.3.1::*GLDPA*-Ft-7::*GUS*	*SULTR2;2*-At-1.2-2.1-2.3.1	At Sultr2;2-20	At Sultr2;2-9	pBIMCS4
	GLDPA-Ft-7	Ft GLDPA-7-2	gdcsPA-XMA-verandert	

Materials and methods used at UoC

Cloning of the promoter-reporter gene constructs

The promoter regions were cloned from *Arabidopsis thaliana* Columbia-0 (Col-0) genomic DNA, which was extracted using a Plant DNeasy Mini-Kit (Qiagen, Hilden, Germany). The fragments were amplified by PCR using oligonucleotides described in Supplementary Table 4. In Supplemental Table 5, the combinations of oligonucleotides and the respective constructs are shown. The pENTR™/D-TOPO® (Thermo Fisher Scientific, Waltham, USA)

was used to clone blunt-ended PCR products into the vector in an orientation-dependent manner. Gateway recombination (Thermo Fisher Scientific, Waltham, USA) was then used to fuse promoter fragments to the *GUS* reporter gene in the binary vector pGWB3 (Nakagawa *et al.* 2007). The construct *SULTR2;2*-I-IIinv-VI*::GUS* was generated by Gibson Assembly (Gibson *et al*. 2009) using primers described in Supplementary Table 4.

Transformation of *Arabidopsis thaliana*

Stable transformants of *A. thaliana* ecotype Col-0 were generated by the floral dip method according to Clough and Bent (1998) using the *Agrobacterium tumefaciens* strain GV3101 (Koncz and Schell 1986).

Growth of plant material

Positive T_0 transformants were selected with kanamycin in tissue culture before transplanting to compost. *A. thaliana* seeds were sterilised by a five minute wash in 70 % ethanol (v/v), followed by a 20 min incubation in 13 % sodium hypochlorite (v/v) at room temperature. The seeds were then washed four times in sterilised water and resuspended in sterilised 0.5 % agarose (w/v) before spreading onto the selective growth medium (0.25 % (w/v) Murashige-Skoog basal salts (MS) (Duchefa Biochemie, Haarlem, Netherlands) solidified by 1 % (w/v) agar (Melford Laboratories, Ipswich, UK), 50 mg ml^{-1} kanamycin (Melford Laboratories, Ipswich, UK), final pH 5.8). The petri dishes were then wrapped in aluminium foil and placed at 4 °C for 48 h for stratification. Following stratification, the dishes were transferred to a long day (16 h light, 8 h dark) growth cabinet with a constant temperature of 22 °C, relative humidity of 65 %, ambient CO_2 concentration and a light intensity of 200 µmol m^{-2} s^{-1} PFD.

Visual and quantitative analysis of GUS accumulation in situ

The histochemical GUS analysis was performed on three-week old rosette leaves according to Brown *et al.* (2011). Transverse sections were made manually using a razor blade. The stained plants and transverse sections were visualised using light microscopy. Samples of whole aerial tissue from three-week old T_0 plants at the mature rosette stage were used to quantify the GUS-activity via the fluorimetric assay according to Jefferson *et al.* (1987). For each construct, at least ten independent T_0 lines were analysed.

Supplemental Table 4: Oligonucleotides used for generating the *AtSULTR2;2* constructs (UoC)

Oligonucleotid name	Sequence (5' to 3')
AtSULTR AF	CACCTCGACATCAAGTACCAAGTAAT
AtSULTR BF	CACCACTACAGGAACACCAGTGTG
AtSULTR CF	CACCAGAACAACTTATATGACTCATGC
AtSULTR DF	CACCATCATCTAACATTGTTGGTATGC
AtSULTR EF	CACCCATGTTCTACTATACCAGGTAA
AtSULTR FF	CACCACACAGTTTAAGAAACCATAAATG
AtSULTR R	TTTGCTAGCCATGGGCTCTTCTGCAGGAC
Sul Inv F	TAATTCTTCAGATATCGTGACTATCTTTCCACTACGCATGA
Sul Inv R	TGAGTCATATAAGTTGTTCTACTACAGGAACACCAGTGTG

Supplemental Table 5: Promoter-reporter constructs, oligonucleotide combinations and vector used (UoC)

Construct	5'-oligonucleotid	3'-oligonucleotid
SULTR2;2-I-VI*::GUS*	AtSULTR AF	AtSULTR R
SULTR2;2-II-VI*::GUS*	AtSULTR BF	AtSULTR R
SULTR2;2-III-VI*::GUS*	AtSULTR CF	AtSULTR R
SULTR2;2-IV-VI*::GUS*	AtSULTR DF	AtSULTR R
SULTR2;2-V-VI*::GUS*	AtSULTR EF	AtSULTR R
SULTR2;2-VI*::GUS*	AtSULTR FF	AtSULTR R
SULTR2;2-I-IIinv-VI*::GUS*	Sul Inv F	Sul Inv R

Supplemental Data

The sequences of the 5' regions of the Brassicaceae *SULTR2;2* genes can be found at the attached SD memory card.

Manuscript 2

Transcriptome analysis of maize subjected to chilling stress

Introduction

C_4 photosynthesis has evolved in arid places of tropic, subtropical and warm temperate climate (Sage 2004) of North and South America, central Asia, northeast Africa and Arabia as well as southern Africa and Australia. Concerning the origin of C_4 grasses, South America has been identified as the major hot spot (Sage *et al.* 2011). Due to their origins, C_4 plants are optimised for photosynthesis at habitats characterised by high light conditions and temperatures (Hatch 1987, Hatch 1992, Sage 2004, Yamori *et al.* 2014) but are maladapted to chilling. Thus, they are susceptible to low temperature (Long and Spence 2013, Pearcy and Ehleringer 1984, Sage *et al.* 2015). Hence, C_4 plants are commonly found in warm climates and hardly in cool environments. Plants using C_4 photosynthesis are rarely native to areas with a mean summer temperature below 8 °C to 10 °C (Kubien and Sage 2003, Long 1983). For example, C_4 grasses are predominant in warm grassland and savannahs of low altitudes and latitudes (Edwards *et al.* 2010). However, there are exceptions, like the perennial grass *Miscanthus* x *giganteus* or *Muhlenbergia glomerata* that are able to endure cold and unfavourable weather conditions in England or boreal fens of Canada, respectively (Beale *et al.* 1996, Kubien and Sage 2003).

One of the most prominent C_4 plants is the crop maize that has its origin in the tropical and subtropical regions of America. Nevertheless, by now maize is cultivated not only in its original area of natural selection but also in more northern latitudes (Greaves 1996). Amongst others, the strong increase in biofuel production led to an enormous expansion of maize cultivation. The yields increased from 592 Mt in the year 2000 to 1016 Mt in 2013 world-wide. Hence, maize is now the most important cereal (FAO 2015). Yet this is only possible due to the use of early flowering varieties as well as those exhibiting a short vegetation period. As a consequence of its origin and photosynthesis type, maize has its growth optimum in a range of 30 °C to 35 °C. Processes like germination, initial shoot, root and leaf extension are repressed at temperatures below 8 °C to 10 °C (Miedema 1982), and hence, maize is chilling sensitive. Temperatures below 20 °C already lead to a reduction in growth and a further decrease below 10 °C causes cellular and tissue injuries (Greaves 1996). Especially the combination of high light and low temperatures can be detrimental for maize seedlings. Low temperatures slow down reaction rates, resulting in an abundance of excitation energy. The consequence is oxidative damage, preferentially of photosystem II (Allen and Ort 2001). At temperatures of 10 °C to 15 °C, chlorosis may occur, mainly in young and developing tissues (Greaves 1996). These temperatures are warm enough for slight leaf extension. However, in the region of growth, chlorophyll is broken down due to photo-oxidation. This

occurs before it is even integrated alongside with the photosystems and the light-harvesting complexes into the thylakoids. These chilling injuries are usually not visible during the phase of chilling stress but appear after subsequent temperature increase. According to the grade of severity, the chlorosis can be irreversible (Miedema 1982). Additionally, the division of labour between the bundle sheath and mesophyll cells, a characteristic of C_4 plants, might be a target for chilling stress. As the maize bundle sheath chloroplasts conduct mainly cyclic electron transport, they lack the reducing power of NADPH (Ghirardi and Melis 1983). Thus, the crucial regeneration of antioxidants mainly takes place in the mesophyll cells. If the chilling disturbs the transport, antioxidant formation or regeneration, the bundle sheath cells are committed to oxidative stress (Doulis *et al.* 1997, Foyer *et al.* 2002, Pastori *et al.* 2000). In general, chilling can lead to a reduction in thylakoid pigments and proteins (Nie and Baker 1991). Moreover, a decline of photosynthetic capacity for CO_2 assimilation was observed at low temperature (Nie *et al.* 1992). Furthermore, cold nights result in smaller leaves due to a slower cell cycle (Rymen *et al.* 2007).

Since chilling particularly affects maize seedlings, early vigour is an important trait for breeders. This trait comprises a robust photosynthetic performance during chilling, an early canopy closure and a quick leaf development (Hund *et al.* 2004, Trachsel *et al.* 2010). Even though the correlation of the chilling tolerance of seedlings and final biomass might be weak (Leipner *et al.* 2008), it is known that early vigour nevertheless has some advantages. The ability of maize to cope with weeds is increased and the risk of soil erosion and nitrate leaching decreases (Leipner *et al.* 2008, Presterl *et al.* 2007). Additionally, early vigour can result in an improved water use efficiency (Trachsel *et al.* 2010). The benefits of an improved early vigour due to chilling tolerance have been displayed in a study performed by Dohleman and Long (2009). In this study, maize and the closely related but chilling tolerant C_4 grass *Miscanthus* x *giganteus* were compared in field trials. Partly due to the strong and early growth of photosynthetic active leaves (and their maintenance) at low temperatures, *Miscanthus* x *giganteus* achieved a 61 % higher biomass yield compared to maize (Dohleman and Long 2009).

It is known that the genetic improvement of maize leads to a better yield even under cold stress conditions (Dwyer and Tollenaar 1989). With the rise of DNA markers, the advent of quantitative trait loci (QTL) studies began (Paterson 1995). In the last decades, many QTL studies with maize have been performed for a better understanding of chilling tolerance as well as to support breeders in their selection work. Representative QTL analyses in maize have been conducted by Fracheboud et al. (2004), Jompuk et al. (2005), Leipner et al. (2008),

Rodríguez et al. (2014) and Trachsel et al. (2010). In a QTL study of Presterl et al. (2007) and Wilde et al. (2005), a major QTL for early vigour in maize was identified. The study was based on a segregating population of double-haploids produced from a cross between the European dent inbred line SL, exhibiting poor early vigour at chilling stress, and the chilling tolerant TH line. The doubled-haploid population as well as the testcrosses were analysed by field trials at different locations in 2001 and 2002. As a criterion for early vigour, the fresh matter yield of plants at the sixth to eighth leaf-stage (beginning of shoot elongation) was chosen. The growth period varied depending on the geographical location over 44 to 86 days. Seven QTL were identified in the lines per se and ten in the testcrosses. The most prominent QTL was found to be located on chromosome 4 (QTL4) and explained 33.7 % of the phenotypic variance for fresh matter yield in the lines per se. The QTL was verified with near isogenic lines (NILs), which contained the positive allele derived from the chilling tolerant parent TH in the background of SL (Presterl *et al.* 2007, Wilde *et al.* 2005).

The QTL4 was coarse-mapped between 26 and 155 Mb, thus comprising more than half of chromosome 4 (Figure 1). By generation of new molecular markers, NILs, subNILs and F_2 segregating populations, the QTL4 was fine-mapped. These mapping studies were facilitated by a surrogate phenotype (Baliashvili (2010); compare Addendum 1). In this process, two closely related NILs that differ only in a nearly 60 kb TH fragment (Figure 1) were created. This fragment contains the putative QTL4. Field studies attested a high early vigour and thus chilling tolerance for the NIL N4-8X-tol containing this TH fragment. Conversely, the NIL N4-8X-sen that lacks the TH fragment exhibited a poor early vigour in the field studies. Therefore, it was concluded that the QTL4 is located in these 60 kb (Figure 1).

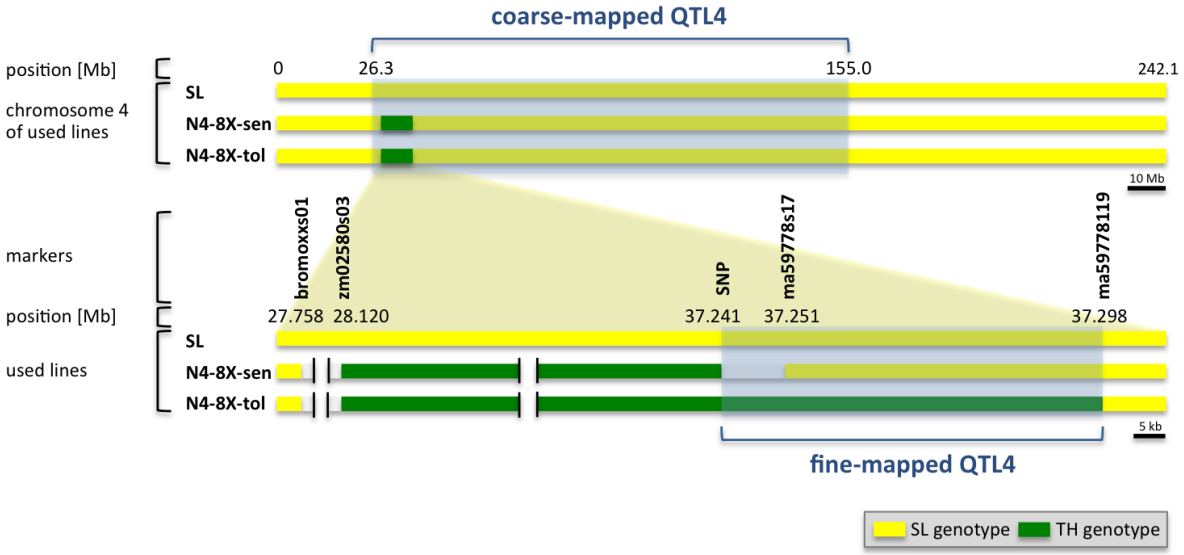

Figure 1: Locations of the coarse- and fine-mapped QTL4 in the analysed lines
Schematic display exhibiting the locations of the coarse- and fine-mapped QTL4 in the chilling sensitive inbred line SL, the susceptible NIL N4-8X-sen and the tolerant NIL N4-8X-tol. The upper panel shows for each line the genotype of chromosome 4. Yellow marks the SL genotype, green the genotype of the tolerant inbred line TH. The pale blue box highlights the location of QTL4 that was coarse-mapped by Presterl *et al*. (2007). This region comprises about 129 Mb. The lower panel illustrates in more detail the parts of chromosome 4 containing the TH introgressions. Both NILs differ in a segment of nearly 60 kb. This segment corresponds to the fine-mapped QTL4. Note the different size of scale bars.

Consequently, this comes down to the questions which gene or locus within the QTL4 region is the actual QTL4, how it is regulated and how it affects chilling tolerance. To establish whether differences in RNA abundance between the TH allele and the SL allele of the QTL4 are responsible for the chilling tolerance, an analysis of the transcriptome could be supportive. RNA-seq experiments allow the simultaneous and quantitative analysis of the expression of thousands of gene transcripts. Transcriptome data obtained from microarray already provided deep insight into the transcriptome changes of maize lines during chilling stress (e.g. Sobkowiak *et al.* (2016), Sobkowiak *et al.* (2014), Trzcinska-Danielewicz *et al.* (2009)). Furthermore, candidate genes for chilling tolerance of maize and for various QTLs were identified by transcriptomics (Sobkowiak *et al.* 2014).

Therefore, we relied on RNA-seq to achieve two goals of our study: (1) We assessed the response of the recurrent parent SL to chilling stress to get a general idea of the expression behaviour of this breeding material. SL was chosen since high grades of homozygosity should prevent perturbing effects originating of heterozygous loci. (2) Subsequently, we analysed the expression differences of N4-8X-tol and N4-8X-sen in the QTL4 region and of the whole genome. As those two lines differ only in the QTL4 region, they provide a good starting position to unravel the molecular basis of QTL4.

Results

Experimental design of the study

For the RNA-seq experiment, we chose three lines (Figure 1): SL, the recurrent parent of the NILs, for global analysis of chilling response, and the two NILs N4-8X-tol and N4-8X-sen. The introgressed genomic segments of TH in the NILs are each about 9.5 Mb in size and cover most of the distal part of the coarse-mapped QTL4. The TH introgression of the susceptible NIL is nearly 60 kb shorter. This region harbours the fine-mapped QTL4 (henceforward solely referred as QTL4).

The plants were grown in two separate but identical growth chambers. Each chamber contained the same set of plants. Thus, two individual experiments were performed simultaneously. The QTL4 has only an impact on the plant performance at low temperatures. Therefore, chilling stress was applied after two weeks of growth at optimal temperatures. The change in temperature should induce a change of the transcriptome between the two NILs that enables the investigation of QTL4. Furthermore, the drop in temperature should trigger a general chilling response that was analysed in SL. Since we focused on the primary response and not on acclimation, the low temperatures lasted only 24 h. The plant material was harvested according to the scheme in Figure 2: at the beginning of chilling (control, t0), after 4 h (t4) and after 24 h (t24).

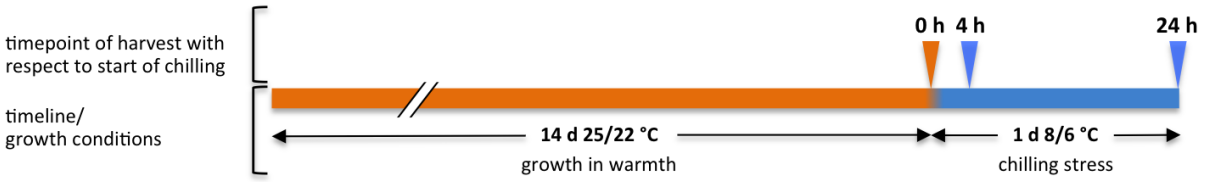

Figure 2: Growth conditions and experimental design
Illustration of the plant growth and harvest procedure. The plants of all three maize lines were grown together in a growth chamber in warmth for 14 d and then subjected to chilling stress. The harvest was performed for three timepoints: at the beginning of chilling (t0, control), after 4 h chilling (t4) and after 24 h (t24). The second experiment was performed in a second growth chamber of the same type at the same time

In order to study the transcriptome of both shoots and roots individually, aerial parts without the first leaf (shoot samples) and roots minus the kernel (root samples) were harvested separately. From the RNA preparations of these samples, libraries were prepared and RNA-seq was performed.

Reorganisation of the transcriptome of the chilling sensitive maize line SL in response to chilling stress

Changes in the global signature of highly abundant transcripts during chilling stress

It was one objective to analyse the changing response of SL to 4 h and 24 h exposition to chilling stress. To get an overview, the unique and shared transcripts of significantly differential abundance were visualised in Venn diagrams for both chilling periods (Figure 3).

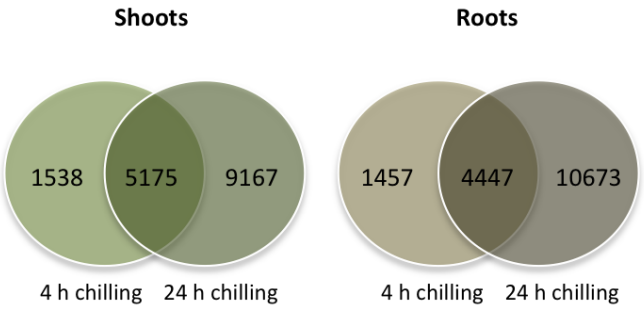

Figure 3: Quantification and comparison of differential gene expression
Venn diagrams showing the numbers of transcripts displaying differential abundance in the shoot and root samples of SL after 4 h and 24 h chilling in comparison to the control (0h). The transcripts exhibiting a FDR *p*-value correction with the cut-off of 0.05 were subjected to analysis.

As expected, the exposition of the SL plants to low temperatures drastically changed the transcriptional program. Compared to 4 h chilling, differential gene expression was strongly pronounced after prolonged chilling. Most of the transcripts of differential abundance after the first 4 h under chilling stress exhibited also differential abundance after 24 h chilling. This indicates that the associated genes are chilling-responsive. The other transcripts probably show circadian variation. There were only slight differences in the numbers of transcripts between shoot and root transcriptomes.

Furthermore, we evaluated the high abundance transcripts and their functions in the SL shoots and roots. Thereby, we achieved a first insight into the gene expression of SL. All transcripts with a RPKM mean of ≥ 500 were assigned to the major MapMan (Thimm *et al.* 2004) gene categories (Figure 4).

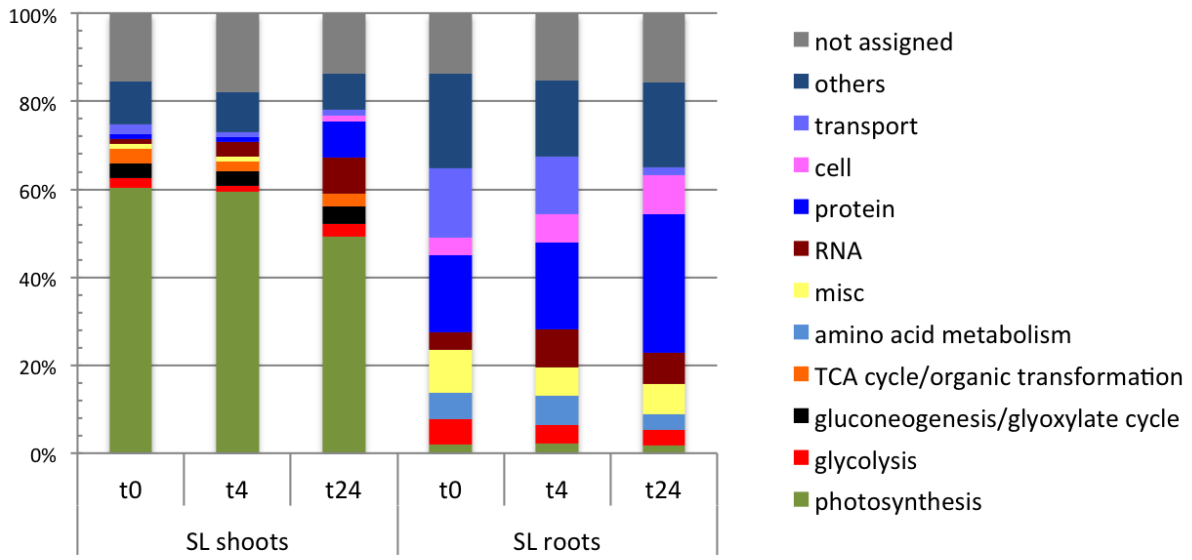

Figure 4: Distribution of high abundance transcripts of the shoot and root samples over time
Percentage distribution of transcripts with RPKMs ≥ 500 assigned to the major MapMan categories. The category "photosynthesis" contains transcripts associated with components of the light reaction, the Calvin-Benson-Bassham cycle and the photorespiration. "Glycolysis", "gluconeogenesis/glyoxylate cycle" and "TCA cycle/organic transformation" comprise transcripts for enzymes catalysing these pathways and cycles. The category "amino acid metabolism" encompasses transcripts encoding enzymes responsible for the synthesis and degradation of amino acids. "Misc" is a category containing transcripts that serve many purposes; in this case they encode Ferredoxin/Rieskedomain proteins, protease inhibitor/seed storage/lipid transfer protein (LTP) family proteins, plastocyanin-like proteins and glutathione S-transferases. "RNA" encompasses transcripts related to RNA-processing, (regulation of) transcription and RNA binding. "Protein" is a broad category and encompasses transcripts responsible for amino acid activation, protein synthesis, protein targeting, diverse (post) translational modification processes, degradation and folding. "Cell" is associated with the organisation of the cells, the cell cycle, division and cell death but also vesicle transport. The category "transport" is very diverse and contains transcripts encoding many different specialised transporters of the cell and organelles like aquaporins etc. "Others" combines all remaining major Mapman categories which exhibited only few hits.
TCA, tricarboxylic acid cycle

Concerning the shoots, the category "photosynthesis" draws attention at first. The amount of photosynthetic transcripts did not decrease after the first 4 h chilling but the category's percentages declined after persistent chilling. The reduction of photosynthesis during prolonged chilling stress was expected; similar findings were also made in rice varieties subjected to low temperature stress (Yang *et al.* 2015, Zhao *et al.* 2015). Contrastingly, the fractions of transcripts associated with transport processes declined during the last 20 h chilling stress in SL roots. Also this response is not uncommon since several studies indeed indicated a downturn of transport processes due to chilling (e.g. Chen *et al.* (2015), Shabala and Shabala (2002), Sowinski *et al.* (1998)). Interestingly, both organs shared responses: the increase of the categories "RNA" and "protein" over time. It seems that low temperature affected gene expression processes and their regulation in shoots and roots. As a comparison and to consolidate the results, we searched for gene ontology (GO) categories enriched in transcript subsets that comprised those being significantly increased or decreased in

abundance (Supplemental Table 1). This analysis confirmed all previous results and also suggested a pivotal role for transcription factors in the chilling response. Additionally, we found an enrichment of the GO category “regulation of cellular process” during the first 4 h chilling in both categories. This category comprises many aspects, for example signal transduction, phytohormone secretion and signalling as well as redox homeostasis. Altogether, the results specified which aspects should be analysed in more detail.

Evaluation of transcripts related to regulation, signalling and the redox system

We have observed that chilling stress profoundly changed the transcriptional landscape. In both examined organs, we identified changes related to diverse regulatory and protection processes using MapMan (Figure 4) and GO enrichment (Supplemental Table 1). Subsequently, we wanted to draw a more comprehensive picture and used MapMan to identify and visualise single transcripts related to the above-mentioned pathways. Those transcripts exhibited moderate to strong changes in abundance during chilling. The shortened graphical output of the most relevant categories is shown in Figure 5, the complete data in Supplemental Figure 1. Most strongly regulated transcripts are listed in Supplemental Table 2.

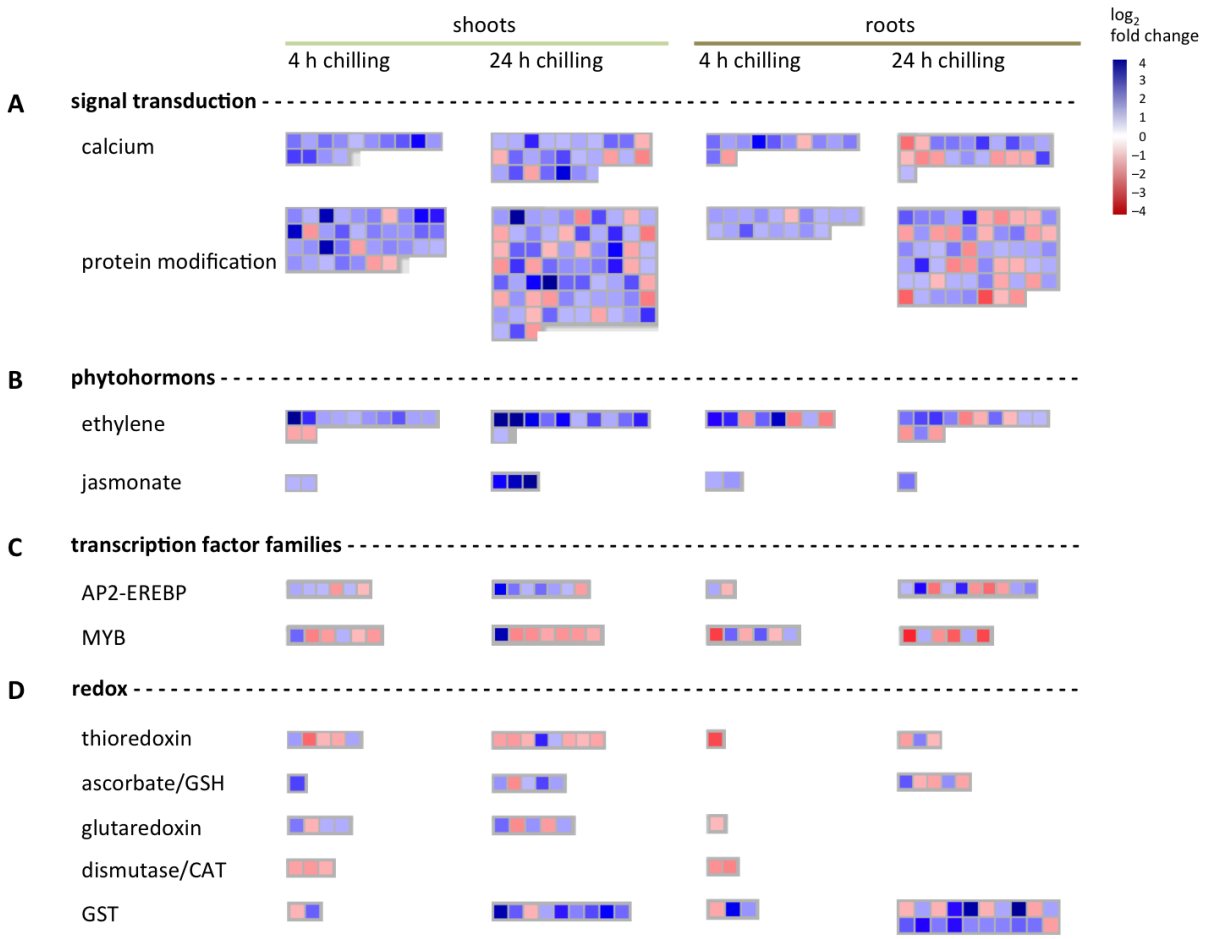

Figure 5: Differential abundance of transcripts related to regulatory and protection processes
Transcripts exhibiting an increase or decrease in abundance after exposure to 4 h and 24 h chilling were assigned to selected subsets of the MapMan categories. Each box represents one transcript. The colour or the boxes designates the degree of differential abundance. Blue indicates an increase in abundance, red a decrease in abundance.
(A) Transcripts related to signal transduction. The bin "signalling.calcium" (calcium) comprises transcripts associated with calcium signalling components. The bin "posttranslational modification" (protein modification) encompasses transcripts encoding diverse protein kinases and phosphatases.
(B) Transcripts of the bin "hormone metabolism". This bin encompasses transcripts related to synthesis, degradation, regulation and the output of given phytohormones.
(C) Transcripts of the bin "regulation of transcription". This bin contains diverse transcription factor families and their members.
(D) Transcripts of the bins "redox" and "glutathione S-transferases". The bins comprise transcripts associated with diverse enzymes and mechanisms that protect against oxidative stress.
Only transcripts with a FDR *p*-value correction ≤ 0.05 and a $\log_2$ fold change of ≥ 1.5 or ≤ –1.5 were considered for analysis.
GSH, glutathione; CAT, catalase; GST, glutathione S-transferase

The results draft a rough picture of the integration and output of chilling response in SL. It seems that signal transduction was strongly affected and upregulated by chilling (Figure 5A, Supplemental Figure 1A). Calcium signalling and various kinases that are commonly induced by low temperature stress (Heidarvand and Amiri 2010, Huang *et al.* 2012, Shi *et al.* 2015, Yadav 2010, Ye *et al.* 2016) might have mediated the signal transduction. In more detail, calcium signalling comprised enhanced quantity of transcripts encoding diverse calcium-

binding proteins, calmodulin-binding proteins (CBPs) and to a lesser extent calcium-transporting ATPases and kinases. The transcripts related to protein modification mostly encoded various types of protein kinases like MAP kinases, receptor-like kinases but rarely protein phosphatases. Downstream of the cascades, the phytohormone network might operate, which is another general response of chilling and cold stress (Kazan 2015, Shi *et al.* 2015). We found evidences for a complex phytohormone response (Figure 5B, Supplemental Figure 1B). In shoots and roots, the change of abundance largely implied a strong upregulation of ethylene synthesis and active ethylene signalling. Contrastingly, the level of active gibberellin was probably reduced in shoots after 4 h and 24 h chilling as suggested by the increased abundance of presumable gibberellin 2-oxidase transcripts (GA2ox, misplaced in the ethylene bin, see also Table 1). The accumulation of certain transcripts in shoots and roots after 4 h and 24 h exposure to chilling suggested an upregulation of jasmonic acid synthesis. Also a decrease of methyl jasmonate formation in shoots at both chilling phases could be implied. Phytohormone or calcium signalling subsequently might have led to a differential expression of transcription factor genes. A strong expression change of many transcription factors of diverse families was induced by low temperature (Figure 5C, Supplemental Figure 1C). Of particular interest are the AP2-EREBP and MYB transcription factor families since they contain players of different chilling-induced regulons, which in turn control and direct the chilling response output (Baldoni *et al.* 2013, Gilmour *et al.* 1998, Park *et al.* 2010). The MYB transcription factors transcripts exhibited a trend to a decrease in abundance whereas the AP2-EREBP transcripts tended to increase in abundance, with the exception of the 24 h chilling phase in roots. The output of these cascades might have led to the manipulation of the redox homeostasis. Chilling stress induces oxidative stress with elevated reactive oxygen species (ROS) levels that can be detrimental to the plants (Prasad 1996, Prasad *et al.* 1994). MapMan analyses (Figure 5D, Supplemental Figure 1D) revealed a striking increase in abundance of numerous glutathione S-transferase (GST) transcripts. Conversely, transcripts commonly associated with redox regulation and ROS scavenging exhibited only slight differential abundance or even a drop in quantity. In general, the roots showed less differential expression of genes associated with redox homeostasis (with the exception of *GST* genes). But certainly, the roots were not exposed to light.

Assessment of transcripts most responsive to chilling

We already assessed chilling-dependant changes of the transcript abundance of transcripts related to various pathways and functions. In order to detect other putative important

transcripts, we concentrated on transcripts that show the strongest changes in abundance evoked by chilling in SL. We chose the $\log_2$ fold changes of ≥ 4 and ≤ –4 (fold change 16) as cut-offs. A selection of transcripts of particular interest is shown in Table 1; the complete results are listed in the Supplemental Table 3 and visualised in the Supplemental Figures 3 and 4.

Table 1: Transcripts of SL shoot and root samples most responsive to chilling
Displayed is a selection of significantly differentially expressed transcripts (FDR *p*-value correction ≤ 0.05) exhibiting a $\log_2$ fold ($\log_2$ fc) change of ≥ 4 or ≤ –4. These are differentiated between 4 h and 24 h chilling stress. If no annotation for a transcript was available, the corresponding ortholog of *Oryza sativa* ssp. *japonica* or *Arabidopsis thaliana* is specified. The locations of transcripts are displayed in Mb; first number indicates the respective chromosome. The transcripts regulated in shoots are highlighted in green, those in the roots in brown.

	Transcript ID	Location	Name/Ortholog	$\log_2$ fc	*p*-value
4 h chilling	GRMZM2G018375_1	8:137.6	THI1-1 Thiamine thiazole synthase 1, chloroplastic	6.177	8.4E–73
$\log_2$ fc ≥ 4	GRMZM2G018375_2	8:137.6	THI1-1 Thiamine thiazole synthase 1, chloroplastic	4.474	2.5E–80
	GRMZM2G006964_1	2:28.3	Uncharacterized protein OS04G0522500 gibberellin 2-beta-dioxygenase 8	4.362	4.0E–59
	GRMZM2G081949_1	7:158.9	Uncharacterized protein OS07G0569100 OsREM4.1 Remorin 4.1 (Gui *et al.* 2016)	4.087	3.1E–31
	GRMZM2G074097_1	3:218.9	THI1-2 Thiamine thiazole synthase 2, chloroplastic	4.054	9.8E–119
24 h chilling	GRMZM2G018375_2	8:137.6	THI1-1 Thiamine thiazole synthase 1, chloroplastic	5.840	6.9E–110
$\log_2$ fc ≥ 4	GRMZM2G018375_1	8:137.6	THI1-1 Thiamine thiazole synthase 1, chloroplastic	4.683	2.7E–54
	GRMZM2G006964_1	2:28.3	Uncharacterized protein OS04G0522500 gibberellin 2-beta-dioxygenase 8	4.642	5.7E–63
	GRMZM2G022679_1	3:196.1	unknown OS01G0757200 gibberellin 2-beta-dioxygenase	4.353	2.6E–22
	GRMZM2G074097_1	3:218.9	THI1-2 Thiamine thiazole synthase 2, chloroplastic	4.196	7.1E–123
	GRMZM2G086763_1	5:19.4	Chloroplast post-illumination chlorophyll fluorescence increase protein	4.080	4.0E–85
$\log_2$ fc ≤ –4	GRMZM2G177229_5	7:133.5	Zm-U2AF35a (Fouquet *et al.* 2011)	–4.046	4.1E–64
24 h chilling	GRMZM2G018375_2	8:137.6	THI1-1 Thiamine thiazole synthase 1, chloroplastic	5.101	7.9E–40
$\log_2$ fc ≥ 4	GRMZM2G044383_2	1:81.7	Glutathione S-transferase GST 30; Uncharacterized protein OS10G0530900 GSTU6 Probable glutathione S-transferase GSTU6	4.323	1.1E–85
	GRMZM2G074097_1	3:218.9	THI1-2 Thiamine thiazole synthase 2, chloroplastic	4.132	5.5E–66
$\log_2$ fc ≤ –4	GRMZM2G136032_1	9:6.4	PIP1-6 Aquaporin	–5.467	4.9E–181
	GRMZM2G177229_5	7:133.5	Zm-U2AF35a (Fouquet *et al.* 2011)	–4.083	1.3E–24

In general, transcripts exhibiting a strong increase in abundance during both chilling phases were more prominent than those displaying a decrease. Furthermore, several transcripts exhibited differences in abundance in shoots as well as in roots, demonstrating that those organs share mechanisms for stress responses. The expression patterns of transcripts that showed an increase in quantity during the first 4 h chilling in both organs resembled mostly expression patterns of circadian regulated genes (Supplemental Figures 3 and 4). However, many of them exhibited expression values that did not reach the same level at t24 as at t0. This indicates a possible dysfunction of the circadian clock. Disturbances of the circadian system by low temperature stress have been demonstrated for Arabidopsis and maize before (Sobkowiak *et al.* 2014, Trzcinska-Danielewicz *et al.* 2009, Bieniawska *et al.* 2008, Espinoza *et al.* 2008, Espinoza *et al.* 2010). Several identified transcripts reflected also the results of the previous sections, e.g. GA2oxs transcripts or a transcript encoding a GST. Interestingly, a

transcript encoding an aquaporin displayed an increase in quantity in the root samples after exposure to 24 h low temperature stress. This might be related to the presumable decrease in transport processes described in Figure 1 and Supplemental Table 1. Other transcripts are novel and provide new information. Remarkably, two thiamine thiazole synthetase genes (*THI1-1* and *THI1-2*) were strongly upregulated after 4 h (shoots) and 24 h chilling (shoots and roots). Conversely, GRMZM2G177229_5 encoding an ortholog of a rice splicing factor subunit experienced also a decrease in amount in both organs at prolonged chilling.

Comparison of transcriptomes of the chilling sensitive NIL N4-8X-sen and the chilling tolerant NIL N4-8X-tol

Principal component analyses of N4-8X-sen and N4-8X-tol

The QTL4 has a large effect on the early vigour and thus on chilling tolerance. How strong is the influence in genetic terms? A principle component analysis (PCA) should reveal to which degree QTL4 affects the global gene expression between the two NILs N4-8X-sen and N4-8X-tol (Figure 6).

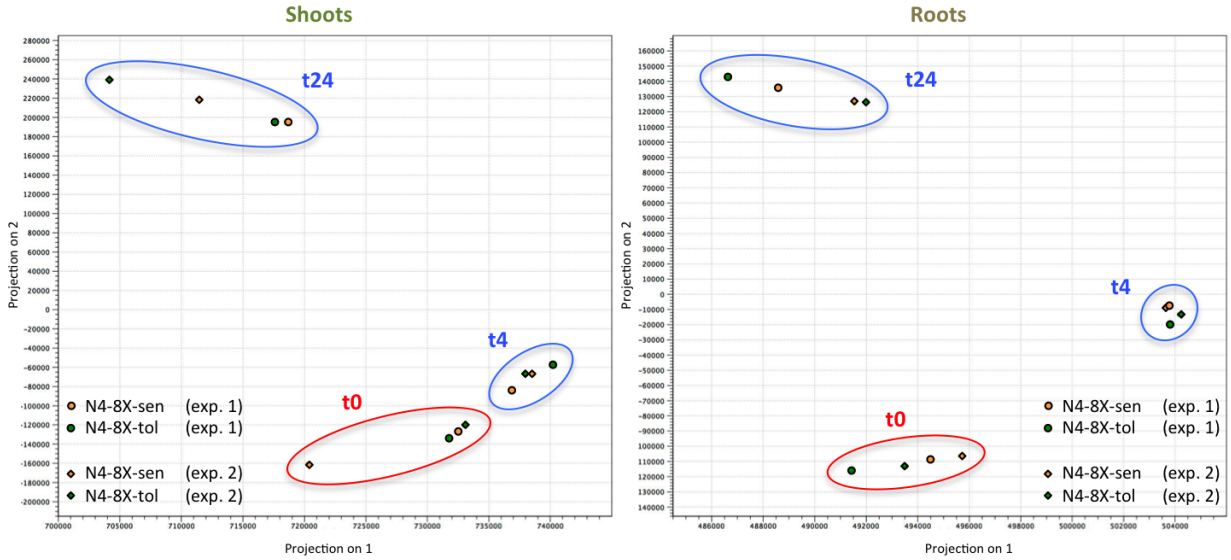

Figure 6: Principal component analyses of the N4-8X-sen and N4-8X-tol transcriptomes
Principal component analyses reveal scattering and clustering of the NIL transcriptome samples of both organs. The horizontal axis represents the principal component 1 and the vertical axis the principal component 2.
t0, timepoint 0 h chilling; t4, timepoint 4 h chilling; t24, timepoint 24 h chilling; exp., experiment

The transcriptome data of the sensitive and the tolerant NIL do not show substantive differences since they cluster together for each timepoint. This was expected as the NILs only differ in a nearly 60 kb long sequence which accounts for less than 0.003 % of the total genome. Additionally, the outcomes of the PCA analyses do not support the existence of a

master regulator in QTL4. This master regulator would have strongly influenced gene expression genome-wide, leading to the observed improved early vigour in N4-8X-tol. It seems that a different mechanism confers the chilling tolerance of N4-8X-tol.

Genome-wide evaluation of differential gene expression between N4-8X-sen and N4-8X-tol

We have shown that the transcriptomes of N4-8X-sen and N4-8X-tol do not differ much, even under chilling conditions. Subsequently, we presumed that no master regulator is active in QTL4. However, some variation must exist and might help to understand the effects of QTL4. We evaluated significant differential gene expression between the two NILs. 102 transcripts in the shoots and 111 transcripts in the shoots exhibited significant differences in abundance for at least one time point (available via attached SD memory card). In order to verify differential gene expression, each transcript was checked visually (Figure 7).

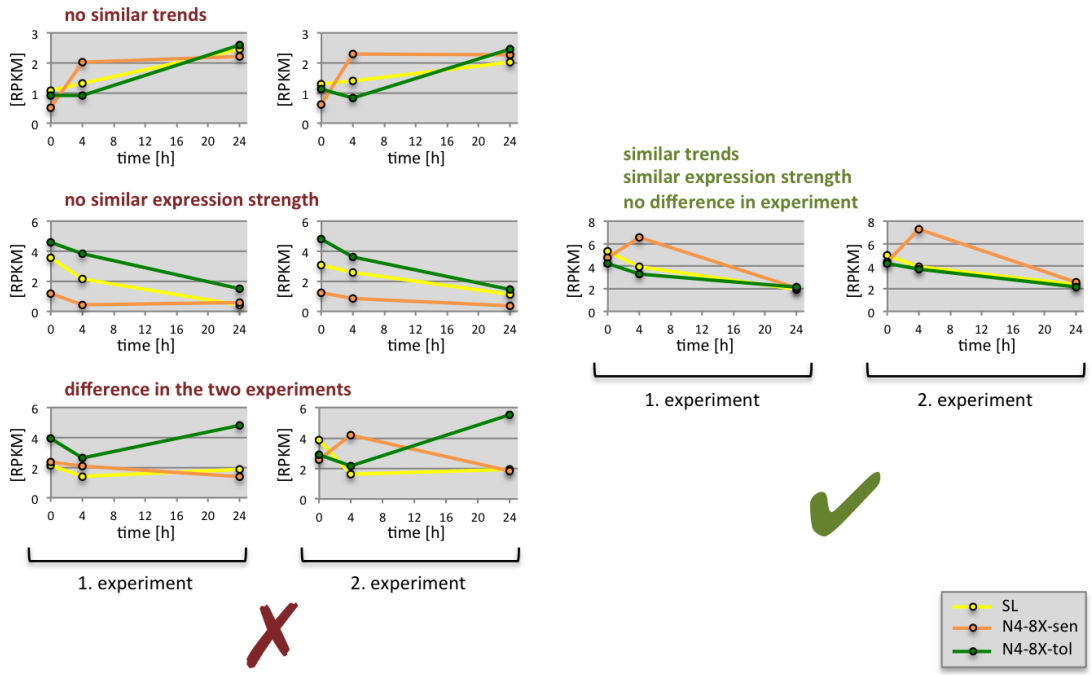

Figure 7: Criteria for distinguishing non-differential and true differential gene expression
Empirical analysis for differential gene expression takes only two comparative figures into account: the mean counts of the two lines for one given time point and not for all three time points. Therefore, three additional constraints, shown on the left-hand side panel, were set up to differentiate between non-differential and true differential expression. Firstly, SL as being chilling sensitive should have the same trend as N4-8X-sen and secondly also a comparable expression strength. Thirdly, trends for both experiments should be the same for all three analysed lines. The right-hand side panel displays an example fulfilling all constraints. The constraints were all checked visually for each transcript.

Between N4-8X-sen and N4-8X-tol, ten transcripts for shoot and 18 for root samples displayed significant differential abundance for at least one timepoint (Table 2, Supplemental Figure 5).

Table 2: Differential expression between the tolerant NIL N4-8X-tol and the sensitive NIL N4-8X-sen
Filtered outcomes of the empirical analysis of differential gene expression (DGE) of N4-8X-tol and N4-8X-sen at the three different time points. Shown are the $\log_2$ fold changes ($\log_2$ fc) and the FDR *p*-value corrections. Highlighted in green are differentially expressed transcripts of the shoot samples and in brown those of the root samples. *P*-values ≤ 0.05 are bolded. If no annotation for a transcript was available, the corresponding ortholog of *Oryza sativa* ssp. *japonica* or *Arabidopsis thaliana* is specified. The locations of transcripts are displayed in Mb; the first number designates the respective chromosome.

			t0		t4		t24	
Transcript ID	Location	Name/Ortholog	$\log_2$ fc	*p*-value	$\log_2$ fc	*p*-value	$\log_2$ fc	*p*-value
GRMZM2G377311_2	1:13.3	Uncharacterized protein OS12G0485400 Cyclin-T1-4	0.614	**0.014**	0.156	1.000	0.289	1.000
GRMZM2G127739_3	1:165.4	Unknown AT2G23460 EXTRA-LARGE G-PROTEIN1 ATXLG1	–0.273	0.799	0.364	1.000	0.993	**0.006**
GRMZM2G127739_2	1:165.4	Unknown AT2G23460 EXTRA-LARGE G-PROTEIN1 ATXLG1	0.857	**0.007**	–0.299	1.000	–0.969	**0.007**
GRMZM2G099328_4	1:167.0	Zinc ion binding protein	1.646	**0.003**	–0.021	1.000	0.240	1.000
GRMZM2G160184_3	2:114.8	Phosphoglycerate mutase-like protein; Uncharacterized protein AT1G58280 Phosphoglycerate mutase family protein	0.296	0.772	–0.591	0.911	–1.163	**0.000**
GRMZM2G122762_1	3:222.7	unknown OS01G0594500	–1.222	**0.000**	–1.046	**0.001**	–0.307	0.122
GRMZM2G110192_1	4:159.7	Uncharacterized protein OS02G0704000 9-cis-epoxycarotenoid dioxygenase 1	–0.582	**0.026**	–0.102	1.000	–0.182	1.000
GRMZM2G420812_1	4:37.2	SAUR31-auxin-responsive SAUR family member	–1.063	**0.047**	–0.396	1.000	–0.545	0.498
GRMZM2G173756_3	7:79.0	ZmUBC52 Ubiquitin conjugating enzyme 52 (Jue *et al.* 2015)	0.819	0.377	1.479	**0.001**	1.124	**0.010**
GRMZM2G085254_3	8:14.2	IWS1 family protein; Uncharacterized protein AT1G32130 ATIWS1, HIGH NITROGEN INSENSITIVE 9, HNI9	–1.165	**0.010**	0.296	1.000	0.264	1.000
GRMZM2G156486_3	1:15.9	ω-Amidase protein (Ellens *et al.* 2015)	–1.193	**0.008**	–1.685	**0.000**	–0.891	0.165
GRMZM2G171111_3	1:194.2	Uncharacterized protein OS06G0112200 Methylthioadenosine/S-adenosyl homocysteine nucleosidase	–1.444	**0.008**	–0.409	1.000	–0.305	1.000
GRMZM2G144995_2	1:60.2	Uncharacterized protein OS03G0352300 Nucleolar protein Nop56, putative, expressed	0.830	**0.010**	–0.028	1.000	–0.210	1.000
GRMZM2G057044_1	3:164.4	Uncharacterized protein OS01G0909150 histone deacetylase HDT2-like	0.599	0.549	0.732	0.053	0.611	**0.022**
GRMZM2G054811_3	3:191.2	Uncharacterized protein OS01G0778700 vacuole membrane protein KMS1	–0.256	1.000	0.901	**0.020**	–0.050	1.000
GRMZM2G121878_2	3:215.5	Carbonic anhydrase CA1 (Studer *et al.* 2014)	0.106	1.000	0.250	1.000	1.380	**0.025**
GRMZM2G061695_2	3:219.4	ZmGR2c protein	0.267	1.000	0.170	1.000	0.814	**0.030**
GRMZM2G000510_1	4:0.03	ZmPUMP (Brandalise *et al.* 2003)	–0.890	**0.004**	–0.951	**0.001**	0.304	1.000
GRMZM2G059618_3	4:67.6	Uncharacterized protein OS08G0270200 nuclear nucleic acid-binding protein C1D	0.954	**0.004**	0.888	**0.015**	0.858	**0.010**
GRMZM2G143627_2	5:215.7	Tubulin folding cofactor A (KIESEL)	0.770	0.847	1.234	0.327	1.426	**0.048**
GRMZM2G108355_1	5:3.6	Serine/threonine-protein phosphatase	–0.930	0.278	0.390	1.000	–1.372	**0.015**
GRMZM2G083076_1	5:45.4	Uncharacterized protein OS01G0511300 Putative 26S proteasome subunit RPN9b; Uncharacterized protein	0.604	**0.009**	0.333	1.000	0.284	0.792
GRMZM2G134284_1	7:174.8	Unknown AT5G01400 ENHANCED SILENCING PHENOTYPE 4 ESP4	0.585	**0.006**	0.409	0.349	0.606	**0.001**
GRMZM2G047732_2	8:39.1	Polyubiquitin-like protein isoform 1; Polyubiquitin-like protein isoform 2	1.185	**0.035**	1.555	**0.001**	1.652	**0.000**
GRMZM2G047161_2	8:39.1	Uncharacterized protein AT5G30490	0.091	1.000	–2.231	**0.000**	–3.082	**0.000**
GRMZM2G047161_4	8:39.1	Uncharacterized protein AT5G30490	0.013	1.000	0.180	1.000	0.846	**0.000**
GRMZM2G416644_2	9:91.9	Uncharacterized protein ?	1.079	**0.008**	1.086	**0.016**	0.849	**0.005**
GRMZM2G097289_2	10:89.2	Chromatin complex subunit A; Uncharacterized protein AT3G06010 CHROMATIN REMODELING 12 CHR12	–0.281	0.953	–0.231	1.000	–0.546	**0.048**

No transcript was found in both shoot and root subsets. This is interesting as it indicates that chilling tolerance might rely on specific differential gene expression in one part of the plant.

The genes encoding the detected transcripts are situated on all maize chromosomes with the exception of chromosome 6. Four of them are located on chromosome 4. Interestingly, one of these transcripts belongs to the only gene located in the QTL4 region and exhibited significant differential abundance for t0 in the shoot samples. This transcript encodes the small auxin-up RNA protein SAUR31 (GRMZM2G420812) and might be a good candidate gene for chilling tolerance. However, the gene was expressed on a low level. Moreover, regarding the functions of the gene products which were determined by annotations, known roles of orthologs or annotated domains, more than one third of the transcripts are associated with gene expression processes. These include chromatin remodelling, (regulation of) transcription, RNA processing and protein turnover. It seems that the differential regulation of gene expression is one aspect of chilling tolerance.

qRT-PCR analyses of the candidate gene and adjacent genes

The preceding analysis revealed that the only gene located in QTL4 was significantly differentially expressed. Field experiments of the used NILs and other NILs with even shorter introgressed genomic TH sequences as well as the outcomes of this transcriptome analysis support the hypothesis that this gene, *SAUR31*, is the actual QTL4. Therefore, the gene was renamed to *kühleempfindlich-1* (*ke-1;* Karin Ernst, personal communication). However, due to the low expression levels of *ke-1*/*SAUR31*, verification of the expression trends and level was required. We evaluated the expression of *ke-1* and three adjacent genes in the shoots by means of qRT-PCR (Figure 8). *GST26* was the only other adjacent gene exhibiting differential, albeit not significant gene expression in the RNA-seq experiment. The other two genes, *ETIF3SU4* and *ACR8* displayed no changes and served together with *GST26* as a control.

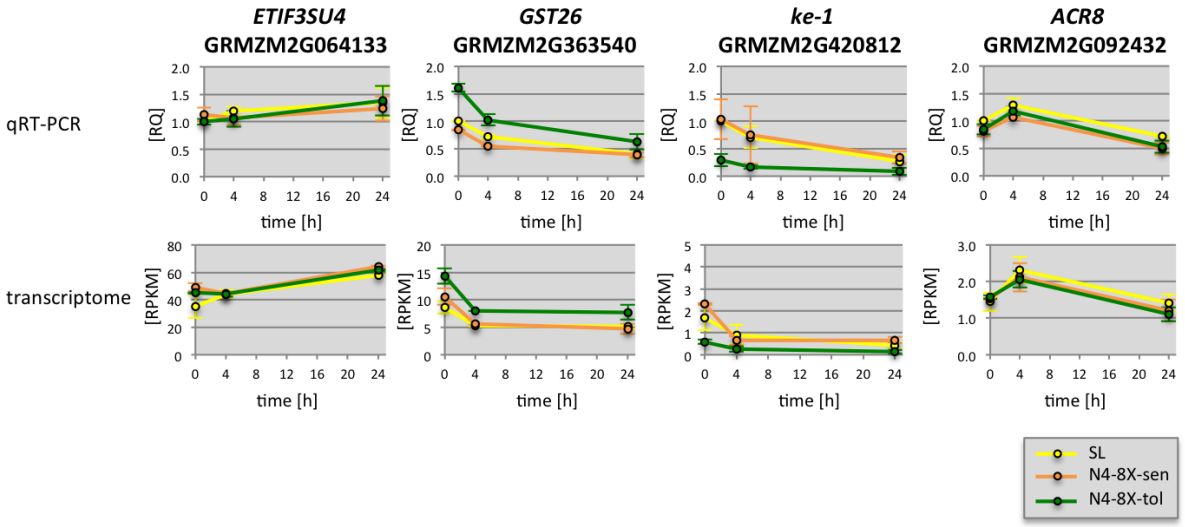

Figure 8: Changes of RNA-abundance of *ke-1* and adjacent genes determined by RNA-seq and qRT-PCR
Expression patterns of four genes analysed via transcriptome and qRT-PCR. The *ke-1* gene is the only gene located in the QTL4 region. *ETIF3SU4* and *GST26* are directly upstream of *ke-1* located, *ACR8* nearly directly downstream. The expression values in terms of the RPKM or the RQ values, respectively, are plotted against the time. The error bars show the standard variation.
RQ, relative quantification; *ETIF3SU4*, eukaryotic translation initiation factor 3 subunit 4; *GST26*, glutathione S-transferase 26; *SAUR31*, small auxin-up RNA 31; *ACR8*, ACT domain repeat 8; RPKM, reads per kilobase per million mapped reads

The qRT-PCR results resembled those of the RNA-seq. The expression patterns were nearly identical (Figure 8) and the expression level correlated with each other (data not shown). There was also a significant correlation ($R^2 = 0{,}787$, $p < 0.0001$) between the qRT-PCR and RNA-seq data (Supplemental Figure 6). These outcomes demonstrate that *ke-1* is indeed differentially expressed and they additionally show that the transcriptome data are reliable, even those of low-abundance transcripts.

Discussion

Maize seedlings grown at low temperatures show a low photosynthetic efficiency in growth chambers (Fryer *et al.* 1995) and also – more importantly – in field experiments, resulting in a low dry matter yield (Stirling *et al.* 1991). Thus, chilling can compromise early vigour which is an important trait for maize breeders (Presterl *et al.* 2007, Trachsel *et al.* 2010). To support breeding, we studied the response of maize to chilling stress. For this purpose, we adopted the technique of RNA-seq to analyse the chilling response of three maize genotypes. We used the inbred line SL to get a general idea of the impact of low temperature stress on transcription of maize. Furthermore, we were interested in unveiling the mechanisms of chilling tolerance. We therefore selected two NILs with introgressed genomic segments of the chilling tolerant parent TH in the SL background. The tolerant NIL N4-8X-tol contains – in contrast to the

susceptible NIL N4-8X-sen – the TH allele of the QTL4. The seedlings of these lines were subjected to 4 h and 24 h chilling stress. Samples were obtained from aerial parts and roots to distinguish the organ-specific responses. The transcriptomes of these samples were sequenced. The exposure to chilling stress induced differential gene expression. Concerning SL, the number of transcripts exhibiting differential abundance was roughly double upon prolonged temperature stress. This was in compliance with a study conducted in rice where differential gene expression depending on the genotype and organ doubled or tripled from 3 h to 24 h cold stress (Yang *et al.* 2015). At the same time, our results contradicted a maize study, in which differential gene expression of leaves was approximately halved after 28 h at 14 °C when compared to 4 h chilling (Trzcinska-Danielewicz *et al.* 2009). However, we applied a more severe chilling stress. Concerning differential expression in roots and shoots, both parts of the plant showed similar amounts of transcripts displaying differential abundance. This was not in agreement with the rice study performed by Yang *et al.* (2015). In this study, both analysed genotypes exhibited higher differential gene expression in roots. But in contrast to our experiments, the rice plants were cultivated in hydroponic and only tested under cold conditions (and not chilling) (Yang *et al.* 2015). The differential gene expression in our experiment was further analysed by MapMan in order to visualise pathway-specific gene expression changes, and partly in a transcript-by-transcript manner. In case of the chilling response in SL, a detailed image of chilling-affected processes was obtained.

Chilling response of the susceptible maize line SL

Perception and integration of the chilling signal in SL

We have observed that chilling stress changed the mRNA abundance of calcium- and calmodulin-binding proteins and diverse kinases (Figure 5A, Supplemental Figure 1A). We therefore hypothesise that the chilling perception and signalling in SL involves calcium signalling. Ca^{2+} is an important second messenger not only in the cold response (Huang *et al.* 2012, Sanders *et al.* 2002, Shi *et al.* 2015). Furthermore, calcium signalling and kinase cascades link the chilling or cold signal perception and the *CBF* regulon (Huang *et al.* 2012, Marozsan-Toth *et al.* 2015, Shi *et al.* 2015, Ye *et al.* 2016). Surprisingly, there were no indications that the signal cascades stimulated the *CBF* regulon in our experiment. The *CBF* regulon is conserved between mono- and eudicots (Akhtar *et al.* 2012) and activates cold-responsive genes. It is regulated by ICE1 and consists of AP2-EREBP family members of the *DREB* subgroup, in Arabidopsis namely *CBF*/*DREB1A*, *CBF2*/*DREB1C* and *CBF3*/*DREB1B* (Akhtar *et al.* 2012, Gilmour *et al.* 1998, Shi *et al.* 2015). However, only several transcripts of

the DREB-A6 group were amongst the transcripts in the MapMan analysis but the maize orthologs of the aforementioned genes were not expressed at all. The already characterised and cold-regulated *ZmDREB1A* (GRMZM2G124037) gene (Qin *et al.* 2004) was also not expressed in shoots and roots. Riva-Roveda *et al.* (2016) showed that this gene was expressed in the cell division and elongation zones of maize leaves after one day chilling (10 °C day/4 °C night). Hence, one can presume that the *CBF* regulon was not active in SL. After all, only about 12 % of the genes responding to cold are regulated by the *CBF* regulon in Arabidopsis. Consequently, this implies the existence of other signalling components (Fowler and Thomashow 2002, Shi *et al.* 2015). This may also apply to SL and there were also hints that a different network was active in this maize line. Two transcripts encoding OsMYB4-like proteins, orthologous to the rice MYB4 transcription factor and its putative paralog OS02G41510, exhibited an increased abundance during the first 4 h chilling. GRMZM2G095904_1 was found in shoots and roots and GRMZM2G127857_1 in roots (Figure 5C, Supplemental Figures 1C and 2). The rice MYB4 (and possibly its paralogs) regulates independently of the *CBF* regulon a broad transcriptional network, partly in response to cold. The network includes many transcription factors related to stress but also those involved in growth and development. Moreover, genes associated with stress, redox homeostasis, signal transduction, detoxification, cellular communication and protein modifications are influenced by *MYB4* (Baldoni *et al.* 2013, Park *et al.* 2010). Strikingly, we observed similar responses in SL. A number of transcription factors genes associated with stress responses, like *WRKY* (Chen *et al.* 2012, Rushton *et al.* 2012) or *NAC* genes (Puranik *et al.* 2012), were strongly upregulated (Supplemental Figure 1C). In contrast, the typical output of the *CBF* regulon was missing. It is therefore not unreasonable to suggest that the MYB4 orthologs instead of the *CBF* regulon induced in SL downstream genes to cope with chilling stress.

Growth reduction in response to chilling

Chilling clearly affected the phytohormone synthesis and signalling (Figure 5B, Supplemental Figure 1B). Quite evident was the impact of low temperature on the ethylene synthesis and signalling. Both processes were possibly mostly enhanced, similar to a study in rice conducted by Yang *et al.* (2015). Ethylene has many functions, e.g. controlling and impeding growth in response to cold (Eremina *et al.* 2016). Consequently, ethylene probably contributed to the observed growth arrest of SL during chilling (compare also Addendum 1). This growth reduction could have been partially achieved by the regulation of orthologs of the

transcriptional co-activators found in the ethylene bin, *AtMBF1A* (GRMZM2G101480_5, decreased abundance after the first 4 h chilling in both organs; Supplemental Figure 2A/B) and *AtMBF1C* (GRMZM2G051135_1, increased abundance after 4 h exposition to chilling in shoots; Supplemental Figure 2A). The *CaMBF1* gene of pepper that is similar to *AtMBF1A*/*B* was shown to be supressed by cold, analogous to this study. When overexpressed in Arabidopsis, the plants displayed larger leaves and during cold stress severe leaf damage (Guo *et al.* 2014). Similarly, *AtMBF1C* controls leaf extension through cell expansion (Tojo *et al.* 2009). It might be that the maize orthologs have fine-tuned leaf growth in order to protect the plants against low temperature induced injuries.

Interestingly, also the other observed changes in gene expression concerning phytohormones might be associated with the growth arrest. We found an increased abundance of GRMZM2G081949_1, an ortholog of *OsREM4.1*, after 4 h chilling stress in SL shoots (Table 1, Supplemental Figure 3). *OsREM4.1* is one node for the cross-talk between abscisic acid (ABA) and brassinosteroids. The gene is induced by ABA and its product negatively regulates brassinosteroid signalling via suppression of an active OsSERK1/OsBRI1 complex. Plants overexpressing *OsREM4.1* exhibited a dwarf-like phenotype, which indicates that ABA signalling stunted the brassinosteroids-promoted plant growth (Gui *et al.* 2016). Conveniently, brassinosteroids, being responsible for diverse cell elongation and proliferation processes (Singh and Savaldi-Goldstein 2015), were presumably less synthesised and supressed in SL during chilling (Supplemental Figure 1B). This implicates that the action of ABA in SL inhibited the action of brassinosteroids through the *OsREM4.1* ortholog, which in turn repressed growth.

Furthermore, several transcripts encoding GA2oxs increased in quantity during chilling, a response commonly found in plants treated with low temperatures (Achard *et al.* 2008, Colebrook *et al.* 2014, Mao *et al.* 2017, Yang *et al.* 2015). Enhanced expression of GA2oxs leads to a reduction of bioactive gibberellins and thus to a stabilisation of DELLA proteins (Achard *et al.* 2008). A stabilisation of DELLAs subsequently triggers growth restriction (Achard *et al.* 2006, Jiang and Fu 2007), thus providing a fast answer to unfavourable environment conditions (Achard *et al.* 2006). A *DELLA* transcript that encodes Dwarf plant9 exhibited an increased abundance after the first 4 h chilling in SL shoots (GRMZM2G024973_1, $\log_2$ fold change: 1,510, Supplemental Figure 2A). Interestingly, the *D9-1* allele was reported to confer dwarfism of both Arabidopsis and maize plants when constitutively expressed (Lawit *et al.* 2010). Furthermore, synthesis of the gibberellin antagonist jasmonate (Wasternack 2014) was possibly increased (Figure 5B, Supplemental

Figure 1B). Jasmonate represses growth through suppression of mitosis and cell proliferation (Wasternack 2014). Enhanced jasmonate levels and upregulation of synthesis in response to low temperature have been reported in various studies (Du *et al.* 2013, Maruyama *et al.* 2014, Yang *et al.* 2015). Incidentally, jasmonate signalling suppresses expression of photosynthesis-related genes in Arabidopsis (Attaran *et al.* 2014, Chen *et al.* 2011). To conclude, the action of phytohormons might have supported the growth reduction in SL.

But not only phytohormons might have promoted growth arrest, also the U2 auxiliary factor 35a (ZmU2AF35a) was probably implicated. The major transcript exhibited a strong decline in abundance in both shoots and roots after 24 h low temperature stress (Table 1, Supplemental Figures 3 and 4). U2AF35S proteins are involved in pre-mRNA splicing (Black 2003, Pacheco *et al.* 2004). In contrast to Arabidopsis and maize (Fouquet *et al.* 2011), humans have only one *U2AF35* gene but alternative splicing gives rise to three isoforms (Pacheco *et al.* 2004). The knockdown of the isoform *U2AF35a* by RNAi in human HeLa cells results in a severe phenotype. The cells exhibit impaired proliferation and increased apoptosis rates. The authors proposed that a reduction of splicing proteins generally lead an arrest of the cell cycle (Pacheco *et al.* 2006), which might be transferred to SL.

Altogether, these finding strongly imply that SL actively encounters environmental stress with an arrest or reduction in growth, a response found in growth chamber and field experiments (Karin Ernst, personal communication). It was proposed that growth restriction enhances the survival of plants at adverse environmental conditions since the saved resources could be better invested in plant defence reactions. Moreover, smaller plants present a smaller target (Achard *et al.* 2006). In a study with European maize lines, a growth reduction was observed in response to chilling. However, plants rapidly restarted to grow during the recovery at warm temperatures. The authors suggested that the maize plants have entered a standby mode during chilling that enabled the plants to recover quickly during improved conditions (Riva-Roveda *et al.* 2016).

Photosynthesis, cyclic electron transport and energy supply during chilling

The prolonged chilling stress resulted in a decreased abundance of photosynthesis-related transcripts in SL (Figure 4, Supplemental Table 1). A similar reaction was observed in a cold tolerant rice variety: the GO term “photosynthesis” was significantly enriched among the downregulated genes, but not before 24 h and 48 h cold stress (Zhao *et al.* 2015). Furthermore, the photosynthetic capacity of two rice varieties started to decrease after 6 h cold treatment. In contrast to the susceptible variety, the cold tolerant variety exhibited

enhanced expression of glycolysis- and TCA cycle-related genes. The authors argued that these pathways provided the necessary ATP to compensate for the impaired photosynthesis (Yang *et al.* 2015). In the current study, the analysed high abundance transcripts did not indicate an upregulation of glycolysis or TCA in SL (Figure 4). Instead, we observed a strongly increased abundance of a transcript encoding the chloroplast post-illumination chlorophyll fluorescence increase (PIFI) protein (Table 1, Supplemental Table 3). The Arabidopsis ortholog PIFI (AT3G15840) possibly contributes to the control of electron donation of the plastid-encoded NAD(P)H-dehydrogenase (Ndh) complex (Peltier and Cournac 2002, Wang and Portis 2007). In bundle sheath chloroplasts of maize, the Ndh complex and photosystem I drive in concert cyclic electron transport to produce ATP (Darie *et al.* 2006). Consequently, a higher amount of the maize PIFI can thus lead to an increased Ndh complex activity. Subsequently, this would donate to the cyclic electron transport around photosystem I, resulting in an enhanced ATP supply that compensates for the downturn of photosynthesis.

ROS signalling and scavenging

Chilling induces accumulation of H_2O_2 in maize (Kingston-Smith *et al.* 1999) which causes oxidative damage of leaves (Pastori *et al.* 2000) through lipid peroxidation and oxidation of proteins (Prasad 1996). ROS are mainly produced in the mitochondria (Møller 2001) and chloroplasts (Foyer *et al.* 1994). But they are also involved in different pathways in response to abiotic stress and phytohormones (Bartoli *et al.* 2013, Maruta *et al.* 2012, Xia *et al.* 2015). We found some indications that ROS signalling was active in SL, for instance by the enhanced abundance of *ZmMKK4* transcripts after 4 h (roots) and 24 h (shoots) chilling stress (Figure 5A, Supplemental Figures 1A and 2). In a study conducted by Kong *et al.* (2011), this MAP kinase kinase gene was not only upregulated by cold but also by salt stress and H_2O_2, which indicates a connection to ROS signalling. Nevertheless, excess ROS need to be scavenged. The plants take advantage of the different ROS scavenging enzymes and the antioxidant system in order to dispose of these harmful molecules (Foyer and Noctor 2009, Noctor and Foyer 1998). Intriguingly, most transcripts that encode primary antioxidant enzymes, enzymes for recycling of reduced antioxidants and those necessary for the biosynthesis of antioxidants did not change in abundance or even decreased in our study (Figure 5D). These findings are similar to the outcomes of previous works conducted in rice and wheat. In these studies, it was shown that ROS scavenging largely depended either on GSTs or the glutathione system in general, respectively (Winfield *et al.* 2010, Zhao *et al.*

2015). We noted a strong upregulation of *GST* expression (Figure 5D, Supplemental Figure 1D) upon 24 h exposure to low temperatures in both organs. Since other studies implicate GSTs with the disposal of ROS (e.g. Dixit *et al.* (2001), Yang *et al.* (2014), Yang *et al.* (2016)) it is not unreasonable to suggest that GSTs also play a pivotal role in ROS scavenging in SL. Furthermore, transcripts encoding two thiamine thiazole synthases (THI1-1/2) displayed a strong increase in abundance in both organs of SL (Table 1, Supplemental Figures 3 and 4). Thiamine thiazole synthases are involved in thiamine biosynthesis (Belanger *et al.* 1995, Roje 2007). Thiamine (vitamin B_1) serves in form of thiamine disphosphate as a cofactor for metabolic enzymes but it is also important during stress (Goyer 2010). Increased levels of thiamine were observed in maize seedlings treated with water, salt and oxidative stress (Rapala-Kozik *et al.* 2008). Arabidopsis seedlings exhibited a higher thiamine content in response to cold stress. It was reported that a thiamine treatment decreased the levels of ROS. Intriguingly, the authors suggested that thiamine functions as an alternative antioxidant (Tunc-Ozdemir *et al.* 2009). The observed upregulation of the *THI1* genes indicates an accumulation of thiamine in SL plants during chilling. Therefore, thiamine might serve as an alternative antioxidant in SL, too.

QTL4 and chilling tolerance

A master regulator for chilling tolerance?

A number of studies have been conducted to evaluate the differential transcription between chilling/cold tolerant and susceptible plant lines and to discover the fundament of chilling/cold tolerance. In the study of Yang *et al.* (2015), several hundred genes were differentially expressed between two rice genotypes. One main aspect of cold tolerance was presumably a high expression of TCA cycle and glycolysis genes that compensate for downregulation of photosynthesis (Yang *et al.* 2015). In a Sorghum study, also several hundred genes were differentially expressed between two lines with contrasting susceptibility to chilling. Noteworthy were the differential expression of *GST* genes, cytochrome-like transcripts and transcription factors (Chopra *et al.* 2015).

These studies are not consistent with our finding. We used two NILs with contrasting chilling tolerance that differ only in a nearly 60 kb segment, the fine-mapped QTL4. The QTL4 did not have a large effect on the transcriptomes. This finding was independent of the prevailing temperature. We merely found few transcripts with a significantly differential abundance with regard to the whole genome (Table 2). The PCA analyses of the transcriptome samples (Figure 6) supported these observations. For both organs, the

transcriptomes of the two NILs cluster together. These findings indicate that there does not seem to be a master regulator of transcription located and active in QTL4. A master regulator would be a gene or locus that has a great impact on the residual transcriptome and its output, like the *teosinte branched1* locus from maize that is able to drastically change the plant's architecture (Doebley 2004, Doebley *et al.* 1995).

Regulation of gene expression in N4-8X-sen and N4-8X-tol

We have evaluated the global mRNA abundance differences between the tolerant and the susceptible NIL. Interestingly, several of the detected transcripts showed constitutive differences between the lines, i.e. one NIL exhibited higher expression values for all three timepoints (Table 2, Supplemental Figure 5). Most of these transcripts were found in the root samples. Remarkably, many transcripts are associated with the regulation of gene expression and protein levels. These include GRMZM2G097289_2 that exhibit a higher abundance in N4-8X-sen and SL. The Arabidopsis ortholog is the ATP chromatin remodelling factor *CHR12*. Mlynarova *et al.* (2007) found out that the overexpression of *CHR12* resulted in an ABA-independent and reversible growth arrest of stems. The phenotype was independent of those mediated by DELLA proteins (Mlynarova *et al.* 2007). A similar but more severe phenotype was observed in tomatoes: overexpression of the tomato ortholog *SICHR* under non-stress conditions led to more compact seedlings, shorter roots and even smaller fruits (Folta *et al.* 2016).

The capability of plants to endure abiotic stress depends on their ability to adapt their proteome rapidly and efficiently to environmental cues. Not only the proteasome functions in the process but also the upstream ubiquitin system (Stone 2014). We found two components exhibiting a higher transcript abundance in N4-8X-tol compared to N-84X-sen and SL. GRMZM2G083076_1 is orthologous to the Arabidopsis *REGULATORY PEPTIDE NON-TRIPLE ATPASE 9B* (*RPN9B*) gene and the product is a component of the Arabidopsis 26S proteasome (Book *et al.* 2010). In tobacco, a reduced 26S proteasome activity mediated by the silencing of *RPN9B* triggered programmed cell death (Kim *et al.* 2003). Additionally, it was suggested that the cell division rates correlate with the 26S proteasome activity (Kurepa *et al.* 2009a, Kurepa *et al.* 2009b). Furthermore, we identified a transcript encoding the E2 conjugating enzyme ZmUBC52. Several studies demonstrate the importance of the ubiquitin system in the stress response. For example, high levels of ROS lead to the degradation of the translocon of the outer chloroplast membrane (TOC) complex mediated by the ubiquitin E3 ligase SSP. Consequently, the import into the chloroplasts declines and thus photosynthesis is

affected. This prevents further formation of ROS (Ling and Jarvis 2015, Ling and Jarvis 2016).

More transcripts exhibited differential mRNA abundance at normal and chilling conditions and thus might be associated with chilling tolerance, e.g. an ortholog (GRMZM2G134284_1) of the Arabidopsis ESP4 protein involved in pre-mRNA processing and alternative splicing (Herr *et al.* 2006, Misra and Green 2016, Misra *et al.* 2015) or a transcript (GRMZM2G059618_3) containing the Rrp47/DNA strand repair C1D domain (IPR011082) associated with RNA processing and DNA repair (Erdemir *et al.* 2002, Jackson *et al.* 2016, Mitchell 2010, Mitchell *et al.* 2003). Moreover, several transcripts associated with gene expression regulation displayed differential abundance only at exposure to low temperature stress. One of these is GRMZM2G047161_4 that exhibits an increase in quantity in in the roots of N4-8X-tol after 4 h and 24 h chilling. The transcript features a BCNT-C (IPR11421) and a SWR1-complex protein 5/Craniofacial development protein (IPR027124) domain (in contrast to GRMZM2G047161_4; Table 2). Bucentaur (BCNT) proteins are strongly conserved in animals and plants and are components of chromatin remodelling complexes (Messina *et al.* 2015). GRMZM2G047161 is an ortholog of *SWC5* and its product is a part of the chromatin remodelling complex SWR1 of Arabidopsis (March-Diaz and Reyes 2009). In this plant, the SWR1 complex exchanges the normal histone H2A with the variant H2A.Z (Berriri *et al.* 2016, Kumar and Wigge 2010, Messina *et al.* 2015). The activity of the SWR1 complex as well as the histone exchange are inherently connected with growth, development, adaption to the environment and pathogen resistance (Berriri *et al.* 2016). Intriguingly, H2A.Z was enriched after environmental stress in fission yeast (Sadeghi *et al.* 2011). In a further study, it has been shown that incorporation of H2A.Z is most important for the thermosensory response. In case of a non-functional SWR1 complex, the transcriptome resembled one induced by warm temperature – independent of the actual temperature (Kumar and Wigge 2010). Probably, N4-8X-tol might be superior to N4-8X-sen in perceiving and integrating temperature changes.

All in all, it seems that N4-8X-tol has already an advantage at non-stress conditions. This advantage can be mostly sustained during chilling stress and might buffer and attenuate the detrimental impact of low temperatures. The here-discussed transcripts indicate that N4-8X-tol has an improved capacity of gene expression and protein turnover coordination to withstand stress.

Root growth during chilling stress

Chilling stress of the maize shoots and roots triggered differential gene expression between the tolerant and the sensitive NIL. One transcript is associated with growth processes and was found in the root samples. GRMZM2G143627_2 encodes the tubulin folding cofactor A (KIESEL). The transcript exhibited a higher abundance in N4-8X-tol at prolonged chilling (Table 2, Supplemental Figure 5). In Arabidopsis, KIESEL is required for the α-β-heterodimerisation of microtubules and is essential in situations that require a rapid cell expansion (Kirik *et al.* 2002, Lu *et al.* 2010). Baluška *et al.* (1993) discovered that cold led to a reorientation and enhanced depolymerisation of microtubules in the elongation zones of maize roots. Presumably, the upregulation of *KIESEL* in N4-8X-tol enabled the plant to maintain the microtubule formation. Moreover, an enhanced growth can be implied. After all, microtubules are necessary for the normal plant growth since they are components of the interphase cortical array, pre-prophase band, mitotic spindle and the phragmoplast (Kirschner and Mitchison 1986, Lu *et al.* 2007). We hypothesise two theories why N4-8X-tol upregulated the KIESEL. Firstly, it is possible that a different growth program takes over at adverse environmental conditions. The pursued root growth results in a normal and adequate nutrient uptake. This might explain – at least partially – the improved early vigour of the tolerant NIL. Secondly, an upregulation of the genes can prepare the plant to resume normal growth after chilling stress. It was previously reported that two expansin genes were upregulated during chilling in the leaves of a maize hybrid (Riva-Roveda *et al.* 2016). These enzymes are likewise associated with growth processes (Goh *et al.* 2012). Yet, the stressed leaves ceased in growing. Riva-Roveda *et al.* (2016) argued that the maize plants entered a 'get ready to grow' state upon chilling stress. Their assumptions were supported by the plant's rapid resumption of growth during recovery (Riva-Roveda *et al.* 2016). We also observed a fast return to growth during recovery in growth chamber experiments (unpublished results). Possibly, N4-8X-tol has with regard to the growth uptake an advantage over the sensitive NIL. As we have hitherto concentrated in our experiments on the shoots and not on the roots, the role of the roots requires further investigations.

ke-1 *and other chilling tolerance regulation levels*

For elucidating the mechanism of the chilling tolerance mediated by the QTL4, we chose the tolerant NIL N4-8X-tol and the susceptible NIL N4-8X-sen that differ only in nearly 60 kb, the QTL4. The SAUR gene *ke-1* (and only this gene) is located in this section and hence is a possible candidate gene for chilling tolerance. The differential expression between the NILs

during and especially before chilling was confirmed by qRT-PCR and RNA-seq (Table 2, Figure 8). What are the functions and the role of *ke-1* in chilling tolerance? The *SAUR* family is the largest amongst the early auxin response gene families (Ren and Gray 2015). For instance, the maize genome contains 79 *SAUR* genes (Chen *et al.* 2014). The functions of the *SAUR* genes in general are diverse, but for some genes a growth-stimulating function has been reported (Chae *et al.* 2012, Li *et al.* 2015, Spartz *et al.* 2012, Spartz *et al.* 2014, Xu *et al.* 2017). However, *ke-1* has not yet been described. A subcellular localisation experiment of ke-1 strongly indicates that the protein is located in the mitochondria (Addendum 2). Many SAUR proteins are possibly targeted to this organelle (Chen *et al.* 2014, Huang *et al.* 2016, Wu *et al.* 2012, Xie *et al.* 2015), but none of these has been investigated in detail. Moreover, ke-1 seems to be quite unstable. A *ke-1-GFP*-fusion construct under control of the constitutive 35SCaMV promoter exhibited only very weak fluorescence signals (Addendum 2) and it was not possible to detect ke-1 with specific antibodies (unpublished results). Furthermore, *ke-1* might be regulated by auxin as its promoter contains an ARF-binding site with respect to B73 (Chen *et al.* 2014). However, the low expression of *ke-1* and the relative low amount of results concerning the expression analysis of N4-8X-tol and N4-8X-sen raise issues. How can a gene with such low mRNA levels and low protein stability affect the chilling tolerance? Moreover, the PCA negates the existence of a single master regulator. Is *ke-1* really the basis of the QTL4? Can the expression differences between the NILs explain the improved early vigour of N4-8X-tol? After all, we analysed only mRNA levels in this study. Since the last decade, miRNAs came to the fore. They are generally involved in biotic and abiotic stress response and might also be used to generate abiotic stress-resistant crops (Kumar 2014). Several studies in different plant species revealed that miRNAs are differentially expressed in response to chilling or cold stress (Cao *et al.* 2014, Chen *et al.* 2015, Lv *et al.* 2010). In a rice study, several putative miRNA targets have been identified (Lv *et al.* 2010). Intriguingly, genes with the same functions were differentially regulated in our study in SL: calmodulin binding proteins (Figure 5A, Supplemental Figure 1A), GSTs (Figure 5D, Supplemental Figure 1D, Table 1), a remorin (Table 1, Supplemental Table 3, Supplemental Figure 3) and abscisic stress-ripening proteins (Supplemental Table 3, Supplemental Figures 3 and 4). Moreover, most of the upstream sequences of the miRNA host genes exhibited phytohormone- or stress-related elements (Lv *et al.* 2010). The miRNA studies emphasise that this type of RNA is also involved in the chilling response of the investigated maize lines in this study and presumably also in chilling tolerance. But considering that miRNAs are only one of many regulatory mechanisms, the further studies on

QTL4 require diversified research. It is possible that an intricate regulatory network, consisting of many different genes regulated on many levels and by many ways, might confer the chilling tolerance.

Conclusion

Our extensive and genome-wide study of the maize inbred SL regarding the transcriptome provided a comprehensive insight into processes and pathways modulated by low temperatures. We have shown that the chilling stress rapidly stimulated differential gene expression in both shoots and roots. Many of the chilling-responsive transcripts are associated with the regulation of expression, signal transduction, phytohormone regulation and ROS signalling and scavenging. The obtained data suggest that SL actively suspended growth to endure the unfavourable phase. Similar to previous studies, a late downregulation of photosynthesis was observed and a perturbation of the circadian clock was indicated. Concerning the chilling tolerance mediated by the QTL4, a less deep insight was provided and the actual mechanism is still unclear. From the expression profiles of N4-8X-sen and N4-8X-tol, we suggest that the tolerant NIL has already an efficient expression regulation system at ambient temperatures. This system is largely maintained during less favourable conditions. The chilling stress also caused differential gene expression between the lines for several genes related to other various functions. The function of one identified transcript indicates that the roots of N4-8X-tol either changed to a different growth program or that the roots prepared for a quick reuptake of growth during chilling stress. The exact function of *ke-1*, the candidate gene for QTL4, requires further investigations. A role for *ke-1* as a master regulator was precluded.

Methods

Plant material and growth conditions

For the RNA-seq and qRT-PCR, the European inbred line SL and two different NILs were used (N4-8X-sen: TH-N4-8X x SL_211_006_00113_011 and N4-8X-tol: TH-N4-8X x SL_211_006_00113_003). All lines are property of the KS SAAT SE (Einbeck, Germany). Two independent experiments were performed simultaneously in two growth chambers. Plants were allowed to grow for 14 d at 25/22 °C (day/night). At this time, the third leaf was usually fully developed, i.e. the leaf blade was clearly bent from the auricle. Then, plants were subjected to 24 h chilling stress with temperatures of 8/6 °C (day/night). For both conditions,

light was applied for 14 h and the dark period stretched over 10 h. The light intensity for all experiments was adjusted to 350 to 400 µmol m^{-2} s^{-1}. The change of temperature occurred at 10:30 am for the first and at 11:00 am for the second experiment. Accordingly, the light period of the second experiment started 30 min later. The seedlings were grown in single square pots in Floraton 1 compost (Floragard Vertriebs GmbH, Oldenburg, Germany). The plant material was harvested directly before chilling (t0), at 4 h chilling (t4) and at 24 h (t24) chilling stress. Eight whole shoots (without the first leaf, "shoots") and eight whole roots (without kernel, "roots") per line and timepoint were harvested separately, resulting in a total of 36 samples. The roots were cleaned from soil in water of ambient temperature (t0) or in pre-cooled water (t4, t24) and quickly dried with paper towels. The plant material was immediately frozen in liquid nitrogen and stored at –80 °C until further use.

RNA isolation

The total RNA was isolated as described in Westhoff *et al.* (1991) and subsequently treated with DNase I (Thermo Fisher Scientific, Waltham, USA). The RNA was purified with a phenol/chloroform extraction, precipitated with NaAc and isopropyl alcohol and washed with 70 % ethanol. The pure RNA was then dissolved in RNase-free dH_2O. The quality was checked by means of agarose gels and the Agilent 2100 Bioanalyzer (Agilent Technologies, Santa Clara, USA) and the quantity using the NanoDrop (VRW Life Science Competence Center, Erlangen, Germany).

cDNA synthesis and qRT-PCR

1 µg total RNA per sample was used to generate cDNA with the QuantiTect® Reverse transcription Kit (Qiagen, Hilden, Germany). The qRT-PCR was conducted according to the manufacturer's instructions of the KAPA SYBR® Fast Mix (2X) Universal Kit using the Applied Biosystems® 7500 Fast Real-Time PCR System (Applied Biosystems, Foster City, USA). Specific oligonucleotides to GRMZM2G152466, encoding the tubulin α-4 chain, were used as an endogenous control. For each reaction, 5 ng (*ETIF3SU4*), 10 ng (*GST26*) or 25 ng (*ke-1*, *ACR8*) cDNA was used. For data analysis, the $2^{-\Delta\Delta CT}$ method was applied (Livak and Schmittgen 2001). All used oligonucleotides are listed in Supplemental Table 4. To determine the correlation with the transcriptome data, the Pearson R^2 and the corresponding *p*-value were calculated with Prism 6 (GraphPad Software, La Jolla, USA). The linear regression was visualised with the same program.

Library preparation and Illumina sequencing

For the library preparation, the total RNA was set to 1 µg in a total volume of 50 µL for each sample. The Illumina cDNA library construction was generated with the TruSeq® RNA Sample Preparation Kit v2 (Illumina, San Diego, USA) according to the Low Sample (LS) Protocol (TruSeq® RNA Sample Preparation v2 Guide, Part #15026495, Revision F, March 2010). The quality of the obtained libraries was tested with the Agilent 2100 Bioanalyzer (Agilent Technologies, Santa Clara, USA). The cluster generation was performed by the use of the TruSeq® SR Cluster Kit v3 (Illumina, San Diego, USA) with regard to the Reagent Preparation Guide of the Illumina cBot device. The single read sequencing was conducted with the Illumina HiSeq2500, using the TruSeq® SBS Kit v3 (Illumina, San Diego, USA). Between 30,128,980 and 45,857,003 reads per library were obtained from sequencing, whereas the percentages of reads with Q30 quality scores (Ewing and Green 1998) ranged from 87.30 % to 89.09 % (Supplemental Table 5). These values account for a good sequencing quality. The Agilent 2100 Bioanalyzer analyses, pooling of libraries, cluster generation and sequencing were conducted at the "Biologisch-Medizinisches Forschungszentrum" (BMFZ) of the HHU Düsseldorf.

Transcriptome mapping and data analysis

Following the quality control and processing, the Illumina reads were mapped to the *Zea mays* B73 AGPv3.24 transcriptome with the software CLC Genomics Workbench (Qiagen, Hilden, Germany) using standard parameters. The shoot and root samples were separately processed in two different experiments; further proceedings were conducted for both sets in the same way. The following procedures – as not stated differentially – were performed with CLC Genomics Workbench. The read counts were normalised to reads per million mapped reads and kb transcript length (RPKM). To filter for background, each transcript should have exhibited for at least one sample (out of 18) a RPKM ≥ 2. The total numbers of transcripts were thereby reduced from 62,892 to 31,939 for shoots and 32,221 for roots, respectively. The associated genes were considered as being expressed and thus these transcripts were subjected to the further analyses. For the principal component analysis (PCA), the read counts were normalised using the Quantile method. The Empirical analysis of differential gene expression (Robinson and Smyth 2008) that incorporates the EdgeR Bioconductor package (Robinson *et al.* 2010) was run with the non-normalised counts. The genes were considered as significantly differentially expressed when they exhibited a false discovery rate (FDR) *p*-value correction $\leq 0{,}05$. For the $\log_2$ fold change calculation, the absolute term 1 was added to the RPKM

means in order to prevent 0 values. These calculations were executed with Excel (Microsoft, Redmond, USA).

Global analysis with MapMan

In order to analyse individual SL transcripts of certain categories, we chose transcripts moderately to strongly responsive for the comparisons t0 vs. t4 and t0 vs. t24. Their genes exhibited significant differential gene expression during the chilling periods and transcript quantities showed $\log_2$ fold changes ≥ 1.5 and ≤ -1.5 (corresponding to fold changes of ≥ 2.8 and ≤ -2.8). Those were processed with MapMan (Thimm *et al.* 2004). A filter for *p*-values ≤ 0.05 was activated. The *Zea mays* mapping data (Zmays_181) were downloaded from http://mapman.gabipd.org/web/guest/mapmanstore.

Analysis of differential gene expression between the tolerant and the sensitive NIL

For analysing differential gene expression between the tolerant and the sensitive NIL, the transcripts of both organs that exhibited a significant differential gene expression (FDR *p*-value correction ≤ 0.05) for at least one time point were chosen. To verify the differential expression, the expression patterns of SL, N4-8X-sen and N4-8X-tol were checked visually with Excel. Apart from the constraints of the Empirical analysis of differential gene expression, three other constraints were set up (Figure 7). Firstly, as being both chilling sensitive, SL and N4-8X-sen should exhibit a similar trend and secondly display a comparable strength of expression. Thirdly, the trends for both experiments should be the same.

Enrichment analysis for gene ontology categories

For the global analysis of differential gene expression in SL, we chose the same subsets as for MapMan analysis (see previous section). The total amount of eight subsets was examined for a significant enrichment of gene ontology (GO) categories. The transcript IDs for each subsets were subjected to singular enrichment analysis (SEA) with the online tool agriGO (Du *et al.* 2010). The Fisher statistical test was applied with the Hochberg (FDR) multi-adjustment method. A cut-off of 0.05 was selected and five transcripts as the minimum number of mapping entries. The plant GO slim ontology type was chosen. The results were visualised with the cross comparison of SEA (SEACOMPARE) (Du *et al.* 2010) which conveniently displays the overrepresented GO categories for all data subsets within one table.

Literature

Achard, P., Cheng, H., De Grauwe, L., Decat, J., Schoutteten, H., Moritz, T., Van Der Straeten, D., Peng, J. and Harberd, N.P. (2006) Integration of plant responses to environmentally activated phytohormonal signals. *Science*, **311**, 91-94.

Achard, P., Gong, F., Cheminant, S., Alioua, M., Hedden, P. and Genschik, P. (2008) The cold-inducible CBF1 factor-dependent signaling pathway modulates the accumulation of the growth-repressing DELLA proteins via its effect on gibberellin metabolism. *Plant Cell*, **20**, 2117-2129.

Akhtar, M., Jaiswal, A., Taj, G., Jaiswal, J.P., Qureshi, M.I. and Singh, N.K. (2012) DREB1/CBF transcription factors: their structure, function and role in abiotic stress tolerance in plants. *J Genet*, **91**, 385-395.

Allen, D.J. and Ort, D.R. (2001) Impacts of chilling temperatures on photosynthesis in warm-climate plants. *Trends Plant Sci*, **6**, 36-42.

Attaran, E., Major, I.T., Cruz, J.A., Rosa, B.A., Koo, A.J., Chen, J., Kramer, D.M., He, S.Y. and Howe, G.A. (2014) Temporal Dynamics of Growth and Photosynthesis Suppression in Response to Jasmonate Signaling. *Plant Physiol*, **165**, 1302-1314.

Baldoni, E., Genga, A., Medici, A., Coraggio, I. and Locatelli, F. (2013) The OsMyb4 gene family: stress response and transcriptional auto-regulation mechanisms. *Biol Plant*, **57**, 691-700.

Baliashvili, N. (2010) Feinkartierung eines QTL (Quantitative Trait Locus) für Kühletoleranz auf Chromosom 4 in Mais und dessen molekularbiologische und phänotypische Charakterisierung. *PhD thesis, HHU Düsseldorf, Düsseldorf, Germany*.

Baluška, F., Parker, J.S. and Barlow, P.W. (1993) The microtubular cytoskeleton in cells of cold-treated roots of maize (Zea mays L.) shows tissue-specific responses. *Protoplasma*, **172**, 84-96.

Bartoli, C.G., Casalongué, C.A., Simontacchi, M., Marquez-Garcia, B. and Foyer, C.H. (2013) Interactions between hormone and redox signalling pathways in the control of growth and cross tolerance to stress. *Environ Exp Bot*, **94**, 73-88.

Beale, C.V., Bint, D.A. and Long, S.P. (1996) Leaf photosynthesis in the C4-grass Miscanthus x giganteus, growing in the cool temperate climate of southern England. *J Exp Bot*, **47**, 267-273.

Belanger, F.C., Leustek, T., Chu, B. and Kriz, A.L. (1995) Evidence for the thiamine biosynthetic pathway in higher-plant plastids and its developmental regulation. *Plant Mol Biol*, **29**, 809-821.

Berriri, S., Gangappa, S.N. and Kumar, S.V. (2016) SWR1 Chromatin-Remodeling Complex Subunits and H2A.Z Have Non-overlapping Functions in Immunity and Gene Regulation in Arabidopsis. *Mol Plant*, **9**, 1051-1065.

Bieniawska, Z., Espinoza, C., Schlereth, A., Sulpice, R., Hincha, D.K. and Hannah, M.A. (2008) Disruption of the Arabidopsis circadian clock is responsible for extensive variation in the cold-responsive transcriptome. *Plant Physiol*, **147**, 263-279.

Black, D.L. (2003) Mechanisms of alternative pre-messenger RNA splicing. *Annu Rev Biochem*, **72**, 291-336.

Book, A.J., Gladman, N.P., Lee, S.S., Scalf, M., Smith, L.M. and Vierstra, R.D. (2010) Affinity purification of the Arabidopsis 26 S proteasome reveals a diverse array of plant proteolytic complexes. *J Biol Chem*, **285**, 25554-25569.

Brandalise, M., de Godoy Maia, I., Borecky, J., Vercesi, A.E. and Arruda, P. (2003) ZmPUMP encodes a maize mitochondrial uncoupling protein that is induced by oxidative stress. *Plant Sci*, **165**, 329-335.

Cao, X., Wu, Z., Jiang, F., Zhou, R. and Yang, Z. (2014) Identification of chilling stress-responsive tomato microRNAs and their target genes by high-throughput sequencing and degradome analysis. *BMC Genomics*, **15**, 1130.

Chae, K., Isaacs, C.G., Reeves, P.H., Maloney, G.S., Muday, G.K., Nagpal, P. and Reed, J.W. (2012) Arabidopsis SMALL AUXIN UP RNA63 promotes hypocotyl and stamen filament elongation. *Plant J*, **71**, 684-697.

Chen, H., Chen, X., Chai, X., Qiu, Y., Gong, C., Zhang, Z., Wang, T., Zhang, Y., Li, J. and Wang, A. (2015) Effects of low temperature on mRNA and small RNA transcriptomes in

Solanum lycopersicoides leaf revealed by RNA-Seq. *Biochem Biophys Res Commun*, **464**, 768-773.

Chen, L., Song, Y., Li, S., Zhang, L., Zou, C. and Yu, D. (2012) The role of WRKY transcription factors in plant abiotic stresses. *Biochim Biophys Acta*, **1819**, 120-128.

Chen, Y., Hao, X. and Cao, J. (2014) Small auxin upregulated RNA (SAUR) gene family in maize: Identification, evolution, and its phylogenetic comparison with Arabidopsis, rice, and Sorghum. *J Integr Plant Biol*, **56**, 133-150.

Chen, Y., Pang, Q., Dai, S., Wang, Y., Chen, S. and Yan, X. (2011) Proteomic identification of differentially expressed proteins in Arabidopsis in response to methyl jasmonate. *J Plant Physiol*, **168**, 995-1008.

Chopra, R., Burow, G., Hayes, C., Emendack, Y., Xin, Z. and Burke, J. (2015) Transcriptome profiling and validation of gene based single nucleotide polymorphisms (SNPs) in Sorghum genotypes with contrasting responses to cold stress. *BMC Genomics*, **16**, 1040.

Colebrook, E.H., Thomas, S.G., Phillips, A.L. and Hedden, P. (2014) The role of gibberellin signalling in plant responses to abiotic stress. *J Exp Biol*, **217**, 67-75.

Darie, C.C., De Pascalis, L., Mutschler, B. and Haehnel, W. (2006) Studies of the Ndh complex and photosystem II from mesophyll and bundle sheath chloroplasts of the C4-type plant Zea mays. *J Plant Physiol*, **163**, 800-808.

Dixit, V., Pandey, V. and Shyam, R. (2001) Differential antioxidative responses to cadmium in roots and leaves of pea (Pisum sativum L. cv. Azad)1. *J Exp Bot*, **52**, 1101-1109.

Doebley, J. (2004) The Genetics of Maize Evolution. *Annu Rev Genet*, **38**, 37-59.

Doebley, J., Stec, A. and Gustus, C. (1995) teosinte branched1 and the origin of maize: evidence for epistasis and the evolution of dominance. *Genetics*, **141**, 333-346.

Dohleman, F.G. and Long, S.P. (2009) More productive than maize in the Midwest: How does Miscanthus do it? *Plant Physiol*, **150**, 2104-2115.

Doulis, A.G., Debian, N., Kingston-Smith, A.H. and Foyer, C.H. (1997) Differential Localization of Antioxidants in Maize Leaves. *Plant Physiol*, **114**, 1031-1037.

Du, H., Liu, H. and Xiong, L. (2013) Endogenous auxin and jasmonic acid levels are differentially modulated by abiotic stresses in rice. *Front Plant Sci*, **4**, 397.

Du, Z., Zhou, X., Ling, Y., Zhang, Z. and Su, Z. (2010) agriGO: a GO analysis toolkit for the agricultural community. *Nucleic Acids Res*, **38**, W64-70.

Dwyer, L.M. and Tollenaar, M. (1989) Genetic improvement in photosynthetic response of hybrid maize cultivars, 1959 to 1988. *Can J Plant Sci*, **69**, 81-91.

Edwards, E.J., Osborne, C.P., Stromberg, C.A., Smith, S.A., Bond, W.J., Christin, P.A., Cousins, A.B., Duvall, M.R., Fox, D.L., Freckleton, R.P., Ghannoum, O., Hartwell, J., Huang, Y., Janis, C.M., Keeley, J.E., Kellogg, E.A., Knapp, A.K., Leakey, A.D., Nelson, D.M., Saarela, J.M., Sage, R.F., Sala, O.E., Salamin, N., Still, C.J. and Tipple, B. (2010) The origins of C4 grasslands: integrating evolutionary and ecosystem science. *Science*, **328**, 587-591.

Ellens, K.W., Richardson, L.G., Freli, O., Collins, J., Ribeiro, C.L., Hsieh, Y.F., Mullen, R.T. and Hanson, A.D. (2015) Evidence that glutamine transaminase and omega-amidase potentially act in tandem to close the methionine salvage cycle in bacteria and plants. *Phytochemistry*, **113**, 160-169.

Erdemir, T., Bilican, B., Cagatay, T., Goding, C.R. and Yavuzer, U. (2002) Saccharomyces cerevisiae C1D is implicated in both non-homologous DNA end joining and homologous recombination. *Molr Microbiol*, **46**, 947-957.

Eremina, M., Rozhon, W. and Poppenberger, B. (2016) Hormonal control of cold stress responses in plants. *Cell Mol Life Sci*, **73**, 797-810.

Espinoza, C., Bieniawska, Z., Hincha, D.K. and Hannah, M.A. (2008) Interactions between the circadian clock and cold-response in Arabidopsis. *Plant Signal Behav*, **3**, 593-594.

Espinoza, C., Degenkolbe, T., Caldana, C., Zuther, E., Leisse, A., Willmitzer, L., Hincha, D.K. and Hannah, M.A. (2010) Interaction with diurnal and circadian regulation results in dynamic metabolic and transcriptional changes during cold acclimation in Arabidopsis. *PLoS One*, **5**, e14101.

Ewing, B. and Green, P. (1998) Base-calling of automated sequencer traces using phred. II. Error probabilities. *Genome Res*, **8**, 186-194.

FAO (2015) FAO Statistical Pocketbook World food and agriculture 2015. *Food and Agriculture Organization of the United Nations, Rome, 2015, ISBN 978-92-5-108802-9*.

Folta, A., Bargsten, J.W., Bisseling, T., Nap, J.P. and Mlynarova, L. (2016) Compact tomato seedlings and plants upon overexpression of a tomato chromatin remodelling ATPase gene. *Plant Biotechnol J*, **14**, 581-591.

Fouquet, R., Martin, F., Fajardo, D.S., Gault, C.M., Gomez, E., Tseung, C.W., Policht, T., Hueros, G. and Settles, A.M. (2011) Maize rough endosperm3 encodes an RNA splicing factor required for endosperm cell differentiation and has a nonautonomous effect on embryo development. *Plant Cell*, **23**, 4280-4297.

Fowler, S. and Thomashow, M.F. (2002) Arabidopsis transcriptome profiling indicates that multiple regulatory pathways are activated during cold acclimation in addition to the CBF cold response pathway. *Plant Cell*, **14**, 1675-1690.

Foyer, C.H., Lelandais, M. and Kunert, K.J. (1994) Photooxidative stress in plants. *Physiol Plant*, **92**, 696-717.

Foyer, C.H. and Noctor, G. (2009) Redox regulation in photosynthetic organisms: signaling, acclimation, and practical implications. *Antioxid Redox Signal*, **11**, 861-905.

Foyer, C.H., Vanacker, H., Gomez, L.D. and Harbinson, J. (2002) Regulation of photosynthesis and antioxidant metabolism in maize leaves at optimal and chilling temperatures: review. *Plant Physiol Biochem*, **40**, 659-668.

Fracheboud, Y., Jompuk, C., Ribaut, J.M., Stamp, P. and Leipner, J. (2004) Genetic analysis of cold-tolerance of photosynthesis in maize. *Plant Mol Biol*, **56**, 241-253.

Fryer, M.J., Oxborough, K., Martin, B., Ort, D.R. and Baker, N.R. (1995) Factors Associated with Depression of Photosynthetic Quantum Efficiency in Maize at Low Growth Temperature. *Plant Physiol*, **108**, 761-767.

Ghirardi, M.L. and Melis, A. (1983) Localization of photosynthetic electron transport components in mesophyll and bundle sheath chloroplasts of Zea mays. *Arch Biochem Biophys*, **224**, 19-28.

Gilmour, S.J., Zarka, D.G., Stockinger, E.J., Salazar, M.P., Houghton, J.M. and Thomashow, M.F. (1998) Low temperature regulation of the Arabidopsis CBF family of AP2 transcriptional activators as an early step in cold-induced COR gene expression. *Plant J*, **16**, 433-442.

Goh, H.H., Sloan, J., Dorca-Fornell, C. and Fleming, A. (2012) Inducible repression of multiple expansin genes leads to growth suppression during leaf development. *Plant Physiol*, **159**, 1759-1770.

Goyer, A. (2010) Thiamine in plants: aspects of its metabolism and functions. *Phytochemistry*, **71**, 1615-1624.

Greaves, J.A. (1996) Improving suboptimal temperature tolerance in maize— the search for variation. *J Exp Bot*, **47**, 307-323.

Gui, J., Zheng, S., Liu, C., Shen, J., Li, J. and Li, L. (2016) OsREM4.1 Interacts with OsSERK1 to Coordinate the Interlinking between Abscisic Acid and Brassinosteroid Signaling in Rice. *Dev Cell*, **38**, 201-213.

Guo, W.L., Chen, R.G., Du, X.H., Zhang, Z., Yin, Y.X., Gong, Z.H. and Wang, G.Y. (2014) Reduced tolerance to abiotic stress in transgenic Arabidopsis overexpressing a Capsicum annuum multiprotein bridging factor 1. *BMC Plant Biol*, **14**, 138.

Hatch, M.D. (1987) C4 photosynthesis: a unique blend of modified biochemistry, anatomy and ultrastructure. *Biochim Biophys Acta, ER. Reviews on bioenergetics*, **895**, 81-106.

Hatch, M.D. (1992) C4 Photosynthesis: An Unlikely Process Full of Surprises. *Plant Cell Physiol*, **33**, 333-342.

Heidarvand, L. and Amiri, R.M. (2010) What happens in plant molecular responses to cold stress? *Acta Physiol Plant*, **32**, 419-431.

Herr, A.J., Molnar, A., Jones, A. and Baulcombe, D.C. (2006) Defective RNA processing enhances RNA silencing and influences flowering of Arabidopsis. *Proc Natl Acad Sci U S A*, **103**, 14994-15001.

Huang, G.T., Ma, S.L., Bai, L.P., Zhang, L., Ma, H., Jia, P., Liu, J., Zhong, M. and Guo, Z.F. (2012) Signal transduction during cold, salt, and drought stresses in plants. *Molecular biology reports*, **39**, 969-987.

Huang, X., Bao, Y., Wang, B.O., Liu, L., Chen, J., Dai, L., Baloch, S.U. and Peng, D. (2016) Identification of small auxin-up RNA (SAUR) genes in Urticales plants: mulberry (Morus notabilis), hemp (Cannabis sativa) and ramie (Boehmeria nivea). *J Genet,* **95**, 119-129.

Hund, A., Fracheboud, Y., Soldati, A., Frascaroli, E., Salvi, S. and Stamp, P. (2004) QTL controlling root and shoot traits of maize seedlings under cold stress. *Theor Appl Genet*, **109**, 618-629.

Jackson, R.A., Wu, J.S. and Chen, E.S. (2016) C1D family proteins in coordinating RNA processing, chromosome condensation and DNA damage response. *Cell division*, **11**, 2.

Jasso-Robles, F. I., Jiménez-Bremont, J. F., Becerra-Flora, A., Juárez-Montiel, M., Gonzalez, M. E., Pieckenstain, F. L., García de la Cruz, R.F. and Rodríguez-Kessler, M. (2016). Inhibition of polyamine oxidase activity affects tumor development during the maize-Ustilago maydis interaction. *Plant Physiol Biochem*, **102**, 115-124.

Jiang, C. and Fu, X. (2007) GA action: turning on de-DELLA repressing signaling. *Curr Opin Plant Biol*, **10**, 461-465.

Jompuk, C., Fracheboud, Y., Stamp, P. and Leipner, J. (2005) Mapping of quantitative trait loci associated with chilling tolerance in maize (Zea mays L.) seedlings grown under field conditions. *J Exp Bot*, **56**, 1153-1163.

Jue, D., Sang, X., Lu, S., Dong, C., Zhao, Q., Chen, H. and Jia, L. (2015) Genome-Wide Identification, Phylogenetic and Expression Analyses of the Ubiquitin-Conjugating Enzyme Gene Family in Maize. *PLoS One*, **10**, e0143488.

Kazan, K. (2015) Diverse roles of jasmonates and ethylene in abiotic stress tolerance. *Trends Plant Sci*, **20**, 219-229.

Kim, M., Ahn, J.W., Jin, U.H., Choi, D., Paek, K.H. and Pai, H.S. (2003) Activation of the programmed cell death pathway by inhibition of proteasome function in plants. *J Biol Chem*, **278**, 19406-19415.

Kingston-Smith, A.H., Harbinson, J. and Foyer, C.H. (1999) Acclimation of photosynthesis, H2O2 content and antioxidants in maize (Zea mays) grown at sub - optimal temperatures. *Plant Cell Environ*, **22**, 1071-1083.

Kirik, V., Grini, P.E., Mathur, J., Klinkhammer, I., Adler, K., Bechtold, N., Herzog, M., Bonneville, J.M. and Hulskamp, M. (2002) The Arabidopsis TUBULIN-FOLDING COFACTOR A gene is involved in the control of the alpha/beta-tubulin monomer balance. *Plant Cell*, **14**, 2265-2276.

Kirschner, M. and Mitchison, T. (1986) Beyond self-assembly: from microtubules to morphogenesis. *Cell*, **45**, 329-342.

Kong, X., Pan, J., Zhang, M., Xing, X., Zhou, Y., Liu, Y., Li, D. and Li, D. (2011) ZmMKK4, a novel group C mitogen-activated protein kinase kinase in maize (Zea mays), confers salt and cold tolerance in transgenic Arabidopsis. *Plant Cell Environ*, **34**, 1291-1303.

Kubien, D.S. and Sage, R.F. (2003) C4 grasses in boreal fens: their occurrence in relation to microsite characteristics. *Oecologia*, **137**, 330-337.

Kumar, R. (2014) Role of microRNAs in biotic and abiotic stress responses in crop plants. *Appl Biochem Biotechnol*, **174**, 93-115.

Kumar, S.V. and Wigge, P.A. (2010) H2A.Z-containing nucleosomes mediate the thermosensory response in Arabidopsis. *Cell*, **140**, 136-147.

Kurepa, J., Wang, S., Li, Y. and Smalle, J. (2009a) Proteasome regulation, plant growth and stress tolerance. *Plant Signal Behav*, **4**, 924-927.

Kurepa, J., Wang, S., Li, Y., Zaitlin, D., Pierce, A.J. and Smalle, J.A. (2009b) Loss of 26S proteasome function leads to increased cell size and decreased cell number in Arabidopsis shoot organs. *Plant Physiol*, **150**, 178-189.

Lawit, S.J., Wych, H.M., Xu, D., Kundu, S. and Tomes, D.T. (2010) Maize DELLA proteins dwarf plant8 and dwarf plant9 as modulators of plant development. *Plant Cell Physiol*, **51**, 1854-1868.

Leipner, J., Jompuk, C., Camp, K.-H., Stamp, P. and Fracheboud, Y. (2008) QTL studies reveal little relevance of chilling-related seedling traits for yield in maize. *Theor Appl Genet*, **116**, 555-562.

Li, Z.G., Chen, H.W., Li, Q.T., Tao, J.J., Bian, X.H., Ma, B., Zhang, W.K., Chen, S.Y. and Zhang, J.S. (2015) Three SAUR proteins SAUR76, SAUR77 and SAUR78 promote plant growth in Arabidopsis. *Scientific reports*, **5**, 12477.

Ling, Q. and Jarvis, P. (2015) Regulation of Chloroplast Protein Import by the Ubiquitin E3 Ligase SP1 Is Important for Stress Tolerance in Plants. *Curr Biol*, **25**, 2527-2534.

Ling, Q. and Jarvis, P. (2016) Plant Signaling: Ubiquitin Pulls the Trigger on Chloroplast Degradation. *Curr Biol*, **26**, R38-40.

Livak, K.J. and Schmittgen, T.D. (2001) Analysis of relative gene expression data using real-time quantitative PCR and the 2(-Delta Delta C(T)) Method. *Methods*, **25**, 402-408.

Long, S.P. (1983) C4 photosynthesis at low temperatures. *Plant Cell Environ*, **6**, 345-363.

Long, S.P. and Spence, A.K. (2013) Toward cool C4 crops. *Annu Rev Plant Biol*, **64**, 701-722.

Lu, B., Gong, Z., Wang, J., Zhang, J. and Liang, J. (2007) Microtubule dynamics in relation to osmotic stress-induced ABA accumulation in Zea mays roots. *J Exp Bot*, **58**, 2565-2572.

Lu, L., Nan, J., Mi, W., Li, L.F., Wei, C.H., Su, X.D. and Li, Y. (2010) Crystal structure of tubulin folding cofactor A from Arabidopsis thaliana and its beta-tubulin binding characterization. *FEBS Lett*, **584**, 3533-3539.

Lv, D.K., Bai, X., Li, Y., Ding, X.D., Ge, Y., Cai, H., Ji, W., Wu, N. and Zhu, Y.M. (2010) Profiling of cold-stress-responsive miRNAs in rice by microarrays. *Gene*, **459**, 39-47.

Mao, J., Yu, Y., Yang, J., Li, G., Li, C., Qi, X., Wen, T.J. and Hu, J. (2017) Comparative transcriptome analysis of sweet corn seedlings under low-temperature stress. *Crop J*.

March-Diaz, R. and Reyes, J.C. (2009) The beauty of being a variant: H2A.Z and the SWR1 complex in plants. *Mol Plant*, **2**, 565-577.

Marozsan-Toth, Z., Vashegyi, I., Galiba, G. and Toth, B. (2015) The cold response of CBF genes in barley is regulated by distinct signaling mechanisms. *J Plant Physiol*, **181**, 42-49.

Maruta, T., Noshi, M., Tanouchi, A., Tamoi, M., Yabuta, Y., Yoshimura, K., Ishikawa, T. and Shigeoka, S. (2012) H2O2-triggered retrograde signaling from chloroplasts to nucleus plays specific role in response to stress. *J Biol Chem*, **287**, 11717-11729.

Maruyama, K., Urano, K., Yoshiwara, K., Morishita, Y., Sakurai, N., Suzuki, H., Kojima, M., Sakakibara, H., Shibata, D., Saito, K., Shinozaki, K. and Yamaguchi-Shinozaki, K. (2014) Integrated analysis of the effects of cold and dehydration on rice metabolites, phytohormones, and gene transcripts. *Plant Physiol*, **164**, 1759-1771.

Messina, G., Celauro, E., Atterrato, M.T., Giordano, E., Iwashita, S. and Dimitri, P. (2015) The Bucentaur (BCNT) protein family: a long-neglected class of essential proteins required for chromatin/chromosome organization and function. *Chromosoma*, **124**, 153-162.

Miedema, P. (1982) The effects of low temperature on Zea mays. *Adv Agron*, **35**, 93-128.

Misra, A. and Green, M.R. (2016) From polyadenylation to splicing: Dual role for mRNA 3' end formation factors. *RNA biology*, **13**, 259-264.

Misra, A., Ou, J., Zhu, L.J. and Green, M.R. (2015) Global Promotion of Alternative Internal Exon Usage by mRNA 3' End Formation Factors. *Mol Cell*, **58**, 819-831.

Mitchell, P. (2010) Rrp47 and the function of the Sas10/C1D domain. *Biochem Soc Trans*, **38**, 1088-1092.

Mitchell, P., Petfalski, E., Houalla, R., Podtelejnikov, A., Mann, M. and Tollervey, D. (2003) Rrp47p is an exosome-associated protein required for the 3' processing of stable RNAs. *Mol Cell Biol*, **23**, 6982-6992.

Mlynarova, L., Nap, J.P. and Bisseling, T. (2007) The SWI/SNF chromatin-remodeling gene AtCHR12 mediates temporary growth arrest in Arabidopsis thaliana upon perceiving environmental stress. *Plant J*, **51**, 874-885.

Møller, I.M. (2001) PLANT MITOCHONDRIA AND OXIDATIVE STRESS: Electron Transport, NADPH Turnover, and Metabolism of Reactive Oxygen Species. *Annu Rev Plant Physiol Plant Mol Biol*, **52**, 561-591.

Nie, G.Y. and Baker, N.R. (1991) Modifications to Thylakoid Composition during Development of Maize Leaves at Low Growth Temperatures. *Plant Physiol*, **95**, 184-191.

Nie, G.Y., Long, S.P. and Baker, N.R. (1992) The effects of development at sub - optimal growth temperatures on photosynthetic capacity and susceptibility to chilling - dependent photoinhibition in Zea mays. *Physiol Plant*, **85**, 554-560.

Noctor, G. and Foyer, C.H. (1998) ASCORBATE AND GLUTATHIONE: Keeping Active Oxygen Under Control. *Annu Rev Plant Physiol Plant Mol Biol*, **49**, 249-279.

Pacheco, T.R., Gomes, A.Q., Barbosa-Morais, N.L., Benes, V., Ansorge, W., Wollerton, M., Smith, C.W., Valcarcel, J. and Carmo-Fonseca, M. (2004) Diversity of vertebrate splicing factor U2AF35: identification of alternatively spliced U2AF1 mRNAS. *J Biol Chem*, **279**, 27039-27049.

Pacheco, T.R., Moita, L.F., Gomes, A.Q., Hacohen, N. and Carmo-Fonseca, M. (2006) RNA interference knockdown of hU2AF35 impairs cell cycle progression and modulates alternative splicing of Cdc25 transcripts. *Molr Biol Cell*, **17**, 4187-4199.

Park, M.R., Yun, K.Y., Mohanty, B., Herath, V., Xu, F., Wijaya, E., Bajic, V.B., Yun, S.J. and De Los Reyes, B.G. (2010) Supra-optimal expression of the cold-regulated OsMyb4 transcription factor in transgenic rice changes the complexity of transcriptional network with major effects on stress tolerance and panicle development. *Plant Cell Environ*, **33**, 2209-2230.

Pastori, G., Foyer, C.H. and Mullineaux, P. (2000) Low temperature-induced changes in the distribution of H2O2 and antioxidants between the bundle sheath and mesophyll cells of maize leaves. *J Exp Bot*, **51**, 107-113.

Paterson, A.H. (1995) Molecular dissection of quantitative traits: progress and prospects. *Genome research*, **5**, 321-333.

Pearcy, R.W. and Ehleringer, J. (1984) Comparative ecophysiology of C3 and C4 plants. *Plant Cell Environ*, **7**, 1-13.

Peltier, G. and Cournac, L. (2002) Chlororespiration. *Annu Rev Plant Biol*, **53**, 523-550.

Pérez-Díaz, J., Wu, T. M., Pérez-Díaz, R., Ruíz-Lara, S., Hong, C. Y. and Casaretto, J. A. (2014). Organ-and stress-specific expression of the ASR genes in rice. *Plant Cell Rep*, ***33***, 61-73.

Prasad, T.K. (1996) Mechanisms of chilling-induced oxidative stress injury and tolerance in developing maize seedlings: changes in antioxidant system, oxidation of proteins and lipids, and protease activities. *Plant J*, **10**, 1017-1026.

Prasad, T.K., Anderson, M.D., Martin, B.A. and Stewart, C.R. (1994) Evidence for Chilling-lnduced Oxidative Stress in Maize Seedlings and a Regulatory Role for Hydrogen Peroxide. *Plant Cell*, **6**, 65-74.

Presterl, T., Ouzunova, M., Schmidt, W., Möller, E.M., Röber, F.K., Knaak, C., Ernst, K., Westhoff, P. and Geiger, H.H. (2007) Quantitative trait loci for early plant vigour of maize grown in chilly environments. *Theor Appl Genet*, **114**, 1059-1070.

Puranik, S., Sahu, P.P., Srivastava, P.S. and Prasad, M. (2012) NAC proteins: regulation and role in stress tolerance. *Trends Plant Sci*, **17**, 369-381.

Qin, F., Sakuma, Y., Li, J., Liu, Q., Li, Y.Q., Shinozaki, K. and Yamaguchi-Shinozaki, K. (2004) Cloning and Functional Analysis of a Novel DREB1/CBF Transcription Factor Involved in Cold-Responsive Gene Expression in Zea mays L. *Plant Cell Physiol*, **45**, 1042-1052.

Rapala-Kozik, M., Kowalska, E. and Ostrowska, K. (2008) Modulation of thiamine metabolism in Zea mays seedlings under conditions of abiotic stress. *J Exp Bot*, **59**, 4133-4143.

Ren, H. and Gray, W.M. (2015) SAUR Proteins as Effectors of Hormonal and Environmental Signals in Plant Growth. *Mol Plant*, **8**, 1153-1164.

Riva-Roveda, L., Escale, B., Giauffret, C. and Perilleux, C. (2016) Maize plants can enter a standby mode to cope with chilling stress. *BMC Plant Biol*, **16**, 212.

Robinson, M.D., McCarthy, D.J. and Smyth, G.K. (2010) edgeR: a Bioconductor package for differential expression analysis of digital gene expression data. *Bioinformatics*, **26**, 139-140.

Robinson, M.D. and Smyth, G.K. (2008) Small-sample estimation of negative binomial dispersion, with applications to SAGE data. *Biostatistics (Oxford, England)*, **9**, 321-332.

Rodríguez, V.M., Butrón, A., Rady, M.O.A., Soengas, P. and Revilla, P. (2014) Identification of quantitative trait loci involved in the response to cold stress in maize (Zea mays L.). *Mol Breeding*, **33**, 363-371.

Roje, S. (2007) Vitamin B biosynthesis in plants. *Phytochemistry*, **68**, 1904-1921.

Rushton, D.L., Tripathi, P., Rabara, R.C., Lin, J., Ringler, P., Boken, A.K., Langum, T.J., Smidt, L., Boomsma, D.D., Emme, N.J., Chen, X., Finer, J.J., Shen, Q.J. and Rushton, P.J. (2012) WRKY transcription factors: key components in abscisic acid signalling. *Plant Biotechnol J*, **10**, 2-11.

Rymen, B., Fiorani, F., Kartal, F., Vandepoele, K., Inzé, D. and Beemster, G.T.S. (2007) Cold Nights Impair Leaf Growth and Cell Cycle Progression in Maize through Transcriptional Changes of Cell Cycle Genes. *Plant Physiol*, **143**.

Sadeghi, L., Bonilla, C., Stralfors, A., Ekwall, K. and Svensson, J.P. (2011) Podbat: a novel genomic tool reveals Swr1-independent H2A.Z incorporation at gene coding sequences through epigenetic meta-analysis. *PLoS computational biology*, **7**, e1002163.

Sage, R.F. (2004) The evolution of C4 photosynthesis. *New Phytol*, **161**, 341-370.

Sage, R.F., Christin, P.A. and Edwards, E.J. (2011) The C4 plant lineages of planet Earth. *J Exp Bot*, **62**, 3155-3169.

Sage, R.F., de Melo Peixoto, M., Friesen, P. and Deen, B. (2015) C4 bioenergy crops for cool climates, with special emphasis on perennial C4 grasses. *J Exp Bot*, **66**, 4195-4212.

Sanders, D., Pelloux, J., Brownlee, C. and Harper, J.F. (2002) Calcium at the crossroads of signaling. *Plant Cell*, **14 Suppl**, S401-417.

Shabala, S. and Shabala, L. (2002) Kinetics of net H+, Ca2+, K+, Na+, , and Cl– fluxes associated with post-chilling recovery of plasma membrane transporters in Zea mays leaf and root tissues. *Physiol Plant*, **114**, 47-56.

Shi, Y., Ding, Y. and Yang, S. (2015) Cold signal transduction and its interplay with phytohormones during cold acclimation. *Plant Cell Physiol*, **56**, 7-15.

Singh, A.P. and Savaldi-Goldstein, S. (2015) Growth control: brassinosteroid activity gets context. *J Exp Bot*, **66**, 1123-1132.

Sobkowiak, A., Jonczyk, M., Adamczyk, J., Szczepanik, J., Solecka, D., Kuciara, I., Hetmanczyk, K., Trzcinska-Danielewicz, J., Grzybowski, M., Skoneczny, M., Fronk, J. and Sowinski, P. (2016) Molecular foundations of chilling-tolerance of modern maize. *BMC Genomics*, **17**, 125.

Sobkowiak, A., Jonczyk, M., Jarochowska, E., Biecek, P., Trzcinska-Danielewicz, J., Leipner, J., Fronk, J. and Sowinski, P. (2014) Genome-wide transcriptomic analysis of response to low temperature reveals candidate genes determining divergent cold-sensitivity of maize inbred lines. *Plant Mol Biol*, **85**, 317-331.

Sowinski, P., Richner, W., Soldati, A. and Stamp, P. (1998) Assimilate transport in maize (Zea mays L.) seedlings at vertical low temperature gradients in the root zone. *J Exp Bot*, **49**, 747-752.

Spartz, A.K., Lee, S.H., Wenger, J.P., Gonzalez, N., Itoh, H., Inzé, D., Peer, W.A., Murphy, A.S., Overvoorde, P.J. and Gray, W.M. (2012) The SAUR19 subfamily of SMALL AUXIN UP RNA genes promote cell expansion. *Plant J*, **70**, 978-990.

Spartz, A.K., Ren, H., Park, M.Y., Grandt, K.N., Lee, S.H., Murphy, A.S., Sussman, M.R., Overvoorde, P.J. and Gray, W.M. (2014) SAUR Inhibition of PP2C-D Phosphatases Activates Plasma Membrane H+-ATPases to Promote Cell Expansion in Arabidopsis. *Plant Cell*, **26**, 2129-2142.

Stirling, C.M., Nie, G.Y., Aguilera, C., Nugawela, A., Long, S.P. and Baker, N.R. (1991) Photosynthetic productivity of an immature maize crop: changes in quantum yield of CO2 assimilation, conversion efficiency and thylakoid proteins. *Plant Cell Environ*, **14**, 947-954.

Stone, S.L. (2014) The role of ubiquitin and the 26S proteasome in plant abiotic stress signaling. *Frontiers in plant science*, **5**, 135.

Studer, A. J., Gandin, A., Kolbe, A. R., Wang, L., Cousins, A. B. and Brutnell, T. P. (2014) A limited role for carbonic anhydrase in C4 photosynthesis as revealed by a ca1ca2 double mutant in maize. *Plant Physiol*, **165**, 608-617.

Thimm, O., Blasing, O., Gibon, Y., Nagel, A., Meyer, S., Kruger, P., Selbig, J., Muller, L.A., Rhee, S.Y. and Stitt, M. (2004) MAPMAN: a user-driven tool to display genomics data sets onto diagrams of metabolic pathways and other biological processes. *Plant J*, **37**, 914-939.

Tojo, T., Tsuda, K., Yoshizumi, T., Ikeda, A., Yamaguchi, J., Matsui, M. and Yamazaki, K. (2009) Arabidopsis MBF1s control leaf cell cycle and its expansion. *Plant Cell Physiol*, **50**, 254-264.

Trachsel, S., Messmer, R., Stamp, P., Ruta, N. and Hund, A. (2010) QTLs for early vigor of tropical maize. *Mol Breeding*, **25**, 91-103.

Trzcinska-Danielewicz, J., Bilska, A., Fronk, J., Zielenkiewicz, P., Jarochowska, E., Roszczyk, M., Jonczyk, M., Axentowicz, E., Skoneczny, M. and Sowinski, P. (2009) Global analysis

of gene expression in maize leaves treated with low temperature I. Moderate chilling (14 °C). *Plant Sci*, **177**, 648-658.

Tunc-Ozdemir, M., Miller, G., Song, L., Kim, J., Sodek, A., Koussevitzky, S., Misra, A.N., Mittler, R. and Shintani, D. (2009) Thiamin confers enhanced tolerance to oxidative stress in Arabidopsis. *Plant Physiol*, **151**, 421-432.

Wang, D. and Portis, A.R., Jr. (2007) A novel nucleus-encoded chloroplast protein, PIFI, is involved in NAD(P)H dehydrogenase complex-mediated chlororespiratory electron transport in Arabidopsis. *Plant Physiol*, **144**, 1742-1752.

Wasternack, C. (2014) Action of jasmonates in plant stress responses and development--applied aspects. *Biotechnol Adv*, **32**, 31-39.

Westhoff, P., Offermann-Steinhard, K., Höfer, M., Eskins, K., Oswald, A. and Streubel, M. (1991) Differential accumulation of plastid transcripts encoding photosystem II components in the mesophyll and bundle-sheath cells of monocotyledonous NADP-malic enzyme-type C4 plants. *Planta*, **184**, 377-388.

Wilde, K., Presterl, T., Möller, E.M., Ouzunova, M., Schmidt, W. and Geiger, H.H. (2005) Untersuchungen zur Züchtung auf Kühletoleranz bei Mais. *Bericht über die 56. Tagung 2005 der Vereinigung der Pflanzenzüchter und Saatgutkaufleute Österreichs*.

Winfield, M.O., Lu, C., Wilson, I.D., Coghill, J.A. and Edwards, K.J. (2010) Plant responses to cold: Transcriptome analysis of wheat. *Plant Biotechnol J*, **8**, 749-771.

Wu, J., Liu, S., He, Y., Guan, X., Zhu, X., Cheng, L., Wang, J. and Lu, G. (2012) Genome-wide analysis of SAUR gene family in Solanaceae species. *Gene*, **509**, 38-50.

Xia, X.J., Zhou, Y.H., Shi, K., Zhou, J., Foyer, C.H. and Yu, J.Q. (2015) Interplay between reactive oxygen species and hormones in the control of plant development and stress tolerance. *J Exp Bot*, **66**, 2839-2856.

Xie, R., Dong, C., Ma, Y., Deng, L., He, S., Yi, S., Lv, Q. and Zheng, Y. (2015) Comprehensive analysis of SAUR gene family in citrus and its transcriptional correlation with fruitlet drop from abscission zone A. *Funct Integr Genomics*, **15**, 729-740.

Xu, Y.X., Xiao, M.Z., Liu, Y., Fu, J.L., He, Y. and Jiang, D.A. (2017) The small auxin-up RNA OsSAUR45 affects auxin synthesis and transport in rice. *Plant Mol Biol*, **94**, 97-107.

Yadav, S.K. (2010) Cold stress tolerance mechanisms in plants. A review. *Agron Sustain Dev*, **30**, 515-527.

Yamori, W., Hikosaka, K. and Way, D.A. (2014) Temperature response of photosynthesis in C3, C4, and CAM plants: temperature acclimation and temperature adaptation. *Photosynth Res*, **119**, 101-117.

Yang, G., Wang, Y., Xia, D., Gao, C., Wang, C. and Yang, C. (2014) Overexpression of a GST gene (ThGSTZ1) from Tamarix hispida improves drought and salinity tolerance by enhancing the ability to scavenge reactive oxygen species. *Plant Cell Tissue Organ Cult*, **117**, 99-112.

Yang, G., Xu, Z., Peng, S., Sun, Y., Jia, C. and Zhai, M. (2016) In planta characterization of a tau class glutathione S-transferase gene from Juglans regia (JrGSTTau1) involved in chilling tolerance. *Plant Cell Rep*, **35**, 681-692.

Yang, Y.W., Chen, H.C., Jen, W.F., Liu, L.Y. and Chang, M.C. (2015) Comparative Transcriptome Analysis of Shoots and Roots of TNG67 and TCN1 Rice Seedlings under Cold Stress and Following Subsequent Recovery: Insights into Metabolic Pathways, Phytohormones, and Transcription Factors. *PLoS One*, **10**, e0131391.

Ye, Y., Ding, Y., Jiang, Q., Wang, F., Sun, J. and Zhu, C. (2016) The role of receptor-like protein kinases (RLKs) in abiotic stress response in plants. *Plant Cell Rep*.

Zhao, J., Zhang, S., Yang, T., Zeng, Z., Huang, Z., Liu, Q., Wang, X., Leach, J., Leung, H. and Liu, B. (2015) Global transcriptional profiling of a cold-tolerant rice variety under moderate cold stress reveals different cold stress response mechanisms. *Physiol Plant*, **154**, 381-394.

Supplemental Figures

Supplemental Figure 1: Differential abundance of transcripts related to regulatory and protection processes
Transcripts exhibiting an increase or decrease in abundance during 4 h and 24 h chilling were assigned to subsets of the MapMan categories. Each box represents one transcript. The colour or the boxes designates the degree of differential abundance. Blue indicates an increase in abundance, red a decrease in abundance.
(A) Transcripts related to signal transduction. The bin “signalling.calcium” (calcium) comprises transcripts associated with calcium signalling components. The bin “posttranslational modification” (protein modification) encompasses transcripts encoding diverse protein kinases and phosphatases.

(B) Transcripts of the bin "hormone metabolism". This bin encompasses transcripts related to synthesis, degradation, regulation and output of given phytohormones.
(C) Transcripts of the bin "regulation of transcription". This bin contains diverse transcription factor families and their members.
(D) Transcripts of the bins "redox" and "glutathione S-transferases". The bins comprise transcripts associated with diverse enzymes and mechanisms that protect against oxidative stress.
Only transcripts with a FDR *p*-value correction ≤ 0.05 and a $\log_2$ fold change of ≥ 1.5 were considered for analysis.
ABA, abscisic acid; ARF, auxin response factor; bHLH, basic helix-loop-helix; BR, brassinosteroids; CAT, catalase; GA, gibberellin; GSH, glutathione; GST, glutathione S-transferase; HB, homeobox; HSF, heat shock factor

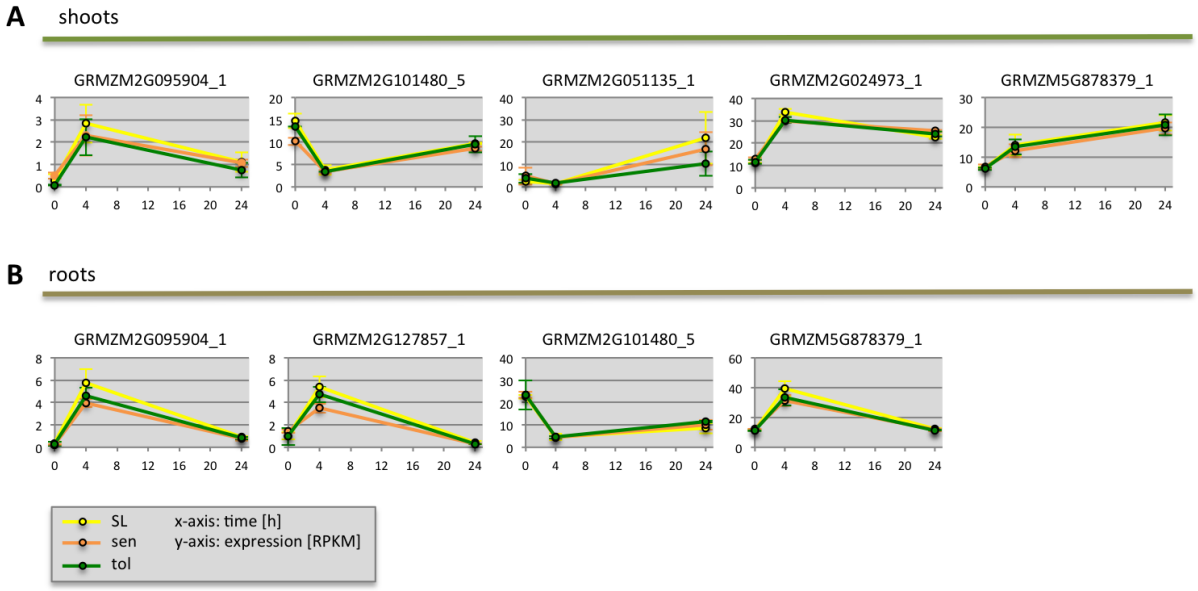

Supplemental Figure 2: Expression patterns of selected transcripts
Plotted are the transcripts amounts normalised to RPKM over time exhibiting different quantities. These transcripts were found with MapMan (with the exception of GRMZM2G024973_ 1/Dwarf plant9) and presumably play important roles in the SL response to chilling. The error bars show the standard deviation.

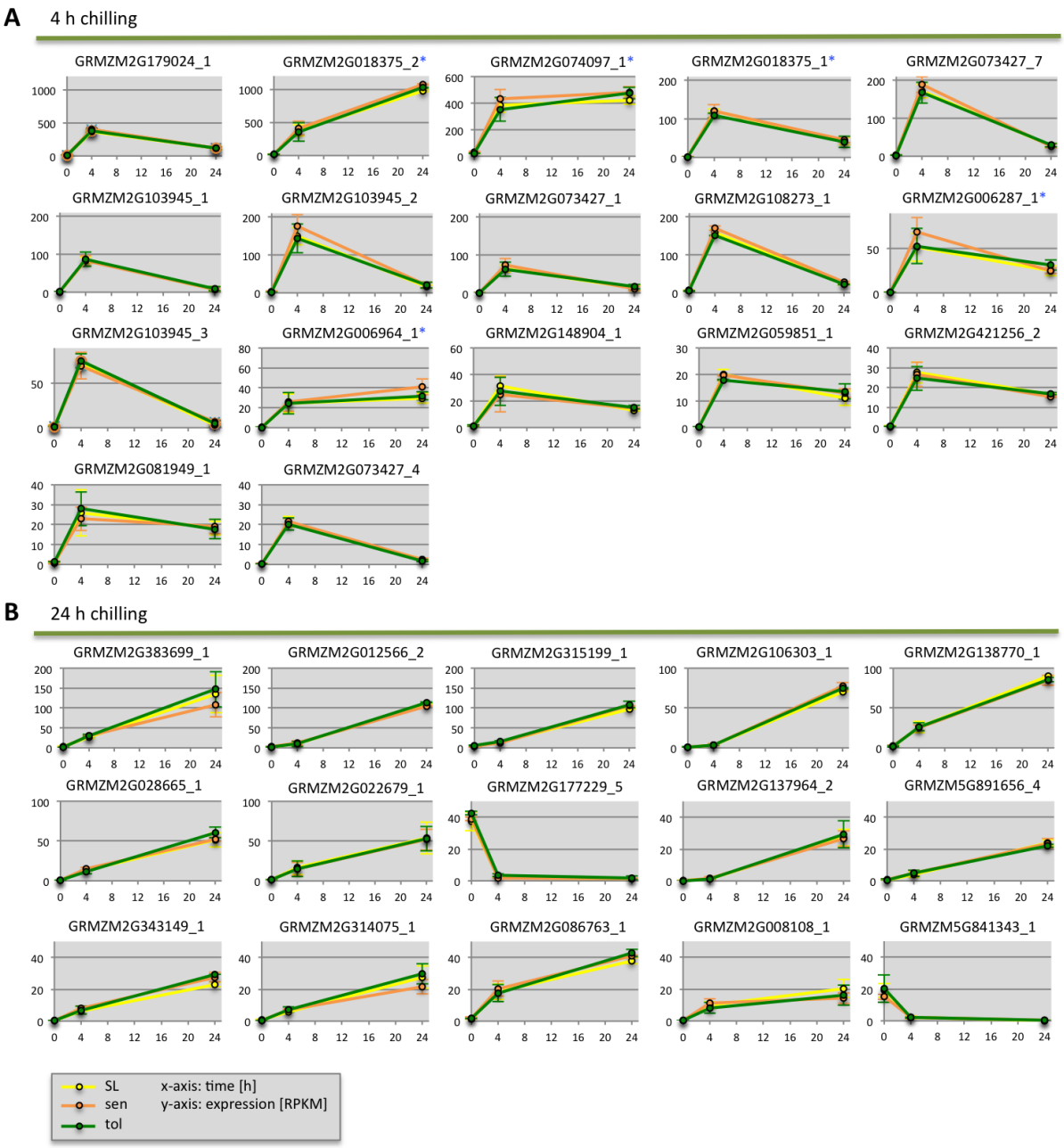

Supplemental Figure 3: Expression patterns of shoot transcripts most responsive to chilling
Plotted are the transcripts amounts normalised to RPKM over time for transcripts displaying significantly different quantities (FDR *p*-value correction ≤ 0.05) and exhibiting a $\log_2$ fold change ≥ 4 or ≤ –4 at 4 h chilling stress (A) and 24 h chilling stress (B). Blue asterisks mark the transcripts that show a different abundance at 4 h and 24 h chilling stress. The error bars show the standard deviation.

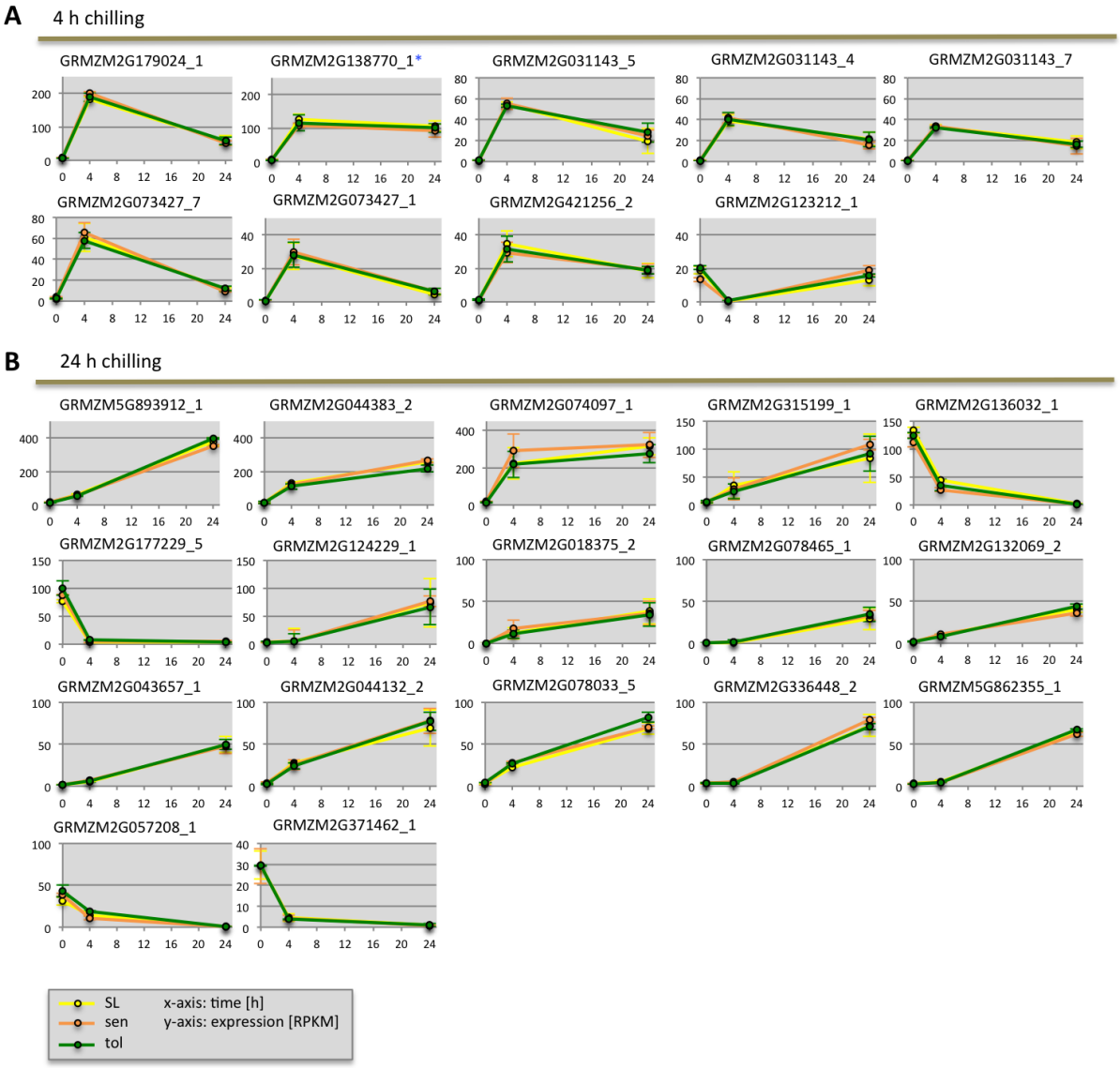

Supplemental Figure 4: Expression patterns of root transcripts most responsive to chilling
Plotted are transcripts amounts normalised to RPKM over time for transcripts displaying significantly different quantities (FDR *p*-value correction ≤ 0.05) and exhibiting a $\log_2$ fold change ≥ 4 or ≤ –4 at 4 h chilling stress (A) and 24 h chilling stress (B). Blue asterisks mark the transcripts that show a different abundance at 4 h and 24 h chilling. The error bars show the standard deviation.

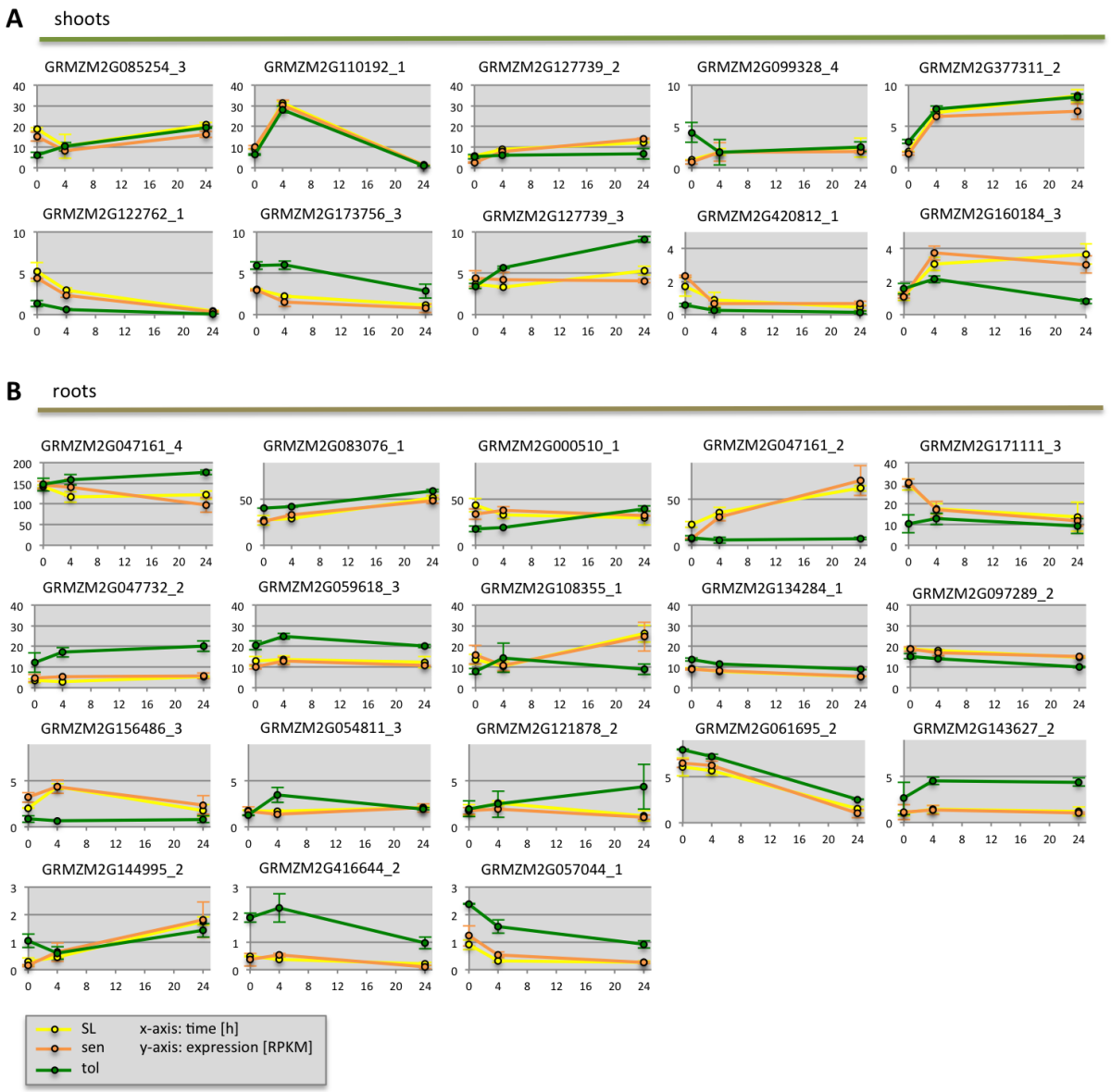

Supplemental Figure 5: Expression patterns of transcripts with significantly differential abundance between N4-8X-tol and N4-8X-sen

Plotted are the transcripts amounts normalised to RPKM over time of transcripts exhibiting significantly differential abundance (FDR *p*-value correction ≤ 0.05) between N4-8X-tol and N4-8X-sen in shoots (A) and roots (B). The error bars show the standard deviation.

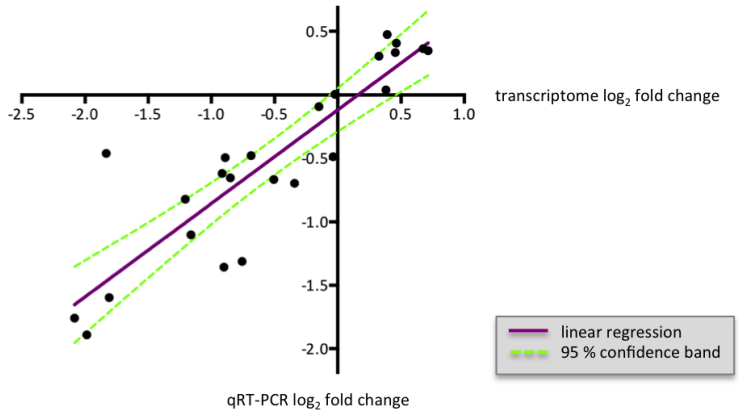

Supplemental Figure 6: Correlation analysis between transcriptome and qRT-PCR data
The graphical output of the linear regression analysis of the transcriptome and qRT-PCR data is shown. The $\log_2$ fold changes of the expression values obtained from the four genes *ETIF3SU4*, *GST26*, *ke-1* and *ACR8* are plotted. The horizontal axis represents the $\log_2$ fold changes obtained from the RNA-seq (RPKMs) and the vertical axis the $\log_2$ fold changes from the qRT-PCR (RQ).

Supplemental Tables

Supplemental Table 1: Overrepresented gene ontology terms in subsets of SL transcripts responsive to exposure to 4 h and 24 h chilling stress
The relevant major terms of hierarchical ontology trees, the related categories (categ.) and the obtained Hochberg FDR *p*-value corrections are shown. The table is sorted by the three main GO categories: the biological process (BP) category, the molecular function (MF) category and the cellular compartment (CC) category. *P*-values of high significance levels are highlighted in red, of high to medium in dark orange, of medium in orange and those of lower level in yellow. Only transcripts showing significantly differential changes in quantity with a $\log_2$ fold change ≥ 1.5 and ≤ 1.5 were considered for analysis.

			p-value shoots				*p*-value roots			
			4 h chilling		24 h chilling		4 h chilling		24 h chilling	
GO-Term	categ.	description	≥ 1.5	≤ –1.5	≥ 1.5	≤ –1.5	≥ 1.5	≤ –1.5	≥ 1.5	≤ –1.5
GO:0010468	BP	regulation of gene expression	1.2E–08				7.8E–05	8.7E–03		
GO:0050794	BP	regulation of cellular process	1.2E–08				1.9E–04	1.3E–02		
GO:0006350	BP	transcription	4.6E–08				1.7E–04	1.3E–02		
GO:0019725	BP	cellular homeostasis	4.8E–02			2.8E–02				
GO:0015979	BP	photosynthesis				3.1E–06				
GO:0006950	BP	response to stress				8.0E–03		3.9E–02		6.2E–03
GO:0009605	BP	response to external stimulus				1.4E–02				
GO:0009628	BP	response to abiotic stimulus				1.5E–02				
GO:0044267	BP	cellular protein metabolic processes						8.7E–03		
GO:0006810	BP	transport								1.8E–04
GO:0005975	BP	carbohydrate metabolic process								1.7E–02
GO:0003700	MF	transcription factor activity	8.9E–08		4.7E–02		4.3E–03	2.3E–03	3.7E-02	
GO:0005515	MF	protein binding						2.3E–03		
GO:0008135	MF	translation factor activity, nucleic acid binding							4.6E-02	
GO:0005215	MF	transporter activity								6.5E–06
GO:0009579	CC	thylakoid				2.0E–03				
GO:0005618	CC	cell wall				1.9E–02				
GO:0005576	CC	extracellular region				1.9E–02				
GO:0005634	CC	nucleus						2.4E–03		
GO:0016020	CC	membrane								1.1E–02

Supplemental Table 2: Highly regulated transcripts of SL related to signal transduction, phytohormones, transcriptional and redox regulation.

Displayed are the transcripts obtained from MapMan analyses and exhibiting significantly differential abundance (FDR *p*-value correction ≤ 0.05) and a $\log_2$ fold ($\log_2$ fc) change ≥ 3 or ≤ –3. If no annotation for a transcript was available, the corresponding ortholog of *Oryza sativa* ssp. *japonica* or *Arabidopsis thaliana* is specified. The locations of transcripts are displayed in Mb; the number in front of the colon indicates the respective chromosome. The transcripts regulated in shoots are highlighted in green, those in the roots in brown.

4 h chilling	Transcript ID	Location	Name/Ortholog	$\log_2$ fc	*p*-value
Calcium regulation	GRMZM2G033846_1	9:134.9	Caltractin	3.111	2.9E–33
	GRMZM2G178074_2	5:214.7	ZmPPCK1	3.770	8.3E–39
Protein modification	GRMZM2G378852_1	9:137.7	Putative MAPKKK family protein kinase AT2G30040 MITOGEN-ACTIVATED PROTEIN KINASE KINASE KINASE 14 MAPKKK14	3.075	1.4E–33
	GRMZM2G472643_1	1:253.3	Uncharacterized protein OS03G0634400 CBL-interacting protein kinase 7 CIPK7	3.636	1.4E–58
	GRMZM2G178074_1	5:214.7	ZmPPCK1	3.784	3.5E–103
Auxin	GRMZM2G146108_1	1:258.8	ZmSAUR11	3.405	6.8E–12
bZIP	GRMZM2G073427_6	1:170.5	Uncharacterized protein AT5G28770 ATBZIP63 ARABIDOPSIS THALIANA BASIC LEUCINE ZIPPER 63	3.240	3.4E-44
	GRMZM2G073427_1	1:170.5	Uncharacterized protein AT5G28770 ATBZIP63 ARABIDOPSIS THALIANA BASIC LEUCINE ZIPPER 63	5.593	7.2E–52
	GRMZM2G073427_7	1:170.5	Uncharacterized protein AT5G28770 ATBZIP63 ARABIDOPSIS THALIANA BASIC LEUCINE ZIPPER 63	5.968	1.4E–136
	GRMZM2G073427_4	1:170.5	Uncharacterized protein AT5G28770 ATBZIP63 ARABIDOPSIS THALIANA BASIC LEUCINE ZIPPER 63	4.041	5.4E–50
HSF	GRMZM2G059851_1	5:158.2	Heat shock factor protein 2	4.172	1.2E–101
MYB-related	GRMZM2G421256_2	2:14.7	Uncharacterized protein Os04g0583900	4.168	3.1E–87
NAC	GRMZM2G068973_2	8:170.4	Putative NAC domain transcription factor superfamily protein; Uncharacterized protein OS01G0816100 NAC68	3.498	4.3E-55
Pseudo ARR	GRMZM2G367834_1	2:196.3	Two-component response regulator-like PRR95	3.945	2.3E-98
	GRMZM2G488465_1	4:196:6	Uncharacterized protein AT5G24470 ARABIDOPSIS PSEUDO-RESPONSE REGULATOR 5 PRR5	3.711	2.8E-56
	GRMZM2G179024_1	7:143.1	Uncharacterized protein OS09G0532400 Two-component response regulator-like PRR95	4.746	8.8E–132
	GRMZM2G148453_1	5:185.4	Unknown OS02G0618200 Two-component response regulator-like PRR1	3.269	9.3E-48
WRKY	GRMZM2G101405_1	3:203.1	Unknown AT5G26170 WRKY DNA-BINDING PROTEIN 50 WRKY50	3.358	7.6E-14
	GRMZM2G449681_2	8:109.7	Putative WRKY DNA-binding domain superfamily protein isoform 1/2 AT2G38470 WRKY DNA-BINDING PROTEIN 33 WRKY33	3.250	1.7E-33
	GRMZM2G012724_3	6:141.6	Putative WRKY DNA-binding domain superfamily protein AT2G38470 WRKY DNA-BINDING PROTEIN 33 WRKY33	3.373	8.5E-22
24 h chilling	Transcript ID	Location	Name/Ortholog	$\log_2$ fc	*p*-value
Protein modification	GRMZM2G178074_2	5:214.7	ZmPPCK1	3.939	3.7E–41
	GRMZM2G053987_2	9:138.6	Putative MAP kinase family protein isoform 1/2; Uncharacterized protein AT3G45640 MITOGEN-ACTIVATED PROTEIN KINASE 3 MPK3	3.177	5.1E–55
	GRMZM2G013236_4	7:5.1	CBL-interacting protein kinase 23	3.132	8.1E–19
	GRMZM2G178074_1	5:214.7	ZmPPCK1	3.984	2.6E–109
Ethylene	GRMZM2G006964_1	2:28.3	Uncharacterized protein OS04G0522500 gibberellin 2-beta-dioxygenase 8	4.642	5.7E–63
	GRMZM2G022679_1	3:196.1	unknown OS01G0757200 gibberellin 2-beta-dioxygenase	4.353	2.6E–22
	GRMZM2G007249_2	7:124.3	Uncharacterized protein OS09G0451400 1-aminocyclopropane-1-carboxylate oxidase 1 ACO1	3.115	2.1E–62
Jasmonate	GRMZM5G822593_1	1:188.1	lipoxygenase 2	3.120	1.8E–84
	GRMZM2G000236_1	9:7.3	12-oxophytodienoate reductase 2	3.714	2.0E–17
	GRMZM2G106303_1	9:7.3	12-oxo-phytodienoic acid reductase; Uncharacterized protein OS06G0216200 OPR2 Putative 12-oxophytodienoate reductase 2	5.664	4.1E–25
Salicylic acid	GRMZM2G050307_1	4:197.9	Jasmonate O-methyltransferase; Uncharacterized protein AT5G66430 S-adenosyl-L-methionine-dependent methyltransferases superfamily protein	–3.390	4.6E–76
	GRMZM2G136857_1	6:44.9	jasmonic acid carboxyl methyltransferase	–3.936	1.1E–64
	GRMZM2G136857_2	6:44.9	jasmonic acid carboxyl methyltransferase	–3.493	2.6E–56

24 h chilling	Transcript ID	Location	Name/Ortholog	log_2 fc	*p*-value
AP2-EREBP	GRMZM2G149756_1	3:175.5	Unknown Os01g0868000 AP2 domain transcription factor-like	3.312	1.3E-18
bZIP	GRMZM2G073427_1	1:170.5	Uncharacterized protein AT5G28770 ATBZIP63 ARABIDOPSIS THALIANA BASIC LEUCINE ZIPPER 63	3.405	2.7E-27
	GRMZM2G073427_7	1:170.5	Uncharacterized protein AT5G28770 ATBZIP63 ARABIDOPSIS THALIANA BASIC LEUCINE ZIPPER 63	3.436	2.7E-27
HSF	GRMZM2G059851_1	5:158.2	Heat shock factor protein 2	3.378	1.4E-81
MYB-related	GRMZM2G421256_2	2:14.7	Uncharacterized protein Os04g0583900	3.462	1.7E-70
MYB	GRMZM2G005066_1	9:9.7	Anthocyanin regulatory C1 protein	3.788	1.7E-20
NAC	GRMZM2G068973_2	8:170.4	Putative NAC domain transcription factor superfamily protein; Uncharacterized protein OS01G0816100 NAC68	3.501	7.8E-55
Pseudo ARR	GRMZM2G135446_1	2:141.5	Uncharacterized protein OS11G0157600 CCT motif family protein, expressed	3.017	4.0E-57
	GRMZM2G179024_1	7:143.1	Uncharacterized protein OS09G0532400 Two-component response regulator-like PRR95	3.075	1.9E-77
	GRMZM2G148453_1	5:185.4	Unknown OS02G0618200 Two-component response regulator-like PRR1	3.217	7.5E-47
Redox	GRMZM2G475059_2	1:8.1	Uncharacterized protein OS10G052800 Glutathione S-transferase GSTU31	3.808	4.1E–05
	GRMZM2G032856_1	5:211.0	Glutathione S-transferase GST 24; Uncharacterized protein AT3G09270 ATGSTU8 GLUTATHIONE S-TRANSFERASE TAU 8	3.221	9.3E–30
4 h chilling	Transcript ID	Location	Name/Ortholog	log_2 fc	*p*-value
Calcium regulation	GRMZM2G061723_3	3:219.4	Uncharacterized protein OS01G0570800 Putative calmodulin-binding protein	3.214	1.0E–24
Ethylene	GRMZM5G894619_1	10:136.1	Uncharacterized protein AT4G11280 1-AMINOCYCLOPROPANE-1-CARBOXYLIC ACID (ACC) SYNTHASE 6 ACS6	3.658	1.2E–16
Auxin	GRMZM2G146108_1	1:258.8	ZmSAUR11	3.187	4.6E–22
bZIP	GRMZM2G073427_1	1:170.5	Uncharacterized protein AT5G28770 ATBZIP63 ARABIDOPSIS THALIANA BASIC LEUCINE ZIPPER 63	4.244	4.0E–29
	GRMZM2G073427_7	1:170.5	Uncharacterized protein AT5G28770 ATBZIP63 ARABIDOPSIS THALIANA BASIC LEUCINE ZIPPER 63	4.267	2.4E–116
MYB-related	GRMZM2G421256_2	2:14.7	Uncharacterized protein Os04g0583900	4.136	4.2E–72
NAC	GRMZM2G068973_2	8:170.4	Putative NAC domain transcription factor superfamily protein; Uncharacterized protein OS01G0816100 NAC68	3.055	1.6E-85
Pseudo ARR	GRMZM2G367834_1	2:196.3	Two-component response regulator-like PRR95	3.184	1.4E-69
	GRMZM2G179024_1	7:143.1	Uncharacterized protein OS09G0532400 Two-component response regulator-like PRR95	4.697	2.9E–161
	GRMZM2G148453_1	5:185.4	Unknown OS02G0618200 Two-component response regulator-like PRR1	3.039	8.0E-59
Redox	GRMZM2G044383_2	1:81.7	Glutathione S-transferase GST 30; Uncharacterized protein OS10G0530900 GSTU6 Probable glutathione S-transferase GSTU6	3.352	2.7E–60
24 h chilling	Transcript ID	Location	Name/Ortholog	log_2 fc	*p*-value
Auxin	GRMZM2G030465_1	5:214.4	IAA9-auxin-responsive Aux/IAA family member	3.037	1.3E–81
Aux/IAA	GRMZM2G030465_1	5:214.4	IAA9-auxin-responsive Aux/IAA family member	3.037	1.3E-81
bHLH	GRMZM2G107672_1	2:160.5	Unknown AT2G28160 FE-DEFICIENCY INDUCED TRANSCRIPTION FACTOR 1 FIT1	-3.214	1.8E-45
	GRMZM2G313756_1	10:108.3	Putative HLH DNA-binding domain superfamily protein AT2G28160 FE-DEFICIENCY INDUCED TRANSCRIPTION FACTOR 1 FIT1	-3.006	7.2E-55
MYB-related	GRMZM2G421256_2	2:14.7	Uncharacterized protein Os04g0583900	3.264	7.9E-58
Pseudo ARR	GRMZM2G179024_1	7:143.1	Uncharacterized protein OS09G0532400 Two-component response regulator-like PRR95	3.094	5.1E-102
	GRMZM2G148453_1	5:185.4	Unknown OS02G0618200 Two-component response regulator-like PRR1	3.184	1.6E-65
WRKY	GRMZM2G101405_1	3:203.1	Unknown AT5G26170 WRKY DNA-BINDING PROTEIN 50 WRKY50	3.307	2.6E-38
	GRMZM2G125653_2	7:115.3	Uncharacterized protein; WRKY DNA-binding protein AT1G80840 WRKY DNA-BINDING PROTEIN 40 WRKY40	3.734	5.6E-52
Redox	GRMZM2G462243_2	9:155.8	Uncharacterized protein	3.863	1.3E–105
	GRMZM2G044383_2	1:81.7	Glutathione S-transferase GST 30; Uncharacterized protein OS10G0530900 GSTU6 Probable glutathione S-transferase GSTU6	4.323	1.1E–85

Supplemental Table 3: Transcripts of SL shoot and root samples most responsive to chilling

Displayed are significantly differentially expressed transcripts (FDR *p*-value correction ≤ 0.05) exhibiting a log_2 fold (log_2 fc) change of ≥ 4 or ≤ –4. These are differentiated between 4 h and 24 h chilling stress. If no annotation for a transcript was available, the corresponding ortholog of *Oryza sativa* ssp. *japonica* or *Arabidopsis thaliana* is specified. The locations of transcripts are displayed in Mb; first number indicates the respective chromosome. The transcripts regulated in shoots are highlighted in green, those in the roots in brown.

	Transcript ID	Location	Name/Ortholog	log_2 fc	*p*-value
4 h chilling	GRMZM2G018375_1	8:137.6	THI1-1 Thiamine thiazole synthase 1, chloroplastic	6.177	8.4E–73
log_2 fc ≥ 4	GRMZM2G073427_7	1:170.5	Uncharacterized protein AT5G28770 ATBZIP63 ARABIDOPSIS THALIANA BASIC LEUCINE ZIPPER 63	5.968	1.4E–136
	GRMZM2G103945_1	6:133. 5	TIP4-1Aquaporin	5.769	6.4E–36
	GRMZM2G103945_2	6:133.5	TIP4-1Aquaporin	5.698	9.9E–64
	GRMZM2G073427_1	1:170.5	Uncharacterized protein AT5G28770 ATBZIP63 ARABIDOPSIS THALIANA BASIC LEUCINE ZIPPER 63	5.593	7.2E–52
	GRMZM2G006287_1	10:19.5	Maternal protein pumilio; Uncharacterized protein AT178160 APUM7 PUMILIO 7	5.038	3.5E–88
	GRMZM2G103945_3	6:133.5	Aquaporin TIP4-1	4.807	3.9E–11
	GRMZM2G179024_1	7:143.1	Uncharacterized protein OS09G0532400 Two-component response regulator-like PRR95	4.746	8.8E–132
	GRMZM2G018375_2	8:137.6	THI1-1 Thiamine thiazole synthase 1, chloroplastic	4.474	2.5E–80
	GRMZM2G108273_1	8:110.2	TIP4-2Aquaporin	4.409	1.1E–164
	GRMZM2G006964_1	2:28.3	Uncharacterized protein OS04G0522500 gibberellin 2-beta-dioxygenase 8	4.362	4.0E–59
	GRMZM2G059851_1	5:158.2	Heat shock factor protein 2	4.172	1.2E–101
	GRMZM2G421256_2	2:14.7	Uncharacterized protein Os04g0583900	4.168	3.1E–87
	GRMZM2G081949_1	7:158.9	Uncharacterized protein OS07G0569100 OsREM4.1 Remorin 4.1 (Gui *et al.* 2016)	4.087	3.1E–31
	GRMZM2G148904_1	8:34.5	S-adenosyl-L-methioninE–dependent methyltransferases superfamily protein	4.079	4.7E–31
	GRMZM2G074097_1	3:218.9	THI1-2 Thiamine thiazole synthase 2, chloroplastic	4.054	9.8E–119
	GRMZM2G073427_4	1:170.5	Uncharacterized protein AT5G28770 ATBZIP63 ARABIDOPSIS THALIANA BASIC LEUCINE ZIPPER 63	4.041	5.4E–50
log_2 fc ≤ –4	none	-	-	-	-
24 h chilling	GRMZM2G018375_2	8:137.6	THI1-1 Thiamine thiazole synthase 1, chloroplastic	5.840	6.9E–110
log_2 fc ≥ 4	GRMZM2G106303_1	9:7.3	12-oxo-phytodienoic acid reductase; Uncharacterized protein OS06G0216200 OPR2 Putative 12-oxophytodienoate reductase 2	5.664	4.1E–25
	GRMZM2G383699_1	3:65.7	ZmASR7-3 ABA-, stress-, and ripening-induced protein 7-3 (Pérez-Díaz *et al.* 2014)	5.249	2.2E–55
	GRMZM2G138770_1	2:35.1	Uncharacterized protein OS12G0431100 AAA-ATPase ASD, mitochondrial	5.203	7.0E–65
	GRMZM2G012566_2	1:38.5	Uncharacterized protein OS03G0265900	5.152	6.2E–48
	GRMZM2G028665_1	3:114.1	Uncharacterized protein OS01G0702000 BBD1 Bifunctional nuclease 1	5.150	6.2E–138
	GRMZM2G018375_1	8:137.6	THI1-1 Thiamine thiazole synthase 1, chloroplastic	4.683	2.7E–54
	GRMZM2G006964_1	2:28.3	Uncharacterized protein OS04G0522500 gibberellin 2-beta-dioxygenase 8	4.642	5.7E–63
	GRMZM2G137964_2	2:75.8	Uncharacterized protein ?	4.597	7.0E–56
	GRMZM5G891656_4	9:153.0	Monooxygenase; Uncharacterized protein AT4G38540 FAD/NAD(P)-binding oxidoreductase family protein	4.430	8.3E–12
	GRMZM2G022679_1	3:196.1	unknown OS01G0757200 gibberellin 2-beta-dioxygenase	4.353	2.6E–22
	GRMZM2G343149_1	10:47.5	DNAJ heat shock N-terminal domain-containing protein	4.290	1.3E–98
	GRMZM2G315199_1	6:156.3	Uncharacterized protein ?	4.204	3.0E–121
	GRMZM2G074097_1	3:218.9	THI1-2 Thiamine thiazole synthase 2, chloroplastic	4.196	7.1E–123
	GRMZM2G314075_1	3:65.6	ZmASR7-2 ABA-, stress-, and ripening-induced protein 7-2 (Pérez-Díaz *et al.* 2014)	4.101	1.1E–28
	GRMZM2G086763_1	5:19.4	Chloroplast post-illumination chlorophyll fluorescence increase protein	4.080	4.0E–85
	GRMZM2G006287_1	10:19.5	Maternal protein pumilio; Uncharacterized protein AT178160 APUM7 PUMILIO 7	4.031	3.1E–69
	GRMZM2G008108_1	7:73.5	Putative uncharacterized protein ?	4.027	1.1E–27
log_2 fc ≤ –4	GRMZM5G841343_1	6:146.2	ZmMBD120 Methyl-CpG-binding domain protein 120	–4.158	1.8E–28

	Transcript ID	Location	Name/Ortholog	log_2 fc	*p*-value
log_2 fc ≤ –4	GRMZM2G177229_5	7:133.5	Zm-U2AF35a (Fouquet *et al*. 2011)	–4.046	4.1E–64
4 h chilling log_2 fc ≥ 4	GRMZM2G031143_5	2:212.3	Uncharacterized protein ?	4.930	9.9E–56
	GRMZM2G179024_1	7:143.1	Uncharacterized protein OS09G0532400 Two-component response regulator-like PRR95	4.697	2.9E–161
	GRMZM2G031143_4	2:212.3	Uncharacterized protein ?	4.667	6.1E–61
	GRMZM2G138770_1	2:35.1	Uncharacterized protein OS12G0431100 AAA-ATPase ASD, mitochondrial	4.524	3.2E–112
	GRMZM2G031143_7	2:212.3	Uncharacterized protein ?	4.416	2.0E–54
	GRMZM2G073427_7	1:170.5	Uncharacterized protein AT5G28770 ATBZIP63 ARABIDOPSIS THALIANA BASIC LEUCINE ZIPPER 63	4.267	2.4E–116
	GRMZM2G073427_1	1:170.5	Uncharacterized protein AT5G28770 ATBZIP63 ARABIDOPSIS THALIANA BASIC LEUCINE ZIPPER 63	4.244	4.0E–29
	GRMZM2G421256_2	2:14.7	Uncharacterized protein Os04g0583900	4.136	4.2E–72
log_2 fc ≤ –4	GRMZM2G123212_1	2:214.2	Ubiquitin-protein ligase CIP8	–4.004	2.4E–63
24 h chilling log_2 fc ≥ 4	GRMZM2G018375_2	8:137.6	THI1-1 Thiamine thiazole synthase 1, chloroplastic	5.101	7.9E–40
	GRMZM5G893912_1	1:180.0	Uncharacterized protein OS12G0431100 AAA-ATPase ASD, mitochondrial	4.594	8.3E–265
	GRMZM2G044383_2	1:81.7	Glutathione S-transferase GST 30; Uncharacterized protein OS10G0530900 GSTU6 Probable glutathione S-transferase GSTU6	4.323	1.1E–85
	GRMZM2G078465_1	7:140.0	Uncharacterized protein AT2G43840 UGT74F1, UDP-GLYCOSYLTRANSFERASE 74 F1	4.317	3.3E–23
	GRMZM2G138770_1	2:35.1	Uncharacterized protein OS12G0431100 AAA-ATPase ASD, mitochondrial	4.270	1.0E–108
	GRMZM2G132069_2	3:6.8	Uncharacterized protein OS01G0191700 ATP-dependent 6-phosphofructokinase 6	4.235	6.7E–91
	GRMZM2G315199_1	6:156.3	Uncharacterized protein ?	4.146	1.1E–14
	GRMZM2G124229_1	5:4.6	Uncharacterized protein OS03G0790500 probable carboxylesterase 15	4.143	9.1E–142
	GRMZM2G043657_1	5:3.0	unknown ?	4.134	1.8E–56
	GRMZM2G044132_2	2:54.4	ZmASR3 ABA-, stress-, and ripening-induced protein 3 (Pérez-Díaz *et al.* 2014)	4.134	9.9E–68
	GRMZM2G074097_1	3:218.9	THI1-2 Thiamine thiazole synthase 2, chloroplastic	4.132	5.5E–66
	GRMZM2G078033_5	2:2.3	Polyamine oxidase 6 ZmPAO6 (Jasso-Robles *et al.* 2016)	4.103	4.3E–57
	GRMZM2G336448_2	4:186.6	Carbohydrate transporter/sugar porter/transporter; Uncharacterized protein AT5G13750 ZIFL1, ZINC INDUCED FACILITATOR-LIKE 1	4.037	3.9E–114
	GRMZM5G862355_1	6:97.2	Uncharacterized protein OS06G0642650	4.024	8.3E–128
log_2 fc ≤ –4	GRMZM2G136032_1	9:6.4	PIP1-6 Aquaporin	–5.467	4.9E–181
	GRMZM2G057208_1	7:104.2	unknown OS02G0503900 isoflavone 2'-hydroxylase	–4.428	8.5E–109
	GRMZM2G177229_5	7:133.5	Zm-U2AF35a (Fouquet *et al*. 2011)	–4.083	1.3E–24
	GRMZM2G371462_1	1:137.1	Uncharacterized protein ?	–4.039	2.3E–23

Supplemental Table 4: Oligonucleotide sequences for the qRT-PCR.
Shown are the designations of oligonucleotides, the respective sequences and their purposes.

Oligonucleotide name	Sequence (5' to 3')	Usage
ETIF3fw-5	GTGGTTTGGTTGGACGAGAATAAC	qRT-PCR *ETIF3SU4*
ETIF3rv-6	ACGGCATGCGAACTCAATATAAAA	qRT-PCR *ETIF3SU4*
GST26fw-1	GAGTACATCGAGCAGGACCTGTTC	qRT-PCR *GST26*
GST26rv-2	CAGACCTCATCGACGTACTCCAC	qRT-PCR *GST26*
SAURfw-5	AGACCGAGTTCGCTCACATC	qRT-PCR *SAUR31*
SAURrv-6	GAACTGGAAGCGGAATTAATCTA	qRT-PCR *SAUR31*
ACR8fw-11	GCTACTCCGTGGTGACCGTGCAGTG	qRT-PCR *ACR8*
ACR8rv-12	CCTCTAGCGACCTCCGGTCTATGGC	qRT-PCR *ACR8*
EP_TUA4-F	TGCTCTGAACGTTGATGTGA	qRT-PCR Endogenous control
EP_TUA4-R	GCAGAAATGACTGGAGCGTA	qRT-PCR Endogenous control

Supplemental Table 5: Statistics of sequencing data
Shown are the obtained reads and the percentages of reads with a Q30 quality score ≥ 30 for each Illumina library prepared. Libraries obtained from the shoot samples are highlighted in green, those obtained from the root samples in brown.

SL	Number of reads	% of ≥ Q30 bases	N4X-sen	Number of reads	% of ≥ Q30 bases	N4X-tol	Number of reads	% of ≥ Q30 bases
t0 (1. exp.)	37,604,340	87.62	t0 (1. exp.)	38,598,888	87.30	t0 (1. exp.)	38,811,477	88.20
t0 (2. exp)	32,498,119	88.98	t0 (2. exp)	30,128,980	88.10	t0 (2. exp)	38,083,402	88.22
t4 (1. exp)	38,699,194	88.09	t4 (1. exp)	41,792,314	88.23	t4 (1. exp)	40,205,899	87.78
t4 (2. exp)	36,883,495	88.01	t4 (2. exp)	40,328,618	88.25	t4 (2. exp)	39,176,262	88.59
t24 (1. exp)	38,086,907	87.66	t24 (1. exp)	35,766,146	87.55	t24 (1. exp)	42,959,006	88.04
t24 (2. exp)	37,169,322	88.51	t24 (2. exp)	31,249,386	88.46	t24 (2. exp)	42,259,334	87.93
t0 (1. exp.)	33,356,139	88.86	t0 (1. exp.)	31,371,833	88.91	t0 (1. exp.)	41,493,209	88.66
t0 (2. exp)	37,725,962	89.09	t0 (2. exp)	35,592,182	89.04	t0 (2. exp)	40,833,285	87.85
t4 (1. exp)	40,976,637	88.59	t4 (1. exp)	45,466,703	88.62	t4 (1. exp)	35,142,980	88.99
t4 (2. exp)	38,860,154	87.83	t4 (2. exp)	44,231,796	88.00	t4 (2. exp)	39,838,858	89.07
t24 (1. exp)	35,483,293	88.68	t24 (1. exp)	31,680,322	88.66	t24 (1. exp)	43,768,193	88.17
t24 (2. exp)	37,780,866	88.67	t24 (2. exp)	33,888,289	88.87	t24 (2. exp)	45,857,003	87.42

VI. Addendum

1. **Bundle sheath cells are more susceptible to chilling than mesophyll cells**
2. **ke-1 contains a functional mitochondrial target sequence**

1. Bundle sheath cells are more susceptible to chilling than mesophyll cells

Introduction

Maize is of tropical and subtropical origin (Greaves 1996) and exhibits a temperature optimum of 30 to 35 °C with respect to processes like germination, initial shoot extension as well as shoot- and root extension. Below 8 °C no shoot elongation and below 7 °C no leaf formation is possible (Miedema 1982). However, by now maize is also cultivated in regions that do not fulfil the plants' optimum requirements. Low temperatures can lead to injuries of maize seedlings like leaf chlorosis. This injury is often described to appear after cold treatment in the dark followed by illumination. For example, etiolated maize seedlings grown at 16 °C in the dark did not green after transfer to light, in contrast to etiolated seedlings cultivated at 28 °C. It has been postulated that the final phase of chlorophyll synthesis was prolonged during chilling and exposure to light caused a faster destruction than formation of the photosynthetic pigment (McWilliam and Naylor 1967). Further studies with maize seedlings revealed that one cold night could lead to the formation of strong yellow transverse bands – so called Faris bands – of maize seedlings leaves and that the severity of the effect depended on age, temperature and genotype (Sellschop *et al.* 1962). A similar analysis was conducted by Slack *et al.* (1974). *Sorghum bicolor* seedlings, raised at optimal temperatures, were subjected to one night at 4 °C. After 36 hours recovery at ideal temperature chlorotic bands appeared in a region that was hidden in the stem during chilling. In the chlorotic region, most of the mesophyll (M) chloroplasts displayed a pale green or yellow phenotype (Slack *et al.* 1974). Impairment of M chloroplasts was also found in maize seedlings exposed to 4 °C in the dark for 3 days (Miedema *et al.* 1987). Moreover, chilling stress during a normal diurnal light cycle can also lead to leaf chlorosis. For instance, two weeks of chilling stress (10 °C day/4 °C night) resulted in large cross bands on leaves of maize seedlings that did not recover completely. It was argued that chlorosis was the result of photo-oxidation of chlorophyll in consequence of high light intensity and chilling. In general, low temperatures of 7 to 16 °C still allowed for slight leaf extension but not for chlorophyll accumulation (Miedema *et al.* 1987). In contrast to full-grown or meristematic zones, the cell extension zone of maize leaves is particularly chilling sensitive (Miedema 1982). Another cross band chlorosis was described in Baliashvili (2010) where two European inbred lines, the chilling tolerant TH and the chilling sensitive SL, a population of double haploid (DH) lines and a population of (sub) near isogenic lines (NILs) were investigated. The DH lines were derived from a crossing of TH and SL, the (sub) NILs from repeated backcrossing of one DH line to SL. These lines were

allowed to grow for 14 days at near-optimum temperatures (25 °C day/22 °C night) until the third leaf was fully developed. Subsequently, the seedlings were subjected to 7 days chilling stress (8 °C day/6 °C night) in which the growth nearly ceased. Following recovery at near-optimum temperatures, chlorotic bands exclusively appeared on the 4th and 5th leaf of lines that have exhibited chilling sensitivity concerning early vigour in field experiments (Baliashvili 2010, Presterl *et al.* 2007, Wilde *et al.* 2005). Further experiments showed that the chlorotic lesions developed in the tissue above the extension zone. During chilling, the susceptible tissue was enclosed in the stems formed by leaf sheaths from older leaves. However, the nature of the chlorosis remained elusive. Cross-sections of TH and chlorotic SL did not exhibit anatomic changes. Similar, leaf protein levels of chilling-treated SL, TH and NILs were not different between chilling sensitive and tolerant lines (Baliashvili 2010). These results were surprising and incomprehensible as they contradicted the obvious appearance of chlorosis. To uncover the foundation of chlorosis an in-depth analysis of the chilling-induced chlorosis was performed using different strategies. In contrast to Baliashvili (2010), cross-sections were neither bleached nor kept in 70 % ethanol prior microscopy to reveal changes in chloroplast distribution and pigment levels. Secondly, protein levels of chlorotic sections and equivalent green tissues were examined, not of whole leaves as in Baliashvili (2010).

Results

Experimental design

Chilling sensitivity related to poor early vigour is linked to a chlorotic phenotype that can be induced in growth chamber experiments. During recovery after previous chilling stress a yellow band appeared on the 4th and 5th leaves of the analysed chilling sensitive lines (see previous section and Figure 2A). We were interested in unravelling the cause of the chlorosis and decided on two approaches to elucidate this issue. Firstly, cross-sections were investigated by light microscopy and secondly, the protein levels of a subset of proteins involved in photosynthesis were compared. For these experiments, we used the chilling sensitive parent SL and three different NILs (Figure 1).

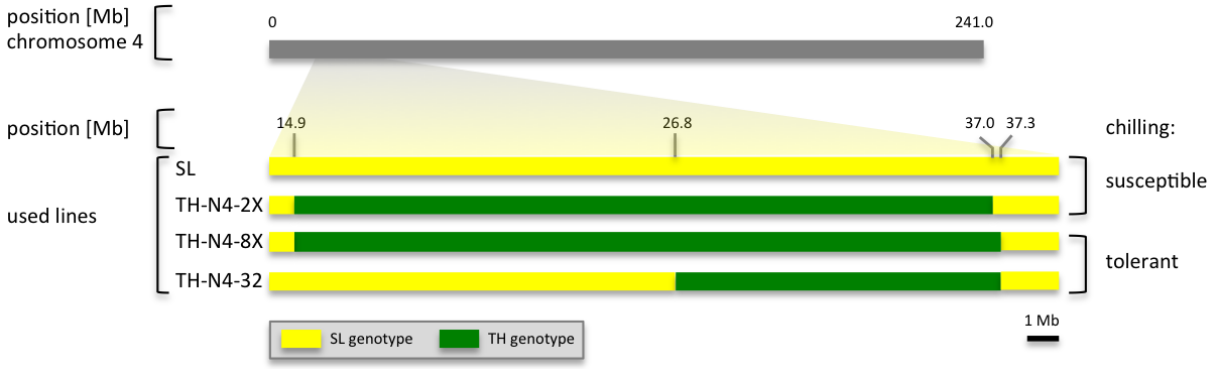

Figure 1: Genotypes of chromosome 4 of investigated lines that contrast in chilling susceptibility
A schematic illustration of chromosome 4 of the chilling sensitive lines SL and TH-N4-2X and the chilling tolerant lines TH-N4-8X and TH-N4-32 is shown. Yellow regions indicate the SL genotype and green regions the TH genotype. According to this illustration the QTL4 is located between 37.0 and 37.3 Mb (compare Manuscript 2).

Each NIL contains a different long TH fragment in the SL background on chromosome 4. TH-N4-2X is chilling sensitive and contains a 22.1 Mb long TH fragment that is located between 14.9 and 37.0 Mb. TH-N4-8X and TH-N4-32 are chilling tolerant and comprise a 22.4 Mb (14.9 Mb to 37.3 Mb) or a 10.5 Mb (26.8 Mb to 37.3 Mb) long TH fragment, respectively.

Analysis of chilling-induced chlorosis by light microscopy

To analyse leaf chlorosis at the cellular level, the chlorotic and equivalent green fragments should be harvested. As maize shows a developmental gradient alongside the leaf blade from the base to the tip (Li *et al.* 2010, Sharman 1942), the following procedure was applied to identify equivalent regions of chlorosis. Stems of the shoots containing the developing leaves were punctured with a syringe at the auricles of the second and third leaf at the beginning and the end of chilling stress. After six days of recovery, chloroses were clearly visible in the sensitive lines around the holes punctured after chilling treatment at the second auricle (Figure 2B).

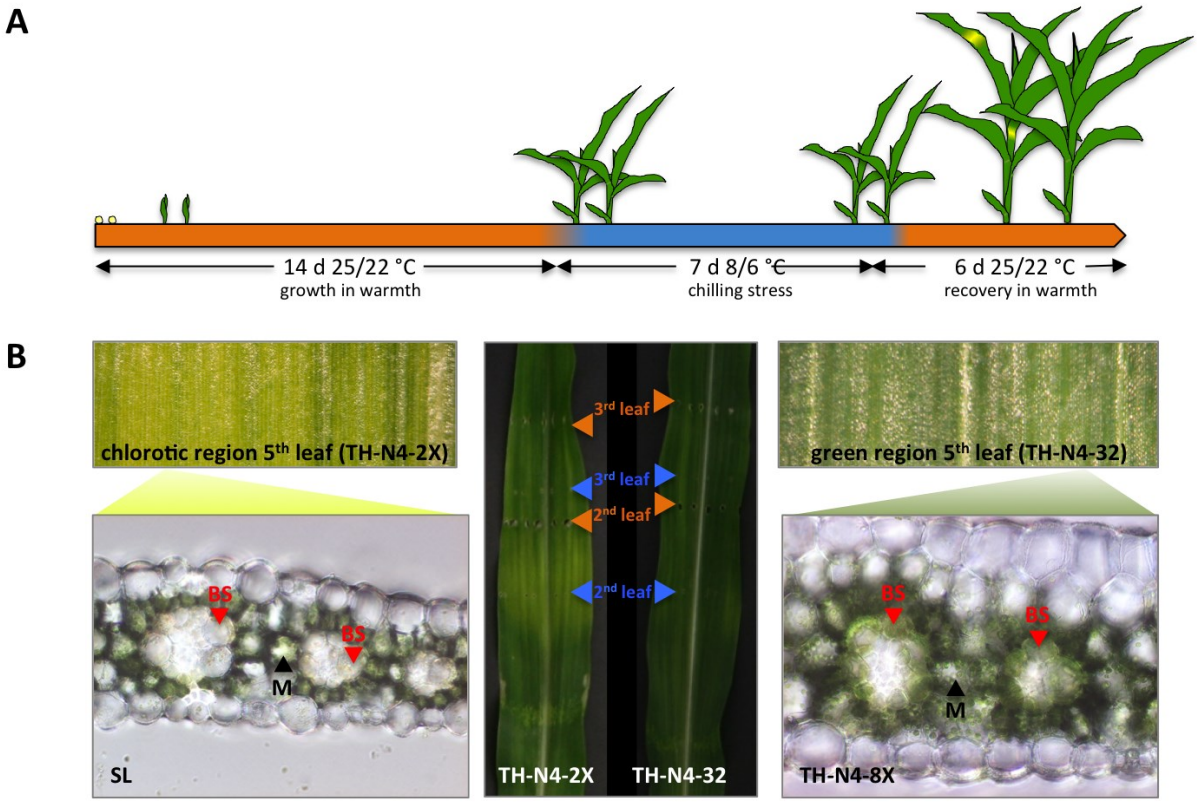

Figure 2: Chlorosis induction and analysis of chlorosis and corresponding green regions in chilling sensitive and tolerant maize plants
(A) Illustration of growth conditions inducing chlorosis. The plant on the left-hand side of each pair displays a chilling sensitive genotype; that on the right-hand side a chilling tolerant genotype.
(B) The location of green and chlorotic segments of the 5th leaf, top view in detail of these segments and cross-sections of chlorotic and corresponding green tissue. Arrowheads mark the holes made before (orange arrowheads) and after cold treatment (blue arrowheads) of the sensitive and tolerant line. The used maize lines are stated in every image.
M, mesophyll; BS, bundle sheath

Subsequently, the chlorotic segments of the chilling sensitive lines TH-N4-2X and SL as well as the equivalent green segments of the chilling tolerant lines TH-N4-8X and TH-N4-32 were harvested.

The chlorotic segments were not completely yellow; especially the cells around major veins and at the edges were less pale. The cross-sections within the yellow parts exhibited pale and less chloroplasts in the bundle sheath (BS) cells. M cells appeared slightly paler. The cross-sections of the corresponding green segments of the tolerant NILs showed green chloroplasts in the BS cells. Those were tightly packed and averted from the vascular tissue and close to the adjacent M cells. Taken together, chilling mainly affects the number and chlorophyll content of BS chloroplasts in the chlorotic regions.

Immunoblot analysis of photosynthetic proteins in chlorotic regions

As pale chloroplasts within leaf chlorosis indicate perturbations of photosynthesis, immunoblots were performed to detect major photosynthetic proteins. For this purpose, plant material of the 5th leaves was harvested at the sixth day of recovery (compare Figure 2A). We gathered chlorotic segments of the chilling sensitive TH-N4-2X and green segments of the chilling tolerant TH-N4-32. Total protein extracts were isolated from two chlorotic or equivalent green segments, respectively. The proteins were subsequently transferred to nitrocellulose membranes and detected with immuno staining (Figure 3).

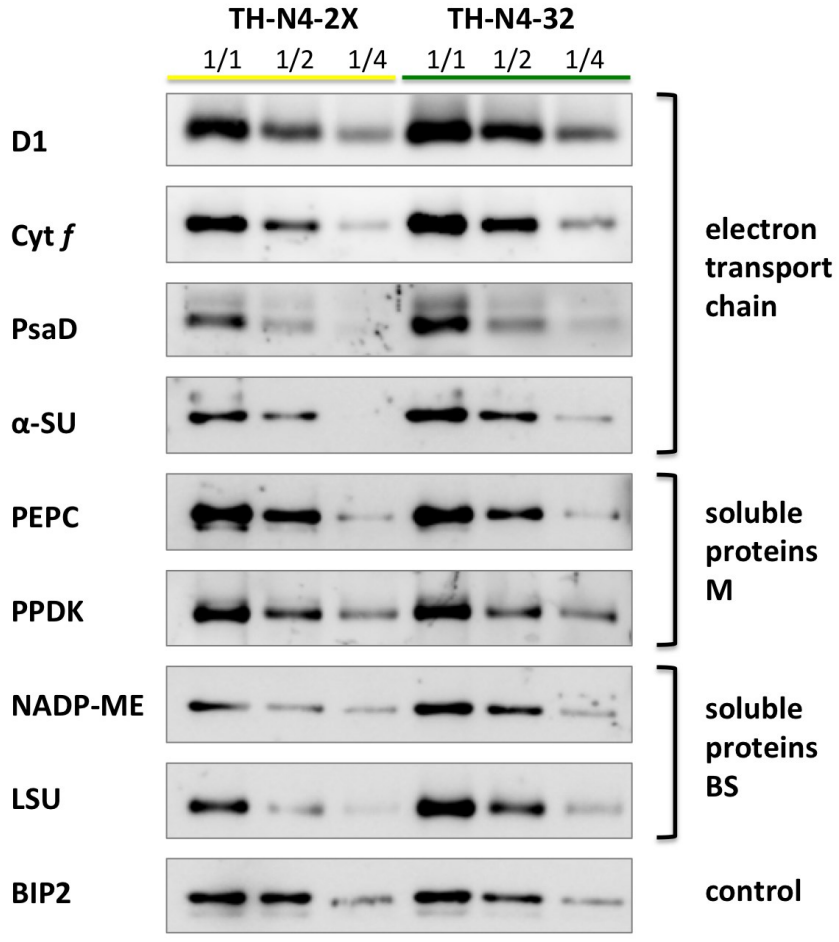

Figure 3: Immunoblot analysis of chlorotic and corresponding green regions from chilling sensitive and tolerant plants

Aliquots of whole protein extracts from chlorotic regions of the sensitive TH-N4-2X and corresponding green regions of the tolerant TH-N4-32 were separated via SDS-PAGE and transferred to a nitrocellulose membrane. A subset of first antibodies was applied, followed by visualisation by means of utilisation of a peroxidase-linked secondary antibody. Protein amounts: 1.00/0.50/0.25 µg (D1), 6.0/3.0/1.5 µg (Cyt *f*, PsaD, NADP-ME), 2.0/1.0/0.5 µg (α-SU, PEPC, PPDK, LSU) and 20/10/5 µg (BIP2).

D1, D1 subunit of photosystem II; Cyt f, Cytochrom f; PsaD, PsaD subunit of photosystem I; α-SU, α-Subunit of ATPase complex; PEPC, Phospho*enol*pyruvate carboxylase; PPDK, Pyruvate, orthophosphate dikinase; LSU, Large subunit of Ribulose-1,5-bisphosphate carboxylase/oxygenase; BIP2, Binding immunoglobulin protein 2; M, mesophyll; BS, bundle sheath

Four antibodies against representative subunits of the electron transport chain complexes were chosen. Westernblot signals of antibodies against photosystem II subunit D1 (D1), cytochrome b_6f complex subunit cytochrome *f* (Cyt *f*), photosystem I subunit PsaD (PsaD) and ATPase α-subunit (α-SU) were reduced to about 50 % in the chlorotic tissues. Additionally, antibodies against each two soluble photosynthetic enzymes restricted to the M or BS, respectively, were applied. The signals of antibodies against phospho*enol*pyruvate carboxylase (PEPC) and pyruvate, orthophosphate dikinase (PPDK) did not exhibit a reduction in chlorotic segments but showed equal levels in chlorotic and green regions. Both enzymes are located in the M that displayed less changes within the chlorotic parts of cross-sections compared to BS (Figure 2B). In contrast, the signals of antibodies against the NADP malic enzyme (NADP-ME) and the large subunit of Rubisco (LSU) revealed a reduction of about 50 % in protein levels of the chlorotic segments. These enzymes are expressed solely in the BS that revealed a drastic change in the cross-sections. This led to the conclusion that chilling and following recovery at normal temperatures particularly affect the BS of sensitive lines.

Discussion

Leaf chlorosis is a frequently observed phenotype in maize plants subjected to chilling stress (Greaves 1996, Miedema 1982). Studies about leaf chlorosis in chilling sensitive grasses exhibited perturbations like abnormal etioblast and chloroplast structures (McWilliam and Naylor 1967, Yoshida *et al.* 1996), pale M cells' chloroplasts and reduced amounts of photosynthetic proteins (Slack *et al.* 1974). During phenotypic experiments consisting of 14 days growing in warmth and 7 days chilling stress at 8 °C/6 °C (day/night) followed by 6 days of recovery, leaf chlorosis emerged in chilling sensitive maize lines (Baliashvili 2010) (Figure 2A). These cross band chloroses were analysed by microscopy to reveal reasons for the lesion at the cellular level. Whilst M cells of chlorotic regions displayed green chloroplasts, the BS cells contained less and yellowish chloroplasts (Figure 2B), which indicates increased chilling sensitivity of BS cells. Hence, the levels of photosynthetic proteins were checked via Westernblots. It was anticipated – due to the abnormal BS chloroplasts – that the protein levels for C_4 cycle enzymes located in the BS, as well as those for electron transport chain complexes, were reduced in chlorotic tissues. The results mostly met the expectations. While antibody signals of PEPC and PPDK (enzymes located in M cells) exhibited no differences between chlorotic and green tissue, signals of antibodies against representative proteins of the electron transport chain, the large subunit of Rubisco

and NADP-ME (both enzymes restricted to BS cells) displayed a reduction of about 50 % in chlorotic tissue. These results indicate that BS cells were essentially affected in the chlorosis. In addition, the M cells also seemed to be slightly affected since maize – like other C_4 plants – lack the photosystem II in the BS (Ghirardi and Melis 1983).

These results contradict the outcomes of several studies. For example in Slack *et al.* (1974), Sorghum seedlings were cold-treated for one night. Yellow bands appeared on leaves after 1.5 days. Interestingly, M chloroplasts were stronger affected than BS chloroplasts. M chloroplasts were pale and exhibited an altered thylakoid ultrastructure. Correspondingly, the activities of PEPC and NADP-malate dehydrogenase, both located in the M, were more strongly reduced than the activities of Rubisco and NADP-ME, which are both restricted to the BS (Slack *et al.* 1974). Furthermore, Robertson *et al.* (1993) and Nie *et al.* (1995) raised maize at 14 °C/12 °C (day/night). During recovery at 25 °C/ 22 °C (day/night), pigments and thylakoid proteins accumulated rapidly close to control levels. Yet photosynthetic capacity was limited when compared to control plants. However, similar to Slack *et al.* (1974), the M cells were more affected. About 20-30 % of the M cells were devoid of thylakoid proteins (Nie *et al.* 1995, Robertson *et al.* 1993). The apparent contradiction to our study might be explained by use of different plant species (Slack *et al.* 1974), genotypes (Nie *et al.* 1995, Robertson *et al.* 1993) or experimental layouts (e. g. chilling treatment).

But what is the molecular reason of the establishment of chlorosis? Probably, the chlorosis may be caused by increased reactive oxygen species (ROS) formation. It is known that chilling, especially in combination with high light, leads to enhanced production of ROS which can cause lipid peroxidation and degradation of proteins and nucleic acids (Prasad 1996, Prasad *et al.* 1994). To diminish effects caused by ROS, plants have evolved an efficient antioxidant system to reduce their accumulation or to dispose of them (Alscher *et al.* 1997, Foyer *et al.* 1994). Interestingly, the antioxidant system also underwent a spatial separation due to the compartmentalisation of C_4 photosynthesis. Since BS cells of maize not only lack photosystem II but also the Ferredoxin-$NADP^+$ reductase (Furbank and Foyer 1988, Ghirardi and Melis 1983), this tissue has less NADPH available. Consequently, the NADPH-using glutathione reductase as well as the dehydroascorbate reductase are restricted to the M cells (Doulis *et al.* 1997, Foyer *et al.* 2002). These enzymes are required for the reduction of oxidised glutathione disulphide to glutathione and dehydroascorbic acid to ascorbate, respectively (Foyer *et al.* 1994). Therefore, the BS cells have to rely on the supply of reduced glutathione and ascorbate from the M cells for scavenging ROS (Doulis *et al.* 1997, Foyer *et al.* 2002). Hence, this system is very fragile to any perturbations that affect transport of

antioxidants between BS and M cells (Foyer *et al.* 2002, Kingston-Smith and Foyer 2000). Thus, it is possible that ROS accumulate during chilling treatment in the photosynthetic cells (Foyer *et al.* 2002), but cannot be scavenged at a decent level in the BS. In the developing leaf, chlorophyll might not be incorporated into the thylakoid membrane, leading to the pale phenotype of chlorosis (Greaves 1996), which is worsened by illumination of the susceptible tissue. This effect has also been described by Kingston-Smith and Foyer (2000).

To sum up, the BS cells are particularly sensitive to chilling in the analysed chlorosis. A ROS-dependant mechanism may cause the disturbances.

Methods

Plant material and growth conditions

For cross-sections, the European inbred line SL, TH-N4-2X (both chilling sensitive), TH-N4-8X and TH-N4-32 (both chilling tolerant) were used. TH-N4-2X and TH-N4-32 were also utilised for protein isolation. All lines are the property of KWS SAAT SE (Einbeck, Germany). Up to 24 kernels were planted in propagator trays filled with Floraton 1 compost (Floragard Vertriebs GmbH, Oldenburg Germany) and grown in the Conviron CMP4030 growth chamber (Conviron, Manitoba, Canada). The seedlings were cultivated for 14 days at 25/22 °C (day/night) until the third leave was fully developed. A 7-day period of chilling stress was applied with temperatures of 8/6 °C (day/night) followed by 6 days recovery at 25/22 °C (day/night). The light period stretched over 14 hours and the dark period over 10 hours. The light intensity was set to a photosynthetic photon flux density (PPFD) of 350 to 400 µmol m^{-2} s^{-1}. The changes of temperatures were executed at 10:30 am. At every change of temperature, the stems were punctured with a syringe at the second and third auricle to analyse the position of chlorosis and to mark the corresponding green segment in tolerant plants.

Visual analysis of cross-sections

The 5th leaves were harvested after 6 days of recovery of chilling stress. The chloroses of the sensitive TH-N4-2X and SL were neatly cut with scissors. Orientating at the holes, corresponding green segments of the tolerant TH-N4-8X/TH-N4-32 were cut. The segments were stored in water until use. The cross-sections were manually made with razor blades and visualised by means of light microscopy at the same day of harvest. Three independent experiments were performed.

Protein isolation, SDS-PAGE and Westernblot

The 5th leaves were harvested after 6 days recovery of chilling stress for protein isolation. By using scissors chlorotic leaf parts of sensitive NIL plants were neatly cut. Leaf segments of 4 cm length were cut from the equivalent green material of tolerant TH-N4-32 plants. The obtained plant material was immediately frozen in liquid nitrogen and stored at –80 °C until further use. Whole protein extracts were isolated according to Shen *et al.* (2007) by using two leaf segments per sample that were ground with mortar and pestle in the presence of liquid nitrogen. Protein concentrations were determined by means of the RC DC™ Protein Assay (BioRad, Hercules, USA). Three different protein amounts per sample in a range of 0.25 to 20.00 µg, depending on the expression strength of the examined protein, were applied to SDS-polyacrylamide gels. SDS-polyacrylamide gel electrophoreses were performed as described in Schagger and von Jagow (1987). The proteins were semi-dry electroblotted to Amersham Protan 0.1 nitrocellulose membranes (GE Healthcare Life Science, Little Chalfont, UK). Immunodecorations of blotted proteins were executed as described in Harlow and Lane (1999). For the visualisation of peroxidase activity, membranes were incubated in SuperSignal™ West Femto Maximum Sensitivity Substrate (Thermo Fisher Scientific, Waltham, USA) and exposed in a LAS-4000 mini (GE Healthcare Life Science, Little Chalfont, UK). Two independent experiments with two biological replicates each were performed.

Literature

Alscher, R.G., Donahue, J.L. and Cramer, C.L. (1997) Reactive oxygen species and antioxidants: Relationships in green cells *Physiol Plant*, **100**, 224-233.

Baliashvili, N. (2010) Feinkartierung eines QTL (Quantitative Trait Locus) für Kühletoleranz auf Chromosom 4 in Mais und dessen molekularbiologische und phänotypische Charakterisierung. *PhD thesis, HHU Düsseldorf, Düsseldorf, Germany*.

Doulis, A.G., Debian, N., Kingston-Smith, A.H. and Foyer, C.H. (1997) Differential Localization of Antioxidants in Maize Leaves. *Plant Physiol*, **114**, 1031-1037.

Foyer, C.H., Lelandais, M. and Kunert, K.J. (1994) Photooxidative stress in plants. *Physiol Plant*, **92**, 696-717.

Foyer, C.H., Vanacker, H., Gomez, L.D. and Harbinson, J. (2002) Regulation of photosynthesis and antioxidant metabolism in maize leaves at optimal and chilling temperatures: review. *Plant Physiol Biochem*, **40**, 659-668.

Furbank, R.T. and Foyer, C.H. (1988) C4 plants as valuable model experimental systems for the study of photosynthesis. *New Phytol*, **109**, 265-277.

Ghirardi, M.L. and Melis, A. (1983) Localization of photosynthetic electron transport components in mesophyll and bundle sheath chloroplasts of Zea mays. *Arch Biochem Biophys*, **224**, 19-28.

Greaves, J.A. (1996) Improving suboptimal temperature tolerance in maize— the search for variation. *J Exp Bot*, **47**, 307-323.

Harlow, E. and Lane, D. (1999) Using Antibodies. A Laboratory Manual. *Coldspring-Harbour Laboratory Press, UK*.

Kingston-Smith, A.H. and Foyer, C.H. (2000) Bundle sheath proteins are more sensitive to oxidative damage than those of the mesophyll in maize leaves exposed to paraquat or low temperatures. *J Exp Bot*, **51**, 123-130.

Li, P., Ponnala, L., Gandotra, N., Wang, L., Si, Y., Tausta, S.L., Kebrom, T.H., Provart, N., Patel, R., Myers, C.R., Reidel, E.J., Turgeon, R., Liu, P., Sun, Q., Nelson, T. and Brutnell, T.P. (2010) The developmental dynamics of the maize leaf transcriptome. *Nat Genet*, **42**, 1060-1067.

McWilliam, J.R. and Naylor, A.W. (1967) Temperature and plant adaptation. I. Interaction of temperature and light in the synthesis of chlorophyll in corn. *Plant Physiol*, **42**, 1711-1715.

Miedema, P. (1982) The effects of low temperature on Zea mays. *Adv Agron*, **35**, 93-128.

Miedema, P., Post, J. and Groot, P.J. (1987) The effects of low temperatures on seedling growth of maize genotypes. *Pudoc Wageningen*.

Nie, G.Y., Robertson, E.J., Fryer, M.J., Leech, R.M. and Baker, N.R. (1995) Response of the photosynthetic apparatus in maize leaves grown at low temperature on transfer to normal growth temperature. *Plant Cell Environ*, **18**, 1-12.

Prasad, T.K. (1996) Mechanisms of chilling-induced oxidative stress injury and tolerance in developing maize seedlings: changes in antioxidant system, oxidation of proteins and lipids, and protease activities. *Plant J*, **10**, 1017-1026.

Prasad, T.K., Anderson, M.D., Martin, B.A. and Stewart, C.R. (1994) Evidence for Chilling-lnduced Oxidative Stress in Maize Seedlings and a Regulatory Role for Hydrogen Peroxide. *Plant Cell*, **6**, 65-74.

Presterl, T., Ouzunova, M., Schmidt, W., Möller, E.M., Röber, F.K., Knaak, C., Ernst, K., Westhoff, P. and Geiger, H.H. (2007) Quantitative trait loci for early plant vigour of maize grown in chilly environments. *Theor Appl Genet*, **114**, 1059-1070.

Robertson, E.J., Baker, N.R. and Leech, R.M. (1993) Chloroplast thylakoid protein changes induced by low growth temperature in maize revealed by immunocytology. *Plant Cell Environ*, **16**, 809-818.

Schagger, H. and von Jagow, G. (1987) Tricine-sodium dodecyl sulfate-polyacrylamide gel electrophoresis for the separation of proteins in the range from 1 to 100 kDa. *Anal Biochem*, **166**, 368-379.

Sellschop, W., Makkinkm, J.P.F. and Baier, A.E. (1962) Cold chlorosis and other abnormalities in maize seedlings. *South African Journal of Agricultural Science*, **5**, 199-209.

Sharman, B.C. (1942) Developmental Anatomy of the Shoot of Zea mays L. . *Ann Bot*, **6**, 245-282.

Shen, Y., Khanna, R., Carle, C.M. and Quail, P.H. (2007) Phytochrome induces rapid PIF5 phosphorylation and degradation in response to red-light activation. *Plant Physiol*, **145**, 1043-1051.

Slack, C.R., Roughan, P.G. and M., B.H.C. (1974) Selective Inhibition of Mesophyll Chloroplast Development in Some C4-Pathway Species by Low Night Temperature. *Planta*, **118**, 57-73.

Wilde, K., Presterl, T., Möller, E.M., Ouzunova, M., Schmidt, W. and Geiger, H.H. (2005) Untersuchungen zur Züchtung auf Kühletoleranz bei Mais. *Bericht über die 56. Tagung 2005 der Vereinigung der Pflanzenzüchter und Saatgutkaufleute Österreichs*.

Yoshida, R., Kanno, A., Sado, T. and Kameya, T. (1996) Cool-Temperature-Induced Chlorosis in Rice Plants (I. Relationship between Induction and a Disturbance of Etioplast Development). *Plant Physiol*, **110**, 997-1005.

2. *ke-1* contains a functional mitochondrial target sequence

Introduction

The gene *kühleemfindlich-1* (*ke-1*) is a candidate for conferring chilling tolerance in the maize inbred line TH. It is located in a QTL region that was found to be mainly responsible for early plant vigour (Presterl *et al.* 2007, Wilde *et al.* 2005) and furthermore exhibited differential gene expression between a chilling tolerant and a chilling sensitive NIL in a transcriptome experiment (Manuscript 2). The *ke-1* gene is also annotated as *SAUR31* and thus belongs to the *SMALL AUXIN-UP RNA* (*SAUR*) family. The *SAUR* family is one of the three early auxin response gene families besides the *AUX/IAA* and the *GRETCHENHAGEN3* (*GH3*) families (Hagen and Guilfoyle 2002, Ren and Gray 2015). The first *SAUR* genes have been identified in a differential hybridisation screen in soybean where their transcripts quickly accumulated after auxin treatment (McClure and Guilfoyle 1987). By now, *SAUR* genes have been detected in many different plant species – and only in plant species (Ren and Gray 2015). The genes are characterised by several features. Most *SAUR* genes have no introns and are partly organised in clusters (Chen *et al.* 2014, Hagen and Guilfoyle 2002, Xie *et al.* 2015). The encoded proteins are small and share a highly conserved, about 60 amino acids long domain, which is characterised by hydrophobic amino acids (Ren and Gray 2015). The *SAUR* genes often contain auxin response elements (AuxREs) within their promoters (Chen *et al.* 2014, Hagen and Guilfoyle 2002, Jain *et al.* 2006, Wu *et al.* 2012). Additionally, many *SAUR* genes possess the so-called downstream (DST) element within their 3' UTRs (Jain *et al.* 2006, McClure *et al.* 1989, Wu *et al.* 2012). This element consists of three highly conserved sequences that are intercepted by two variable sequences. In total, the DST element is about 40 bp long and is able to destabilise transcripts in heterologous systems (Newman *et al.* 1993). The regulation of *SAUR* expression is affected at different levels. On the transcriptional level, *SAUR* genes can be – as mentioned before – regulated by auxin. However, regulation by this phytohormone cannot only be stimulated in a positive (Chen *et al.* 2014, Hagen and Guilfoyle 2002) but also in a negative manner (Paponov *et al.* 2008, Xie *et al.* 2015). It is also known that *SAUR* genes are partially regulated by other phytohormones (Bai *et al.* 2012, Nemhauser *et al.* 2006, Ren and Gray 2015, Wang *et al.* 2012). Furthermore, regulation also occurs posttranscriptionally due to mRNA instability. Owing to the above-mentioned DST element, *SAUR* mRNAs containing this element are rapidly degraded (Gil and Green 1996, Newman *et al.* 1993). Additionally, SAUR proteins can also be regulated at the posttranslational level. Not only their mRNAs, but also the derived proteins can be highly

unstable (Chae *et al.* 2012, Knauss *et al.* 2003, Li *et al.* 2015, Spartz *et al.* 2012). The individual SAUR proteins have different functions and may be involved in various pathways. The role of SAUR19 from *Arabidopsis thaliana* is well characterised in terms of cell expansion. Upon auxin treatment, *SAUR19* gets quickly upregulated, leading to an inhibition of the PP2C-D phosphatase that negatively regulates a PM H^+-ATPase. Once active, the PM H^+-ATPase stimulates cell expansion in an acid growth manner (Spartz *et al.* 2012, Spartz *et al.* 2014). Additionally, SAUR proteins are involved in apical hook development and leaf senescence of Arabidopsis (Hou *et al.* 2013, Park *et al.* 2007). Furthermore, they control fruitlet abscission of citrus (Xie *et al.* 2015). However, considering that the *SAUR* family is the largest family within the early auxin response genes (Ren and Gray 2015), it has to be admitted that only little is known about the diverse functions of SAUR proteins.

Similarly, not much is known about *ke-1*. In a study of the *SAUR* gene family of maize, it was predicted that ke-1 is located within the mitochondria (Chen *et al.* 2014). In this study, we wanted to experimentally prove this assumption by means of a comprehensive subcellular localisation study. We show that ke-1 contains a functional mitochondrial targeting sequence and discuss possible functions of the protein.

Results

The gene *SAUR31* from *Zea mays* was found to be a candidate for chilling tolerance related to early vigour (Manuscript 2) and was therefore called *kühleempfindlich-1* (*ke-1*). The gene has not been characterised on the experimental level before. However, a localisation of ke-1 to the mitochondria was predicted recently (Chen *et al.* 2014). To confirm the prediction, the analysis was repeated with a different program. By using the online tool MitoProtII (Claros and Vincens 1996) the outcome of the analysis exhibited a probability of 0.83 for mitochondrial import of ke-1. The first 21 amino acids were outlined as the cleaved target sequence (Figure 1).

```
1          10         20         30         40         50         60
MAAGKLGQQLMTRLHLARTRSSATADVPRGHLAVYVGEGRKRLVIPTACLSHPAFVTLLK
           70         80         90         100
RVEDEFGFDHRCGGLTIPCASETEFAHIVGAAAAAGDDHHHH
```

Figure 1: Protein sequence of ke-1 including the mitochondrial target sequence
The 102 amino acids long protein sequence of ke-1 is shown. Highlighted in red is the putative mitochondrial target sequence.

To experimentally verify the transport of ke-1 to the mitochondria, three constructs were designed based on the CDS of *ke-1* of the TH genotype (Figure 2A). Construct *35S::ke-1::GFP* contained the full-length *ke-1* CDS without the stop codon. Construct *35S::Δ_{63bp}ke-1::GFP* lacked the predicted mitochondrial target sequence (63 bp) and the stop codon of *ke-1* (an ATG was added with the forward oligonucleotide by PCR). The reciprocal construct *35S::ke-1Δ_{243bp}::GFP* only contained the predicted mitochondrial target sequence of *ke-1*. All *ke-1* parts were cloned between the CaMV35S promoter and the *GFP* gene. A fusion of *GFP* with the CaMV35S promoter served as control. These constructs were transiently transformed into leaves of *Nicotiana benthamiana* and isolated protoplasts were subjected to fluorescence microscopy (Figure 2B).

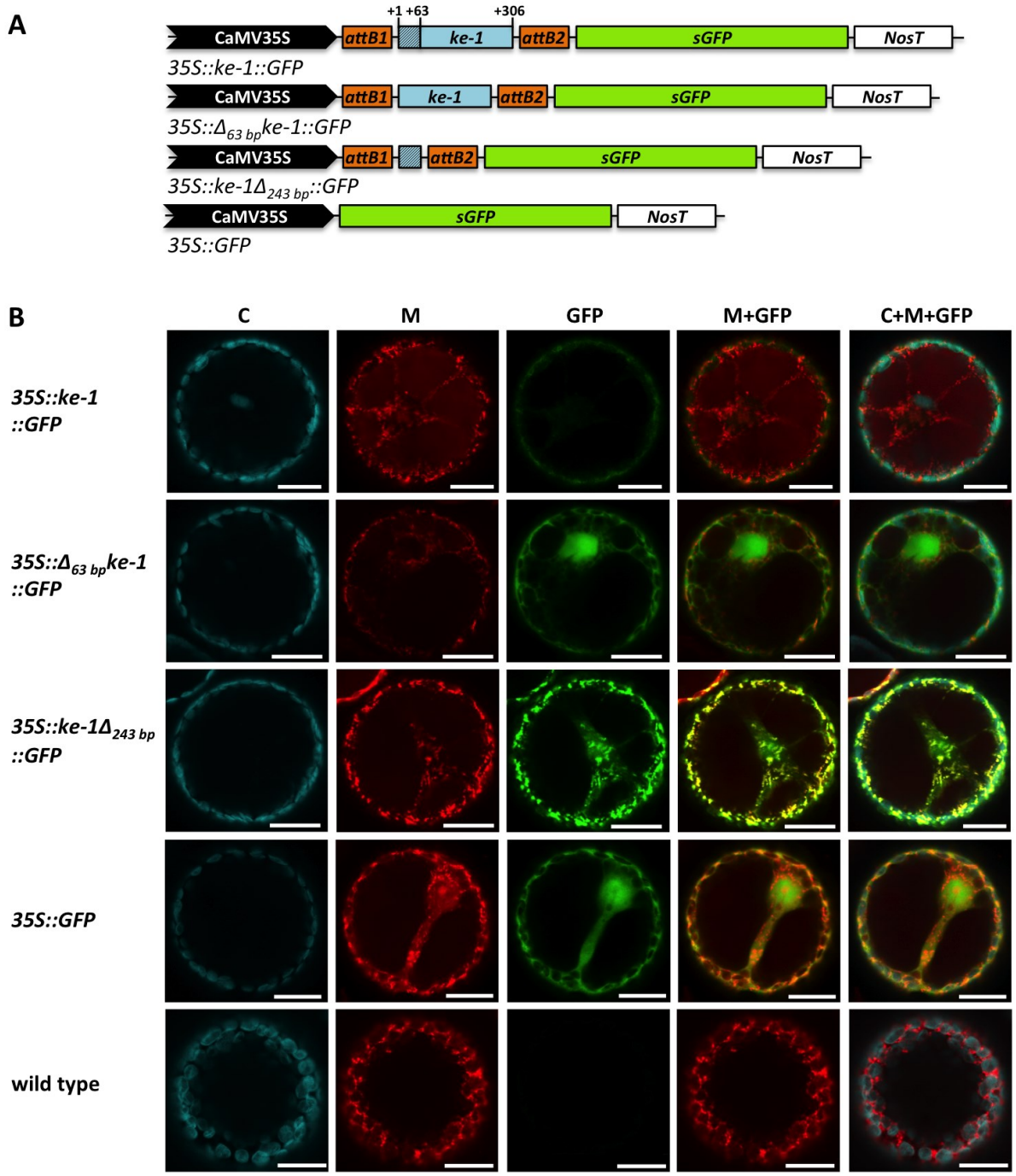

Figure 2: Localisation of ke-1 constructs in tobacco protoplasts

(A) Schematic illustration of the *ke-1* constructs transformed into tobacco leaves. Three constructs with various *ke-1* CDS parts fused to the *GFP* gene and one control consisting of solely *GFP* were generated. All constructs were under the constitute control of the CaMV35S promoter. The mitochondrial target sequence is indicated as a shaded box.

(B) Transient expression of the *ke-1* constructs in tobacco protoplasts. The constructs described above were transformed into tobacco leaves and isolated protoplasts were treated with MitoTracker® Orange CMTMRos to label mitochondria. Wild type protoplasts served as a negative control. Images of chlorophyll, MitoTracker® Orange CMTMRos, GFP fluorescence as well as overlays were generated. For each construct and the controls, representative pictures are shown. The same settings for exposure time and gain were used for all shown images.

Scale bars = 20 µm. *att*, *attachment site*; *ke-1*, *kühleempfindlich-1*; *NosT*, Nopaline synthase terminator; *GFP*, *Green Fluorescent Protein*; C, chlorophyll; M, MitoTracker® Orange CMTMRos

According to the MitoProtII prediction, the GFP fluorescence generated by construct *35S::ke-1::GFP* was expected to be restricted to the mitochondria. However, the GFP signal was detected exclusively in the cytosol. The fluorescence strength was only slightly stronger than the background signal of wild type protoplasts. In contrast, the construct *35S::Δ$_{63bp}$ke-1::GFP*, missing the predicted mitochondrial target sequence, exhibited a strong GFP signal in the cytosol and the nucleus, thus resembling the control *35S::GFP*. The target sequence alone was sufficient to direct transport to the mitochondria since the GFP signal of *35S::ke-1Δ$_{243bp}$::GFP* displayed co-localisation with the fluorescence of the MitoTracker. In conclusion, ke-1 contains a functional target sequence for the mitochondria.

Discussion

The *SAUR* gene *ke-1* may be involved in chilling tolerance of maize (Manuscript 2). No comprehensive study about *ke-1* has been conducted so far. Based on the prediction that ke-1 is targeted to the mitochondria, an extensive localisation study was performed. Curiously, the ke-1-GFP fusion was barely visible in tobacco protoplasts (Figure 2B). However, it is known that at least several SAUR proteins are unstable. In a metabolic labelling experiment, ZmSAUR2 from maize exhibited a half-life of 7 min and it was not possible to detect the protein in a Westernblot (Knauss *et al.* 2003). In another study, overexpressed AtSAUR19 from Arabidopsis was hardly detectable in an immunoblot assay and endogenous AtSAUR19 could not be visualised at all. Interestingly, N-terminal GFP- or StrepII-tags were able to stabilise AtSAUR19 (Spartz *et al.* 2012). The whole ke-1 protein also seems to be unstable, which made the interpretation of the GFP signal difficult. Even though the entire ke-1 protein may be located in the mitochondria, the weak signal did not allow to draw a solid conclusion. However, further experiments with ke-1 and a double GFP fusion revealed a fluorescence signal within the mitochondria and the nucleus (Karin Ernst, personal communication). The extra GFP might have a stabilising effect on ke-1. But it is more likely that the double GFP led to a double signal strength that eased the detection. Intriguingly, cleavage of the mitochondrial target sequence suppressed the degradation of ke-1 since either the target sequence or the residual ke-1 sequence fused to GFP conferred a strong fluorescence signal in the mitochondria or the cytoplasm and nucleus, respectively (Figure 2B). This indicates that the signal for degradation is located at the target sequence cleavage site and needs to be intact for functioning. However, the true nature of ke-1 degradation remains to be elucidated. No known degradation sequence, for example the PEST sequence (Rogers *et al.* 1986), can be found in the ke-1 amino acid sequence.

The target sequence of ke-1 was able to direct GFP accumulation in the mitochondria (Figure 2B). However, the function of ke-1 is still enigmatic. Subcellular localisation prediction studies revealed that many SAUR proteins are possibly targeted to the mitochondria (Chen *et al.* 2014, Huang *et al.* 2016, Wu *et al.* 2012, Xie *et al.* 2015). To date, none of these *SAUR* genes have been analysed in detail and thus their functions remain unclear. As indicated before, several *SAUR* genes are regulated by the phytohormone auxin that influences many processes in plant growth (Hagen and Guilfoyle 2002). In line with this, *ke-1* may be regulated by auxin since the maize B73 *SAUR31* promoter exhibits an auxin response factor (ARF) binding site (Chen *et al.* 2014). This possibility as well as the probable localisation of ke-1 in the mitochondria may imply a connection between the reactive oxygen species (ROS) second messenger, *ke-1* and auxin signalling in relation to chilling stress. ROS, for example H_2O_2, are not only produced in the chloroplasts but also in the mitochondria (Hossain *et al.* 2015, Møller 2001). As second messengers, ROS are involved amongst others in developmental processes, cell growth (Gapper and Dolan 2006) and hormone signalling (Xia *et al.* 2015). There are implications that auxin is engaged, too. For example, the mitochondrial AtFtsH4 protease from Arabidopsis mediates between H_2O_2 and auxin homeostasis for regulation of plant growth and development (Zhang *et al.* 2014). Additionally, the Arabidopsis J-protein AtDjB1 is required for the mitochondrial Complex I activity and the corresponding mutant exhibited increased H_2O_2, decreased IAA content – the most important auxin (Jia *et al.* 2016, Simon and Petrasek 2011) – and reduced growth (Jia *et al.* 2016). Hence, it is possible that *ke-1* is involved in mediation and integration of mitochondrial ROS generation, auxin signalling and the resulting enhanced early vigour in tolerant maize plants. Further experiments may provide a deeper insight. Stabilisation of the whole ke-1 sequence with an N-terminal GFP as conducted in Spartz *et al.* (2012) may reveal mitochondrial localisation for good. Additionally, it would be of great interest whether ke-1 responds to auxin or not and which proteins interact with ke-1. In conclusion, this study revealed that ke-1 has a functional mitochondrial target sequence, but the proteins function still remains enigmatic.

Methods

Cloning of protein-GFP-fusion constructs

DNA manipulations were executed as described in Sambrook and Russell (2001). Karin Ernst provided template TH DNA for the generation of *ke-1* constructs. Reverse oligonucleotides

contained an extra adenine to ensure that *ke-1* fragments were expressed in frame with *GFP*. DNA fragments were inserted into pENTR3C™ Dual Selection Vector (Invitrogen, Carlsbad, USA) by means of blunt-end cloning. Via LR reaction, *ke-1* fragments were incorporated into the destination vector pGWB5 (Nakagawa *et al.* 2007). Inserts within the pENTR3C™ Dual Selection Vector and pGWB5 were confirmed and checked by DNA sequencing. All oligonucleotides are listed in Supplemental Table 1. The control *35S::GFP* was provided by Christian Wiludda.

Transient transformation of *Nicotiana benthamiana* and isolation of protoplasts

All prepared protein-*GFP*-fusion constructs were transformed into the *Agrobacterium tumefaciens* strain GV3101 (Koncz and Schell 1986) via electroporation. Leaves of four week-old *N. benthamiana* plants were infiltrated with Agrobacteria containing the respective construct and with the *Agrobacterium* strain p19 to suppress gene silencing (Voinnet *et al.* 2003) according to the protocol of Waadt and Kudla (2008). After three to five days incubation in the greenhouse, protoplasts of tobacco leaves were isolated, treated with MitoTracker® Orange CMTMRos (Invitrogen, Carlsbad, USA) (final concentration of 150 nM) and washed as described in Wiludda *et al.* (2012). Three independent experiments (first one without the *35S::GFP* control) were performed.

Fluorescence microscopy of protoplasts

Protoplasts were imaged using confocal laser-scanning microscope Leica TCS SP8 STED 3X (Leica Microsystems, Wetzlar, Germany) equipped with the HC PL APO 40x/1.0 water immersion objective. For excitation of EGFP, MitoTracker and chlorophyll fluorescence, we used the wavelength 488 nm and 561 nm of a pulsed white light laser in combination with the corresponding notch filters. Emission was detected by using hybrid detectors (EGFP and MitoTracker) or a photomultiplier tube (chlorophyll) in a range of 492–530 nm for EGFP, 563–615 nm for MitoTracker and between 650 and 740 nm (chlorophyll). Pictures were taken with a scan frequency of 100 Hz, a line average of 4 and a pixel size of 90 nm.

Acknowledgments

We thank the Center for Advanced imaging (HHU Düsseldorf) for provision and Stefanie Weidtkamp-Peters for technical assistance of the confocal laser-scanning microscope Leica TCS SP8 STED 3X.

Literature

Bai, M.Y., Shang, J.X., Oh, E., Fan, M., Bai, Y., Zentella, R., Sun, T.P. and Wang, Z.Y. (2012) Brassinosteroid, gibberellin and phytochrome impinge on a common transcription module in Arabidopsis. *Nature cell biology*, **14**, 810-817.

Chae, K., Isaacs, C.G., Reeves, P.H., Maloney, G.S., Muday, G.K., Nagpal, P. and Reed, J.W. (2012) Arabidopsis SMALL AUXIN UP RNA63 promotes hypocotyl and stamen filament elongation. *Plant J*, **71**, 684-697.

Chen, Y., Hao, X. and Cao, J. (2014) Small auxin upregulated RNA (SAUR) gene family in maize: Identification, evolution, and its phylogenetic comparison with Arabidopsis, rice, and Sorghum. *J Integr Plant Biol*, **56**, 133-150.

Claros, M.G. and Vincens, P. (1996) Computational method to predict mitochondrially imported proteins and their targeting sequences. *Eur J Biochem*, **241**, 779-786.

Gapper, C. and Dolan, L. (2006) Control of plant development by reactive oxygen species. *Plant Physiol*, **141**, 341-345.

Gil, P. and Green, P.J. (1996) Multiple regions of the Arabidopsis SAUR-AC1 gene control transcript abundance: the 3' untranslated region functions as an mRNA instability determinant. *The EMBO journal*, **15**, 1678-1686.

Hagen, G. and Guilfoyle, T. (2002) Auxin-responsive gene expression: genes, promoters and regulatory factors. *Plant Mol Biol*, **49**, 373-385.

Hossain, M.A., Bhattacharjee, S., Armin, S.M., Qian, P., Xin, W., Li, H.Y., Burritt, D.J., Fujita, M. and Tran, L.S. (2015) Hydrogen peroxide priming modulates abiotic oxidative stress tolerance: insights from ROS detoxification and scavenging. *Front lant Sci*, **6**, 420.

Hou, K., Wu, W. and Gan, S.S. (2013) SAUR36, a small auxin up RNA gene, is involved in the promotion of leaf senescence in Arabidopsis. *Plant Physiol*, **161**, 1002-1009.

Huang, X., Bao, Y., Wang, B.O., Liu, L., Chen, J., Dai, L., Baloch, S.U. and Peng, D. (2016) Identification of small auxin-up RNA (SAUR) genes in Urticales plants: mulberry (Morus notabilis), hemp (Cannabis sativa) and ramie (Boehmeria nivea). *J Genetics*, **95**, 119-129.

Jain, M., Tyagi, A.K. and Khurana, J.P. (2006) Genome-wide analysis, evolutionary expansion, and expression of early auxin-responsive SAUR gene family in rice (Oryza sativa). *Genomics*, **88**, 360-371.

Jia, N., Lv, T.T., Li, M.X., Wei, S.S., Li, Y.Y., Zhao, C.L. and Li, B. (2016) The J-protein AtDjB1 is required for mitochondrial complex I activity and regulates growth and development through ROS-mediated auxin signalling. *J Exp Bot*, **67**, 3481-3496.

Knauss, S., Rohrmeier, T. and Lehle, L. (2003) The auxin-induced maize gene ZmSAUR2 encodes a short-lived nuclear protein expressed in elongating tissues. *J Biol Chem*, **278**, 23936-23943.

Koncz, C. and Schell, J. (1986) The promoter of TL-DNA gene 5 controls the tissue-specific expression of chimaeric genes carried by a novel type of Agrobacterium binary vector. *Mol Gen Genet*, **204**, 383-396.

Li, Z.G., Chen, H.W., Li, Q.T., Tao, J.J., Bian, X.H., Ma, B., Zhang, W.K., Chen, S.Y. and Zhang, J.S. (2015) Three SAUR proteins SAUR76, SAUR77 and SAUR78 promote plant growth in Arabidopsis. *Scientific reports*, **5**, 12477.

McClure, B.A. and Guilfoyle, T. (1987) Characterization of a class of small auxin-inducible soybean polyadenylated RNAs. *Plant Mol Biol*, **9**, 611-623.

McClure, B.A., Hagen, G., Brown, C.S., Gee, M.A. and Guilfoyle, T.J. (1989) Transcription, organization, and sequence of an auxin-regulated gene cluster in soybean. *Plant Cell*, **1**, 229-239.

Møller, I.M. (2001) PLANT MITOCHONDRIA AND OXIDATIVE STRESS: Electron Transport, NADPH Turnover, and Metabolism of Reactive Oxygen Species. *Annu Rev Plant Physiol Plant Mol Biol*, **52**, 561-591.

Nakagawa, T., Kurose, T., Hino, T., Tanaka, K., Kawamukai, M., Niwa, Y., Toyooka, K., Matsuoka, K., Jinbo, T. and Kimura, T. (2007) Development of series of gateway binary vectors, pGWBs, for realizing efficient construction of fusion genes for plant transformation. *J Biosci Bioeng*, **104**, 34-41.

Nemhauser, J.L., Hong, F. and Chory, J. (2006) Different plant hormones regulate similar processes through largely nonoverlapping transcriptional responses. *Cell*, **126**, 467-475.

Newman, T.C., Ohme-Takagi, M., Taylor, C.B. and Green, P.J. (1993) DST sequences, highly conserved among plant SAUR genes, target reporter transcripts for rapid decay in tobacco. *Plant Cell*, **5**, 701-714.

Paponov, I.A., Paponov, M., Teale, W., Menges, M., Chakrabortee, S., Murray, J.A. and Palme, K. (2008) Comprehensive transcriptome analysis of auxin responses in Arabidopsis. *Mol Plant*, **1**, 321-337.

Park, J.E., Kim, Y.S., Yoon, H.K. and Park, C.M. (2007) Functional characterization of a small auxin-up RNA gene in apical hook development in Arabidopsis. *Plant Sci*, **172**, 150-157.

Presterl, T., Ouzunova, M., Schmidt, W., Möller, E.M., Röber, F.K., Knaak, C., Ernst, K., Westhoff, P. and Geiger, H.H. (2007) Quantitative trait loci for early plant vigour of maize grown in chilly environments. *Theor Appl Genet*, **114**, 1059-1070.

Ren, H. and Gray, W.M. (2015) SAUR Proteins as Effectors of Hormonal and Environmental Signals in Plant Growth. *Mol Plant*, **8**, 1153-1164.

Rogers, S., Wells, R. and Rechsteiner, M. (1986) Amino acid sequences common to rapidly degraded proteins: the PEST hypothesis. *Science*, **234**, 364-368.

Sambrook, J. and Russell, D.W. (2001) Molecular cloning: a laboratory manual 3rd edition. *Coldspring-Harbour Laboratory Press, UK*.

Simon, S. and Petrasek, J. (2011) Why plants need more than one type of auxin. *Plant Sci*, **180**, 454-460.

Spartz, A.K., Lee, S.H., Wenger, J.P., Gonzalez, N., Itoh, H., Inzé, D., Peer, W.A., Murphy, A.S., Overvoorde, P.J. and Gray, W.M. (2012) The SAUR19 subfamily of SMALL AUXIN UP RNA genes promote cell expansion. *Plant J*, **70**, 978-990.

Spartz, A.K., Ren, H., Park, M.Y., Grandt, K.N., Lee, S.H., Murphy, A.S., Sussman, M.R., Overvoorde, P.J. and Gray, W.M. (2014) SAUR Inhibition of PP2C-D Phosphatases Activates Plasma Membrane H+-ATPases to Promote Cell Expansion in Arabidopsis. *Plant Cell*, **26**, 2129-2142.

Voinnet, O., Rivas, S., Mestre, P. and Baulcombe, D. (2003) An enhanced transient expression system in plants based on suppression of gene silencing by the p19 protein of tomato bushy stunt virus. *Plant J*, **33**, 949-956.

Waadt, R. and Kudla, J. (2008) In Planta Visualization of Protein Interactions Using Bimolecular Fluorescence Complementation (BiFC). *CSH protocols*, **2008**, pdb.prot4995.

Wang, Z.Y., Bai, M.Y., Oh, E. and Zhu, J.Y. (2012) Brassinosteroid signaling network and regulation of photomorphogenesis. *Annu Rev Genet*, **46**, 701-724.

Wilde, K., Presterl, T., Möller, E.M., Ouzunova, M., Schmidt, W. and Geiger, H.H. (2005) Untersuchungen zur Züchtung auf Kühletoleranz bei Mais. *Bericht über die 56. Tagung 2005 der Vereinigung der Pflanzenzüchter und Saatgutkaufleute Österreichs*.

Wiludda, C., Schulze, S., Gowik, U., Engelmann, S., Koczor, M., Streubel, M., Bauwe, H. and Westhoff, P. (2012) Regulation of the Photorespiratory GLDPA Gene in C4 Flaveria: An Intricate Interplay of Transcriptional and Posttranscriptional Processes. *Plant Cell*, **24**, 137-151.

Wu, J., Liu, S., He, Y., Guan, X., Zhu, X., Cheng, L., Wang, J. and Lu, G. (2012) Genome-wide analysis of SAUR gene family in Solanaceae species. *Gene*, **509**, 38-50.

Xia, X.J., Zhou, Y.H., Shi, K., Zhou, J., Foyer, C.H. and Yu, J.Q. (2015) Interplay between reactive oxygen species and hormones in the control of plant development and stress tolerance. *J Exp Bot*, **66**, 2839-2856.

Xie, R., Dong, C., Ma, Y., Deng, L., He, S., Yi, S., Lv, Q. and Zheng, Y. (2015) Comprehensive analysis of SAUR gene family in citrus and its transcriptional correlation with fruitlet drop from abscission zone A. F*unct Integr Genomics*, **15**, 729-740.

Zhang, S., Zhang, D. and Yang, C. (2014) AtFtsH4 perturbs the mitochondrial respiratory chain complexes and auxin homeostasis in Arabidopsis. *Plant Signal Behav*, **9**, e29709.

Supplemental Table

Supplemental Table 1: Oligonucleotides used for construction and verification of *ke-1* constructs.
Shown are the designations of oligonucleotides, the respective sequences and their purposes.

Oligonucleotide designation	Sequence (5’ to 3’)	Usage
ATG_SAUR_fw1	ATGTCGGCGACGGCGGACGT	Construct *35S::Δ$_{63bp}$ke-1::GFP*
ATG_TSS_fw1	ATGGCGGCGGGAAAGCTG	Constructs *35S::ke-1::GFP 35S::ke-1Δ$_{243bp}$::GFP*
SAUR_A_rv2	TGTGATGGTGGTGGTCGTCCC	Constructs *35S::ke-1::GFP 35S::Δ$_{63bp}$ke-1::GFP*
TSS_SAUR_A_rv	TCGATCGGGTCCTCGCGAGGT	Construct *35S::ke-1Δ$_{243bp}$::GFP*
pENTR3C fw	TGCGTTTCTACAAACTCTTCCTG	Sequencing, colony PCR
pENTR3C rv	GTAACATCAGAGATTTTGAGACAC	Sequencing, colony PCR
3’sGFP301105	GTCGTGCTGCTTCATGTGGTC	Sequencing, colony PCR
35S_pGWB5_fw	CATCGTGGAAAAAGAAGACGTTC	Sequencing, colony PCR

VII. Acknowledgements

Ich danke...

...Prof. Dr. Peter Westhoff für die Möglichkeit, meine Doktorarbeit an seinem Institut durchführen zu können und für die hilfreiche Betreuung während dieser Zeit.

...Prof. Dr. Maria von Korff Schmising für die Übernahme des Korreferates.

...Karin und **Udo** für die Betreuung, Ratschläge und Tipps.

> Die Doktorarbeitszeit war – zumindest die letzten 2 Jahre – für mich eine sehr schwierige Zeit. Ohne eine Vielzahl von Menschen hätte ich das nicht geschafft. Deswegen **danke ich ebenfalls...**

...meiner Familie, insbesondere **Mama** und **Papa** und meinem Bruder **Marco**! Ihr habt mich viel unterstützt und durch schwierige Zeiten geholfen. Vielen Dank **Marco** für das Korrekturlesen von Biologen-Kauderwelsch und vielen Dank **Papa** (und teilweise **Mama**) fürs stundenlange Päppeln und viele Tierarzttransportdienste. Lieber **Opa Artur**, wenn du das da oben lesen kannst: bald kannst du mich – wenn alles gut geht – völlig legal Frau Doktor nennen!

> Und nun in alphabetischer Reihenfolge:

...Anja (die hier als einzige namentlich 2x auftaucht, s.u.) und **Kenan**, dafür, dass ihr mir den größten Gefallen überhaupt getan habt, indem ihr meine liebe Fluse aufgenommen habt, als ich nicht mehr konnte! Und natürlich für die Grill- und Spieleabende, die Mittelaltermärkte, die Transportdienste und vor allem für die Freundschaft!

...Borjana for nice talks, painting my walls, postcards and watching together Hobbit in the cinema! It's sad, that there are only three movies...

...der **Botanik IV**, mit allen bekannten ehemaligen und derzeitigen **Mitarbeitern**. Ich war sehr gerne bei euch!

...Christiane, die ich seit Anbeginn des Studiums kenne und mit der ich immer noch stundenlang telefonieren kann!

...Christian Wever für die ultragenialen Kuchen und dein lexikonartiges Pflanzenwissen! Für das Zusammenhalten bei dem verfluchten Transkriptom!

...Christian Wiludda, dafür, dass du mich nie vergessen hast! Mich immer wieder aufgeheitert und aufgebaut hast und mir soooo viel Entspannungsmaterial geschickt hast!

...Daniela für das Zusammenhalten beim Transkriptom, Hilfe beim Renovieren, die Meerschweinchenhege (du brauchst immer noch kein schlechtes Gewissen haben) und die Holland-Trips!

...Elena, die mich in die Geheimnisse des Transkriptoms eingeweiht hat, fürs Aufmuntern und Korrekturlesen!

...den **Gärtnern Andrea**, **Anja** und **Jochen** nicht nur für die liebevolle Pflege von meinen Versuchspflanzen. Sondern auch für die vergnüglichen Zeiten im Dachgewächshaus, für den ganzen Spaß und die vielen Pflegetipps für meinen Dschungel! Schade, dass ich kein Gärtner bin...

...meiner Nachnamensvetterin **Gwen** und ihrer **Shalima**, die mir beide eine ganz andere Art des Reitens gezeigt haben! Und – was **Gwen** angeht – für die netten Intergroup Seminare!

...Jan und **Steffi Schulze** für den ganzen Spaß zusammen, die vielen Tipps und Tricks und Kreuzworträtsel in der Mittagspause!

...Jasmin, für blaue Haare, Krallenschneiden und tolle Spieleabende mit dir und **Otto**!

...Judith, die mir fast seit Anfang des Studiums eine liebe Freundin war und ist! Für die interessanten Ärztegeschichten, die tollen Klamotten (ich brauche bald einen neuen Kleiderschrank), die Klamottenberatung, die alljährliche Pizzasuppe, die schöne Reise nach Dublin, das immer offene Ohr und und und...

...Katharina für das Erbe des interessanten *SULTR2;2* Projekts und die Starthilfe im neuen Job!

...Kumari. I know I should not thank friends. Sorry, dear, I do it again! Thanks for delicious chai in times I needed a break (transcriptome...), the beautiful panjabi dress and for getting familiar with Indian culture (especially food)!

...dem **KWS-Team** aus **Claude**, **Daniela**, **Milena** und **Thomas** für die interessanten Projekttreffen, die Zusammenarbeit und die tollen Restaurantbesuche!

...Linda, für die noch nicht so lange bestehende (wen man so beim Tierarzt trifft...) aber hoffentlich lebenslang andauernde Freundschaft! Und dafür, dass du – im Gegensatz zu anderen Laien – dir immer hast erklären lassen, was ich für mysteriöse Sachen im Labor mache!

...Lyssa, für die nun schon so lange währende Email-Freundschaft! Dafür, dass du immer ein „offenes Postfach“ hast und für die Reise nach Mittelerde!

...Mara für die schönen Stunden bei Esprit oder beim Stoffmarkt! Für deine fröhliche Art! Und für die Scones mit Marmelade, Clotted Cream und Tea!

...Maria, für sooo vieles! Die unzähligen Start-in-den-Tag-Gespräche mit Kaffee und Tee (und die einsamen Tassenfotos per WhatsApp, wenn ich nicht da war), dafür, dass du mich wieder ans Autofahren gebracht hast (Sandra und polnische Landstraße...), der wunderschöne Trip nach Polen (Grüße an Mama und Bernadette!) und und und...

...meinen **Meerschweinchen**, die mich so lange begleitet haben und mich soooo oft aufgeheitert haben! Leider habt ihr nicht mit mir bis zum Ende durchgehalten. Ich vermisse euch so sehr!

...der **Mittelaltermarktfraktion** bestehend aus **Hilde**, **Marcus** und **Michael** für die schöne Zeit mit euch auf den Mittelaltermärkten!

...Myles für die zahlreichen „Kompleidigungen“ und die vielen lustigen Gespräche und lebhaften Diskussionen (bei denen ich meist unterlag)! Und zusammen mit **Tatjana** für die lustigen Aktionen wie der legendäre Peter Pepper Chili-Wettbewerb!

...Nina und **Florian** für die unzähligen schönen Spieleabende und den ebenso unzähligen tollen Postkarten! Ich hoffe, es folgen noch unzählige (Spielabende und Postkarten)! **Nina** auch dafür, dass sie mich beim Schreiben nicht vergessen hat und immer wieder gefragt hat, wie es mir geht! Und **Florian** für das Korrekturlesen und die Expertentipps!

...Sonja, die neben Judith meine zweite 827 Freundschaft ist (auch wenn wir uns eigentlich schon seit dem Kindergarten kennen)! Danke für die tollen Postkarten von deinen traumhaften Reisezielen und für das Korrekturlesen!

...Steffi Hartings für die tollen Stunden im Reitstall und bei den Isländern. Und zusammen mit **Martin** für die tolle Freundschaft!

...meiner möglichen Cousine x-ten Grades **Susanne** (sorry, konnte ich mir nicht verkneifen) für die vielen Ratschläge, netten Gespräche, gemeinsames Lachen, Shoppen bei Esprit, Geburtstagsüberraschungen, Nachhause fahren, ... Die Liste ließe sich sehr lange weiterführen!

...und den anderen, die hier hinein gehören aber die ich **vergessen** habe. Tut mir leid...